

**EFFECT OF COMBINATION OF THE MAMMALIAN LIGNAN,
ENTEROLACTONE, WITH TYROSINE KINASE INHIBITORS ON
MARKERS OF HEPATIC FIBROSIS**

A Thesis Submitted to the
College of Graduate and Postdoctoral Studies
In Partial Fulfillment of the Requirements
For the Degree of Doctor of Philosophy
In the College of Pharmacy and Nutrition
At the University of Saskatchewan
Saskatoon

By

Xiaolei Yang

© Copyright Xiaolei Yang, December 2020. All rights reserved.

Unless otherwise noted, copyright of the material in this thesis belongs to the author

PERMISSION TO USE

In presenting this thesis in partial fulfilment of the requirements for a Postgraduate degree from the University of Saskatchewan, I agree that the Libraries of this University may make it freely available for inspection. I further agree that permission for copying of this thesis in any manner, in whole or in part, for scholarly purposes may be granted by the professor or professors who supervised my thesis work or, in their absence, by the Dean of the College in which my thesis work was done. It is understood that any copying or publication or use of this thesis or parts thereof for financial gain shall not be allowed without my written permission. It is also understood that due recognition shall be given to me and to the University of Saskatchewan in any scholarly use which may be made of any material in my thesis.

Requests for permission to copy or to make other use of material in this thesis in whole or part should be addressed to:

Dean of the College of Pharmacy and Nutrition
University of Saskatchewan
107 Wiggins Road
Saskatoon, Saskatchewan S7N 5E5
Canada

Dean
College of Graduate and Postdoctoral Studies
University of Saskatchewan
116 Thorvaldson Building, 110 Science Place
Saskatoon, Saskatchewan S7N 5C9
Canada

ABSTRACT

Current treatments for hepatic fibrosis are still elusive because of the lack of efficient and safe drugs. The pathogenesis of hepatic fibrosis suggests multi-target drugs might have therapeutic potential. This dissertation research aimed to confirm the antifibrotic effects of the combination of the bioactive mammalian lignan, enterolactone (ENL), and selected tyrosine kinase inhibitors (TKIs) and to explore whether these effects involve peroxisome proliferator-activated receptor gamma (PPAR γ), oxidative stress, and/or endoplasmic reticulum (ER) stress, known pathways of lignan and TKI action.

A standard PPAR γ competitive binding assay was conducted to assess whether three multi-target TKIs and ENL were PPAR γ agonists. Binding affinity to the rosiglitazone binding site of PPAR γ was low. However, a PPAR γ transactivation assay and PPAR γ -related biological functional assays, adipogenesis and glucose uptake assays, provided evidence of potential PPAR γ partial agonism by gefitinib and ENL. Evaluation of the expression changes of several fibrotic markers (e.g., collagen I, α -SMA, MMP2/MMP9, and TIMP-1,) using human hepatic stellate cells (HSC), LX-2 cells, at both mRNA and protein level by real-time PCR and ELISA/western blot, respectively, demonstrated that Gefitinib had the greatest ability to attenuate HSC activation and ECM production and was chosen as the model TKI for further investigation.

Next, qPCR was used to quantify changes in the expression of biomarkers of HSC proliferation and activation (e.g., α -SMA, collagen I, TIMP-1, and MMP2) and possible pathways (e.g., PPAR γ , β -catenin/Wnt, Nrf2) for the antifibrotic effects of ENL and/or gefitinib in TGF- β 1-stimulated LX-2 cells. The combination of gefitinib and ENL attenuated the fibrotic biomarkers to a greater extent than using each compound alone. In further experiments evaluating reactive oxygen species (ROS) production, caspase-3/7 apoptosis, and changes in the expression of PPAR γ , Nrf2, and ER stress markers, the data suggested that PPAR γ , oxidative stress, and ER stress-induced apoptosis might be involved in the antifibrotic response of gefitinib and ENL.

The antifibrotic role of secoisolariciresinol diglucoside (SDG) and its metabolites were also investigated in a hypercholesterolemic rat model of hepatic lipidosis. This study indicated that SDG caused modest improvement in serum lipid parameters and hepatic lipidosis, with mild effects on fibrotic biomarkers of non-alcoholic fatty liver disease in hypercholesterolemic rats.

In conclusion, these studies suggest the potential of the combination of ENL and gefitinib as a therapeutic approach in hepatic fibrosis. PPAR γ , oxidative stress, and the ER stress-induced apoptosis can be potential pathways to attenuate markers of hepatic fibrosis. Further studies should be done to clarify whether ENL and gefitinib attenuate hepatic fibrosis through PPAR γ , oxidative stress, and/or the ER stress response *in vivo*.

ACKNOWLEDGEMENTS

I would like to thank my supervisor Dr. Jane Alcorn for her constant mentorship, support, guidance, and expertise that led me to complete this thesis. I truly appreciate Dr. Alcorn's full support during the coronavirus pandemic. Dr. Alcorn's dedication and passion to her own work and life have inspired me greatly.

I also would like to give thanks to my advisory committee members: Dr. Kate Dadachova, Dr. Darrell Mousseau, Dr. William Kulyk, Dr. Brian Bandy for their constructive suggestions and valuable advice. I would like to thank Dr. Ed Krol and Dr. David Blackburn for chairing my committee meetings and providing support.

APOTEX funded me through an APOTEX scholarship for two years. Laboratory space was provided by the College of Pharmacy and Nutrition and my research was funded by SHRF. I also thank College of Pharmacy and Nutrition for providing me professional development opportunities and travel awards to present my research at different conferences. I appreciate the help by our office staff, Erin, Jenn, and Gen.

I would like to extend my sincere thanks to Deborah Michel for her technical assistance. Special thanks are given to my lab colleagues, Ahmed, Ahlam, Arka, Jim, Stephanie, Shelby, Shanal and Yunyun for their help during my PhD study. I also appreciate the patience, help, and friendship tendered by my officemate/roommate Jennifer Xiao.

I thank my husband, my parents, and my parents-in-law, for their patience, encouragement, and support. I also would like to thank our dog, Shorty, for his companionship and unconditional support.

Dedicated To

My husband Guo, Yang

My parents Li, Suyun and Yang, Sizhen

My parents-in-law Bao, Xiurong and Guo, Qingrui

Our dear dog Shorty and forthcoming girl Guo, Shining Yang

TABLE OF CONTENTS

PERMISSION TO USE.....	i
ABSTRACT.....	ii
ACKNOWLEDGEMENTS	iv
TABLE OF CONTENTS	vi
LIST OF FIGURES	xi
LIST OF TABLES	xxiv
LIST OF ABBREVIATIONS	xxv
1. INTRODUCTION.....	1
2. RESEARCH QUESTION	3
3. HYPOTHESES	3
4. OBJECTIVES	3
5. LITERATURE REVIEW	5
5.1 Hepatic Fibrosis	5
5.1.1 Pathology of Hepatic Fibrosis	6
5.1.2 Current Therapeutic Approaches	10
5.1.3 Possible Antifibrotic Mechanisms and Potential Targets	11
5.1.3.1 TGF- β and PDGF.....	12
5.1.3.2 Oxidative stress	15
5.1.3.3 PPAR γ	16
5.1.3.3.1 Pan-agonists or Dual agonists of PPARs	19
5.1.3.3.2 PPAR γ full agonists	20
5.1.3.3.3 PPAR γ partial agonists and non-agonist ligands.....	21
5.1.3.3.4 PPAR γ in Hepatic fibrosis.....	22
5.1.3.4 ER Stress-induced Apoptosis in HSCs.....	25
5.1.3.5 Wnt/ β -catenin Pathway in HSCs.....	26
5.1.4 Experimental Models of Hepatic Fibrosis	27
5.1.4.1 In Vitro Models of Hepatic Fibrosis.....	28
5.1.4.1.1 Primary HSCs	28

5.1.4.1.2	Hepatic Stellate Cell Lines	29
5.1.4.1.3	Co-culture Models.....	30
5.1.4.2	<i>Ex vivo</i> Models of Hepatic Fibrosis	31
5.1.4.3	<i>In vivo</i> Models of Hepatic Fibrosis	32
5.1.4.3.1	Diet- or Chemical-stimulated Models	32
5.1.4.3.2	Infection- or Surgery-induced Models.....	33
5.1.4.3.3	Genetic models for Hepatic Fibrosis	33
5.2	TKIs and Possible Mechanisms of TKI Action in Hepatic Fibrosis.....	34
5.2.1	RTKs	35
5.2.1.1	EGFR	36
5.2.1.2	FGFR/VEGFR/PDGFR.....	39
5.2.1.3	Other RTKs	40
5.2.2	Non-RTKs.....	40
5.3	Flaxseed Lignans.....	41
5.3.1	Brief Overview on Natural Products.....	41
5.3.2	Flaxseed Lignans	42
5.3.2.1	Biological Function of Flaxseed Lignans	43
5.3.2.2	Pharmacokinetics and Safety Properties of Flaxseed Lignans	44
5.3.2.2.1	Bioavailability of Flaxseed Lignans.....	44
5.3.2.2.2	Distribution of Flaxseed Lignans.....	45
5.3.2.2.3	Metabolism and Elimination of Flaxseed Lignans.....	46
5.3.2.2.4	Safety of Flaxseed Lignans	48
5.3.3	Flaxseed Lignans' Antifibrotic Potential in Hepatic Fibrosis.....	48
5.3.3.1	Flaxseed Lignans and PPAR γ	49
5.3.3.2	Flaxseed Lignans and TGF- β	50
5.3.3.3	Flaxseed Lignans and ER Stress-induced Apoptosis.....	50
5.3.3.4	Flaxseed Lignans and Cholesterol.....	50
5.3.3.5	Flaxseed Lignans and Other Possible Mechanisms	51
6.	MATERIALS AND METHODS	53
6.1	Objective 1: Are TKIs and ENL full agonists or partial agonists of PPAR γ ? ..53	
6.1.1	Chemicals, Reagents, and Supplies	53
6.1.2	PPAR γ Competitive Binding assay	53

6.1.3	PPAR γ Transactivation assay.....	54
6.1.4	Adipogenic and Glucose uptake assays.....	55
6.2	Objective 2: To determine whether certain TKIs (ibrutinib, gefitinib, and dabrafenib) and ENL can suppress HSC activation through modulation of PPARγ or other pathways in activated human HSCs, LX-2 cells.	56
6.2.1	HSC Culture.....	56
6.2.2	MTT assays for TKIs in TGF- β 1-stimulated LX-2 cells	57
6.2.3	Calcein-AM assay for ENL in TGF- β 1-stimulated LX-2 cells.....	57
6.2.4	Scratch wound healing assay	58
6.2.5	Apoptosis assay.....	58
6.2.6	Oxidative stress assay	59
6.2.7	Real-time PCR.....	59
6.2.8	ELISA.....	61
6.2.9	Western blot	62
6.3	Objective 3: Whether flaxseed lignans exhibit antifibrotic effects in high-cholesterol diet-induced fatty liver rats.	63
6.3.1	Comparative oral PK study of purified SDG and SDG-enriched polymer complex in female Wistar rats	63
6.3.2	Comparative efficacy study of purified SDG and SDG-enriched polymer complex in female hypercholesterolemic Wistar rats.....	63
6.3.3	Real-time PCR.....	65
6.3.4	Western blot	66
6.4	Statistical analysis	66
7.	RESULTS	68
7.1	Objective 1: To determine whether TKIs and ENL are either full agonists or partial agonists of PPARγ	68
7.1.1	PPAR γ competitive binding assay	68
7.1.2	PPAR γ transactivation assay	71
7.1.3	Adipogenesis and Glucose uptake assays.....	73
7.2	Objective 2: To determine whether ENL and certain TKIs (ibrutinib, gefitinib, and dabrafenib) can suppress HSC activation in TGF-β1-activated human HSCs (LX-2 cells).....	76

7.2.1	MTT and/or Calcein-AM assays for TKIs and ENL in TGF-β1-stimulated LX-2 cells	76
7.2.1.1	MTT assay for TKIs in TGF-β1-stimulated LX-2 cells.....	76
7.2.1.2	MTT and Calcein-AM assays for ENL in TGF-β1-stimulated LX-2 cells	78
7.2.2	Several factors impact gene expression of fibrotic biomarkers and PPARγ in non-TGF-β1 and TGF-β1-activated LX-2 cells.....	80
7.2.2.1	The concentration of TGF-β1 and the duration of cell-seeding and stimulation impacts the expression of fibrotic biomarkers.....	80
7.2.2.2	mRNA expression changes of the fibrotic biomarkers in TGF-β1-activated LX-2 cells.....	82
7.2.2.3	The time of administration of TKIs after stimulation impacts the expression of fibrotic biomarkers.....	84
7.2.3	Changes in fibrotic biomarkers in TGF-β1-stimulated LX-2 cells.....	86
7.2.4	Scratch wound healing assay for gefitinib and ENL in TGF-β1-stimulated LX-2 cells	96
7.2.5	Possible mechanisms of the attenuation of activated LX-2 cells by gefitinib and ENL.....	99
7.2.5.1	PPARγ-related changes by gefitinib and ENL in LX-2 cells	99
7.2.5.1.1	PPARG mRNA expression changes by ibrutinib in Non-TGF-β1-stimulated LX-2 cells	99
7.2.5.1.2	PPARG and PKM2 mRNA expression changes by TKIs in TGF-β1-stimulated LX-2 cells	101
7.2.5.1.3	Protein changes of PPARγ by gefitinib and ENL in TGF-β1-stimulated LX-2 cells	103
7.2.5.2	Preliminary study on gene expression of Wnt pathway	108
7.2.5.3	Oxidative stress assay for gefitinib and ENL in TGF-β1-activated LX-2 cells	110
7.2.5.3.1	Mitochondrial ROS production changes by gefitinib and ENL in TGF-β1-activated LX-2 cells.....	110
7.2.5.3.2	Nrf2 protein changes by gefitinib and ENL in TGF-β1-activated LX-2 cells	112
7.2.5.4	Apoptosis-related assays for gefitinib and ENL in TGF-β1-stimulated LX-2 cells	114

7.2.5.4.1	Caspase-3/7 apoptosis induction by gefitinib and ENL in TGF- β 1-activated LX-2 cells.....	114
7.2.5.4.2	ER-stress related pathway	116
7.3	Objective 3: Whether flaxseed lignans exhibit antifibrotic effects in fatty livers of high cholesterol diet-fed rats.	121
7.3.1	Comparative oral PK study of purified SDG and SDG-enriched polymer complex in female Wistar rats	121
7.3.2	Comparative efficacy of purified SDG and SDG-enriched polymer complex in female hypercholesterolemic Wistar rats.....	124
7.3.3	The gene and protein expression changes in the rat liver from SDG treated group	131
8.	DISCUSSION	134
8.1	PPAR γ agonism of the tested compounds.....	134
8.2	The antifibrotic potential and possible mechanisms of PPAR γ -related TKIs with ENL.....	138
8.3	Other possible antifibrotic mechanisms of TKIs with ENL.....	147
8.4	The antifibrotic potential of SDG in hypercholesterolemia rats	148
9.	SUMMARY AND CONCLUSIONS	152
10.	FUTURE WORK.....	153
	REFERENCES.....	156
	APPENDIX A.....	189
	APPENDIX B	192

LIST OF FIGURES

- Figure 5.1** The cellular mechanisms of hepatic fibrogenesis and resolution of fibrosis in the liver. Chronic hepatic insults stimulate inflammatory responses and profibrotic cytokine/chemokine secretion which subsequently induce the activation of quiescent hepatic stellate cells (HSCs), contributing to the fibrogenesis in the liver. In contrast, with the removal of stimuli, the production of existing extracellular matrix (ECM) degrading enzymes and deactivation factors for myofibroblasts, the existing ECM, and the activated HSCs can be eliminated to resolve the fibrosis within the liver. Adapted from Pellicoro et al (Permission license number: 4831430631176)³⁷.9
- Figure 5.2** The 3D configuration model of PPAR γ ligand binding domain (LBD) with superposition of known agonists. Full (orange) and partial (cyan) agonists are binding to different sites with PPAR γ . Helix 12 (H12, yellow), β -sheet binding pocket (blue), and Ω -loop (red) are shown with all the other regions (grey). The 3D model was made by Waku (Permission license number: 4831421286787)¹⁴⁸. 18
- Figure 5.3** The main transduction pathways regulated by the epidermal growth factor receptors (EGFR) family members—EGFR/HER1, HER2, HER3, and HER4. Many pathways are involved in the modulation of EGFR, playing roles in many cellular processes such as cell proliferation and nuclear transcription. Adapted from Fornaro et al (Permission license number: 4831430901474)³⁰⁵.38
- Figure 5.4** Metabolic pathway of flaxseed lignan, secoisolariciresinol diglucoside (SDG) in the GI tract. SDG undergoes glycolysis and fermentation to yield its aglycone form secoisolariciresinol (SECO). SECO is then converted into enterodiol (END) by diverse bacteria, most of which is metabolized to ENL by serial reactions³⁷¹. ENL, as well as END and SECO, undergo conjugation to yield its glucuronidated or sulfated forms (not shown in the picture).47
- Figure 7.1** PPAR γ competitive binding assay results for ibrutinib (a), dabrafenib (b), gefitinib (c), enterolactone (ENL), (d), rosiglitazone (e), and FMOC-L-Leucine (FMOC, f), performed as binding percentage using the PolarScreenTM PPAR γ -Competitor Assay Kit. a: ibrutinib has a relative IC₅₀ value over 50 μ M calculated from the concentration range from 0.5 nM to 50,000 nM (could not go higher due to the solubility limitation); b: the relative IC₅₀ value of dabrafenib is not available by the plot (no binding trend from the experimental data); c: gefitinib has a relative

IC₅₀ value of 62 μM; d: ENL has a relative IC₅₀ value of 117μM; e: rosiglitazone has a relative IC₅₀ value of 111.3 nM as a known agonist of PPARγ; f: FMOC has a relative IC₅₀ value of 2 μM. The data were analyzed by a nonlinear regression model of GraphPad Prism v6.0. The data are reported as mean ± SD of six replicates, performed on three occasions.....70

Figure 7.2 The adipogenesis assay was performed to detect PPARγ-mediated biological functions of the compounds in mouse 3T3-L1 adipocytes. The adipogenic activities of different compounds at different concentrations (1 μM, 20 μM, and 50 μM) were detected by absorbance measurement at 490 nm after extraction of the Oil Red staining, using the same concentrations of rosiglitazone as a full agonist positive control and FMOC-L-Leucine (FMOC) as a partial agonist control. The relative lipid accumulation to the vehicle control was plotted. Vehicle control (grey) used DMSO at a final concentration of 1%. Data were reported as mean + SD of six replicates; *P<0.05 when compared with vehicle control using two-way ANOVA followed by Dunnett test.....74

Figure 7.3 The glucose uptake assay was performed to detect PPARγ-mediated biological functions of the compounds in mouse 3T3-L1 adipocytes. The glucose transport activities of different compounds at different concentrations (1 μM, 20 μM, and 50 μM) for 3 days are shown by reading the fluorescence of 2-NBDG at (Ex/Em =485/528 nm) using same concentrations of rosiglitazone as a full agonist positive control and FMOC-L-Leucine (FMOC) as a partial agonist control. Vehicle control (grey) used DMSO at a final concentration of 1%. Data are shown as % of glucose uptake stimulation with vehicle control which was considered 100% insulin stimulation. Data are reported as mean + SD of six replicates; *P<0.05 compared with vehicle control using two-way ANOVA followed by Dunnett test.....75

Figure 7.4 The effects of ibrutinib, gefitinib, and dabrafenib on cell viability in TGF-β1-activated LX-2 cells as determined by MTT assay. Cells were treated with compounds for 72 hours prior to the addition of MTT for cytotoxicity determination. The IC₅₀ values for the test compounds were calculated from the plots by a nonlinear regression model using GraphPad Prism v6.0. a) ibrutinib in nonTGF-β1-stimulated LX-2 cells, the IC₅₀ value calculated from this plot was 26 μM; plot b) ibrutinib in TGF-β1-stimulated LX-2 cells, the IC₅₀ value calculated from this plot was 5 μM; c) gefitinib in TGF-β1-stimulated LX-2 cells, the IC₅₀

value of gefitinib in activated LX-2 cells was 13 μ M; d) dabrafenib in TGF- β 1-stimulated LX-2 cells, the IC₅₀ value of dabrafenib in activated LX-2 cells was over 100 μ M. The data were analyzed by a nonlinear regression model of GraphPad Prism v6.0. The data are reported as mean \pm SD of six replicates (done on two occasions).....77

Figure 7.5 Cell viability of TGF- β 1-activated LX-2 cells following enterolactone (ENL) and FMOC-L-Leucine (FMOC, PPAR γ partial agonist control) treatment determined by MTT and Calcein-AM assays. A) ENL (concentrations from 2 nM to 50 μ M); B) FMOC (concentrations from 1 nM to 50 μ M). Cells were treated with the tested compounds for 72 hours prior to the addition of MTT or Calcein-AM for cytotoxicity determination. The data is reported as relative cell viability comparing with the 1% DMSO treated TGF- β 1-activated LX-2 cells, described as mean + SD of four replicates, done on two occasions. * for MTT assay and # for Calcein-AM assay P<0.05 compared with each assay's vehicle control using one-way ANOVA followed by Tukey test.79

Figure 7.6 The mRNA expression of COL1A1 (A) and ACTA2 (B) in TGF- β 1-stimulated LX-2 cells. The final concentrations of TGF- β 1 were 5, 2.5, 1, and 0 ng/mL. 24 hours (12h/24h-24h) or 28 hours (12h/24h-28h) after seeding cells to 96-well plate, the cells were stimulated with TGF- β 1 for 12h and 24 h. The mRNA expression of COL1A1 and ACTA2 were measured by qPCR, using β -actin as reference gene for the calculation. The data are reported as mean + SD (N=3). * Induction or reduction when the relative mRNA expression beyond 2 or below 0.5, respectively.81

Figure 7.7 The mRNA expression changes of fibrotic biomarkers in nonTGF- β and TGF- β 1-activated LX-2 cells. The cells were stimulated with TGF- β 1 at a final concentration of 2.5 ng/mL for 24 hours. The mRNA expressions of ACTA2, COL1A1, MMP2, TGFB1, and TIMP1 were detected by qPCR, using β -actin as reference gene for the calculation. The data are reported as mean + SD (N=3, performed on three occasions). *Induction or repression when the relative mRNA expression beyond 2 or below 0.5, respectively.83

Figure 7.8 The mRNA expression of COL1A1 (A) and ACTA2 (B) after treatment with ibrutinib at different time points in TGF- β 1-stimulated LX-2 cells. 2.5 ng/mL of TGF- β 1 was applied to Non-TGF- β -stimulated LX-2 cells 24 hours after plating. Ibrutinib was applied at the same time with TGF- β 1, 6 and 12 hours after TGF- β 1

stimulation. The mRNA expression of COL1A1 and ACTA2 was measured by qPCR, using β -actin as reference gene for the calculation. The data are reported as mean + SD (N=3, performed on three occasions). *Induction or repression when the relative mRNA expression was beyond 2 or below 0.5, respectively.85

Figure 7.9 The relative mRNA expression of hepatic fibrotic biomarkers in TGF- β 1-stimulated LX-2 cells after treatment with ibrutinib (0.5, 1, 5 μ M) or gefitinib (1, 2, 10 μ M) for 24 hours (6 hours of stimulation with 18 hours of treatment with different concentrations of compounds), using β -actin as reference gene and the vehicle-treated activated LX-2 cells as control for the calculation. Rosiglitazone (1 μ M) was used as positive control. Data are presented as mean + SD of triplicates on three occasions. * significant induction or repression when the relative mRNA expression beyond 2 or below 0.5, respectively.87

Figure 7.10 Protein expression changes of Pro-collagen I α 1 and MMP9 in TGF- β 1-activated LX-2 cells. The LX-2 cells were treated with or without ibrutinib, dabrafenib, and gefitinib for 24, 48, and 72 hours, using the vehicle-treated TGF- β 1-activated LX-2 as normalization reference and rosiglitazone at 1 μ M as a potential positive control. Pro-collagen I α 1 was detected in cell extract (A) and supernatants (B) at 24 h, 48h (not in cell extracts), and 72 h, while MMP9 was detected in the supernatants of the cell culture at 24 h, 48 h, and 72 h (C). Evaluations were performed in duplicate using TGF- β 1-activated LX-2 cells at the same time point as reference. (Rosi: rosiglitazone, at concentration of 1 μ M; ibrutinib, at concentrations of 0.5, 1, 5 μ M; dabrafenib, at concentrations of 1, 2, 5 μ M; gefitinib, at concentrations of 1, 2, 5 μ M). The data were reported as mean + SD of duplicates on two occasions. #, *, and \blacktriangle means $P < 0.05$, compared with vehicle-treated TGF- β 1-stimulated LX-2 cells at the same time point using one-way ANOVA followed by Tukey test.90

Figure 7.11 The relative mRNA expression of fibrotic biomarkers (collagen I α 1 (COL1A1), MMP2, and TIMP1) in TGF- β 1 stimulated LX-2 cells after treatment with gefitinib (1 and 10 μ M), enterolactone (ENL, 1 and 50 μ M), and the combination of gefitinib (G, 1 and 10 μ M) and ENL (E, 1 and 50 μ M) for 24 hours (6 hours of stimulation with 18 hours of treatment with different concentrations of compounds), using β -actin as reference gene and TGF- β 1-activated LX-2 cells as control for the calculation. Data are presented as mean + SD of triplicates on three occasions.

*Induction or reduction when the relative mRNA expression beyond 2 or below 0.5, respectively.92

Figure 7.12 Protein expression changes of pro-collagen I α 1 in TGF- β 1-stimulated LX-2 cells after treatment with gefitinib and/or enterolactone (ENL). LX-2 cells were stimulated for 6 hours before treatment with or without gefitinib and/or ENL at different concentrations for 24 and 48h, gefitinib at concentrations of 1, 3, and 10 μ M; ENL at concentrations of 1, 10, and 50 μ M; and combination of gefitinib (1 and 10 μ M) and ENL (1, 10, and 50 μ M). Pro-collagen I α 1 was measured in cell extracts (A) and supernatants (B), using TGF- β 1-stimulated LX-2 cells at the same time point as normalization references. The data were reported as mean + SD of duplicates on three occasions. # * means P<0.05, compared with the vehicle-treated TGF- β 1-stimulated LX-2 cells at the same time point using two-way ANOVA followed by Tukey test.94

Figure 7.13 Protein expression of α -SMA in TGF- β 1-activated LX-2 cells after treatment with gefitinib and/or enterolactone (ENL). The LX-2 cells were stimulated for 6 hours before treatment with or without gefitinib and/or ENL at different concentrations for 18 and 42h. A and B) TGF- β 1-activated LX-2 cells were treated with gefitinib of 1 and 10 μ M (lanes 1 and 2) or ENL of 1 and 50 μ M (lanes 3 and 4); C and D) The TGF- β 1-activated LX-2 cells were treated with the combination of gefitinib (1 and 10 μ M) and ENL (1 and 50 μ M) (lanes 5, 6, 7, and 8), using vehicle-treated TGF- β 1-activated LX-2 cells as control (lane 9) and total protein stained by SYPRO Ruby blot stain reagent (A' and B' for A and B, respectively, protein ranges from 10 to 250 kDa according to BioRad Precision Plus Protein Dual Color Standards, where the dual-color bands were stained as the red in panel A' and B') as normalizing reference. The relative expression of α -SMA for each group was normalized to the TGF- β 1-activated LX-2 group, located at the red arrow on the blot. The data were reported as mean + SD of duplicates on two occasions. * and # mean P<0.05, compared with the vehicle-treated TGF- β 1-stimulated LX-2 cells at the same time point using one-way ANOVA followed by Dunnett test.....95

Figure 7.14 The wound healing assay endpoint images for gefitinib (G) and/or enterolactone (ENL or E) for 24 hours, using NonTGF- β -stimulated LX-2 and TGF- β 1-activated LX-2 as controls. LX-2 cells were seeded at appropriate density into 6-well plates for overnight attachment. A scraped gap was made by using a 10 μ L clear

micropipette tip in each well right before the cells were stimulated with TGF- β 1 at 2.5 ng/mL 6 hours before treatment with gefitinib and/or ENL at different concentrations for 18 hours. The cell migration was observed and imaged by Olympus microscope, original magnification 400 \times . The gaps were indicated by two white lines, the inhibition on cell migration was revealed by the number of cells migrated to the gap after treatment, compared with the pre-treatment with both the nonTGF- β -stimulated and TGF- β -stimulated LX-2 cells after 24 hours.....98

Figure 7.15 The relative PPAR γ mRNA expression in nonTGF- β 1-stimulated LX-2 cells after treatment with rosiglitazone and ibrutinib for 12h, 24h, and 72h (compared with the vehicle control group), using β -actin as reference gene for the calculation. Data are presented as mean + SD of triplicates on three occasions. It is considered significant induction or repression when the relative mRNA expression is beyond 2 or below 0.5, respectively.100

Figure 7.16 The relative PPAR γ and PKM2 mRNA expression in TGF- β 1-stimulated LX-2 cells with treatment of ibrutinib at 1 and 5 μ M (A) and gefitinib at 1, 3, and 10 μ M (B) for 18 hours), using β -actin as reference gene and TGF- β 1-activated LX-2 cells as control for the calculation while rosiglitazone at 1 μ M was used as a positive control. Data were presented as mean + SD of triplicates on three occasions. *Induction or reduction when the relative mRNA expression beyond 2 or below 0.5, respectively.102

Figure 7.17 Preliminary study on the protein expression changes of PPAR γ and PKM2 as measured by western blot. The activated LX-2 cells were treated with different concentrations of ibrutinib for 42 hours, using rosiglitazone as positive control and non-TGF- β 1-stimulated LX-2 and TGF- β 1-activated LX-2 as negative controls. The relative expression of both PPAR γ (open), PKM2 (grey), and β -actin (dark) was calculated, using β -Actin as reference protein, and relative expression for each group was normalized to the PPAR γ or PKM2 protein levels of activated LX-2 group.104

Figure 7.18 PPAR γ protein expression changes as measured by western blot in LX-2 cells stimulated with TGF- β 1 for 6 hours followed by treatment with gefitinib or enterolactone (ENL) or their combination for another 18 hours. A and B: The TGF- β 1-activated LX-2 cells were treated with gefitinib (1, 3, and 10 μ M) or ENL (1, 10, 100 μ M); C and D: The TGF- β 1-activated LX-2 cells were treated with the combination of gefitinib (1 and 10 μ M) and ENL (1, 10, and 100 μ M), using

vehicle-treated TGF- β 1-activated LX-2 cells as control and total protein stained by SYPRO Ruby blot stain reagent (A' and C' for A and C, respectively, protein ranges from 10 to 250 kDa according to BioRad Precision Plus Protein Dual Color Standards, where the dual-color bands were stained as the red in panel A' and B') as normalizing reference. The relative expression of PPAR γ for each group was normalized to the TGF- β 1-activated LX-2 group, located at the red arrow on the blot. The data were reported as mean + SD of duplicates on two occasions. * means P<0.05, compared with the vehicle-treated TGF- β 1-stimulated LX-2 cells using one-way ANOVA followed by Dunnett test..... 106

Figure 7.19 PPAR γ protein expression changes as measured by western blot in LX-2 cells stimulated with TGF- β 1 for 6 hours followed by treatment gefitinib or ENL or their combination for another 42 hours. The TGF- β 1-activated LX-2 cells were treated with gefitinib (1 and 10 μ M), ENL (1 and 50 μ M), or the combination of gefitinib (1 and 10 μ M) and ENL (1 and 50 μ M), using vehicle-treated TGF- β -activated LX-2 cells as control and total protein stained by SYPRO Ruby blot stain reagent (A', protein ranges from 10 to 250 kDa according to ThermoFisher PageRuler™ Plus Prestained Protein Ladder) as normalizing reference. The relative expression of PPAR γ for each group was normalized to the TGF- β 1-activated LX-2 group, located at the red arrow on the blot. The data were reported as mean + SD of duplicates on two occasions. * means P<0.05, compared with the vehicle-treated TGF- β 1-stimulated LX-2 cells and # means P<0.05, compared with the treatment of gefitinib at 1 μ M using one-way ANOVA followed by Tukey test. 107

Figure 7.20 The relative mRNA expression of PPARG, COL1A1, and β -catenin/Wnt related targets in TGF- β 1-stimulated LX-2 cells with the treatment of FMOC-L-Leucine (FMOC) and enterolactone (ENL), using β -actin as reference gene and TGF- β 1-activated LX-2 cells as control for the calculation. Data are presented as mean + SD of triplicates on three occasions. *Induction or repression when the relative mRNA expression was beyond 2 or below 0.5, respectively. 109

Figure 7.21 Mitochondrial superoxide production in TGF- β 1-stimulated LX-2 cells treated with gefitinib and enterolactone (ENL). LX-2 cells were stimulated with TGF- β 1 for 6 hours before treatment with gefitinib or ENL or their combination for another 0.5, 1, and 3 hours. The TGF- β -activated LX-2 cells were treated with gefitinib (1 and 10 μ M), ENL (5, 50 μ M), and the combination of gefitinib (1 and 10 μ M) and ENL (1 and 50 μ M), using non-TGF- β stimulated LX-2 cells as a negative control.

Data are presented as mean + SD of triplicates on three occasions. * # means $P < 0.05$, comparing with the vehicle-treated TGF- β 1-stimulated LX-2 cells at the same time point, using two-way ANOVA followed by Tukey test. 111

Figure 7.22 The expression changes of Nrf2 protein were measured by western blot. LX-2 cells were stimulated with TGF- β 1 for 6 hours before treatment with gefitinib, enterolactone (ENL), or their combination for another 0.5h (A) and 1h (C). The TGF- β 1-activated LX-2 cells were treated with gefitinib (1, and 10 μ M), ENL (1, and 50 μ M), or with the combination of gefitinib (1 and 10 μ M) and ENL (1 and 50 μ M), using vehicle-treated TGF- β 1-activated LX-2 cells as control and total protein stained by SYPRO Ruby blot stain reagent (A' and C' for A and C, respectively, protein ranges from 10 to 250 kDa according to ThermoFisher PageRuler™ Plus Prestained Protein Ladder) as normalizing reference. The relative expression of Nrf2 for each group was normalized to the TGF- β 1-activated LX-2 group (B and D), located at the red arrow on the blot. The data were reported as mean + SD of duplicates on two occasions. * means $P < 0.05$, compared with the vehicle-treated TGF- β 1-stimulated LX-2 cells and # means $P < 0.05$, compared with the treatment of gefitinib at 10 μ M using one-way ANOVA followed by Tukey test. 113

Figure 7.23 Caspase-3/7 apoptosis assay results of gefitinib and/or enterolactone (ENL) in TGF- β 1-stimulated LX-2 cells. LX-2 cells were seeded into 96-well plate at appropriate density for overnight attachment. The cells were stimulated with TGF- β 1 at 2.5 ng/mL for 6 hours before treatment with gefitinib (1, 3, and 10 μ M), ENL (1, 10, and 50 μ M), and the combination of gefitinib (1 and 10 μ M) and ENL (1, 10, and 50 μ M) for 6 and 12 hours. Caspase-3/7 caused apoptosis kit was used to detect the apoptosis following the kit manual. The relative fluorescence was calculated to reflect the apoptosis induced by the treatments, expressed as % of the vehicle-treated TGF- β 1-stimulated LX-2 cells as reference. Data were shown as mean + SD of duplicates on two occasions. * and # mean $P < 0.05$ when compared with the vehicle-treated control group at 24 and 48 h, respectively, while \blacktriangle and \triangle mean $P < 0.05$ when compared with the treatment of gefitinib at the same concentration at 24 and 48 h, respectively, using one-way ANOVA followed by Tukey test. 115

Figure 7.24 The relative mRNA expression of ER-stress related markers, including CHOP, ATF4, and ATF6 in TGF- β 1-stimulated LX-2 cells with treatment of gefitinib (1, 3, and 10 μ M), ENL (10, 50, and 100 μ M), and the combination of gefitinib (1 and 10

μM) and ENL (1, 10, 50, and 100 μM), using β -actin as reference gene and TGF- β 1-activated LX-2 cells as control for the calculation (Data were presented as mean + SD of three replicates on three occasions). A) the TGF- β 1 activated LX-2 cells were treated with gefitinib (1, 3, 10 μM) or ENL (10, 50, 100 μM) alone for 24 hours (6 hours of stimulation with 18 hours of treatment with different concentrations of compounds); B) the activated LX-2 cells were treated with the combination of gefitinib (1 or 10 μM) and ENL (1, 10, 50, or 100 μM) for 24 hours. Data were shown as mean + SD of triplicates on three occasions. *Induction or repression when the relative mRNA expression was beyond 2 or below 0.5, respectively. 117

Figure 7.25 ATF4 protein expression changes were measured by western blot in gefitinib and/or enterolactone (ENL) treated LX-2 cells. LX-2 cells were stimulated with TGF- β 1 for 6 hours before the treatment for 42 hours (consider this as 48h treatment for results interpretation). The TGF- β 1-activated LX-2 cells were treated with gefitinib (1 and 10 μM), ENL (1 and 50 μM), or with the combination of gefitinib (1 and 10 μM) and ENL (1 and 50 μM), using vehicle-treated group as negative control and using total protein stained by SYPRO Ruby blot stain reagent (A', protein ranges from 10 to 250 kDa according to ThermoFisher PageRuler™ Plus Prestained Protein Ladder) as normalizing reference. The relative expression of ATF4 for each group was normalized to the TGF- β 1-activated LX-2 group (B), located at the red arrow on the blot. The data were reported as mean + SD of duplicates on two occasions. * means $P < 0.05$, compared with the vehicle-treated TGF- β 1-stimulated LX-2 cells, and # means $P < 0.05$, compared with the treatment of gefitinib at 10 μM using one-way ANOVA followed by Tukey test. 119

Figure 7.26 The changes in CHOP protein expression were measured by western blot in LX-2 cells. LX-2 cells were stimulated with TGF- β 1 for 6 hours before the treatment with gefitinib, enterolactone (ENL), or their combination for 66 hours (with a total treatment time of 72 hours). The TGF- β 1-activated LX-2 cells were treated with gefitinib (1 and 10 μM), ENL (1, 10, 50 μM), or with the combination of gefitinib (1 and 10 μM) and ENL (1 and 50 μM), using vehicle-treated group as negative control and total protein stained by SYPRO Ruby blot stain reagent (A', protein ranges from 10 to 250 kDa according to ThermoFisher PageRuler™ Plus Prestained Protein Ladder) as normalizing reference. The relative expression of CHOP for each group was normalized to the vehicle-treated TGF- β 1-activated LX-2 group (B),

located at the red arrow on the blot. The data were reported as mean + SD of duplicates on two occasions. * means $P < 0.05$, compared with the vehicle-treated TGF- β 1-stimulated LX-2 cells, and # means $P < 0.05$, compared with the treatment of gefitinib at 10 μ M using one-way ANOVA followed by Tukey test. 120

Figure 7.27 Plasma concentration versus time profile for total enterolactone (ENL) and enterodiol (END) in single oral dose pharmacokinetic study in female Wistar rats. Purified secoisolariciresinol diglucoside (SDG) or SDG polymer were administered orally at an equivalent dosage of 12 mg/kg into rats, and jugular blood samples were collected at 0, 15, 30 minutes, and 1, 1.5, 2, 3, 4, 8, 12, 16, 20, 24, 32, 40, and 48 hours from two subgroups of animals. The plasma concentrations of free and total secoisolariciresinol (SECO), END, and ENL were detected by appropriate LC-MS/MS methods. Data were shown as mean + SD of each group, N=5 for purified SDG and N=7 for SDG polymer..... 123

Figure 7.28 The relative final body weight, weight gain, liver weight, and liver body weight ratio of the purified secoisolariciresinol diglucoside (SDG) or SDG polymer treated female Wistar rats. The final body weight (open), weight gain (light grey), liver weight (dark grey), and liver to body weight ratio (black) were normalized to the standard diet group. Data were reported as mean + SD, N=10 (N=5 for the reference group). *, #, Δ , and \triangle $P < 0.05$ suggesting a significant difference from the normal diet group using one-way ANOVA followed by Tukey test. 125

Figure 7.29 Liver histology with hematoxylin and eosin (H&E) staining of female Wistar rats fed 1% high cholesterol diet for 30 days and treated with oral doses of vehicle, purified secoisolariciresinol diglucoside (SDG), or SDG polymer with equivalent SDG dose of 6 mg/kg or fed a standard diet for 30 days and treated with vehicle for 23 days. Liver samples were collected, and H&E stained after 23 days of vehicle control with 1% high cholesterol diet (A), treatment with purified SDG (B) or SDG polymer (C), and the standard diet control group (NC). Representative images are presented at 40X. 127

Figure 7.30 The relative levels of total cholesterol (TC), triglyceride (TG), high-density lipoprotein cholesterol (HDL-C), and low-density lipoprotein (LDL) in purified secoisolariciresinol diglucoside (SDG) or SDG polymer treated female Wistar rats. All four parameters are the measured levels compared to the normal diet group, the high-cholesterol diet group without lignan treatment applied as control (open), high-

cholesterol diet with purified SDG labeled as purified SDG (grey), while high-cholesterol diet with SDG polymer labeled as SDG polymer (black). Data were reported as mean + SEM (N=10 for the high cholesterol diet group, N=5 for the normal diet group), *P<0.05 indicates a significant difference between the groups indicated using two-way ANOVA followed by Tukey test..... 129

Figure 7.31 The AST/ALT ratio of 23-day purified secoisolariciresinol diglucoside (SDG) and SDG polymer treated female Wistar rats. The AST and ALT activities were detected and normalized to the standard diet group. Data were shown as mean + SEM (N=10 for fatty liver groups and N=5 for normal diet group). *indicates a significant difference (P <0.05) from the High-Cholesterol Diet group using one-way ANOVA followed by Dunnett test..... 130

Figure 7.32 The relative mRNA expression of hepatic fibrotic biomarkers (Acta2, Colla1, Mmp2, and Timp1) in the liver tissue of purified secoisolariciresinol diglucoside (SDG) and SDG polymer treated female hypercholesterolaemic Wistar rats. The 1% high cholesterol diet group was used as control and β -actin was used as reference gene for the calculation. Data are presented as mean + SD of triplicates. *Induction or repression when the relative mRNA expression was beyond 2 or below 0.5, respectively. 132

Figure 7.33 The relative expression of Collagen I in rat liver tissue after treatment with purified secoisolariciresinol diglucoside (SDG) in high cholesterol diet induced Wistar rats. The expression of Collagen I in pooled rat liver (A) and the relative expression for each group were normalized to the 1% high cholesterol diet group (B), using total protein stained by SYPRO Ruby blot stain reagent (A', protein ranges from 10 to 250 kDa according to BioRad Precision Plus Protein Dual Color Standards where the dual-color bands were stained dark in panel A') as normalizing reference. Data were shown as mean + SD of the relative expression of Collagen I protein (N=5 for the normal control group and N=10 for high cholesterol diet and SDG groups), located at the red arrow on the blot. * means P<0.05 when comparing with the high cholesterol diet group using one-way ANOVA followed by Tukey test..... 133

Figure 8.1 A schematic model of the possible mechanisms involved in the antifibrotic effects of the combination of gefitinib and enterolactone (ENL) related to PPAR γ , oxidative stress, and ER stress. With chronic liver insults, hepatic stellate cells (HSCs) would be activated possibly involving processes like oxidative stress and

ER stress. PPAR γ would play a central role in the potential antifibrotic effects of antifibrotic agents. Possible agonists may activate PPAR γ which in turn would transcriptionally activate fibrotic downstream factors, including Wnt pathways, antioxidant response, and ER stress-related pathways. These potential mechanisms may cause inhibition of cellular oxidative stress, cell proliferation, and migration as well as induction of apoptosis and antioxidant responses in the fibrotic HSCs. 146

Figure A 1. The expression of collagen I in rat liver tissue after treatment with purified secoisolariciresinol diglucoside (SDG) in high cholesterol diet induced Wistar rats. The expression of collagen I in the individual rat liver samples were run separately, using total protein stained by SYPRO Ruby blot stain reagent (A' and B', protein ranges from 10 to 250 kDa according to ThermoFisher PageRuler™ Plus Prestained Protein Ladder) as normalizing reference. The expression of Collagen I protein was detected for each individual rat, located at the red arrow on the blot. N=5 for the normal control group and N=10 for high cholesterol diet and SDG groups..... 189

Figure A 2. The relative protein expression of Mmp2 in rat liver samples after treatment with purified secoisolariciresinol diglucoside (SDG) in high cholesterol diet induced Wistar rats. The relative expressions of Mmp2 in individual rat liver samples (A) and mean of relative expression for each group was normalized to the 1% high cholesterol diet group (B), using total protein stained by SYPRO Ruby blot stain reagent (A' and B', protein ranges from 10 to 250 kDa according to ThermoFisher PageRuler™ Plus Prestained Protein Ladder) as normalizing reference. Data were shown as mean \pm SD of the relative expression of Mmp2 protein in panel B, located at the red arrow on the blot (N=5 for the normal control group and N=8 for high cholesterol diet and SDG groups). * indicates significantly ($P < 0.05$) different from the High cholesterol diet control, by one-way ANOVA followed by Tukey test. . 190

Figure A 3. The relative protein expression of Timp1 in rat liver samples after treated with purified secoisolariciresinol diglucoside (SDG) in high cholesterol diet supplied Wistar rats. The relative expressions of Timp1 in individual rat liver samples (A) and the mean relative expression for each group were normalized to the 1% high cholesterol diet group (B), using total protein stained by SYPRO Ruby blot stain reagent (A' and B', protein ranges from 10 to 250 kDa according to ThermoFisher PageRuler™ Plus Prestained Protein Ladder) as normalizing reference. Data were shown as mean \pm SD of the relative expression of Timp1 protein in panel B, located

at the red arrow on the blot (N=5 for the normal control group and N=10 for high cholesterol diet and SDG groups). * indicates significantly ($P < 0.05$) different from the High cholesterol diet control, by one-way ANOVA with Tukey test..... 191

LIST OF TABLES

Table 6.1 Primer sequences used for LX-2 cell samples in quantitative Polymerase Chain Reaction (qPCR)	60
Table 6.2 The criteria used for histological scoring of the degree of severity of non-alcoholic fatty liver disease.	64
Table 6.3 Primer sequences used for rat liver samples in quantitative Polymerase Chain Reaction (qPCR)	65
Table 7.1 The competitive binding affinities, represented as relative IC ₅₀ values, of the tyrosine kinase inhibitors and enterolactone (ENL).	69
Table 7.2 The relative luciferase ratio for ibrutinib, dabrafenib, gefitinib, and enterolactone (ENL) in PPAR γ -transfected HepG2 cells.	72
Table 7.3 The width of the wound for three fields per well after treatment with gefitinib and/or enterolactone (ENL) for 24h in TGF β 1-stimulated LX-2 cells.	97
Table 7.4 The area under curve (AUC) for enterolactone (ENL) and enterodiol (END) in 12 mg/kg secoisolariciresinol diglucoside (SDG) treated female Wistar rats after oral administration. AUC was determined for each individual rat in each subgroup and shown as mean \pm SD (N=5 for purified SDG and N=7 for SDG polymer). When P <0.05, it suggests a significant difference between the groups using two-way ANOVA followed by Tukey test.	122
Table 7.5 Hepatic histological scores for female Wistar rats fed a 1% cholesterol diet and treated with daily purified secoisolariciresinol diglucoside (SDG) or SDG-polymer for 23 days (Data shown as mean of each treatment group).....	126

LIST OF ABBREVIATIONS

Abl	Abelson murine leukemia viral oncogene homolog
Akt (PKB)	Protein Kinase B
ALT	Alanine Aminotransferase
AMPK	Adenosine Monophosphate-activated Protein Kinase
AST	Aspartate Aminotransferase
ATF	Activating Transcription Factor
ATP	Adenosine Triphosphate
BCR	Breakpoint Cluster Region
BDL	Bile Duct Ligation
CHOP	C/EBP-homologous Protein
CTGF	Connective Tissue Growth Factor
CYP450	Cytochrome P450
DMEM	Dulbecco's Modified Eagle Medium
DMN	Dimethyl Nitrosamine
DMSO	Dimethyl Sulfoxide
ECM	Extracellular Matrix
EGFR/ErbB	Epidermal Growth Factor Receptor
EMT	Epithelial-to-Mesenchymal Transition
END	Enterodiol
ENL	Enterolactone
ER	Endoplasmic Reticulum
ERK	Extracellular-signal Regulated Kinase
eIF2 α	Eukaryotic Initiation Factor 2 alpha

FBS	Fetal Bovine Serum
FGF	Fibroblast Growth Factor
FMOC/ FMOC-L-Leu	FMOC-L-Leucine, N-[(9H-fluoren-9-ylmethoxy)carbonyl]-L-leucine
GFAP	Glial Fibrillary Acidic Protein
GI	Gastrointestinal
GSH	Glutathione
HDL-C	High-Density Lipoprotein Cholesterol
H&E	Hematoxylin and Eosin
HER	Human Epidermal Growth Factor Receptor
HIF	Hypoxia-Inducible Factor 1
HSC	Hepatic Stellate Cell
ILs	Interleukins
INSIG-1	Insulin Induced Gene-1
InsR	Insulin Receptor
IRE1 α	Inositol-Requiring Protein-1 alpha
JAK	Janus Tyrosine Kinases
JNK	Jun N-Terminal Kinase
LBD	Ligand Binding Domain
LDL-C	Low-Density Lipoprotein Cholesterol
LDLR	Low-Density Lipoprotein Receptor
LPS	lipopolysaccharides
LX	Lieming Xu (cells)
MAPK	Mitogen-Activated Protein Kinase

MMP	Matrix Metalloproteinase
mTOR	The Mammalian Target of Rapamycin
NF- κ B	Nuclear Factor-kappa B
Nrf	Nuclear Erythroid 2-Related Factor
PBS	Phosphate Buffered Saline
PCR	Polymerase Chain Reaction
PDGF	Platelet-Derived Growth Factor
PERK	Protein Kinase RNA-like ER Kinase
PI3K	Phosphoinositide 3'-kinase
PK	Pharmacokinetics
PKM	Pyruvate Kinase Isozyme M
PPAR	Peroxisome Proliferator-Activated Receptor
PPRE	Peroxisome Proliferator Response Element
ROS	Reactive Oxygen Species
RTK	Receptor Tyrosine Kinase
RXR	Retinoid X Receptor
SDG	Secoisolariciresinol Diglucoside
SECO	Secoisolariciresinol
SHBG	Sex Hormone Binding Globulin
SOD	Superoxide Dismutase
SREBP-1	Sterol Regulatory Element-Binding Protein 1
STAT	Signal Transducer and Activator of Transcription
TAM	Tyro3, Axl, and Mer Receptors
TGF- β	Transforming Growth Factor-beta

TIMP	Tissue Inhibitor of Metalloproteinase
TK	Tyrosine Kinase
TKI	Tyrosine Kinase Inhibitor
TNF- α	Tumor Necrosis Factor alpha
TRAIL	Tumor Necrosis Factor-Related Apoptosis-Inducing Ligand
TZD	Thiazolidinedione
UGT	Uridine 5'-diphospho-glucuronosyltransferases
UPR	Unfolded Protein Response
VEGF	Vascular Endothelial Growth Factor
VLDL-C	Very Low-Density Lipoprotein Cholesterol
α -SMA	Alpha-Smooth Muscle Actin

1. INTRODUCTION

Hepatic fibrosis is a worldwide health issue with high risk of complications such as portal hypertension, liver failure, and carcinoma¹. Hepatic fibrosis is defined as a wound-healing response following continuous liver injury and is associated with inflammatory and oxidative stress responses and excessive accumulation of ECM proteins. A variety of liver diseases may cause fibrogenesis, which is characterized as fibrosis or fibrotic scars at the sites of damaged hepatocytes. These diseases include inflammatory conditions, alcohol-induced or non-alcohol-induced liver injuries, and cancer that ultimately result in the development of fibrotic lesions². Despite significant efforts made in the area of antifibrotic therapy in the past decades, specific antifibrotic drugs for the liver are still elusive because of the lack of both efficient and safe drugs on the market, especially for the late stage of liver fibrosis, i.e., cirrhosis²⁻⁴. Increasing evidence supports a view that fibrosis may be reversible, and the degree and recovery of fibrosis depend on the type and duration of the liver injury⁵. Therefore, reliable diagnosis and treatment methods for hepatic fibrosis at an early stage of liver disease are critical to avoid further hepatic health risks⁶.

According to the pathology of liver fibrosis, the resolution of fibrogenesis is a multi-cellular and multi-target process^{7,8}. Multi-target drug families such as the tyrosine kinase inhibitors (TKIs), which are primarily marketed for cancer therapy, are reported to have antifibrotic effects. Literature evidence has demonstrated the ability of some TKI drugs to favorably modulate renal fibrosis, pulmonary fibrosis, and tumour fibrosis⁹⁻¹¹. However, the mechanisms of TKIs' antifibrotic action in the fibrotic pathway are not fully understood. In the literature, PPAR γ is suggested to play a role in the activation of fibroblasts and the fibrogenesis process¹². Computational docking model data suggested a list of TKIs exhibit similar binding affinity to PPAR γ as its known full agonist, rosiglitazone, indicating that TKIs might cause cellular responses *via* PPAR γ agonism¹³. However, an obvious issue of TKI drugs is their toxicity when used in anti-cancer treatments. The adverse effects caused by TKI drugs are significant at their common dose¹⁴.

Natural products and herbal medicines have demonstrated antifibrotic effects in many types of systemic scleroses such as lung fibrosis and liver fibrosis^{15,16}. Over half of the current therapeutic drugs for cancer and liver diseases on the market are natural products or extracts from natural products¹⁷. The use of natural products to prevent liver lesions has been confirmed for many different compounds¹⁸. Among those natural products, lignans have shown anti-inflammatory effects, induction of PPAR γ expression, amelioration of oxidative

stress, and enhanced endoplasmic reticulum (ER) stress response – factors that have key roles in liver fibrosis¹⁹⁻²². Attenuation of oxidative stress relates with PPAR γ activation reduced hepatic fibrosis in rats, and ER stress-related pathways contribute to the hepatic stellate cell (HSC) activation in liver fibrosis^{23, 24}. Both oxidative stress and ER stress are believed to be involved in the pathology of liver fibrosis and there might be a close linkage between the two²⁵. Moreover, the ER stress-induced apoptosis might be an important way to deplete the key player of fibrogenesis, activated HSCs²⁶. Flaxseed lignans are also reported to have long-term safety²⁷. Though the TKI drugs have been shown to have an impact on fibrosis, the effects are neither guaranteed nor always safe because of unexpected adverse effects¹⁴. A possible way to resolve the troublesome toxicity of TKIs is to reduce the dosage of these drugs when used in combination with safer compounds if they may work *via* certain similar pathways. Natural products receive increasing interest for their safety and their potential ability to reduce the dose levels of pharmaceutical agents and thereby decrease the risk of adverse effects while maintaining favorable therapeutic outcomes. The combination of flaxseed lignans with the TKIs for liver fibrosis may result in an enhancement of the TKI effect, which may be mediated through modulation of PPAR γ expression and function, oxidative stress, and/or the ER stress response.

This dissertation research aimed to confirm the antifibrotic effects of the combination of the bioactive mammalian lignan, enterolactone (ENL), and selected TKI drugs, and to explore possible molecular targets of the combination using models of liver fibrosis. A human hepatic stellate cell line, LX-2 cells, was used as *in vitro* hepatic fibrosis model, and transforming growth factor-beta 1 (TGF- β 1) was applied to stimulate LX-2 cells. ENL was used as a model flaxseed lignan, and three TKI model drugs demonstrating high *in-silico* PPAR γ -binding affinity, ibrutinib, gefitinib, and dabrafenib, to understand the combinatorial antifibrotic effects and mechanisms in hepatic fibrosis. Furthermore, the choice of these drugs as my TKI models was also based on their target differences. Ibrutinib is utilized as a multi-target TKI drug, while gefitinib targets epidermal growth factor receptors (EGFR), a key target in cancer signaling and other fibroproliferative diseases, and dabrafenib as a non-EGFR-TKI²⁸⁻³⁰. As severe side effects occur when applying some certain target TKI drugs, we hope to identify generic mechanisms for TKI drugs in hepatic fibrosis and to understand the general interaction of lignans with antifibrotic TKIs in liver fibrosis. The dissertation research may lead to subsequent research that will identify the ability to reduce the administered dosage of TKIs when combined with lignans, which may decrease the risk of toxicity and increase the antifibrotic effects. My dissertation research may then provide experimental preclinical support for the application of

the combination of flaxseed lignans and TKIs as therapeutic alternatives in hepatic fibrosis.

2. RESEARCH QUESTION

Do flaxseed lignans combined with TKI drugs favorably modulate hepatic antifibrotic biomarkers to a further extent than using each compound alone and do these effects involve PPAR γ , oxidative stress, and/or the ER stress response?

3. HYPOTHESES

1. The TKIs, ibrutinib, gefitinib, dabrafenib, and the flaxseed lignan, ENL, are PPAR γ agonists.
2. TKIs, ibrutinib, gefitinib, and/or dabrafenib, will decrease HSC activation, extracellular matrix (ECM) protein production, and proliferation.
3. Reduction in HSC activation will involve PPAR γ , oxidative stress signaling, and/or induction of apoptosis *via* the ER stress response.
4. In combination, ENL will enhance the antifibrotic effects of certain TKI drugs *via* PPAR γ signaling and through modulation of oxidative stress or induction of ER stress-induced apoptosis.
5. In a non-alcoholic fatty liver disease *in vivo* rat model, oral flaxseed lignan administration will modulate hepatic fibrosis biomarkers and reduce hepatic lipidosis.

4. OBJECTIVES

Objective 1: To determine whether TKIs and ENL are agonists of PPAR γ

1. To determine whether TKIs (ibrutinib, gefitinib, and dabrafenib) and ENL bind to and induce transactivation of PPAR γ .
 - Determine the binding affinity of ibrutinib, gefitinib, and dabrafenib to PPAR γ using a competitive binding assay.
 - Assess the ability of ibrutinib, gefitinib, and dabrafenib to cause transactivation of PPAR γ using a transactivation reporter assay in a PPAR γ -transfected cell-based (HepG2) system.
 - Determine if the mammalian flaxseed lignan, ENL, is an agonist of PPAR γ using similar methods for TKIs as indicated above.
2. To confirm the biological response of TKIs and ENL as agonists of PPAR γ .
 - Determine if ENL and TKIs, ibrutinib, dabrafenib, and gefitinib are functional PPAR γ partial agonists by measuring the adipogenic activity as response indicators

of partial agonism in differentiated mouse 3T3-L1 pre-adipocytes.

- Assess the glucose uptake activities of the TKIs and ENL in adipocytes as a second biological functional assay in differentiated mouse 3T3-L1 pre-adipocytes.

Objective 2: To determine whether the flaxseed mammalian lignan, ENL, and certain TKIs (ibrutinib, gefitinib, and dabrafenib) can suppress HSC activation in TGF- β 1-activated human HSCs (LX-2 cells).

- Quantify changes in mRNA and protein expression of biomarkers of HSC proliferation and activation (α -SMA, collagen I, TIMP-1, and MMP2) and possible pathways for their antifibrotic effects (e.g., PPAR γ , β -catenin/Wnt, Nrf2) after stimulation with TGF- β 1 and treatment with or without ENL and/or TKI model drugs (ibrutinib, gefitinib, or dabrafenib) in the human hepatic stellate cell line, LX-2 cell. (Note: Considering the secretion and regulating effects of TGF- β and its crosstalk with PDGF, we will not use TGF- β and PDGF as biomarkers because we are using TGF- β as an initiator of fibrogenesis in LX-2 cells.)
- Assess HSC ER stress-induced apoptotic and oxidative stress response in the presence and absence of ENL or TKIs and detect fibrotic biomarker changes at levels of mRNA and protein expression (induction of ER stress apoptotic response markers such as CHOP and ATF4).

Objective 3: To assess changes in fibrotic biomarker expression following chronic administration of flaxseed lignans in a rat model of non-alcoholic fatty liver disease.

- Assess the histological and lipid profile changes in flaxseed lignan supplemented hypercholesterolemic rats.
- Assess hepatic fibrotic biomarker changes at both mRNA and protein levels in flaxseed lignan supplemented hypercholesterolemic rats.

5. LITERATURE REVIEW

5.1 Hepatic Fibrosis

Chronic fibroproliferative diseases including inflammatory bowel disease, chronic kidney disease, pulmonary fibrosis, and liver fibrosis have become a major health issue³¹. About 45% of all deaths are attributed to fibroproliferative diseases, which make it the leading cause of morbidity and mortality in the developed world and afflicts millions of individuals worldwide³². The Canadian Liver Foundation estimated that one in ten Canadians, more than three million people, has some form of liver disease, and the death rate from liver disease has risen almost 30% over a period of eight years (<https://www.liver.ca/wp-content/uploads/2017/09/Liver-Disease-in-Canada-E-3.pdf>). Chronic liver disease and cirrhosis, the final pathological result of chronic liver disease and a late stage of fibrosis, was one of the top 15 causes of death in 2014 in the United States³³⁻³⁵. In particular, non-alcoholic fatty liver disease (NAFLD), which composes 24% of total chronic liver disease, has been an economic and clinical burden estimated at \$1.005 trillion and €334 billion for the United States and four major European countries over a 10-year period, respectively³³⁻³⁵. Hepatitis C infection and NAFLD are considered the most important liver diseases in the developed world in the 20th and 21st centuries, respectively³⁶. Other causes of liver injury also contribute to liver fibrosis, such as alcoholic fatty liver disease, cholestatic disorder, and metabolic dysfunction³⁷.

The pathology of hepatic fibrosis is quite complicated but most chronic liver diseases follow similar common courses³⁶. Liver fibrosis is defined as a deregulated wound-healing response after continuous injury associated with inflammatory and oxidative stress responses and excessive accumulation of ECM proteins, particularly fibrotic collagen such as type I and type III collagen³⁸. With the formation of fibrotic scars in the hepatic sinusoidal structure, architectural modifications of the liver occur because of liver remodeling and regeneration, which will finally lead to liver dysfunction or carcinoma³⁷. Hepatic fibrogenesis is initiated with hepatic myofibroblast activation, caused by different kinds of stimuli, followed by multicellular processes leading to ECM production and fibrotic scar formation³⁹. Almost all kinds of chronic liver damage initiate hepatic fibrogenesis, which may ultimately lead to cirrhosis, liver failure, and hepatocarcinoma⁴⁰.

The continuous liver insult usually causes inflammatory and oxidative responses in attempts to repair the damaged hepatocytes. Recruitment and migration of macrophages and HSCs occur at the sites of damaged hepatocytes and commence secretion of inflammatory

cytokines and chemokines to initiate fibrogenesis⁴¹. The secretion of cytokines or chemokines can stimulate quiescent HSCs, switching these cells to an activated and proliferative phenotype. Among these cytokines and chemokines, TGF- β and platelet-derived growth factor (PDGF) are considered to be the most predominant profibrogenic factors stimulating the activation of HSCs⁴². HSC activation leads to recruitment and migration of other cells within the liver, release of inflammatory mediators and reactive oxygen species (ROS), and excessive ECM deposition by activated myofibroblasts and differentiated HSCs⁴³. Excessive ECM deposition, which forms the fibrotic scar, follows from an imbalance of synthesis and degradation of ECM due to the changed secretion ratio of matrix metalloproteinases (MMPs) and tissue inhibitor of metalloproteinases (TIMPs)¹⁶. Another major factor involved in liver fibrosis is the oxidative stress pathway. Oxidative stress is implicated in many liver diseases, including hepatitis, fatty liver diseases, and metabolic liver disease⁴⁴. ROS generated by the injured hepatocytes is a well-characterized stimulator of HSCs activation and collagen secretion of these activated HSCs⁴⁵. As these cellular activities proceed, the fibrotic scar is formed in the injured liver, and with further liver remodeling, complete loss of hepatocyte function in the fibrotic scar region ultimately occurs⁴⁶. Subsequently, chronic hepatitis progresses to repeated cycles of hepatocyte apoptosis and regeneration, along with increased fibrotic ECM stiffness and loss of normal functions of cells in the liver, leading to cirrhosis or other serious hepatocellular diseases^{35, 47}.

5.1.1 Pathology of Hepatic Fibrosis

As a wound-healing response to both acute and chronic liver injuries, the pathology of hepatic fibrosis is quite complicated⁴⁸. The most common causes of liver fibrosis are inflammation with hepatitis B or C virus, autoimmune diseases, and metabolic disorders, as well as alcohol abuse and drug toxicity^{1, 49}. The development of liver fibrosis is the result of a multi-cellular process, which implicates the involvement of different cell types, such as hepatocytes, macrophages, endothelial cells, and mesenchymal cells⁵⁰. The injury to hepatocytes results in a complicated inflammatory response with production of pro-fibrotic mediators and fibrogenic cytokines that activate the quiescent HSCs and/or other fibrogenic cells, among which HSCs are considered to be a key and major cell source of myofibroblasts⁴³. The two major ways liver injuries generate stimuli that activate the HSCs are: 1) the migration and accumulation of inflammatory cells, and 2) the activation of macrophages (mainly Kupffer cells)⁵¹. Activated HSCs and macrophages are considered to

be the major cellular source of ECM accumulation, where HSCs are known as “master producers” while macrophages are “master regulators” during the progression of liver fibrosis⁵².

HSCs compose about 5 to 15% of the cells in the normal liver, existing as a non-parenchymal quiescent phenotype, which are considered to be the major ECM-producing cells in injured liver after stimulation^{53, 54}. As non-parenchymal cells, HSCs function to maintain a normal level of ECM. In healthy liver, these fibroblasts stay quiescent and are involved in routine production of ECM to maintain homeostasis⁵⁵. Continuous liver injury causes perpetuation of stellate cell activation, mainly HSCs, in the liver and their transformation to myofibroblasts⁵³. For instance, damage to hepatocytes causes inflammatory reactions that lead to activation and migration of HSCs, subsequently leading to the accumulation of ECM and the formation of fibrotic scars in the injured area within the liver⁵². HSCs undergo complex activation processes in their transformation from a quiescent phenotype to activated fibroblast-like cells that include upregulation of alpha-smooth muscle action (α -SMA), increased accumulation of collagen, mainly type-I and -IV, and the expression of TGF- β and PDGF- β ^{43, 56}. Once activated, HSCs lose vitamin A and switch their phenotype to a highly proliferative and productive form and are also characterized by an enhanced survival because of stimulation of the nuclear factor-kappa B (NF- κ B) pathway^{43, 57}. Quiescent HSCs express a wide range of MMPs and their activators as well as their inhibitors TIMPs⁵⁸. On the other hand, activated HSCs repress the expression of MMPs and increase the expression of TIMPs, which dramatically reduces the collagenolytic activity and degradation of ECM within the liver, causing the accumulation of ECM proteins⁵¹.

The accumulation of myofibroblast precursor cells is identified as an essential feature of tissue fibrosis³⁷. As the major cell source of myofibroblasts, HSCs are responsible for liver fibrosis once activated into the fibrogenic phenotype, secreting fibrotic proteins and cytokines. Activated HSCs are demonstrated to be the primary source of collagen type I and α -SMA, which are the major components of the fibrotic scar in hepatic fibrosis^{59, 60}. However, in addition to HSCs, other cell types involved in the pathogenesis of liver fibrosis are derived from fibroblasts of the liver resident cells such as portal connective tissue, and portal and central veins, and bile duct epithelial cells⁶¹. Bone marrow-derived fibrocytes are also described as fibrogenic myofibroblasts⁶². Similar to HSCs, other sources of myofibroblasts show the same characteristics – highly proliferative and productive ability for ECM components, mainly collagen type I and α -SMA – and the recruitment of

myofibroblast-like cells arise to promote the process of fibrogenesis. Regardless of the origin, myofibroblasts are responsible for liver remodeling and proliferation of hepatocytes, ECM deposition during liver repair, and the enzymes involved in matrix degradation and scar formation^{61, 63}. Evidence suggests a cross-talk between the mechanisms of activated HSCs and other fibroblast-like cells, but the mechanism is still unknown, and conflicting information remains⁶³.

Hepatic macrophages are the major immune cells supporting the progression of liver fibrosis⁶⁴. Liver injury leads to the local recruitment of immune cells and to the activation and migration of macrophages within the liver, which can further promote the fibrotic process *via* secretion of inflammatory and fibrogenic cytokines⁵⁰. Macrophages can promote hepatic fibrogenesis by producing a range of cytokines, chemokines, and other soluble mediators that directly influence the behavior of HSCs and other myofibroblasts, such as TGF- β and galectin-3, tumor necrosis factor-alpha (TNF- α), and the potent mitogen PDGF^{37, 65}. Chronic insults such as inflammatory responses stimulate the pro-fibrotic macrophages to secrete proliferative cytokines and chemokines, which induce the activation and proliferation of the quiescent HSCs (**Figure 5.1**). Activated HSCs are responsible for the secretion and accumulation of ECM proteins, forming the fibrotic scar in the liver. During the resolution of hepatic fibrosis, which is a reverse process of fibrogenesis, macrophages switch to a pro-resolution phenotype leading to the removal of pro-fibrotic stimuli. Concurrently, the antifibrotic cytokines, such as tumor necrosis factor-related apoptosis-inducing ligand (TRAIL) and certain kinds of MMPs, cause the deactivation and apoptosis of the expanded HSC population and the degradation of fibrotic scars, mainly the ECM protein, contributing to the resolution of hepatic fibrosis^{37, 66}.

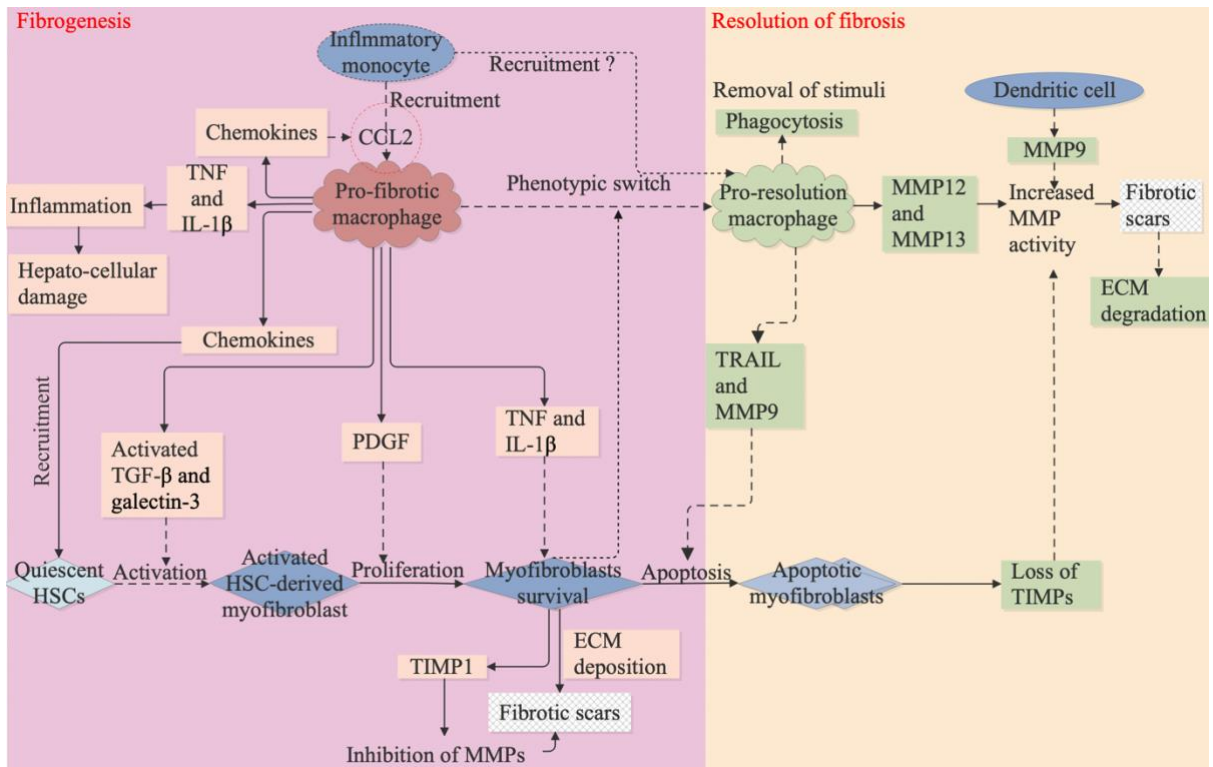


Figure 5.1 The cellular mechanisms of hepatic fibrogenesis and resolution of fibrosis in the liver. Chronic hepatic insults stimulate inflammatory responses and profibrotic cytokine/chemokine secretion which subsequently induce the activation of quiescent hepatic stellate cells (HSCs), contributing to the fibrogenesis in the liver. In contrast, with the removal of stimuli, the production of existing extracellular matrix (ECM) degrading enzymes and deactivation factors for myofibroblasts, the existing ECM, and the activated HSCs can be eliminated to resolve the fibrosis within the liver. Adapted from Pellicoro et al (Permission license number: 4831430631176)³⁷.

Oxidative stress is also implicated in the pathogenesis of liver diseases, contributing to the progression of liver injuries. Oxidative stress induces cell proliferation and ECM synthesis of HSCs, thus promoting hepatic fibrosis⁶⁷. Since the liver is a multifunction organ responsible for detoxification and maintenance of body metabolic homeostasis, it is the first organ exposed to xenobiotics after absorption from the gastrointestinal (GI) tract⁶⁸. A variety of continuous insults cause chronic liver diseases associated with oxidative stress, such as alcohol, drugs, and high-fat diet⁶⁷. As a metabolically active organ, the liver is vulnerable to ROS and has established an antioxidant system to destroy this by-product of normal metabolism in the liver⁶⁹. When elevated and sustained, ROS antioxidant systems of the liver are inadequate thus promoting cellular damage and liver disease⁶⁹. Hence, modulation of hepatic oxidative stress can be a potential approach to treat various liver diseases including liver fibrosis.

5.1.2 Current Therapeutic Approaches

Considerable progress has been made in understanding the pathology and development of hepatic fibrosis in the past decades, especially clarification of the cellular and molecular mechanisms involved in fibrogenesis⁷⁰. Hepatic fibrosis is no longer considered a passive and irreversible process but a reversible process once the stimuli are removed⁴⁶. Increasing evidence supports a view that even advanced fibrosis may be reversible, and the degree and recovery of fibrosis depend on the type and duration of the liver injury⁵. When the injury is acute, fibrosis is taken over by resolution of inflammation, replacement of the apoptotic cells, resolution of the activated HSCs, and removal of accumulated ECM^{5, 71, 72}. However, when the injury is sustained, the regeneration process is insufficient and liver tissue is gradually replaced by scar tissue⁵⁰.

The possible chemotherapies designed to mitigate hepatic fibrosis can be divided into three categories⁶⁰: (1) Inhibition of etiologies: Hepatic fibrosis is the result of the wound-healing response of the liver to repeated injury and is associated with alterations in both the quality and composition of ECM because of increased production as well as decreased degradation². Myofibroblasts may undergo apoptosis and inactivation when the etiologies are cleared. (2) Inactivation of myofibroblasts/HSCs: Although control and clearance of the etiology can retard fibrosis progression and lead to fibrosis regression, antifibrotic therapies that selectively target activated myofibroblasts/HSCs and the increased production of ECM are not yet available⁶⁰. Since ROS and inflammation play important roles in hepatic

fibrogenesis, regulation of ROS and inflammation might be strategies for the treatment of liver fibrosis by inhibiting injury⁷³. As the activated myofibroblasts are crucial for hepatic fibrogenesis by increasing cell proliferation, generating excessive ECM, and expressing α -SMA, it is important to cause inactivation, apoptosis, and quiescence of HSCs or other myofibroblasts to treat liver fibrosis⁷⁴. (3) The degradation of the ECM: Since net deposition of ECM is the final common result of liver fibrosis, the ideal antifibrotic drug should decrease the production of ECM proteins and increase the degradation of accumulated ECM sufficiently⁷⁵.

Currently, there are merely drugs available for the elimination or inhibition of the etiology of liver fibrosis. For different kinds of hepatitis, some anti-inflammatory drugs may be helpful to eliminate the stimuli to HSC activation but not sufficient to remove the fibrotic scars. For alcoholic liver diseases, cessation of drinking is the most effective approach to stop the development of liver fibrosis. Natural or synthetic steroid treatments and nutritional supplements, as well as natural and herbal medications, are all considered to be therapies for alcoholic liver injury⁷⁶. However, the removal of these insults is only effective for early-stage fibrotic patients⁶⁰. Eventually, unresolved liver fibrosis results in end-stage liver disease and requirement for liver transplantation. Transplant rejection remains a significant issue for liver-transplant patients⁷². Hence, a better understanding of the key pathways or targets is needed to develop appropriate therapeutic strategies for hepatic fibrosis at an early stage of the pathogenic process. Therapies targeting myofibroblasts activation and activation-related cytokines, as well as the degradation of the ECM, can be envisioned with a better understanding of hepatic fibrogenesis⁷⁷. Hopefully, synthetic compounds or drugs from natural products will be developed to block the fibrogenesis and resolve the existing fibrosis in the liver⁷⁸.

5.1.3 Possible Antifibrotic Mechanisms and Potential Targets

The most important and common way to treat liver fibrosis is the combination of removing the cause of liver injury, amelioration or resolution of the development of the activated myofibroblasts, and enhancement in the degradation of ECM. Although the pathogenesis of liver fibrosis involves many cytokines, enzymes, and other fibrogenic factors, the usual target for enhanced degradation of ECM is the HSC-derived myofibroblasts, which is considered the major contractile ECM-producing cell source⁵². The molecular mechanisms of HSC activation and liver fibrogenesis involve a complex array of

cytokines and chemokines in HSCs and other cells with enormous crosstalk between different signaling pathways⁷⁹. By removing the pro-inflammatory or pro-fibrotic factors, the activated HSCs will undergo deactivation with senescence, apoptosis, and reversion, switching back to a quiescent state⁸⁰. However, upon switching back to a quiescent state, HSCs can be re-activated more readily in the presence of new fibrogenic initiators such as TGF- β or PDGF⁸¹. This suggests only the elimination of activated HSCs can resolve liver fibrosis effectively⁸².

Apoptosis is considered an essential mechanism for cell clearance, which is significantly important in the resolution of hepatic fibrosis⁸³. There are three major apoptotic signaling pathways: the mitochondrial pathway, the death receptor-associated pathway, and the ER stress-associated pathway. Current literature evidence shows that ER stress-induced apoptosis might play a pivotal role in the elimination of activated HSCs to treat liver fibrosis⁸⁴. ER as a critical organelle in almost every kind of cell in mammals, is essential for cellular homeostasis and can be an important modulator for cell death by inducing the apoptotic response⁸⁵. Since the inactivation of HSCs is not sufficient for the resolution of liver fibrosis (because the deactivated HSCs are more likely to be reactivated by any subsequent insult to the liver), elimination of the deactivated HSCs is essential for the resolution of liver fibrosis without relapse. Thus, current research increasingly focuses on the elimination of the myofibroblasts in the liver by selective induction of HSC apoptosis²⁶.

According to current literature evidence, it is a promising strategy to treat hepatic fibrosis using antifibrotic agents which may cause apoptosis of the activated and/or deactivated HSCs and degradation of accumulated ECM components^{86, 87}. The possible mechanisms may include modulation of different cell signaling pathways such as TGF- β /Smad, NF- κ B, Peroxisome Proliferator-Activated Receptor gamma (PPAR γ), M2-type pyruvate kinase isozyme (PKM2), and/or PI3K-Akt/mTOR are also reported to be crucial for certain fibrosis. Beyond the aforementioned factors, ER stress can trigger pro-apoptotic response in hepatic fibrosis and can also cause apoptosis of the major myofibroblast – the activated HSCs²⁶.

5.1.3.1 TGF- β and PDGF

TGF- β is known as a master modulator of cell proliferation, differentiation, and migration, and TGF- β and PDGF are probably the most important cytokines in the hepatic

fibrogenesis process^{88, 89}. TGF- β , which is secreted by non-parenchymal cells in the liver, controls many cellular processes such as cell growth, morphogenesis, differentiation, and matrix remodeling. Controversially, TGF- β 1 also inhibits the cell cycle in the G1 phase, supporting its role in the inhibition of cell proliferation and induction of apoptosis⁸⁹. There are three isoforms of TGF- β identified in mammals, TGF- β 1, TGF- β 2, and TGF- β 3, with about 80% homology at protein level but reside on different chromosomes⁹⁰. TGF- β 1 is reported as the most prominent isoform and demonstrates an array of profibrotic functions by stimulating fibroblasts and ECM deposition *via* its interaction with certain Smad signaling proteins^{91, 92}. TGF- β 2 and TGF- β 3 are critical for embryonic development and scarless wound healing⁹³.

TGF- β diversely affects a vast range of different cells, stimulating many downstream factors. Any disturbance of TGF- β homeostasis or overexpression of TGF- β may lead to pathological conditions by causing dysfunction in cell proliferation and/or other cellular processes⁹³. Signaling *via* TGF- β begins at the cell surface with binding to its receptor, a constitutively active, membrane-bound kinase⁹⁴. Binding to TGF- β receptors triggers many cellular responses such as the TGF- β /Smad, Wnt/ β -catenin, The Mammalian Target of Rapamycin (mTOR), and EGFR signaling pathways, modulating epithelial-to-mesenchymal transition (EMT), mesenchymal transition, and myofibroblast activation⁹⁵. Subsequently, TGF- β /Smad pathway involves the phosphorylation of certain TGF- β -associated transcriptional regulators, Smads (e.g., Smad2 and Smad3), transforming into a complex state of cellular regulation and crosstalk with other pathways in the liver such as PDGF, Phosphoinositide 3'-kinase (PI3K), and PPAR γ ^{96, 97}. Various studies demonstrated that different kinds of sustained liver injury cause an inflammatory response, and then the immune cells produce active TGF- β as well as ROS or other inflammatory or non-inflammatory factors to generate fibrotic proteins⁵. In mouse and rat HSCs, TGF- β 1 showed upregulation on PDGF- β receptor, which requires the activation of PI3K pathway⁹⁸. TGF- β 1 also has an inhibitory effect on PPAR γ expression and its transactivation *via* β -catenin pathway in rat HSCs⁹⁹. In a bile duct ligation (BDL) rat model, Hypoxia-Inducible Factor 1 α (HIF1 α) induced activation of HSCs and EMT is inhibited by inhibition of TGF- β 1 receptor kinase, which was also confirmed in a human hepatic stellate cell line, LX-2 cells¹⁰⁰.

TGF- β plays a central role in the initiation and maintenance of fibrogenesis and ECM production in many fibrotic diseases, such as dermal fibrosis, pulmonary fibrosis, and hepatic fibrosis¹⁰¹⁻¹⁰³. TGF- β , mainly TGF- β 1, stimulates fibroblast proliferation and synthesis of

ECM proteins, developing or promoting fibrotic scar in different organs¹⁰⁴. The HSC is both a predominant target of this factor and an important source of TGF- β ^{105, 106}. TGF- β 1 stimulates the proliferation of many mesenchymal cells including HSCs, fibroblasts, and osteoblasts both *in vitro* and *in vivo*⁸⁹. Stimulation of the activation and transdifferentiation of HSCs by TGF- β 1 is considered as the key fibrogenic regulator in liver fibrogenesis, subsequently causing the stimulation of matrix protein synthesis, autoinduction of inflammatory cytokines, and the regulation of unbalanced MMPs to TIMPs ratio^{90, 103}. After HSC activation, the autocrine expression of TGF- β 1 by HSCs became an important source of TGF- β 1¹⁰³. Thus, TGF- β 1 can be used as a stimulator for the activation of HSCs and initiate the hepatic fibrogenesis process. Inhibition of TGF- β signaling can be a primary target for the resolution of liver fibrosis.

PDGF signaling is also an important mediator for activated HSCs and fibroblast proliferation, similar to TGF- β 's role in liver fibrosis¹⁰⁷. PDGF stimulates fibroblast-like cells and production of ECM components¹⁰⁸. PDGF receptors (PDGFR) belong to the receptor tyrosine kinases (RTKs). Ligand binding to PDGFRs in human fibrotic livers may have pro-fibrotic effects *via* the modulation of ROS generation and inflammatory response leading to the excessive deposition of ECM and *de novo* expression of fibronectins⁷⁴. Both PDGF antagonists and siRNAs may attenuate fibrogenesis and reduce HSC proliferation in animal models¹⁰⁷. Furthermore, the TKI drugs, Imatinib and Nilotinib, can suppress fibrosis *via* the blockade of PDGF signaling¹⁰⁹. The literature also indicates a close relationship between TGF- β and PDGFR in liver fibrosis. For example, PDGFR mediates induction of ErbB ligands *via* TGF- β with a positive feedback loop through ErbB, while in murine fibroblasts, TGF- β cooperates with RTKs including PDGF and ErbB, which indicates that TGF- β and PDGF have crosstalk during the hepatic fibrogenesis⁹⁴.

Given their significant role as critical pro-fibrotic factors, new therapeutic approaches targeting TGF- β or PDGF secretion, receptor activation, or downstream signal transduction may attenuate HSC activation and its subsequent events in liver fibrogenesis^{96, 110}. In fibrotic diseases, TGF- β controls many pro-fibrotic mediators including PDGF, endothelin, and Wnt signaling directly or indirectly¹¹¹⁻¹¹³. TGF- β also upregulates the expression of PDGFR in activated HSCs⁹⁸. In cultured HSCs, TGF- β is also reported to decrease the expression of PPAR γ *via* β -catenin/Wnt pathway, contributing to the production of collagen I alpha 1 and fibrogenesis^{66, 99}. In conclusion, both TGF- β and PDGFR serve as pro-fibrotic factors in liver fibrogenesis and may serve as therapeutic targets in drug development.

5.1.3.2 Oxidative stress

Oxidative stress-induced damage appears to be a common feature in hepatic fibrogenesis, regardless of the etiology¹¹⁴. Oxidative stress refers to an imbalanced state between reactive oxygen species (ROS) and antioxidant abilities in the body, causing cellular damage if the disturbance continues. Oxidative stress may ultimately contribute to the development of cancer, cardiovascular disease, diabetes, and other diseases¹¹⁵⁻¹¹⁷. ROS include free radicals, which are defined as chemical species containing unpaired electron(s), increasing the reactivity of their molecule or atom¹¹⁸. Examples of common ROS and reactive nitrogen species (RNS) include hydrogen peroxide (H₂O₂), superoxide anion (O₂^{·-}), nitric oxide (NO[·]), hydroxyl radical (·OH), peroxynitrite (ONOO⁻), and formation is often catalyzed by transition metals such as iron and copper^{115, 118}. An important intracellular source of ROS is the mitochondrial electron transport chain when electrons escape from electron carriers to oxygen¹¹⁸⁻¹²⁰.

Defense mechanisms may be stimulated by exposure to free radicals and include preventive and repair systems, as well as physical and antioxidant defences¹²¹. Endogenous antioxidant safeguard systems and dietary exogenous antioxidants defend the body against oxidative damage caused by ROS or other kinds of oxidative stress under normal physiological conditions^{122, 123}. The endogenous antioxidant defense system includes enzymes, such as superoxide dismutase (SOD), glutathione (GSH), GSH peroxidase (GPx), and catalase, and antioxidants such as vitamins C and E, which help maintain a delicate oxidative-antioxidative balance to ensure a low net production of ROS¹¹⁸. Excessive production of ROS and/or a decreased capacity of antioxidants affect cellular functions including those of mitochondria, contributing to the progression of multiple cellular dysfunction or pathogenesis of chronic diseases^{124, 125}. However, ROS production also can be useful. For example, the production of O₂^{·-} and H₂O₂ by phagocytes contributes to their pathogen-killing mechanism, while ROS-induced apoptosis in cancer cells makes ROS an anti-tumorigenic species^{116, 118}.

Both experimental and clinical data suggest that hepatic oxidative stress plays a pivotal role in the initiation and progression of fibrosis and is involved in the activation of HSCs as well as the accumulation of ECM and the formation of fibrotic scar¹²⁶⁻¹²⁸. Oxidative stress is demonstrated not only as the cause of, but also as a mediator in, the fibrogenesis involved in multiple cellular responses¹²⁹. However, activated HSCs are more capable of removing

reactive oxidative intermediates than quiescent cells¹³⁰. At the early stage of liver fibrosis, oxidative stress may directly activate Kupffer cells following liver insults of different etiologies, and subsequently initiate the activation of different cellular pathways including PDGF, TGF- β , MAPK, and PI3K pathways¹¹⁴. In the progression of fibrotic scar, ROS-related mediators also may be involved in the overexpression of ECM with profibrotic cytokines¹³¹. Increased oxidative insults, mainly by ROS, to hepatocytes initiate the progression of fibrosis by inducing the production of profibrogenic mediators, or directly stimulate HSCs into fibrogenic and proliferative myofibroblasts, possibly through the modulation of TGF- β - or MMP2-mediated pathways^{132, 133}. The Nuclear erythroid 2-related factor-2 (Nrf2) plays a considerable role in protecting the liver against disease through regulating a multifaceted cellular antioxidant defense¹³⁴.

Nrf1 and Nrf2, two members of the vertebrate Cap'n'Collar (CNC) transcription factor family, are key regulators of oxidative stress regulating various genes in the antioxidant response¹³⁵. Nrf2 is a master regulator of multi-cytoprotective responses, including cell maintenance, growth, and proliferation, and a new target for drug development and repurposing for a certain cluster of diseases¹³⁶. Nrf2 is repressed by being bound to the cytoskeletal anchoring protein Kelch-like ECH-associated protein (Keap1) on the N-terminal portion¹³⁴. When the complex is stimulated by oxidative or electrophilic stress, Nrf2 dissociates from Keap1 and then translocates to the nucleus, playing a role in detoxification and the elimination of toxic xenobiotics. The activation of Nrf2 shows protective effects against oxidative stress, inflammation, and fibrosis in the liver^{44, 134}. Nrf1 shares similarities with Nrf2 in structure and bioactivity, such as their regulatory transcriptional effects on targeting ER stress¹³⁵. However, some observations suggest that Nrf1 exhibits unique functions separate from Nrf2, such as an ER targeting sequence responsible for anchoring NRF1 to the ER membrane¹³⁷. Taken together, Nrf1 and Nrf2 are implicated in multiple liver diseases and have potential to protect the liver by integrating diverse functions.

5.1.3.3 PPAR γ

PPARs, members of the ligand-activated nuclear hormone receptor superfamily, regulate the expression of many proteins involved in lipid and glucose metabolism, fatty acid oxidation, and energy homeostasis, with subsequent regulation of inflammation, cell proliferation, lipid homeostasis, adipogenesis, and wound healing response¹³⁸⁻¹⁴⁰. The three subtypes of PPARs, PPAR α , PPAR γ , and PPAR β/δ , have isotype-specific but partially

overlapping expression patterns. PPAR α is expressed highly in the liver, kidney, heart, and other tissues and serves as the receptor for endogenous or xenobiotic ligands such as fibrates¹⁴¹. PPAR α plays a crucial role in lipid metabolism and atherogenesis, as well as vascular function. PPAR β/δ is expressed highly in the brain, skin, and adipose tissue, and is known as a promoter for lipid catabolism, but its exact function is not completely known¹⁴². PPAR γ , known as the most researched PPAR isoform, is present in adipocytes at a high level, and now is considered as a multifunctional nuclear receptor for many diseases. PPAR isoforms have many endogenous ligands and a number of synthetic ligands. After ligand binding, the transcriptional activity of all PPARs is mediated by PPAR:RXR heterodimers that subsequently bind to peroxisome proliferator response elements (PPREs), regulating the transcription of their target downstream genes¹⁴³.

PPAR γ is composed of multiple domains including the A/B domain, ligand-independent activation domain (AF-1 region), DNA-binding domain (DBD) (C-domain), hinge region (D-domain), the ligand-binding domain (LBD), and ligand-dependent activation domain (AF-2 region)¹⁴⁴. The LBD consists of 12 α -helices, arranged in an anti-parallel helix sandwich, and four short β strands as an anti-parallel β sheet¹⁴⁵. PPAR γ ligands bind to the LBD, which consists of approximately 250 amino acid near the C-terminal of the protein, and then undergo heterodimerization with retinoid X receptor (RXR) subunit with association of coactivator molecules, and the mediation of the PPAR γ activity is directly caused by the changes of AF-2 domain¹⁴⁶. PPAR γ has a large internal hydrophobic ligand-binding pocket which is located within the LBD¹⁴⁷. As shown in **Figure 5.2**, analyses of 3D crystal structures of the PPAR γ reveal that PPAR γ has a Y-shape ligand binding cavity with an outside Ω -loop¹⁴⁸. The large Y-shaped hydrophobic ligand-binding pocket of PPAR γ can be divided into two sub-pockets, the AF-2 and β -sheet sub-pockets^{149, 150}. Endogenous or synthetic ligands bind to the hydrophobic core within the helix 12 (H12) region, which is referred as the AF-2 binding sub-pocket, or bind to H2'-H3 region, which is referred as the β -sheet binding sub-pocket, or bind to the Ω loop, causing conformational changes by altering or stabilizing the hydrogen bond network of the nuclear receptor^{147, 151-153}. Consequently, the ligand bound may have more than two binding modes in one single binding site. Full agonists bind to both AF-2 and β -sheet sub-pockets, which are near H12 and helix 3 region (H3) of PPAR γ , respectively, and fully activate two sites of the LBD by hydrogen bond with one or more amino acids, such as His323, His449, Ser289, Tyr327, and Tyr473^{148, 154}. Full agonism would induce PPAR γ structural change to a fully activated form, subsequently interfere with its coregulators or heterodimer interfaces, stimulating transcriptional responses to its

downstream factors such as NF- κ B and PKM2, which play important roles in many cellular processes¹⁵⁵⁻¹⁵⁷. Unlike the full agonists, binding to both AF-2 and β -sheet sub-pockets, some partial agonists only bind to the β -sheet sub-pocket or the Ω loop without direct contact with H12, and the binding may occur at different binding sites, such as His266, Ser245, Ser289, Tyr327, and Lys367^{150, 158, 159}. Partial agonists may induce selective conformation changes or partial activation of PPAR γ , which subsequently may improve their pharmacokinetic (PK) properties with wider safety range¹⁶⁰.

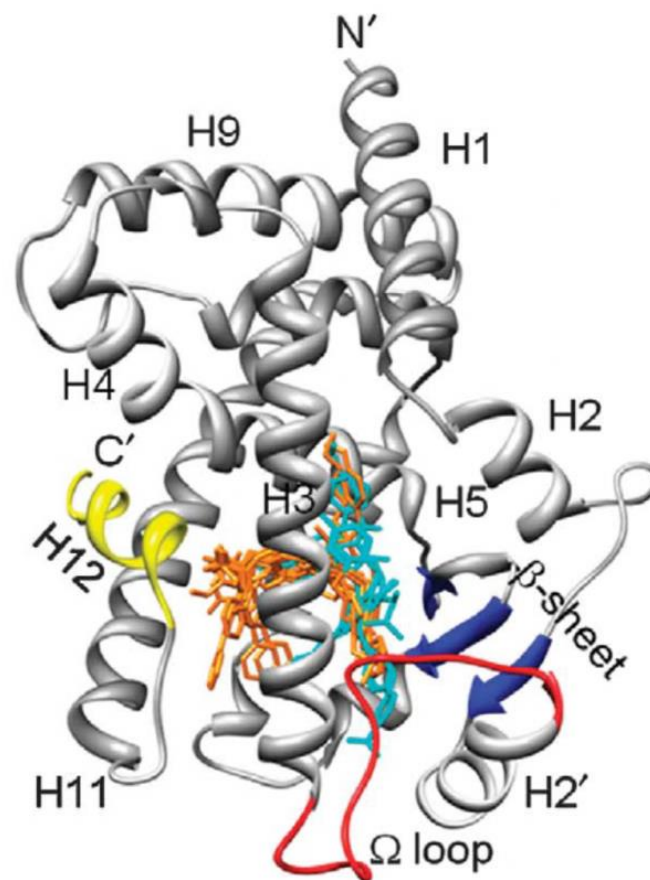


Figure 5.2 The 3D configuration model of PPAR γ ligand binding domain (LBD) with superposition of known agonists. Full (orange) and partial (cyan) agonists are binding to different sites with PPAR γ . Helix 12 (H12, yellow), β -sheet binding pocket (blue), and Ω -loop (red) are shown with all the other regions (grey). The 3D model was made by Waku (Permission license number: 4831421286787)¹⁴⁸.

PPAR γ may regulate HSC activation in liver fibrosis¹⁶¹. PPAR γ depletion is associated with HSC activation, whereas increasing PPAR γ expression induces HSC quiescence and

inhibits activation of markers such as α -SMA and collagen I¹⁶¹. Type I TGF- β can suppress the expression of PPAR γ in HSCs, while deficiency of PPAR γ will lead to constitutive secretion of TGF- β and continuous accumulation of α -SMA and collagen I¹². PPAR γ can also be attenuated by the Erk-MAPK pathway, which is a downstream response of Raf and Ras signaling and can be induced by the PDGF-PI3K-Akt pathway¹⁶². In HSCs, PPAR γ is triggered by macrophage-derived cytokines, Raf-Erk pathway, and p38 pathway, mainly modulating cell differentiation, metabolism, and proliferation^{12, 161}.

The PPAR γ ligands have anti-proliferative and antifibrotic effects on activated HSCs as well as inducing HSCs apoptosis through a mechanism involving the extrinsic apoptosis pathway¹⁶³. In preclinical animal models, rosiglitazone, a known full agonist of PPAR γ , demonstrates antifibrotic activity by inhibiting TGF- β 1-induced expression of connective tissue growth factor (CTGF)¹⁶¹. This suggests PPAR γ might be a key regulator of ECM production in hepatic fibrosis by inhibiting HSC proliferation and inducing apoptosis in HSCs. Therapeutic approaches targeting PPAR γ agonism have been investigated recently. The major studied agonists of PPAR γ are now focusing on the pan agonists of PPARs, full agonists of PPAR γ , and the partial agonists or non-agonist ligands of PPAR γ ^{142, 164}.

5.1.3.3.1 Pan-agonists or Dual agonists of PPARs

Pan agonists of PPARs are considered as potential anti-diabetic drugs and anti-hyperlipidemic drugs with a wide therapeutic window *via* the activation of PPARs¹⁶⁵. Clinically, PPAR pan-agonists are being evaluated with positive observations in diabetes and other metabolic diseases, indicating that PPAR pan-agonists can serve as a new generation of drugs for PPAR-related diseases¹⁶⁶. Individually, PPAR α , as a key activator of lipid metabolism, plays an important role in fatty acid oxidation, promoting the expression of genes required for lipid metabolism *via* hepatic AMPK-SREBP-1 and PPAR α -dependent pathways¹⁶⁷. PPAR γ activation shows high activity towards inhibiting cell growth and inducing apoptosis in human cancer cells¹⁶⁸. Pan agonists of PPARs have received great interest in the past decades, due to the reduced risk of side effects that are typically induced by full activation of one single PPAR or dual PPARs¹⁶⁵. In fact, significant progress in the development of new drugs include pan-agonists and dual agonists of PPARs have been made since 1990^{141, 169}.

Dual agonists for PPAR α and PPAR γ have a potential role in chronic disease due to their homology and ability to regulate lipid homeostasis and the inflammatory response¹⁴¹. Dual

agonists such as ragaglitazar demonstrate anti-hyperglycemic and anti-hyperlipidemic effects in rodents and humans¹⁷⁰. However, PPAR dual agonists may enhance the risk of carcinogenesis due to overexpression of PPAR α in rats¹⁷¹. In liver fibrosis PPAR pan- or dual-agonists may have opposing effects on the pathogenesis process. For example, in human HSCs, PPAR α activity is reduced by inhibition of adenosine monophosphate-activated protein kinase (AMPK) signaling in hepatocytes and is also influenced by mitogen-activated protein kinase (MAPK) and PI3K pathways¹⁶⁷. This is in contrast with the mechanism that attenuates liver fibrosis where activation of AMPK and MAPK pathways are thought to stimulate the production of IL-6, a cytokine involved in the activation of the fibrogenesis processes^{39, 172}. PPAR β/δ 's role in liver injury remains uncertain and its function in liver fibrosis is still unknown, but it is reported that in CCl₄-injured mouse model, activation of PPAR δ increased proliferation and decreased apoptosis of activated HSCs with involvement of PI3K activation¹⁷³. PPAR γ activation has anti-inflammatory effects in macrophages, reduction in the activation of HSCs, and resolution of activated HSCs to the quiescent phase¹⁷⁴. Consequently, pan agonists of PPARs might show a bi-directional effect on liver fibrosis. Challenges remain in the development of pan- or dual agonists of PPARs. PPAR γ agonists, though, have become potential candidates for the treatment of liver fibrosis because the PPAR γ agonism is not dependent on the upstream pathway of MAPK, Janus tyrosine kinases (JAK), and/or PI3K¹⁷⁵.

5.1.3.3.2 PPAR γ full agonists

PPAR γ full agonists, such as thiazolidinediones (TZDs), are widely applied for the therapy of type II diabetes and Alzheimer's disease¹⁷⁶. Full agonists bind to and activate PPAR γ and subsequently stimulate the downstream factors, improving insulin sensitivity, glucose metabolism, and immune response¹⁷⁷. PPAR γ full agonists bind to the helix 12 region of PPAR γ and fully activate the two sites of the LBD, by the hydrogen-bonding interaction with five amino acids, Ser289, His323, His449, Tyr327, and Tyr473¹⁵⁴. Full agonism by PPAR γ full agonists will induce structural change to a fully activated form, subsequently stimulating different responses *via* transactivation or transrepression of the downstream factors such as PKM2 and NF- κ B¹⁵⁵⁻¹⁵⁷. Rosiglitazone, a known full agonist of PPAR γ , has an antifibrotic effect in the liver through its influence on HSCs¹⁷⁸.

Although PPAR γ full agonists have potential for significant clinical efficacy, such

compounds are associated with uncontrolled adverse effects such as weight gain, peripheral edema, bone loss, and heart failure¹⁵⁵. The first TZD, troglitazone, a PPAR γ full agonist, was approved by the Food and Drug Administration (FDA) in 1997 and withdrawn in 2000 due to hepatotoxicity¹⁷⁹. Subsequent TZDs, rosiglitazone (approved in 1999) and pioglitazone (approved in 1999), had black box warnings due to potential adverse effects such as ischemic toxicity and carcinogenicity^{180, 181}. These unwanted adverse effects limit the administration of PPAR γ full agonists. Partial agonists or non-agonist ligands of PPAR γ represent a possible solution to the adverse effects of full agonists¹². A partially activated PPAR γ will have a lower opportunity to cause adverse effects without significant reductions in their bioactivity. Consequently, interest has grown to develop PPAR γ partial agonists rather than full agonists to avoid the significant side effects associated with the full agonists¹⁴⁷.

5.1.3.3.3 PPAR γ partial agonists and non-agonist ligands

Recent studies reported that a moderate reduction of PPAR γ activity by PPAR γ partial agonists improved insulin sensitivity and high-fat diet-induced obesity without serious side effects¹⁷⁶. Due to the lack of safety for the PPAR γ full agonists, many partial agonists have been developed in an attempt to reduce the side effects caused by full agonists¹⁸². An alternative binding behavior of PPAR γ partial agonists occurs during the interaction with PPAR γ . The partially activated form is established by weak hydrogen-bonding at the helix-12 region of the ligand binding domain (LBD)¹⁵⁵. Partial agonists interact mainly with Ser342 in arm III through a hydrogen bond, and several hydrophobic interactions with arm II of the LBD, but do not bind to arm I usually occupied by full agonists¹⁵³. Since the binding of PPAR γ partial agonist is weaker than that of full agonists, the spatial structural modifications of PPAR γ (the transactivation) are weaker than full agonists¹⁵⁵. Alternatively, partial agonists can inhibit the phosphorylation of PPAR γ at a different domain such as Ser273¹⁵³. Partial agonists have a reduced ability to transactivate PPAR γ resulting in lower side effects than the full agonists, yet demonstrate similar biological functions such as improved insulin sensitivity to increase glucose uptake^{153, 183}.

Non-agonist PPAR γ ligands might have potent biological activity while avoiding undesirable adverse effects related to the classic full agonists¹². SR1664, a non-agonist PPAR γ ligand, is identified as an anti-diabetic compound with similar functions as PPAR γ partial agonists, but without the adverse effects of full agonists¹⁸⁴. With a different binding

pattern (binding to helix-11 rather than helix-12), non-agonist ligands of PPAR γ block CDK5-mediated phosphorylation to perform anti-diabetic effects similar to PPAR γ full agonist rosiglitazone¹⁸⁴. This study suggests that non-agonist ligands of PPAR γ may serve as potential drugs for PPAR γ -related diseases.

Identification of PPAR γ partial agonists can be done from both structural and biological aspects. Methods to identify partial agonists include computational 3D modelling for structural binding simulations, PPAR γ competitive binding assay, and PPAR γ -transactivation assay, as well as adipogenesis and/or glucose uptake assay in adipocytes to determine biological function^{185, 186}. With the biological benefits of both partial agonists and non-agonist ligands of PPAR γ , it is possible to identify and develop a new generation of drugs targeting PPAR γ in a selective manner.

5.1.3.3.4 PPAR γ in Hepatic fibrosis

Besides the known role of PPAR γ in the modulation of lipid metabolism and glucose homeostasis, PPAR γ is also reported to be a modulator of HSC proliferation, differentiation, and metabolism at the transcriptional level¹². The basal endogenous expression of PPAR γ is abundant in different types of cells in the liver, including hepatocytes, macrophages, and fibroblasts¹⁸⁷. In mesenchymal cells, such as HSCs and other sources of myofibroblasts, TGF- β 1 is an inhibitor for the expression of PPAR γ *via* the TGF- β /Smad pathway¹⁸⁸. Deficiency of PPAR γ would cause constitutive secretion of TGF- β 1 and enhanced production of collagen I in cell culture models, which suggests that PPAR γ is possibly involved in the processes of hepatic fibrogenesis¹⁸⁹. Two natural PPAR γ partial agonists showed anti-proliferative and proapoptotic effects, as well as modulation of oxidative stress related to their binding properties¹⁵⁸. Moreover, PPAR γ has close linkage with many other cell signaling pathways such as PI3K/Akt-mTOR pathways with subsequent modulation of downstream targets such as PKM2¹⁵⁶.

PKM2, an isoform of pyruvate kinase, is a multifunctional sensor which can act as a metabolic regulator of glycolysis, and therefore plays a role in cell proliferation and apoptosis, interaction with immunological factors, and other physiological effects¹⁹⁰⁻¹⁹². Pyruvate kinases are rate-limited glycolytic enzymes that catalyze the irreversible transphosphorylation between phosphoenolpyruvate and adenosine diphosphate, which produces pyruvate and adenosine triphosphate (ATP)¹⁹³. PKM2 is one of the four isoforms of

pyruvate kinase, which are PKM1, PKM2, PKL, and PKR. PKM2 has an important metabolic function in glycolysis, catalyzing the last step of glycolysis when it exists in the active tetrameric form¹⁹¹. In its less active dimeric form, carbon sources are shunted to macromolecule synthesis curtailing ATP production¹⁹¹. Inhibitors of PKM2 appear to rely on the hypothesis that proliferating cells are highly dependent on energy, and reduced activity of PKM2 inhibits energy regeneration¹⁹³. PKM2 is capable of regulating the production of cytokines and progression of mitosis, which are critical in the activation of inflammatory responses and cell proliferation¹⁹⁰. PKM2 may be modulated by many transcriptional factors such as PPAR γ and HIF1- α ^{156, 194}.

Activated HSCs switch to a glycolytic phenotype with upregulation of several targets, including PKM2, which has an impact on the population of glycolytic cells⁶³. In mice, CCl₄ injection increased the expression of PKM2 protein which was reduced after antifibrotic compound administration¹⁹⁵. In another fibrotic mouse model, PKM2 is recruited *via* the isoform switch from PKM1, causing energy depletion which further leads to fibrosis¹⁹⁶. PKM2 also can be modulated by both PPAR γ and PI3K-Akt/mTOR pathway, and transcription of PKM2 is induced by a signaling cascade including EGFR and NF- κ B¹⁹⁷.

In hepatic fibrosis models, the activation of transcriptional nuclear factor kappa B (NF- κ B) is commonly found in the major myofibroblasts – HSCs – during the fibrogenesis process, and inhibitors of NF- κ B can block the fibrogenesis^{198, 199}. Nuclear factor kappa-light-chain-enhancer of activated B cells (NF- κ B) is a family of protein dimeric complexes which controls the transcription of DNA, production of cytokines, and cell survival. Recent evidence also indicates that NF- κ B is a key regulator for inflammatory responses and cell proliferation in the liver *via* the modulation of a wide range of target genes^{200, 201}. It is also reported that NF- κ B promotes the production of collagen in carbon tetrachloride-induced liver fibrosis in mice²⁰². Thus, blocking of NF- κ B signaling might be a way to inhibit the activation of HSCs and might be a preventive target for liver fibrosis caused by infection²⁰³. NF- κ B is also reported to be triggered by EGFR activation and has close relationships with other signaling pathways such as TGF- β /Smad pathway, JNK (Jun N-Terminal Kinase)/ERK (extracellular-signal regulated kinase) pathway^{200, 203, 204}. Nonetheless, NF- κ B has crosstalk with many different cellular signaling pathways, such as Gli3, TLR5, and MAPK, which can either enhance liver fibrogenesis or inhibit fibrosis depending upon the state of cell signaling pathway activation²⁰².

As another cellular signaling pathway which has close linkage with PPAR γ , PI3Ks can

also regulate many cell functions such as proliferation, migration, adhesion, and survival in cancer cells as well as in the liver probably *via* reprogramming of metabolism, specifically an upregulation in aerobic glycolysis^{205, 206}. Activated PI3K represents a key signaling molecule, along with the activation of the downstream factor, protein kinase B (Akt/PKB), causing stimulation of cell proliferation and inhibition of apoptosis *via* stimulating tyrosine kinase activity²⁰⁷. Akt-mTOR is a critical downstream survival pathway after activation by a PDGF activator in HSCs⁴². Activation of the PI3K pathway is a key pathway for HSC proliferation and collagen I production in activated HSCs, and the inhibition of PI3K can deactivate HSCs and reduce HSCs proliferation and causing a reduction in the production of collagen I and α -SMA without changing the intracellular unprocessed collagen intermediates, a mechanism that might be similar in fibrosis as with cancer²⁰⁷⁻²⁰⁹. Additionally, mTOR upregulates the activity of Sterol regulatory element-binding proteins 1 (SREBP1) and PPAR γ , key transcriptional regulators of lipid and cholesterol homeostasis, while inhibition of mTOR reduces the expression of PPAR γ and other targets involved in lipid metabolism^{210, 211}. Taken together, the PI3K/Akt-mTOR pathway is involved in the development and the resolution of hepatic fibrosis related to PPAR γ . Furthermore, Inhibition of PI3K plays a major role in the regulation of cell autophagy and apoptosis *via* Akt/mTOR modulation, which indicates that the PI3K/Akt-mTOR pathway might be a key signaling pathway to target to control the pathophysiology of pulmonary fibrosis²¹². In liver cirrhosis patients, though, the inhibition of PI3K-Akt pathway regulates the balance of proinflammatory and anti-inflammatory cytokines such as interleukins (ILs) bidirectionally, which suggests modulation of PI3K-Akt/mTOR pathway is not a potential therapeutic target on its own²¹³.

The literature provides evidence that PPAR γ agonists have potential to attenuate liver fibrosis in CCl₄-induced rats *via* non-parenchymal cell apoptosis and PPAR γ activation, working on many downstream factors such as PKM2, PI3K pathway as well as NF- κ B^{156, 210, 214}. Moreover, treatment with PPAR γ ligand reveals the antifibrotic effects of PPAR γ in a liver fibrotic mouse model (Pioglitazone, PPAR γ full agonist), and in activated human HSCs and different fibrotic rat models (rosiglitazone, PPAR γ full agonist)^{174, 215}. Over the past decade, research on the regulatory role of PPAR γ in liver fibrosis has been done at both the pathological and therapeutic levels. Activation of PPAR γ attenuates ECM production and modulates the HSC phenotype during the fibrogenesis^{12, 161}. Collectively, the literature evidence indicates that PPAR γ may be an important novel pathway in regulating fibrosis, and

PPAR γ partial agonists can be potential drug candidates for liver fibrosis.

5.1.3.4 ER Stress-induced Apoptosis in HSCs

ER stress responses may induce cellular dysfunction and cell death *via* apoptosis²¹⁶. In eukaryotic cells, the ER is a central organelle responsible for normal cellular function and cell survival²¹⁷. It is responsible for the folding, post-transcriptional modification, and translocation of proteins, which are then transported to the Golgi complex and subsequently secreted out from the cell or displayed on the plasma surface²¹⁶. The ER is also responsible for the synthesis of lipids and sterols, as well as the storage of free calcium²¹⁸. Disruption of ER homeostasis, known as ER stress, is initiated by accumulation of unfolded, misfolded or excessive protein, lipid imbalances, or changes in the ionic conditions of the ER lumen^{217, 218}. To solve the accumulation of unfolded or misfolded protein in the ER, a group of cellular signaling pathways is activated, termed unfolded protein response (UPR), to induce transcriptional programs²¹⁹.

Three ER-transmembrane protein sensors are activated by prolonged ER stress. These include activating transcription factor 6 (ATF6), protein kinase RNA-like ER kinase (PERK), and inositol-requiring protein-1 (IRE1), mediating UPR pathways²²⁰. ATF6 is a bZIP transcription factor of the CREB/ATF family which is induced *via* regulated-intramembrane proteolysis (RIP) under ER stress²²¹. PERK is a kind of type I ER transmembrane protein with a sensor at the luminal side and a cytoplasmic domain with Ser/Thr kinase activity, and the active PERK can phosphorylate its downstream targets such as eukaryotic initiation factor 2 α (eIF2 α) and Nrf2²²². IRE1 is a serine/threonine protein kinase/endoribonuclease encoded by the ERN1 gene, which consists of an ER luminal domain and two cytosolic domains²²⁰. The IRE1 pathway regulates chaperone induction, ER-associated degradation, and the response of the ER to the stress²²³. Among the action of these signaling proteins, many cellular signals are involved working as downstream or transcriptional factors, eventually leading to cell death *via* intrinsic or mitochondrial-mediated pathways^{222, 224, 225}.

Prolonged ER stress can promote cell death *via* apoptosis in many types of cells, such as macrophages, endothelial cells, and cardiomyocytes^{226, 227}. In cancer cells, an evolved way for cell survival to adapt to unfavorable microenvironment was caused by persistent UPR, for example, the activated IRE1 α induces vascular regeneration and angiogenesis possibly via HIF-1 α and vascular endothelial growth factor (VEGF)²²⁸. Not only the IRE1/XBP1 pathway was impacted, but it is also reported that at least one of the branches of the UPR response

would be activated in a variety of human cancer cells, PERK-eIF2 α -ATF4 pathway is also demonstrated to be activated which plays a complex role in tumor development²²⁹. However, many cancer cells suppress ER stress signaling to promote tumor progression, and the activation of Nrf2 could provide aid for this progress²³⁰. In activated HSCs, the downstream pro-apoptotic signals of ER stress can be triggered to initiate cell apoptosis, including CHOP (C/EBP-homologous protein, also known as GADD153), JNK, and caspase²⁶. As a common target for IRE1, ATF6, and PERK, CHOP may interact with other transcriptional factors or kinases, participating in ER stress-related actions like apoptosis *via* several different pathways, including Bcl-2, JNK, or caspase-12⁸⁵. Another possible mechanism involved in the ER stress-induced apoptosis is the cholesterol-driven pathway²¹¹. Taken together, ER stress-induced apoptosis might serve as a therapeutic target for fibroproliferative disease, however, the complex mechanism remains uncertain, especially in chronic liver diseases.

5.1.3.5 Wnt/ β -catenin Pathway in HSCs

A novel strategy to treat liver fibrosis is to inhibit the Wnt/ β -catenin pathway to deactivate HSCs which are responsible for the hepatic fibrogenesis²³¹. The Wnt signaling pathway is an important regulator for cell proliferation, differentiation, and embryonic development²³². The Wnt signaling pathway contains numerous components, including 19 known Wnt receptors and over 15 co-receptors, which have complicated crosstalk and regulatory mechanisms with many other cellular signaling pathways²³³. Wnt proteins intervene in various biological processes *via* canonical and non-canonical Wnt signaling, the two pathways distinguished by the dependency of β -catenin²³⁴.

At resting state, the Frizzled protein on the cell membrane is not bound by Wnt protein, and β -catenin in the cytoplasm is assembled in a complex with axin, APC, CK1 α , and GSK3 β , and subsequently is phosphorylated and degraded. In the activated phase, Wnt proteins bind to Frizzled/LRP complex on the cell membrane, leading to canonical or noncanonical Wnt pathways activation⁶⁶. In canonical β -catenin/Wnt signaling pathway, β -catenin is the key molecule that mediates the signaling from the cell membrane to the cytoplasm, and eventually to the nucleus, causing transcriptional modulation of its target genes. When Wnt proteins bind to Frizzled protein receptor and its co-receptor, lipoprotein receptor-related protein (LRP)- 5/6, the complex triggers the destruction of the β -catenin complex, which stops the degradation of β -catenin. This allows β -catenin to accumulate in the cytoplasm and translocate to the nucleus, where it activates the transcription of its downstream factors by binding with T-cell factors (TCF) and lymphoid enhancer binding

factor (LEF) proteins²³³. In β -catenin-independent non-canonical Wnt signaling, there are two main pathways which are described. One is the planar cell polarity (PCP) pathway, which is prominently regulating cytoskeleton and cell polarity. PCP and canonical Wnt pathways are characterized as repressing each other. The other noncanonical Wnt signaling is the Wnt-Ca²⁺ pathway, which is involved in inflammation and cancer through the release of Ca²⁺ and activation of transcriptional regulators²³⁵.

Wnt signaling promotes hepatic fibrogenesis by enhancing the activation of HSCs. Wnt3a and Wnt5a are confirmed to participate in the activation and proliferation of HSCs both *in vitro* and *in vivo*^{236, 237}. In HSCs, PPAR γ induction represses Wnt signaling, while Wnt pathway serves to inhibit the trans-differentiation of HSC *via* epigenetic repression of PPAR γ ²³⁸. It is also reported that cholesterol selectively activates canonical Wnt signaling²³⁹. Certain natural products attenuate the degree of hepatic fibrosis by downregulating the canonical β -catenin/Wnt pathway²⁴⁰. Controversially, in metformin treated cultured-HSCs, canonical Wnt signaling is induced²⁴¹. Overall, it is promising that either canonical or non-canonical signaling pathways may be involved in the process of fibrogenesis and can be a therapeutic target pathway for hepatic fibrosis.

Other possible ways reported for the treatment of liver fibrosis include targets such as TAM receptors (Tyro3, Axl, and Mer), which control inflammation and homeostasis and TRAIL-dependent mechanism^{242, 243}. All the involved cell types, as well as the cell signaling pathways, may have crosstalk with each other, pointing to different results of the liver condition. The resolution of hepatic fibrosis, as well as fibrogenesis, is a complex process with multicellular and multi-signaling responses.

Although considerable progress in understanding the process of fibrogenesis and therapeutic targets on hepatic fibrosis has been made in the past years, appropriate clinical therapies for liver fibrosis are still limited^{244, 245}. Current therapeutic options for hepatic fibrosis are limited due to variants of liver fibrosis pathology, severe side effects of the drugs, and clinical complications^{246, 247}. To better understand the pathology, progression, and resolution of hepatic fibrosis, further research is necessary and must involve different experimental models.

5.1.4 Experimental Models of Hepatic Fibrosis

Many different experimental models are available today to mimic the complex hepatic

fibrogenesis processes in many aspects including the cellular interactions and signaling pathways²⁴⁸. Since hepatic fibrosis results from a sustained wound healing response to continuous insults, the progression of the disease is usually related to multicellular dysfunction²⁴⁹. In hepatic fibrosis research, it is important to establish experimental models that can mimic the pathophysiology of liver fibrosis to study the ongoing nature of liver fibrogenesis and the resolution of the process. Currently, liver fibrosis models include *in vitro*, *ex vivo*, and *in vivo* models each with different strengths and weaknesses in the investigation of hepatic fibrogenesis and its resolution.

5.1.4.1 In Vitro Models of Hepatic Fibrosis

In vitro models are essential for in-depth research of the mechanisms involved in hepatic fibrogenesis as well as the resolution of liver fibrosis. Human and animal primary HSCs and cell lines are commonly used *in vitro* models in the investigation of liver fibrosis. The major advantages of using *in vitro* models to study liver fibrosis include: 1) Avoidance of species differences as investigations can involve human cell lines, and 2) Replacement of animal use to understand basic molecular mechanisms of drug action. A major disadvantage for using *in vitro* models is that such models fail to capture the complexity of fibrogenesis, which is a multi-cellular as well as a multi-pathway process with involvement of different cells and mediators⁵⁰. The commonly used *in vitro* models are primary human or animal HSCs, human HSC lines, and co-culture systems.

5.1.4.1.1 Primary HSCs

Primary HSCs serve as a good model to reflect the processes of liver fibrogenesis and the resolution of liver fibrosis *in vitro*²⁴⁸. At present, primary HSCs from both human and animal livers are widely used for the research on liver fibrosis²⁴⁸. HSC isolation and culturing strategies have been developed to mimic the ECM scaffold in the liver, including culturing on Matrigel[®] or in suspension^{250, 251}. The available isolation strategies for HSCs are based on enzymatic digestion by collagenase, pronase, and DNase, followed by purification procedures to ensure a pure population of primary human HSCs for further studies⁵⁴. The development of techniques for primary HSCs isolation and cultivation helps to understand HSC function in liver pathophysiological processes, providing a platform for great achievements in related research areas²⁵². However, a significant limitation for use of primary

human HSCs is the limited availability of healthy human liver for cell isolation, as well as the low transfection efficiency²⁵³. Even if primary HSCs are successfully isolated and cultured, the inability to passage these cells in culture is problematic for continuous studies²⁵³. This suggests a need for a stable and repeatable cell model to duplicate the fibrogenesis process to study human liver fibrosis *in vitro*.

5.1.4.1.2 Hepatic Stellate Cell Lines

Although liver fibrosis is a complex process, HSCs are responsible for as much as 80% of the total fibrillary protein, such as collagen I, in fibrotic liver. Hence, human HSCs can serve as a representative model for liver fibrosis *in vitro*⁴⁶. The usage of cell lines may offer many advantages, such as the ease of culture and reproducibility of results from passage to passage. The human HSC lines Lieming Xu-1 (LX-1) and LX-2 were generated from primary HSCs of a male human liver²⁴⁸. The LX-1 cell line was generated from a primary T antigen immortalized clone culture in Dulbecco's modified eagle medium (DMEM) with 10% fetal bovine serum (FBS), while the LX-2 cell line was selected from a subline of LX-1 cells under low serum media conditions (1-2% FBS). Based upon their genetic characteristics, both LX-1 and LX-2 cell lines are utilized as cell line models for liver fibrosis worldwide. Both cell lines retain key features of activated HSCs, such as expression of PDGFR, glial fibrillary acidic protein (GFAP), and α -SMA, and ability to secrete pro-collagen, TIMPs, and MMPs^{54, 254}. Some other cell lines are applied for specific purposes such as LI90 cell line, which was the first human HSC immortalized cells for the study of drug targets in HSC activation, and TWNT-4 cell line, which was generated for antifibrotic drug testing²⁴⁸.

Undoubtedly, the most commonly used human hepatic stellate cell line is LX-2, with conserved characteristics of gene expression (98.7% similarity with primary HSCs), cytokine secretion, and fibrotic protein production²⁵³. The LX-2 cell line is also widely utilized in the study of lipid metabolism, tissue engineering, and endocrinology, besides the common areas of cellular biology and hepatology²⁵⁴⁻²⁵⁷. LX-2 cells retain key features of cytokine signaling, similar gene expression, relatively high transfection efficiency, and fibrotic responses, making it a highly suitable *in vitro* model for human hepatic fibrosis²⁵³. At low passages, LX-2 cell line is a good *in vitro* hepatic fibrotic model to mimic the pathophysiological response, and the experimental data may be translated to the human disease condition. As normal human stellate cells, LX-2 cells can also be used to assess the differences between quiescent and activated human HSCs with the typical properties as observed in primary culture, but

under low serum culture conditions²⁵⁸. Isolated HSC lines from rat and mouse are also used as tools for liver fibrosis but are not as popular as human cell lines²⁵⁹.

Although the genetic profile and phenotype switch of LX-2 cells are well characterized, the unavoidable disadvantages caused by the subculture of these cells are still bothersome. The expression of cell markers and the functionality of the LX-2 cell line demonstrated stability for only ten passages, and the reported research was usually done within a range of three to ten passages without significant phenotype alterations^{252, 254}. With repeated passaging, LX-2 cells may undergo genotypic or phenotypic drift, which may lead to heterogeneity in their sublines²⁵⁴. An even more important limitation of the monoculture is that LX-2 itself does not perfectly reflect cell migration features observed *in vivo* and the correlation of HSCs with other mesenchymal and parenchymal cells within the process of fibrogenesis and resolution.

5.1.4.1.3 Co-culture Models

Although useful and easy to perform, the research based on monoculture may not adequately reflect the complicated processes of fibrogenesis and the interaction between different therapeutic targets with treatment²⁴⁸. Even though HSCs serve as the central modulator of liver fibrosis and eventually carcinoma, hepatic fibrogenesis is still a multi-cellular process, including the recruitment of inflammatory cells, as well as the migration of different types of cells such as endothelial cells, HSCs, and certain macrophages^{42, 260-262}. Thus, it is necessary to develop reasonable co-culture model(s) to study the dynamic responses of key potential cell types. Currently, there are many well-established methods for hepatic co-cultures that include two and three cell types in attempts to mimic the microenvironment of the liver. Due to the involvement of parenchymal as well as non-parenchymal cells in the sinusoidal structure, endothelial cells, Kupffer cells, and HSCs are usually considered in co-cultures for liver fibrosis²⁶³.

One typical simple example is the co-culture system of hepatocytes and HSCs, usually primary hepatocytes with hepatic stellate cell line in a quiescent state²⁴⁸. Recently, the use of this co-culture system demonstrated that cell interaction is important to stimulate fibrogenesis *via* lipid accumulation²⁶⁴. For this model, several different methods are available to culture hepatocytes and HSCs together for different purposes. LX-2 cells in hanging cell inserts were placed in 6-well plate with Huh7 cells to discover the mechanisms of sorafenib resistance in hepatocellular carcinoma microenvironment with HSCs involvement²⁶⁵. Primary

macrophages and cholangiocytes are isolated and cocultured together onto monolayer to measure apoptosis and cytokine secretion *via* certain mechanisms²⁶⁶. Other models for liver fibrosis such as co-culture of HSCs and macrophages, Kupffer cells, or endothelial cells, with or without hepatocytes, were also established for certain purposes²⁶⁷⁻²⁶⁹. More complicated co-culture systems (i.e., more cell types involved in the model) enhance the opportunity to reflect the real *in vivo* response in liver fibrosis. For instance, a co-culture of four liver cell types was established by plating hepatocytes on top of a precultured confluent layer of non-parenchymal cells²⁷⁰. Another 3D co-culture system consisting of hepatocytes in a collagen gel and a mixture of mesenchymal cells on top of the gel contained all liver cell types but this system did not allow for direct cellular interactions between different cell types²⁷¹. Such systems make it more difficult to determine proper co-culture conditions and result in complications in the interpretation of experimental outcomes. Thus, the cell types composed in the co-culture system, as well as the pattern of the system, should be determined by the purpose of the study, and the interpretation of results would depend upon the system and culture condition.

5.1.4.2 *Ex vivo* Models of Hepatic Fibrosis

Precision-cut liver slices are a common *ex vivo* model and have been used in the study of liver fibrosis. Liver slices are an alternative model to overcome some deficiencies of cell culture models such as the diffusion and penetration of the pathological and therapeutic molecules into the pre-cut organ slices²⁷². Precision-cut liver slices came into attention as a potential model to study liver fibrosis because this model maintained cell-to-cell interactions and cellular interactions with the ECM⁵⁰. Although precision-cut liver slices from human liver have successfully been used to investigate antifibrotic compounds, limitations include diffusion and penetration of the pathological and therapeutic molecules throughout the liver slice, as well as the duration of the slice viability, where incubation times generally could not exceed 72 hours²⁷²⁻²⁷⁴.

The combined usage of different *in vitro* and *ex vivo* models to study fibrogenesis and resolution of liver fibrosis has contributed considerable understanding to the molecular mechanisms of this process. However, their limitations in mimicking the real condition of liver fibrosis necessitate the use of *in vivo* models for hepatic fibrosis to better appreciate the development of fibrosis and possible therapeutic approaches for its resolution.

5.1.4.3 *In vivo* Models of Hepatic Fibrosis

Several common *in vivo* models for hepatic fibrosis are available to address the different causes of liver fibrosis in human. These *in vivo* models overcome the failure of *in vitro* models as they consider the involvement of other tissues and systemic factors such as the immune system and the impact of other organs⁵⁰. Continuous liver injury resulting from chemical, nutritional, and biological stimuli, or interrupted blood flow and reperfusion, often lead to liver fibrosis coupled with a series of subsequent responses including inflammation, oxidative stress, immune cell recruitment, and cell survival, proliferation, migration, and differentiation²⁷⁵. Thus, there could be many ways to induce the development of liver fibrosis *in vivo*.

5.1.4.3.1 Diet- or Chemical-stimulated Models

Diet-induced or chemical-stimulated liver fibrosis animal models are widely used to study nutritional and toxic etiological factors and the underlying mechanisms to reverse fibrogenesis in the liver. Several frequently applied diet-induced *in vivo* animal models have contributed to the study of liver fibrosis for decades²⁷⁶. A high-fat diet fed for seventeen weeks in mice induces liver fibrosis as chronic non-alcoholic steatohepatitis (NASH) or NAFLD²⁷⁷. Fifteen to twenty weeks of dietary Vitamin A depletion for mice and ten-week choline-deficient diet for rats also leads to liver fibrosis^{278, 279}. Ethanol-induced liver fibrosis is also used, which may mimic alcoholic fatty liver diseases and could be a good model, combined with the presence or absence of other dietary factors^{81, 248}.

A number of chemical-stimulated models are available to cause liver fibrosis. The common compounds used in the literature include carbon tetrachloride (CCl₄) and dimethyl-nitrosamine (DMN), usually by intraperitoneal injection to mice or rats. CCl₄ induces hepatotoxicity following bioactivation by hepatic cytochrome P450 (CYP450) enzymes concomitant with lipid peroxidation and eventually leads to liver injury accompanied by fibrogenesis²⁸⁰. DMN modulates the expression of drug-metabolizing enzymes causing hepatocyte necrosis and nodular degeneration²⁸¹. CCl₄ administered twice a week for at least ten weeks, or DMN once daily continuous administration for five weeks, induces hepatic fibrosis in rats or mice^{203, 214}. These chemical derived models are popular because of their reproducibility and similarity of mechanisms in human liver fibrosis²⁴⁸.

Diet- or chemical-induced hepatic fibrosis is not limited to the above models. Different diet or chemicals and their combination along with different durations of administration to stimulate hepatic fibrosis in animals can be considered to reach the diverse goals of fibrosis research.

5.1.4.3.2 Infection- or Surgery-induced Models

In addition to diet-induced models, two additional experimental models of hepatic fibrosis are infection- and surgery-induced liver fibrosis. Although immunologic responses are involved in almost all pathological causes of liver fibrogenesis, other than the inflammatory responses caused by indirect causes, distinct models of infection can result in fibrosis. Surgery-induced models, which are induced by common bile duct ligation (BDL), are also known as biliary derived models²⁸².

Infection-induced liver fibrosis models include but are not limited to infections caused by endotoxin, virus, heterologous serum, or parasites in rodents or other species²⁴⁸. Inhibition of pro-inflammatory cytokine Il-17 signaling results in an antifibrotic effect *via* reductions in collagen production in fibroblasts²⁸³. Hepatitis B virus is also reported to induce fibrosis in mice²⁸⁴. The immune response caused by any kind of infection contributes to the secretion of pro-fibrotic cytokines or chemokines subsequently contributing to HSC activation and thus to hepatic fibrogenesis²⁴⁸. More recently, it was demonstrated that endotoxin, or lipopolysaccharide (LPS), contributes to liver fibrosis by activating HSCs or modulating the immune response²⁰⁵.

Common BDL is a well-known surgery model leading to biliary fibrosis, which is usually applied in rats and mice. The ligation of the bile duct evokes the proliferation of fibroblasts and bile duct cells, with subsequent increases in biliary pressure. This causes inflammatory reactions and pro-fibrotic cytokine production by biliary epithelial cells, generating cholestatic injury to the liver²⁸⁵. Although the BDL model is feasible technically and is an appropriate model for portal hypertension, one of the drawbacks is that BDL results in many secondary complications in the animal, which makes the interpretation of fibrosis difficult²⁸⁶.

5.1.4.3.3 Genetic models for Hepatic Fibrosis

Genetic models are available to investigate liver fibrosis in animals. These models

allow assessment of the role of specific signaling pathways in hepatic fibrosis. Gene knockout technology is popular because it leads to many breakthroughs in liver fibrogenesis research²⁸⁷. For instance, liver TGF- β 1R knockout mice indicated that the absence of TGF- β signaling plays a dominant role in reducing hepatic fibrogenesis²⁸⁸. There are also other knockout models for different targets used to study certain signaling pathways and genetic models have been widely used in the past decades. Additionally, diet combined with genetic models helps to confirm certain pathways – the deficient gene expression in that model, as well as the importance of the diet-related factors^{278, 289}. Despite the availability of different knock-out models, the mechanisms of every single phenotype, as well as the interaction between different genes, are still unclear²⁸⁷. Further progress on genetic models for liver fibrosis is needed.

None of the aforementioned *in vitro*, *ex vivo*, or *in vivo* models accurately reflect the many kinds of chronic liver disease induced fibrosis in human. Often, investigators use two or more models to assess the pathogenesis and reversal of hepatic fibrosis to overcome the weakness of a single model depending upon the purpose of their study⁵⁹. As the development and resolution of liver fibrosis is a multi-cellular and multi-pathway process, *in vivo* models are necessary to study the antifibrotic effects and mechanism(s) of multi-target drugs as potential antifibrotic therapies.

5.2 TKIs and Possible Mechanisms of TKI Action in Hepatic Fibrosis

The traditional therapeutic approach concept of considering “one disease, one medicine” is generally inadequate for a number of human chronic diseases. Since the sequencing of the human genome and our advanced knowledge of molecular networks of disease, an emerging concept, “several diseases, one medicine”, provides a rationale to a new therapeutic approach – drug repurposing^{136, 290}. With a need for network medicine, multi-target drugs provide an opportunity to make this new concept an alternative approach for human disease, especially for chronic diseases.

Tyrosine kinases (TKs) are key regulators of signaling transduction pathways that regulate normal cell processes such as differentiation, metabolism, and apoptosis²⁹¹. TKs also play a key role in many diseases such as hypertension, cancer, and cirrhosis as the pathologic activation of these enzymes may drive the development of processes such as abnormal cell proliferation and activation of fibrotic pathways¹⁰⁹. Transactivation of TKs has an essential

role in inflammation and healing response by activating target proteins *via* interfering with a number of TK transduction cascades²⁹². Consequently, the TKs play key roles in many diseases including sclerosis, and fibrosis and pathological activation of TKs may cause fibrogenesis and other diseases²⁹³. Small molecule TKIs block the kinase domains after entering the cell and inhibit the downstream activities²⁹³. As a class of multi-target drugs, some TKIs show promise as a new therapy for liver fibrosis. Both preclinical and clinical studies have demonstrated antifibrotic effects of TKIs in different fibrotic diseases, such as imatinib, gefitinib, and nintedanib for pulmonary fibrosis, ibrutinib for pancreatic fibrosis, and imatinib and sorafenib for liver fibrosis^{9-11, 281, 294-296}. Increasing evidence suggests that there is a potential for certain TKIs to serve as antifibrotic agents in hepatic fibrosis.

TKs can be classified into receptor and non-receptor TKs. Receptor TKs activate intracellular pathways by transducing extracellular signals into the cell, while non-receptor TKs transduce signals within the cytoplasm²⁹⁷. Tyrosine phosphorylation or autophosphorylation of the intracellular kinase domain then leads to the activation of receptor and non-receptor TKs and regulates a wide variety of cell processes, including metabolism, growth, proliferation, and apoptosis^{109, 292}. Single or multiple kinase inhibitors targeting receptor or non-receptor TKs account for about a quarter of current drug development and have demonstrated promising results in suppressing fibrosis. However, the mechanisms through which the TKI drugs affect the fibrotic pathway are still not clear and little evidence has been reported for hepatic fibrosis specifically²⁹⁸. Based on the understanding of TKs and TKIs, we investigated the antifibrotic effects and possible mechanisms of TKIs as repurposed therapeutic agents in liver fibrosis.

5.2.1 RTKs

RTKs mediate the transfer a phosphate group from ATP to a protein within the cell. This function has considerable influence on cell growth and cytokine signaling pathways²⁹⁹. RTKs contain a transmembrane domain, and therefore act as membrane receptors. Ligand binding to these receptors activates signal transduction pathways that modulate cell growth and cytokine secretion^{300, 301}. Over 58 RTKs have been identified, including EGFR, fibroblast growth factor receptors (FGFR), PDGFR, VEGFR, and hepatocyte growth factor receptors (MET)^{299, 300}. RTKs are common drug discovery targets for a number of proliferation dysfunction diseases and immune disorders²⁹⁹. Except for the insulin receptor (InsR), which are disulfide linked dimers, all known RTKs exist as monomers in the cell membrane. Ligand

binding induces the dimerization of the monomeric receptors, while insulin rearranges a heterotetrameric structure of InsR. Both binding formats induce auto-phosphorylation of the RTK's cytoplasmic domain with the following signaling pathways²⁹¹.

5.2.1.1 EGFR

The EGFR/ErbB family plays a key role in cell proliferation, differentiation, and growth. The EGFR/ErbB family consists of four transmembrane RTKs: EGFR/HER1 (Human Epidermal Growth Factor Receptor 1), ErbB2/HER2, ErbB3/HER3, and ErbB4/HER4³⁰². EGFR is important for the growth of some cancer cells and fibrotic diseases^{109, 303}. Downstream factors of EGFR signaling include the MAPK, PI3K-Akt-mTOR, and JAK, which are all involved in the development and resolution of fibrogenesis (**Figure 5.3**)^{304, 305}. Inhibition of PI3K/Akt-mTOR pathway in cancer with EGFR mutations can suppress glycolysis, promoting cellular glucose metabolism³⁰⁶. Once bound by ligands, EGFR/HER would modulate different pathways including Raf, PI3K, MAPK, and NF- κ B and significant crosstalk exists between these pathways to modulate cell growth and proliferation³⁰⁵. *In vitro* studies suggest EGFR enhances the expression of TGF- β receptor in dermal fibroblasts, but the mechanism is not clear³⁰⁷. As well, evidence suggests that ErbB receptor activation contributes significantly to lung fibrosis and cooperates with PDGF in TGF- β -stimulated responses^{94, 308}. Inhibition of EGFR prohibited the development of pulmonary fibrogenesis in rodents³⁰⁹. PKM2 regulation may pose another possible pathway through which TKI drugs might modulate liver fibrosis at a metabolic level because pyruvate kinase has an intracellular domain with TK activity⁶³. Gefitinib, as an EGFR-TKI, might function through the modulation of nuclear PKM2 followed by signal transducer and activator of transcription (STAT) activation in cancer cells³¹⁰. This suggests a possible link between pyruvate kinase and TK in liver fibrosis. According to the above aspects, PKM2 might be a putative novel mechanism of TKI drugs in fibrosis resolution.

The administration of several EGFR-TKIs increases the production of proinflammatory cytokines, leading to cell apoptosis in intestinal epithelial cells *via* triggering ER stress response³¹¹. In cancer cells treated with erlotinib, an EGFR-TKI, suppression of autophagy acts synergistically with the EGFR-TKI to overcome drug resistance *via* modulating ER stress-induced apoptosis³¹². One of the underlying cellular mechanisms might be that upregulation of CHOP increases PERK and then induces eIF2 α phosphorylation to subsequently switch the ER stress response from pro-adaptive to pro-apoptotic signaling,

finally leading to apoptosis of cancer cells^{313, 314}. Since the ER stress response is involved in EGFR-TKI-stimulated apoptosis of intestinal epithelial and cancer cells, it is promising that EGFR-TKIs might work *via* similar mechanisms in other cell proliferation dysfunction conditions such as hepatic fibrosis.

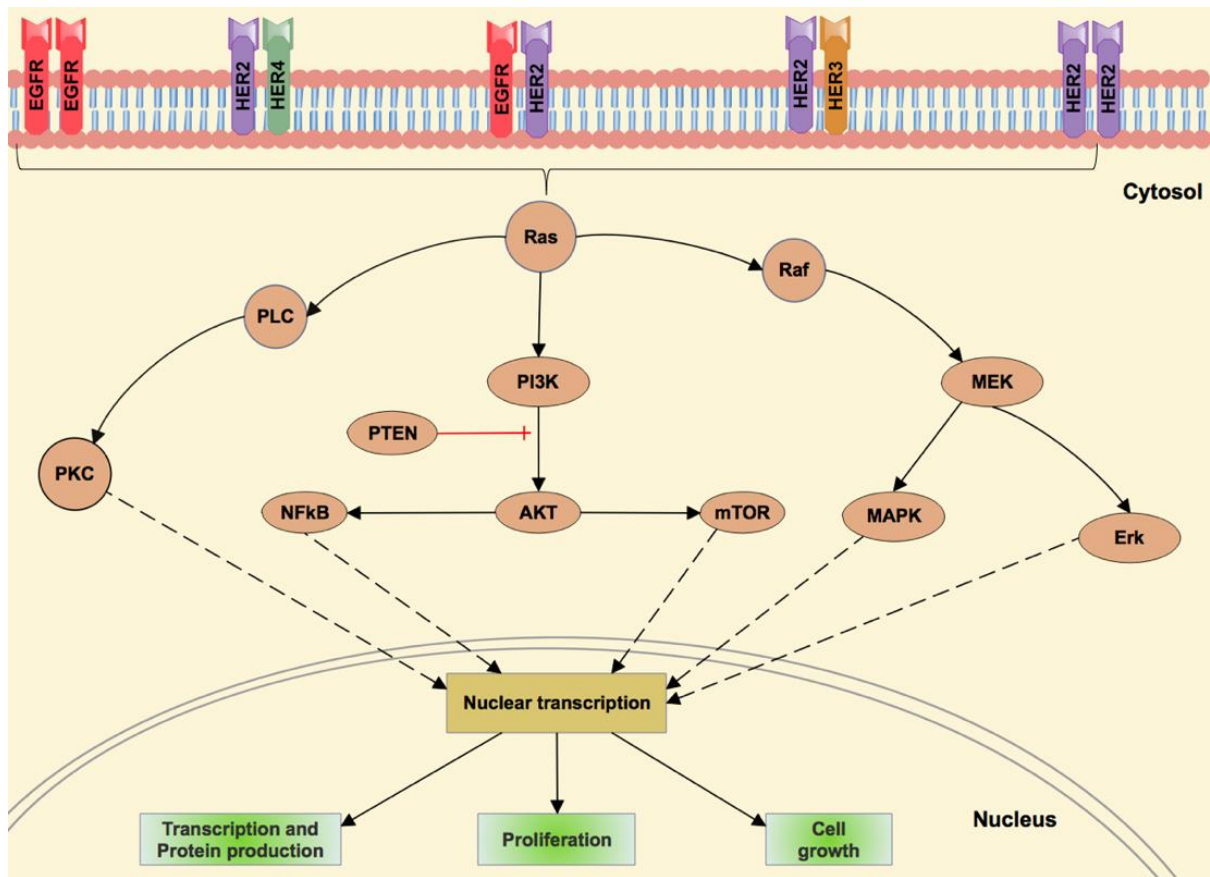


Figure 5.3 The main transduction pathways regulated by the epidermal growth factor receptors (EGFR) family members—EGFR/HER1, HER2, HER3, and HER4. Many pathways are involved in the modulation of EGFR, playing roles in many cellular processes such as cell proliferation and nuclear transcription. Adapted from Fornaro et al (Permission license number: 4831430901474)³⁰⁵.

5.2.1.2 FGFR/VEGFR/PDGFR

Many RTKs are implicated in the development and progression of fibrosis, including FGFR, VEGFR, and PDGFR²⁹³. All these RTKs have shown potential to be antifibrotic targets in hepatic fibrosis, such as sorafenib targeting VEGFR and PDGFR for hepatic and lung fibrosis, and brivanib targeting FGFR and VEGFR for hepatic fibrosis³¹⁵.

The FGFR pathway plays an essential role in angiogenesis, wound healing, and cell migration. Consequently, therapeutic approaches targeting FGFR have become popular in the chemotherapy field³¹⁶. Most FGFs contain a heparin sulfate proteoglycan region and a high sequence homology region, the binding of FGFRs by these ligands may cause the activation of many downstream pathways involved in many cellular processes, such as MAPK/Erk, PKM2, PI3K/Akt, and STAT transcription factors^{317, 318}. Inhibition of FGFRs by sunitinib may contribute to the effect in renal and gastrointestinal stromal tumors³¹⁹. However, in recent decades, FGFR signaling has been well studied for tumorigenesis but not fibrosis.

VEGF signaling can stimulate the production of ECM molecules and may have profibrotic effects in many renal diseases^{320, 321}. VEGF belongs to the VEGF/PDGF family of heparin-binding growth factors with a highly conserved receptor-binding cystine-knot structure³²². There are five ligands for three types of VEGF receptors (VEGFR1, 2, and 3), accounting for the complexity of the downstream modulation by this signaling pathway²⁹³. VEGF is secreted by many cell types including diverse tumor cells, macrophages, and aortic vascular smooth muscle cells³²³. Oxygen tension is reported as a key physiological modulator of VEGF expression *via* binding of the HIF-1 to HRE, which may be involved in the modulation of hepatic fibrogenesis³²². The literature and experimental evidence for the profibrotic role of VEGF, though, is still limited.

Several small molecule TKIs have shown an ability to inhibit certain promising targets for fibrosis such as Abelson murine leukemia viral oncogene homolog (Abl) and PDGF receptor¹⁰⁸. In the progression of hepatic fibrogenesis, PDGF signaling becomes activated due to tissue injury, promoting the wound-healing response¹⁰⁷. As indicated above, PDGF and TGF- β are mediators which can induce the activation of many downstream signaling pathways such as Erk, PI3K/Akt-mTOR in activated HSCs²⁰⁷. Given the crucial role of PDGF in fibrosis, inhibition of PDGFR seems to be a promising therapeutic approach for tissue fibrosis²⁹³.

5.2.1.3 Other RTKs

InsR is another target for TKIs which can show further downstream manipulation on P85 and PI3K, and PPAR γ agonist rosiglitazone modulates insulin sensitivity and insulin-receptor-substrate protein serine phosphorylation³²⁴. Furthermore, there are many non-RTKs that might serve as targets in fibrosis.

5.2.2 Non-RTKs

Compared with the RTKs, non-RTKs cannot bind to ligands but can be activated by TKs in the cytoplasm, consequently initiating transcriptional responses *via* modulating downstream signaling cascades²⁹². There are 32 non-RTK, placed into 10 subfamilies based upon their kinase domain sequence³⁰⁰. Among the non-RTKs, some can mediate the TGF- β -induced fibrotic progression, such as c-Abl, c-Kit, and Src kinases²⁹⁷. Nilotinib, a TKI of breakpoint cluster region (Bcr)-Abl used primarily for chronic myeloid leukemia, has antifibrotic activity to attenuate the development of liver fibrosis in experimental fibrosis *via* multiple pathways¹⁰⁸. Dasatinib and imatinib, also as Bcr-Abl TKIs, show ability to increase PPAR γ expression at both gene and protein level, suggesting that these TKIs have an opportunity to treat disease *via* the modulation of PPAR γ which regulates proliferative or apoptotic downstream targets such as PKM2, PI3K, and STAT^{156, 325}. Bcr-Abl TKIs are also reported to induce the expression of many genes involved in ER stress signaling pathways. Nilotinib shows ability to induce ER stress and apoptosis in H9c2 cells, as well as in imatinib-resistant leukemic cells^{326, 327}. It is believed that members of JNK cell signaling pathway bridge ER stress response and apoptosis *via* the upregulation of cytochrome c-mediated cell death pathways, such as c-Jun and c-Fos mRNA and protein³²⁷⁻³²⁹. Current literature evidence illustrates that ER stress-induced apoptosis might be a pathway involved in TKI's effects on cell proliferation dysfunction diseases.

The accumulated evidence, thus far, indicates that certain selective TKIs that specifically modulate HSCs or other cells or pathways during the fibrogenesis might be repurposed for this disease state³³⁰. Usage of TKIs with ability to inhibit different key receptors, such as gefitinib as an EGFR inhibitor, ibrutinib as a multi-target TKI drug with its major target BTK/BMX, and Dabrafenib as a non-ErbB (B-raf) TKI drug, may help elucidate novel mechanisms involving the well-known pathways through which some TKIs may

favorably modulate liver fibrosis pathogenesis. Use of different targeted TKI drugs might provide a broader map for TKIs in hepatic fibrosis to provide guidance for further drug discovery and development.

Unfortunately, the clinically available TKIs have dose and treatment limiting toxicities such as cardiotoxicity, lung toxicity, hepatotoxicity, and gastrointestinal upset^{14, 315, 331, 332}. An option to improve their clinical effectiveness might be their combined administration with natural products that have additive or synergistic effects to allow for dosage reduction of TKIs for effective treatment of liver fibrosis. Recent studies indicate that the lignans upregulate the expression and activity of PPAR γ and may have a considerable influence on the activity of PPAR γ ³³³. Considering the possibility of lower toxicity with PPAR γ partial agonists and the possible activation effects of lignans on PPAR γ , the combination of lignans and PPAR γ partial agonists might be beneficial for the resolution of liver fibrosis without undesirable adverse responses.

5.3 Flaxseed Lignans

5.3.1 Brief Overview on Natural Products

The medical use of natural products, including herbal remedies, traditional medicines, and other products, has become increasingly popular in the past decades because of their diverse biological and pharmacological activities which indicate a therapeutic potential against many diseases^{334, 335}. Natural products, as a source of numerous therapeutic agents, are usually defined as secondary metabolites produced by organisms that show biological functions against a broad range of challenges including infections, fibrogenesis, as well as cancer^{17,336}. Over the past 85 years, natural products have shown important capability in cancer and infectious diseases, becoming a source of innovation in drug discovery and development³³⁷. The most commonly studied natural products for liver injury are curcumin (the polyphenolic pigment in turmeric), oxymatrine (extracted from the roots of Sophora plants), different kinds of lignans, wogonin (a mono-flavonoid isolated from *Scutellaria radix*), among others^{17, 188, 260, 338}. These studies suggest an ability to treat fibrosis and resolve the progression of fibrosis in the liver.

Nearly half of liver therapy agents today are natural products or derived from natural products. In the US and Europe, approximately 65% of liver disease patients take natural products as a treatment for liver disorders and other pathological conditions¹⁷. Many natural products have clinical efficacy for liver fibrosis. For example, metformin can suppress TGF-

β -induced fibrosis through inhibition of EMT³³⁸. Curcumin has an ability to inhibit many pro-inflammatory and pro-fibrotic cytokines, including inhibition of NF- κ B pathway, as well as exhibiting anti-oxidative responses in many liver diseases *via* modulation of various targets³³⁹. In general, natural products might mediate antifibrotic effects through mechanisms that include anti-inflammatory responses, inhibition of cytokines, modulation of nuclear receptors, and modulation of epithelial-mesenchymal and mesenchymal-epithelial transitions¹⁵.

In the present age of natural product drug discovery, natural products have become a preference for many human diseases due to the low toxicity risk and demonstrated efficacy³⁴⁰. This is true of the plant lignans, an important family of natural products, which exist as glycosides in many foods such as flaxseed, sesame seed, and vegetables³⁴¹. Lignans, as natural plant polyphenols, are secondary plant metabolites derived biosynthetically from phenylpropanoids with low molecular weight³⁴². Lignans are found in various foods including plant seeds, vegetables, and fruits, and are highly concentrated in the hull of flaxseed suggesting that they are major components contributing to the beneficial effects of flaxseed³⁴³. Lignans are a large group of secondary metabolites produced from the oxidative dimerization of two phenylpropanoid units³⁴⁴. Lignans, neolignans, and other types are continuously reported and studied, including the dibenzylbutanes, aryl-naphthalenes, benzofurans, oligomeric lignans, and hybrid lignans³⁴⁵. As lignans are extensively distributed in plants with potent anti-viral, anti-fungal, antioxidant, and insecticidal actions, lignans may play an important role in plant defense against various pathogens³⁴⁶. Lignans receive attention as potential therapeutic compounds because of their diverse bioactivities such as antioxidant and anti-inflammatory activities³⁴². Among plant derived foods, flaxseed contains the highest concentration of the lignan, secoisolariciresinol diglucoside (SDG), which is receiving increasing attention due to its health benefits³⁴⁷.

5.3.2 Flaxseed Lignans

Flaxseed, historically used as an industrial oil, a source of fiber production, as well as food, is gaining increasing interest as a functional supplement because of its biological and pharmacological activities³⁴⁸. Flaxseed contains 35-45% oil, of which around 50% is α -linolenic acid (ALA, omega-3 fatty acids), 20% protein, 25% fiber, lignans, and micronutrients including minerals and vitamins³⁴⁹. Among these components of flaxseed, dietary fiber, ALA, and lignans, have been identified as three major components that elicit

the biological activities of flaxseed³⁵⁰. As one of the richest sources of plant lignans and a rich source of dietary fiber as well as ALA, flaxseed can lower serum and hepatic triglyceride and cholesterol levels in hyperlipidemic patients, as well as maintain the healthy intestinal environment³⁵¹⁻³⁵³. It is also reported that flaxseed consumption improves lipid abnormalities and reduces systemic inflammation in hemodialysis patients with lipid homeostatic problems, but the mechanism is not clear³⁵⁴.

Flaxseed is particularly rich in lignans, mainly SDG, and also contain small quantities of the lignans matairesinol, pinoresinol, and isolariciresinol³⁵⁰. SDG exists in the flaxseed hull as an oligomer complexed with hydroxymethylglutaric acid and following oral consumption may undergo hydrolysis forming Secoisolariciresinol (SECO), with further metabolism to the mammalian lignans, enterodiol (END) and enterolactone (ENL), by the colonic microflora³⁵⁵. SECO, END, and ENL may undergo subsequent phase II metabolism in the mammalian system, usually by uridine 5'-diphospho-glucuronosyltransferases (UGTs) and sulfotransferases and exist systemically primarily as lignan conjugates of glucuronic acid and sulfates³⁵⁶. Previous data of our lab demonstrated that conjugates of SECO, END, and ENL primarily exist in the systemic circulation with low levels of parent SECO, END, and ENL³⁵⁷. Current knowledge of flaxseed lignans shows that these major components are involved in the health benefits attributed to flaxseed or flaxseed extracts^{350, 358}.

5.3.2.1 Biological Function of Flaxseed Lignans

Flaxseed lignans, as a group of unique biphenolic structural compounds, have shown various pharmacological functions such as anti-cancer, antiviral, cardiovascular protection, and antioxidant activities³⁴⁵. Flaxseed consumption is associated with a reduction in the risk of breast cancer possibly due to the abundant SDG as well as its metabolites, END and ENL, *via* suppression of cell proliferation and induction of apoptosis^{350, 359}. END and ENL are also reported to show anti-tumor effects against prostatic carcinoma as well as colon cancer, probably working *via* hormone dependent or independent pathways³⁶⁰. Inverse association between serum concentration of ENL and breast cancer risk has been reported in breast cancer cases^{361, 362}. SDG and its metabolites can inhibit lipid peroxidation with higher antioxidative ability than Vitamin E³⁶³.

Flaxseed lignans also have purported health benefits against many chronic diseases including obesity and diabetes, with reported ability to protect lung and liver function through anti-inflammatory and antioxidant properties^{21, 364, 365}. SDG may inhibit the gene

expression of phosphoenolpyruvate carboxykinase, a key enzyme responsible for gluconeogenesis in the liver³⁶⁶. Epidemiological studies also demonstrated that high concentrations of ENL in the serum are associated with low risk of acute coronary events^{367, 368}. Since the components of flaxseed may provide health benefits, more people turn to the consumption of flaxseed or flaxseed derived products in Canada as well globally for chemoprevention and therapeutic purposes^{369, 370}.

5.3.2.2 Pharmacokinetics and Safety Properties of Flaxseed Lignans

Experimental and clinical studies indicate that the enterolignans, END and ENL, are the major metabolites of flaxseed plant lignans (e.g., SDG) and their aglycones (e.g., SECO)³⁷¹. The oral bioavailability of flaxseed lignans is influenced by the product form, as well as gastrointestinal bacterial populations³⁷². Upon oral consumption, the glucose groups are cleaved from SDG to produce the aglycone SECO. SECO is subsequently catalyzed by bacterial metabolic enzymes to END and then to ENL. During the absorption process, the enterolignans undergo phase II metabolism to produce conjugated forms such as ENL-glucuronide before their entrance into the systemic circulation. Most of the lignan dose is excreted from the body as the conjugated metabolites³⁷¹. SECO, END, and ENL and their conjugated metabolites reach the systemic circulation and may be responsible for the health benefits³⁷⁰.

5.3.2.2.1 Bioavailability of Flaxseed Lignans

The bioavailability of flaxseed lignans depends upon the form and consumption pattern of flaxseed supplementation, as this influences the access to and residence time of the lignan in the GI tract³⁴⁷. Low oral bioavailability of certain lignans limits the usage of flaxseed lignans as a therapeutic agent because of the extensive first-pass effect after oral administration³⁵⁶. Changing the formulation of flaxseed products may help the absorption of flaxseed lignans. For instance, long-term intake of roasted flaxseed powder improved both blood pressure and lipid profiles in dyslipidemic patients, but no bioavailability data have been reported for this formulation yet³⁷³. In a crossover study, the relative bioavailability of enterolignans for crushed flaxseed was increased significantly compared to whole flaxseed from 28% to 43%, possibly due to the improved accessibility of intestinal bacteria to the lignan in crushed flaxseed³⁴⁷. In another reported PK study in male Wistar rats, the oral

bioavailability for SECO is approximately 25%, while the values for END and ENL are less than 1%³⁵⁵. Enterohepatic recirculation of mammalian lignans is reported in humans and pigs^{374, 375}. In a human PK study, an increased exposure of ENL and a second peak of END in plasma after oral administration of purified SDG demonstrated that both END and ENL undergo enterohepatic recycling³⁷⁴.

Disease condition can also alter the absorption of flaxseed lignans. In hepatic fibrotic rats, the relative bioavailability of lignans is significantly higher than in normal rats, suggesting that the absorption of lignans might be enhanced in hepatic fibrosis patients³⁷⁶. Other lifestyle-related diseases may also influence the absorption of flaxseed lignans either through modulation of bacterial metabolism prior to the absorption of lignans into the systemic circulation or through changes in first pass metabolism³⁷⁷. So, it is crucial to determine the intake of flaxseed lignans as precursors of enterolignans which are the likely bioactive compounds mediating the health benefits of flaxseed consumption.

5.3.2.2 Distribution of Flaxseed Lignans

Flaxseed lignans are widely distributed to the whole body as conjugated forms. The apparent volume of distribution and plasma protein binding of flaxseed lignan metabolites increased with hydrophobicity due to greater tissue partitioning of these lignan metabolites, which has been confirmed in rats (SDG<SECO<END)³⁵⁵. SDG is the most polar lignan form, with decreasing polarity observed with the aglycone, SECO, and the mammalian lignans, END and ENL. The serum concentrations of SECO, END, and ENL reaches steady state within 2 weeks³⁷⁸. In rats, lignans accumulate in the GI tract, lung, liver, kidney, skin, and uterus or prostate with considerable concentrations^{379, 380}.

Serum protein binding of flaxseed lignans showed an ascending order with hydrophobicity where SECO, END, and ENL had values of 67%, 93%, and 98%, and ENL showed no partitioning and accumulation into red blood cells³⁵⁵. Furthermore, both END and ENL are reported to bind to human sex binding globulin (SHBG) and the binding affinities are influenced by the substitution pattern of aromatic rings both *in vitro* and in humans³⁸¹. In rats with increasing levels of SDG consumption, END concentrations increased accordingly in the liver, prostate, lung, and testes, indicating that the accumulation of lignans within these organs may suggest a potential benefit under certain pathological conditions³⁸². Overall, the distribution of flaxseed lignans is influenced by many factors and, therefore, impact the effects of flaxseed lignans depending upon the amount of active compounds reaching the site

of action.

5.3.2.2.3 Metabolism and Elimination of Flaxseed Lignans

Flaxseed lignans undergo biotransformation by bacterial and mammalian enzyme systems prior to their entry into the systemic circulation following oral administration. SDG undergoes deglycosylation by microflora in the colon to its aglycone form, SECO. SECO subsequently undergoes dehydroxylation and demethylation to END, which is further oxidized to produce ENL. The enterolignans, END and ENL, undergo limited cytochrome P450 enzyme-mediated metabolism, typically hydroxylation at aromatic and aliphatic sites producing mostly monohydroxylated metabolites^{355, 383}. The flaxseed lignans undergo phase II metabolism such as glucuronidation or sulfation by UGT or sulfotransferase enzymes, respectively, in both intestinal and hepatic cells, and the conjugated END and ENL are the major end-products of flaxseed lignans (**Figure 5.4**)^{357, 384}. The involvement of conjugation in the liver and the GI tract, in addition to enterohepatic recirculation, leads to a considerable increase in the exposure of the intestine to lignans³⁸⁵.

In rats, flaxseed lignans have short beta half-lives in ascending order of SDG (0.5h), END (1.8h), and SECO (4h) and are eliminated within 48 hours after SDG administration³⁵⁵. The elimination half-lives of END and ENL are 4.4 and 12.6 hours, respectively, predicted at steady state after dietary supplementation of lignans in humans³⁴⁷. The flaxseed lignans are mainly excreted by feces and urine. About 77% of the radioactivity detected in the urine after oral administration of radiolabeled SDG in rats existed mainly in the form of conjugates³⁵⁵. Almost 48% of administered lignan is fecally excreted in pigs, and both fecal and urine excretion were observed in humans, presenting as metabolites, not as parent compound^{375, 386}. Food consumption and age impact both the urinary and fecal excretion of flaxseed lignans, for instance, premenopausal women with different diets showed a difference in the lignan urinary excretion while vegetarian diet increased the excretion of ENL in young women but not in senior vegetarians^{387, 388}.

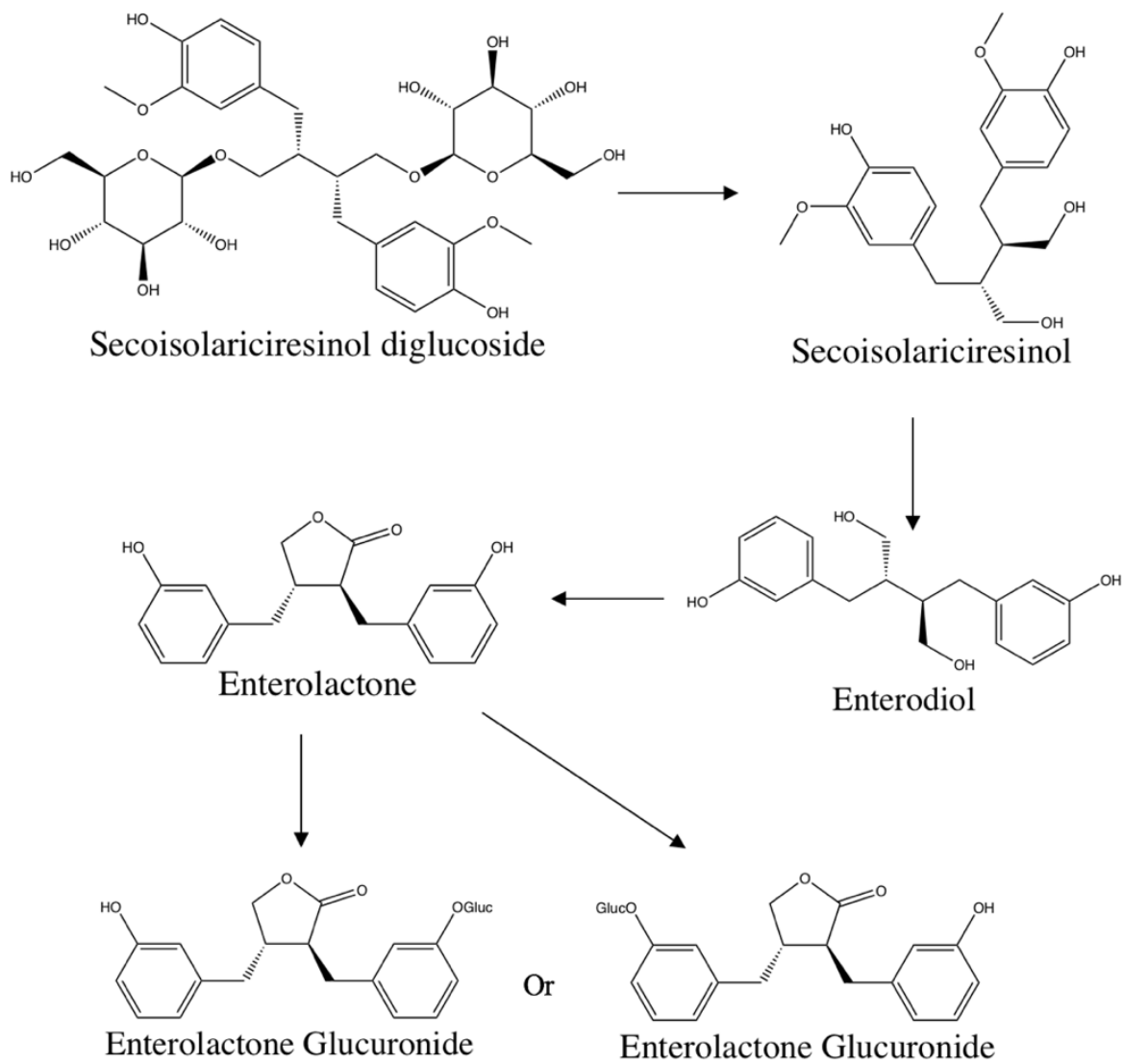


Figure 5.4 Metabolic pathway of flaxseed lignan, secoisolariciresinol diglucoside (SDG) in the GI tract. SDG undergoes glycolysis and fermentation to yield its aglycone form secoisolariciresinol (SECO). SECO is then converted into enterodiol (END) by diverse bacteria, most of which is metabolized to ENL by serial reactions³⁷¹. ENL, as well as END and SECO, undergo conjugation to yield its glucuronidated or sulfated forms (not shown in the picture).

5.3.2.2.4 Safety of Flaxseed Lignans

As research continues into the potential health benefits of flaxseed lignan products, it is necessary to determine the safety properties of long-term use, especially long-term supplementation in both healthy populations and populations with chronic health conditions. Whole flaxseed products contain cyanogenic glycosides and linatine, an anti-pyridoxine factor known to impact the safety and tolerability of flaxseed consumption. Although high doses (e.g., 1 kg) of ground flaxseed could cause acute cyanide toxicity in humans, daily intake of five tablespoons of flaxseed results in cyanide exposures well below the acute toxic dose³⁸⁹. As well, no genotoxicity was found at various endpoints when treated with SECO, END, and ENL in hamster V79 fibroblasts up to 100 μM ³⁹⁰.

Clinically, no adverse effects were observed in a safety evaluation in the healthy population with flaxseed lignan supplementation at a daily dose of 543 mg for six months³⁹¹. This observation is also confirmed in another double blind placebo controlled study of long-term consumption of SDG which caused no adverse effects in older adults who have chronic health conditions³⁹². In a pilot study in cystic fibrosis patients, daily intake of 40 g ground flaxseed was safe and well-tolerated as well²¹. Currently, flaxseed or flaxseed products are considered safe and tolerable without adverse effects when applied daily³⁹¹. However, further study is necessary in the larger population of both healthy subjects and patients. Furthermore, as coadministration of flaxseed lignans with other drugs is attracting more attention, the safety profile for any drug combined with flaxseed or flaxseed products should be investigated to support the usage of combinations without adverse effects.

5.3.3 Flaxseed Lignans' Antifibrotic Potential in Hepatic Fibrosis

Clinical trials of natural products surveyed on the FDA website showed that many natural products, such as curcumin and lignans, have anti-proliferative activity and liver protective effects³⁹³. Lignans extracted from *Schisandra Chinensis* have antifibrotic effects by attenuating TGF- β 1 stimulated phosphorylation and transcriptional activity in cardiovascular fibrosis³⁹⁴. Pharmacological studies demonstrated that flaxseed lignans can exhibit anti-cancer and antifibrotic abilities in liver both *in vitro* and *in vivo*^{395, 396}. In hyperlipidaemic rats, administration of flaxseed lignans contributes to the beneficial effects of hypocholesterolaemia³⁶⁴. In a pilot study, flaxseed had anti-inflammatory and antioxidant properties without serious adverse effects in cystic fibrosis patients²¹. SDG has shown protective properties in various diseases such as liver necrosis and diabetes by modulating

multiple cellular signaling pathways³⁹⁷. ENL and END have demonstrated protective efficacies against breast cancer and prostate cancer, as well as diabetes³⁹⁸. Flaxseed lignans may also reduce the risk of liver diseases when exposed to oxidative stress and/or infections^{364, 399}. Collectively, the research suggests flaxseed lignans have potential ability against proliferative dysfunction disease and inflammation-induced damage.

5.3.3.1 Flaxseed Lignans and PPAR γ

PPAR γ may be involved in the antifibrotic effects of flaxseed lignans⁴⁰⁰. Lignans, including ENL, can reduce circulating cholesterol *via* increasing the expression of PPAR γ and LXR- α , which are key regulators of fatty acid homeostasis and cholesterol efflux transporters^{333, 400-402}. In rats, SECO administration increased the expression of PPAR γ by 17%³⁶⁴. In high-fat fed mice, SDG reduced liver fat accumulation, and the secondary metabolite END induced the mRNA expression of PPAR γ and its DNA binding activity in adipocytes in a concentration-dependent manner³⁴³. In HepG2 cells, the anti-inflammatory effects and PPAR transactivation of lignans are closely related to the upregulation of the three PPARs subtypes and the peroxisome proliferator response elements (PPRE)⁴⁰³. The upregulation of PPAR γ may contribute to the ability of lignans to modulate cholesterol homeostasis and to increase intestinal barrier integrity and anti-inflammatory status, since conjugated ENL, mainly ENL-glucuronide, is reported to upregulate the expression of PPAR γ and insulin induced gene-1 (INSIG-1) while downregulating the expression of SREBP-1, which are major modulators in cholesterol metabolism^{385, 404}. As well, certain lignans, Leoligin and ENL, are reported as weak agonists of PPAR γ ^{343, 405}. Given the potential role of PPAR γ in hepatic fibrosis, treatment with PPAR γ ligands may show antifibrotic effects for liver fibrosis. In rats, overexpression of PPAR γ inhibits fibrotic protein production, and a synthetic PPAR γ agonist reduced liver fibrosis both *in vivo* and *in vitro*⁴⁰⁶. A PPAR γ agonist also showed repression of fibrogenesis *via* PI3K-Akt pathway in TGF- β -induced myofibroblasts⁴⁰⁷. Taken together, it is possible that flaxseed lignans may act as PPAR γ agonists or as transcriptional modulators for PPAR γ to serve as antifibrotic compounds or enhancers of other antifibrotic drugs. However, little experimental evidence is available that supports flaxseed lignans ability to suppress liver fibrosis *via* the upregulation of PPAR γ expression or binding and transactivation of PPAR γ .

5.3.3.2 Flaxseed Lignans and TGF- β

Flaxseed lignans may modulate the activity of the pro-fibrotic cytokine TGF- β and attenuate the activation of HSCs in fibrotic models⁴⁰⁸. For instance, the lignans, sauchinone and sesamin, suppress fibrosis *via* downregulation of TGF- β /Smad signaling pathway in liver fibrosis and myocardial fibrosis, respectively^{409, 410}. In lung-injured mice, flaxseed lignans show radiation mitigating properties on the process of pulmonary fibrosis *via* downregulation of TGF- β 1³⁶⁵. Fibrotic processes associated with high TGF- β 1 in lung tissue, then, might be blunted when the injury is continuing⁴⁰⁸. Another study in a mouse model confirmed dietary flaxseed reduced the proliferative stimulus of TGF- β 1 and prevented the development of fibrosis³⁶⁵. In TGF- β stimulated AML12 cells, lignan schizandrin inhibited fibrogenesis and EMT transition, antagonizing TGF- β -induced fibrosis⁴¹¹. The ability of flaxseed lignans to reduce key cytokines in the liver also suggests flaxseed lignans as a possible therapeutic agent in the resolution of liver fibrogenesis.

5.3.3.3 Flaxseed Lignans and ER Stress-induced Apoptosis

Accumulating evidence suggests that ER stress is involved in a wide range of pathologies including hepatic fibrosis²⁶. A strategy to resolve liver fibrosis is to eliminate the activated HSCs. One of the pathways for this purpose is to induce the ER stress-induced apoptosis of the activated HSCs. Lignans are known to induce ER-stress and cause apoptosis. For instance, arctigenin, a lignan derived from *Arctium lappa L*, is reported to modulate ER stress *via* activating AMPK pathways with subsequent reduction in ATP production in mitochondria, finally protecting cells against ER stress in HepG2 cells⁴¹². Schisandrin B, another active lignan from *Schisandra Chinensis*, induces apoptosis and inhibits proliferation of human hepatoma cells *via* the modulation on ER stress and caspase-3 dependent pathway^{20, 413}. In cancer cells, ENL modulated the lipid and cholesterol metabolism related to the regulation of PPAR γ , ER stress, and mitochondrial function⁴¹⁴. Taken together, it is highly possible that flaxseed lignans may help resolve hepatic fibrosis *via* ER stress, or the resolution could act through ER stress-related pathways, but the exact mechanisms need investigation in hepatic fibrosis models.

5.3.3.4 Flaxseed Lignans and Cholesterol

As both ER stress-mediated apoptosis and hepatic fibroblasts show a relationship with

cholesterol homeostasis, it is possible that flaxseed lignans would have antifibrotic effects *via* modulation of cholesterol-related pathways. Literature evidence suggests that sesamin shows anti-atherogenic effects not only *via* the transactivation of PPAR γ but also has ability to improve cholesterol efflux from macrophages, acting as an anti-atherosclerosis agent⁴¹⁵. This effect is confirmed by another study using arctigenin, which promotes cholesterol efflux to prevent the development of atherosclerosis in THP-1 macrophages *via* the same mechanism – PPAR γ related pathways⁴¹⁶. Chronic supplementation of dietary flaxseed lignans is reported to decrease the serum total and low-density lipoprotein cholesterol (LDL-C) levels and hepatic lipid accumulation independently in a dose-dependent manner in hypercholesterolaemic patients and patients with peripheral artery disease^{364, 378, 417}. In cancer cells, ENL caused modulation of cholesterol metabolism targets including FASN, SREBPs, INSIG-1, and LDL receptor (LDLR), as well as the intracellular vesicular cholesterol trafficking⁴¹⁴. Along with its effects on PPAR γ and ER stress markers, the same study indicated that there might be a linkage between cholesterol, ER stress, and PPAR γ in cancer cells, which might also be a potential mechanism in hepatic fibrosis.

5.3.3.5 Flaxseed Lignans and Other Possible Mechanisms

Other pathways may be involved in the effects of flaxseed lignans in hepatic fibrosis. Lignans show an inhibitory response on TNF α -induced NF- κ B transcriptional activity in HepG2 cells¹⁹. This suggests lignans might have anti-proliferative effects on the progression of fibrosis *via* the NF- κ B pathway. This is also supported by another lignan, arctigenin, which can suppress TGF- β 1-induced secretion of proinflammatory and profibrotic cytokines in epithelial cells *via* the modulation of Erk and ROS/MAPK/NF- κ B pathways⁴¹⁸. Sesamin, a lignan derived from sesame seeds, attenuates liver fibrosis *via* inhibition of EMT, collagen I and α -SMA secretion, and several downstream signaling pathways of TGF- β 1 stimulation both in primary fibroblasts and A549 cells⁴¹⁹. Other natural products such as curcumin also show inhibition of VEGF expression through the PDGF/Erk and mTOR pathways in HSCs⁴⁰¹.

Overall, flaxseed lignans may have antifibrotic effects *via* several different signaling pathways in hepatic fibrosis and may also enhance the response of other drugs, such as TKIs, targeting similar pathways in the suppression and resolution of activated hepatic myofibroblasts in hepatic fibrosis. Furthermore, there might be overlapping mechanisms between the TKIs and flaxseed lignans and their co-administration may show synergistic

effects in liver fibrosis while reducing the risk of side effects caused by TKIs.

6. MATERIALS AND METHODS

6.1 Objective 1: Are TKIs and ENL full agonists or partial agonists of PPAR γ ?

Since PPAR γ is a ligand-activated transcription factor, evaluation of agonist activity of the ENL and TKIs requires assessments of their binding affinity to the LBD of PPAR γ and the capability to modulate the transcription of PPAR γ . Potential partial agonists should have similar biological function as full agonists of PPAR γ with reduced binding affinity and transactivation compared with full agonists. Consequently, the following assays were conducted to determine if the chosen TKIs and ENL are full or partial agonists of PPAR γ .

6.1.1 Chemicals, Reagents, and Supplies

DMEM (Hyclone, Cat.: SH30243.01) was purchased from GE Healthcare Life Sciences (Pittsburgh, PA, USA). Eagle's Minimum Essential Medium (EMEM, Cat: ATCC[®] 30-2003[™]) was purchased from ATCC (Manassas, VA, USA). DMEM (no glucose, Gibco, Cat.: 11966-025), FBS (Gibco, Cat: 12483020), penicillin-streptomycin-glutamine (Gibco, Cat.: 10378016), was purchased from ThermoFisher Scientific (Waltham, MA, USA). PolarScreen[™] PPAR γ -Competitor Assay Kit, Green (Cat.: PV6136) was purchased from Invitrogen (Burlington ON, Canada). Signal PPAR reporter (Luc) Kit (Cat.: CCS-3026L) was purchased from Qiagen (Toronto, ON, Canada) and Dual-Glo luciferase assay system (Cat.: E2920) was purchased from Promega (Madison, WI, USA). Adipogenesis assay kit (Cell-based) (Cat.: ab133102) was purchased from Abcam (Toronto, ON, Canada). 2-(N-(7-Nitrobenz-2-oxa-1,3-diazol-4-yl)amino)-2-deoxyglucose (2-NBDG, CAS: 186689-07-6, MW: 342.26) and rosiglitazone (CAS: 122320-73-4) were purchased from Sigma (Oakville, Ontario, Canada). Ibrutinib (Cat.: S2680, MW: 440.5) and dabrafenib (Cat.: S2807, MW: 519.56) were purchased from Selleck Chemicals LLC (Houston, Texas, USA). Gefitinib (Cat.: 184475-35-2) and FMOC-L-Leucine (FMOC-L-Leu/FMOC, N-[(9H-fluoren-9-ylmethoxy)carbonyl]-L-leucine, CAS: 35661-60-0) were purchased from Cayman Chemical (Ann Arbor, MI, USA).

6.1.2 PPAR γ Competitive Binding assay

To assess the competitive binding affinities of TKIs and flaxseed lignans, the PPAR γ competitive binding assay for ibrutinib, dabrafenib, gefitinib, and ENL was performed with the PolarScreen[™] PPAR γ -Competitor Assay Kit, Green, following the manufacturer's instructions. The kit provides the PPAR γ protein and a novel fluorescent ligand, Fluormone[™]

Tracer, to determine the relative affinity of the tested compounds for PPAR γ . When the PPAR γ protein forms a complex with FluormoneTM Tracer, the polarization value is high, and when compounds displace the FluormoneTM Tracer from the complex, the polarization decreases. Competitive binding affinity was measured through changes in fluorescence using a multi-detection microplate reader SYNERGY HT (BioTek, Winooski VT, USA) at an excitation wavelength of 485 nm and an emission wavelength of 528 nm. Rosiglitazone and FMOC-L-Leu, known full and partial agonists of PPAR γ respectively, were used as positive controls. Fluorescence values were plotted against the log value of the concentrations of rosiglitazone (0.05 – 10,000nM), ibrutinib (0.5 – 50,000 nM), dabrafenib (0.01 – 10,000 nM), gefitinib (0.06 – 33,333 nM), ENL (0.01 – 200,000 nM), FMOC-L-Leu (0.02 – 10,000 nM). The relative affinity of the test compounds for PPAR γ was determined by calculating the relative IC₅₀ values from the binding plots. Curve fitting was performed using a nonlinear regression model (one site-fit Log IC₅₀) of GraphPad Prism v6.0 (GraphPad Software, La Jolla CA, USA).

6.1.3 PPAR γ Transactivation assay

The transactivation potential of the test compounds on the nuclear receptor, PPAR γ , were assessed in PPAR γ -transfected HepG2 cells (purchased from ATCC, cultured according to the recommended method) using the Cignal PPAR reporter (Luc) Kit and Dual-Glo luciferase assay system, according to the manufacturer's instructions. The *Renilla* luciferase is used as a control reporter from the same sample for reporter normalization, and the changes of firefly luciferase are used to interpret the transcriptional changes in the system. For example, a decrease in firefly luminescence with unchanged *Renilla* luminescence indicates a specific impact on the experimental condition. HepG2 cells were transfected with the PPAR γ reporter and negative control plasmids along with the PPAR γ expression vector in 96-well plates. After 16 hours of transfection, cells were treated with the known PPAR γ full agonist rosiglitazone (100 nM, 30 μ M, and 50 μ M), the known partial agonist FMOC-L-Leu (50 μ M), ibrutinib (200 nM, 2 μ M, and 30 μ M), dabrafenib (200 nM, 2 μ M, and 50 μ M), gefitinib (50 μ M), and ENL (50 μ M). The firefly luciferase and *Renilla* luciferase were measured by the aforementioned microplate reader. Transactivation was expressed as relative ratios by normalizing the relative luciferase activity (Firefly/*Renilla*) to the vehicle (0.1% dimethyl sulfoxide/DMSO) treated control group.

6.1.4 Adipogenic and Glucose uptake assays

To evaluate the biological function of the test compounds as potential PPAR γ partial agonists, adipogenic and glucose uptake assays were done in mouse 3T3-L1 preadipocytes to help determine if ENL and the three TKIs (ibrutinib, dabrafenib, and gefitinib) have similar biological functions as the PPAR γ full agonists since adipogenesis and glucose uptake activities are considered as end-point downstream targets of PPAR γ ⁴²⁰. Mouse 3T3-L1 preadipocyte cell line (obtained from the Department of Biology, University of Saskatchewan) was used to detect the adipogenesis and glucose uptake activities of the test compounds, at concentrations of 1 μ M, 20 μ M, and 50 μ M for ibrutinib, dabrafenib, gefitinib, and ENL, using rosiglitazone and FMOC-L-Leu as full and partial agonists of PPAR γ . Undifferentiated 3T3-L1 preadipocytes were cultured in T75 flasks and maintained in a growth medium composed of DMEM with 10% calf serum, and 1% penicillin/streptomycin. For the differentiation of the 3T3-L1 preadipocytes, the cells were propagated into 24-well plates or 96-well plates for the adipogenic assay and glucose uptake assay, respectively. The induction medium used for the preadipocyte differentiation was composed of 0.25 mM dexamethasone, 0.5 mM 3-isobutylmethylxanthine, and 200 nM insulin. The insulin medium used after the induction medium was prepared by adding insulin solution at a final concentration of 200 nM to DMEM containing 10% FBS.

For the adipogenic assay, treated adipocytes were measured by an adipogenesis assay kit (Cell-based) according to the protocol of the manufacturer. The 3T3-L1 preadipocytes were propagated into 24-well plates at a cell density of 1×10^5 per well. Two-days post-confluent, the cells were treated by induction medium with or without the test compounds as indicated in the instructions of the kit on Day 0, using rosiglitazone and FMOC-L-Leu as PPAR γ full and partial agonist controls. On day 3, an insulin medium with the treated compounds was used in the treatment group to replace the induction medium. The medium for all the groups was changed every other day. Briefly, the classic Oil Red O staining for lipid droplets was extracted and quantified by the absorbance measurements at 490 nm by microplate reader after the dye was conveniently extracted from the lipid droplets. On day 7 after differentiation, Oil red staining for the lipid droplets was extracted and transferred into 96-well plates, then absorbance at 490 nm (O.D. value) was measured to quantify the adipogenic activity.

For the glucose uptake assay, 2-(N-(7-Nitrobenz-2-oxa-1,3-diazol-4-yl)Amino)-2-Deoxyglucose (2-NBDG) was used to detect the glucose uptake activities of test compounds

in the treated 3T3-L1 preadipocytes, using rosiglitazone as PPAR γ full agonist control, while FMOCL-Leu as PPAR γ partial agonist control. The 3T3-L1 preadipocytes were propagated into 96-well plates at a density of 1×10^4 per well. The cells were differentiated after 2-days post-confluence with induction medium for two days, then the medium was switched to insulin medium for two more days, and then the same medium without insulin was used for eight more days. With a total differentiation period of ten days, cells were treated with the test compounds in the same medium for 72 hours. After treatment, the treatment medium was switched to glucose- and serum-free medium for three hours, and then insulin was added to the medium for half hour before adding the 2-NBDG compound into the wells. After 15 minutes of incubation with 2-NBDG, the cells were washed with ice-cold Phosphate Buffered Saline (PBS) once and the fluorescence of the cells in 100 μ L PBS was measured immediately at an excitation wavelength of 485 nm and an emission wavelength of 528 nm (excitation/emission = 485/520 nm) to quantify the glucose uptake activity.

6.2 Objective 2: To determine whether certain TKIs (ibrutinib, gefitinib, and dabrafenib) and ENL can suppress HSC activation through modulation of PPAR γ or other pathways in activated human HSCs, LX-2 cells.

To evaluate the antifibrotic abilities of the tested compounds, suppression of HSC activation was evaluated by measuring the changes in expression of fibrotic biomarkers at both mRNA and protein levels in a human hepatic stellate cell line, LX-2, by appropriate methods.

To determine the possible mechanisms of suppression of HSC activation, PPAR γ , PKM2, and key factors of Wnt signaling pathway were assessed by qPCR and western blot assays. All experiments with treatments were done in TGF- β 1-stimulated LX-2 cells, nonTGF- β -stimulated LX-2 cells and/or TGF- β 1-stimulated LX-2 cells treated with the vehicle control (0.1% or 1% DMSO) as negative controls.

6.2.1 HSC Culture

The human hepatic stellate cell line, LX-2 cell, was acquired from Millipore Sigma (Cat: SCC064) and cultured according to company protocols, since the LX-2 human hepatic stellate cell line has been considered as a highly suitable model of hepatic fibrosis²⁵³. DMEM (Hyclone, Cat.: SH30222.01) was purchased from GE Healthcare Life Sciences (Pittsburgh,

PA). DMEM high glucose medium with 2% FBS and 1% of penicillin and streptomycin was used for the cell culture (10% FBS for thawing, medium was changed to 2% FBS after overnight culture) in T75 flasks. LX-2 cells were plated as appropriate into different multi-well cell culture plates one day before and were stimulated for 6 hours with 2.5 ng/mL of TGF- β 1, human recombinant (Cat: TGFB1-005, Empowering Stem Cell R&D, USA) in advance of the presence or absence of the test compounds or vehicle control (0.1% or 1% DMSO). After different treatment periods with the compounds, assessment on activated HSCs involved measurements of cell proliferation, cell migration, total RNA extraction, and qPCR for biomarkers of HSC activation (e.g., α -SMA, TGF- β , collagen I, TIMP-1, MMP2) at mRNA level and western blot or ELISA for these same markers at protein level. Chemicals, reagents, and common cell culture supplies used for the following experiments were as described in Section 6.1.1.

6.2.2 MTT assays for TKIs in TGF- β 1-stimulated LX-2 cells

To determine the appropriate concentrations for the test compounds, MTT assays (Cat: M6494, ThermoFisher, Canada) were used for the TKI drugs and ENL in TGF- β 1-stimulated LX-2 cells. The MTT proliferation assay measures the cell proliferation rate and cell viability when there are metabolic events that lead to apoptosis or necrosis. The yellow tetrazolium MTT can be reduced by metabolically active cells to produce intracellular purple formazan, which can be solubilized and quantified by spectrophotometric methods. LX-2 cells were seeded onto 96-well plates at a density of 10,000 cells/well with an overnight growth/attachment. TGF- β 1 at a final concentration of 2.5 ng/mL was introduced to activate the LX-2 cells for 6 hours before treatment with TKIs. After 72 h incubation in the presence and absence of test compounds, the growth medium was removed followed by one wash with ice-cold PBS. MTT solution (0.5 mg/mL) was added to each well in a volume of 100 μ L growth medium. The incubation with MTT was terminated after 4 hours of incubation in the dark at 37°C, 5% CO₂ by removing the MTT solution. Then, 100 μ L of DMSO was added to each well with 10 minutes of low-speed shaking in the dark. Finally, the absorbance at 570 nm was measured using a multi-detection microplate reader. Then the absorbance (O.D. value) versus concentration curve was drawn to calculate the IC₅₀ value for the compounds by GraphPad Prism v6.0.

6.2.3 Calcein-AM assay for ENL in TGF- β 1-stimulated LX-2 cells

As previous work of our lab suggests the lignans interact with MTT reagent, the effect

of Fmoc-L-Leu, ENL on cell viability of TGF- β 1-stimulated LX-2 cell was confirmed by Calcein-AM assay (Cat: ab228556, Abcam, Canada) according to the kit manual. Calcein-AM is a non-fluorescent, hydrophobic compound that can easily penetrate live cells and undergo hydrolysis by intracellular esterases to produce a hydrophilic and fluorescent compound that can be quantified within the cytoplasm to reflect the number of viable cells. Briefly, LX-2 cells were seeded into 96-well plates at a density of 10,000 cells/well with an overnight growth/attachment. TGF- β 1 at a final concentration of 2.5 ng/mL in the medium was introduced to activate the LX-2 cells for 6 hours before treatment with ENL. After 72 h incubation in the presence and absence of Fmoc-L-Leu and ENL, the medium was removed, and the wells were washed with 200 μ L ice-cold PBS once. Then 100 μ L Calcein-AM working solution (2 μ M) was added to each well. After 30 minutes of incubation in the dark at 37°C, 5% CO₂, the fluorescence was read at an excitation wavelength of 485 nm and an emission wavelength of 528 nm using a multi-detection microplate reader. Then the fluorescence versus concentration bar graph was drawn to indicate the cytotoxicity of the drugs in TGF- β 1-activated LX-2 cells.

6.2.4 Scratch wound healing assay

The effects of gefitinib and ENL on migration potential of LX-2 cells were detected by the scratching wound healing assay. LX-2 cells were seeded into 6-well plates at a density of 3×10^5 cells/well and grown overnight at 37°C, 5% CO₂. Artificial wounds were created in confluent cell monolayers using a sterilized 10 μ L pipette tip to make a straight scratch within each well of the plate containing cells. After washing with PBS, the cells were induced with or without TGF- β 1 for 6 hours before treatment with gefitinib and ENL separately or in combination at different concentrations for another 18 hours. The scratched wounds were photographed at 0-hour and 24-hour after stimulation using an Olympus microscope. Cell migration ability was assessed by measuring the width of the wound for three fields per well at different time points using Image J software (version 1.41).

6.2.5 Apoptosis assay

The effect of gefitinib and ENL on apoptosis of LX-2 cells was detected by Caspase-3/7 fluorescence assay kit (Cat: 1009135; Cayman chemicals, Canada). Cayman's Caspase-3/7 fluorescence assay kit employs a specific substrate, N-Ac-DEVD-N'-MC-R110, which can be cleaved by active caspase-3 or -7 to generate a highly fluorescent product. The activation of caspase-3 and -7 then can be quantified as an endpoint of the apoptotic cascade

irrespective of the cause of apoptosis. LX-2 cells were seeded into 96-well plates at a density of 5×10^4 cells/well and grown overnight at 37°C, 5% CO₂. After washing with PBS, the cells were induced with or without TGF- β 1 for 6 hours before treatment with gefitinib and ENL separately or in combination at different concentrations for 0h, 6h, 12h, 24h, and 48h. After treatment, the apoptosis assay was performed according to the manual script from the company. The fluorescence intensity was read using microplate reader (excitation = 485 nm; emission = 535 nm). Then the fluorescence was normalized to the vehicle control group, the relative apoptosis ratio was calculated to reflect the apoptosis response of the compounds.

6.2.6 Oxidative stress assay

The superoxide production by mitochondria of gefitinib- and/or ENL- treated LX-2 cells was measured by MitoSox Red mitochondrial superoxide indicator (Cat: M36008, Invitrogen, Canada), and the total antioxidant capacity of gefitinib and/or ENL was detected by an antioxidant assay kit (Item No. 709001; Cayman chemicals, Canada). As mitochondria serve as the major intracellular source of ROS, a MitoSOX red mitochondrial superoxide indicator, which is permeant to live cells targeted to the mitochondria and oxidized by superoxide, is used to reflect ROS production in mitochondria by detecting the superoxide in the mitochondria of live cells. LX-2 cells were seeded into 96-well plates at appropriate density and grown overnight at 37°C, 5% CO₂. The cells were stimulated by TGF- β 1 for 6 hours prior to the treatment with gefitinib and/or ENL for 0.5, 1, and 3 hours. Then, superoxide production and total antioxidant capacity were measured by the appropriate kits according to the manufacturer. For superoxide production, the fluorescence was measured, and the relative fluorescence was calculated to determine the effect of the treatments on the production of superoxide in LX-2 cells. Absorbance at 750 nm was read and plotted and the antioxidant concentration was calculated to reflect the total antioxidant capacity of the treatment with gefitinib and/or ENL.

6.2.7 Real-time PCR

Quantitative reverse transcription-polymerase chain reaction (qPCR) analysis for fibrotic biomarkers and possible mechanistic biomarkers (e.g., PPAR γ , PKM2, ER stress-related, and oxidative stress targets) were evaluated in TGF- β 1-activated LX-2 cells. LX-2 cells were plated as appropriate into 6-well plates and stimulated for 6 hours with TGF- β 1 (2.5 ng/mL) before treatments with the presence and absence of the model TKIs and ENL for 18 hours. At the termination of the treatments, the PBS-washed cells were scraped off from

the plates and pelleted for RNA isolation and following procedures.

Total RNA was isolated by RNeasy Plus Mini Kit (Cat: 74136, QIAGEN, Canada) according to the kit manual. The RNA concentration was measured at 260 and 280 nm using NanoVue Plus spectrophotometer (GE lifescience, USA). After the total RNA was isolated, SuperScript™ VILO™ cDNA synthesis kit (Cat: 11754-050 and 11754-250, Life Technologies, Canada) was used for the reverse transcription. The synthesized cDNA was normalized to the same concentration and then used for qPCR, using Power SYBR™ Green PCR Master Mix (Cat: 4367659, ThermoFisher, Canada). The primers were designed using the IDT PrimerQuest Tool and PubMed gene database, the primers' sequence information is shown in **Table 6.1**. The Ct value was detected and analyzed using BioRad CFX96 Touch™ Real-Time PCR detection system, and the results were reported by comparing the $2^{(-\Delta\Delta Ct)}$ values to reflect the expression changes of the target genes after treatment, using β -actin as reference gene for the calculation.

Table 6.1 Primer sequences used for LX-2 cell samples in quantitative Polymerase Chain Reaction (qPCR)

Primers	Sequence (5' to 3')
<i>ACTB</i>	F: GGACCTGACTGACTACCTCAT
	R: CGTAGCACAGCTTCTCCTTAAT
<i>GAPDH</i>	F: CAAGAGCACAAGAGGAAGAGAG
	R: CTACATGGCAACTGTGAGGAG
<i>COL1A1</i>	F: CGATGGATTCCAGTTCGAGTATG
	R: CTTGCAGTGGTAGGTGATGTT
<i>ACTA2</i>	F: TGTTCAGCCATCCTTCATC
	R: GCAATGCCAGGGTACATAGT
<i>TIMP1</i>	F: CTGATGACGAGGTCGGAATTG
	R: TGTTGTTGCTGTGGCTGATA
<i>MMP2</i>	F: TGCTGAAGGACACACTAAAGAA
	R: CGCATGGTCTCGATGGTATT
<i>TGFBI</i>	F: CGTGGAGCTGTACCAGAAATAC
	R: CACAACCTCCGGTGACATCAA
<i>PPARG</i>	F: GTGCAGGAGATCACAGAGTATG
	R: GTGGACTCCATATTTGAGGAGAG

<i>PKM2</i>	F: GCTGACTCCTGCATAGGTTATC R: GCCAATGCCTCAGAGTAGAAA
<i>MMP9</i>	F: CCGGACCAAGGATACAGTTT R: GCGGTACATAGGGTACATGAG
<i>ATF4</i>	F: GGAGATAGGAAGCCAGACTACA R: GGCTCATAACAGATGCCACTATC
<i>ATF6</i>	F: CTTCGAGGATGGGTTTCATAGAC R: CCAGAGCACCCCTGAAGAATAC
<i>CHOP</i>	F: CTCACTCTCCAGATTCCAGTCA R: GACCACTCTGTTTCCGTTTCC
<i>NRF2</i>	F: GCAAGTTTGGGAGGAGCTATTA R: GTTTGGCTTCTGGACTTGGA
<i>CTNNB1</i>	F: TACCATTCCATTGTTTGTGCAG R: TGAAGAGAGAGCTGGTCAGCTC
<i>AXIN2</i>	F: GAGTGGACTTGTGCCGACTTCA R: GGTGGCTGGTGCAAAGACATAG
<i>WNT1</i>	F: GAGCCACGAGTTTGGATGTT R: AGAGAAGAGTGGAGAGGGATTG
<i>WNT3A</i>	F: CCATCCTCTGCCTCAAATTCT R: CTCCGTTGGACAGTGGATATAG
<i>WNT5A</i>	F: CACCAGAGCAGACAACCTATTT R: CATCACAACACGGAGGAATCA

Note: F – forward primer, R – reverse primer

6.2.8 ELISA

To detect changes in expression of fibrotic biomarkers at the protein level, LX-2 cells were plated as appropriate into 12-well plates and stimulated with TGF- β 1 (2.5 ng/mL) for 6 hours in advance of the treatment. Then the cells were treated with test compounds for 24, 48, and 72 hours. The levels of pro-collagen I alpha 1 in the cell extracts as well as in supernatants and MMP9 in the supernatants were measured by standard ELISA kits (Cat: ab210966 (human pro-collagen I alpha 1) and ab100610 (human MMP9); Abcam, Canada), following the manufacturer instructions for pro-collagen I α 1 and MMP9. The concentrations for each protein were measured in duplicate, interpolated from each standard curve, and

corrected for the dilution factor. The dilution factor corrected concentrations were plotted, and two-way ANOVA followed by Dunnett test was performed between the treated groups with the TGF- β 1-stimulated cells at the same time point.

6.2.9 Western blot

To assess possible mechanisms of antifibrotic effects of the tested compounds, changes in certain protein targets were measured by western blot. LX-2 cells were plated as appropriate into 6-well plates for overnight incubation. The cells were stimulated with TGF- β 1 (2.5 ng/mL) for 6 hours in advance of the treatment. Cells were then treated with test compounds or vehicle control for another 18, 30, and 66 hours. The resulting cell pellet was lysed using RIPA lysis buffer (Cat: 89900, ThermoFisher, Canada) with Halt™ Protease and Phosphatase Inhibitor Single-Use Cocktail (Cat: 78843S, ThermoFisher, Canada), the lysates were centrifuged at 14,000 \times g for 15 minutes and the protein samples were collected for further measurement.

The total protein level was measured by Pierce™ BCA protein assay kit (Cat: 23225, ThermoFisher, Canada) according to the manuals. Changes in expression of PPAR γ , PKM2, α -SMA, ATF4, CHOP, and Nrf2 protein were done by western blot. The samples, at reducing condition, with Bolt LDS agent were heated at 70°C for 10 minutes and then an equal amount of protein was loaded for electrophoresis in MES running buffer at 200V for 23 minutes through 10% SDS polyacrylamide gels at an equal amount of protein. Blots were transferred to nitrocellulose membranes at 10V for 60 minutes. Total protein was stained by SYPRO® Ruby protein blot stain (Cat: S11791, ThermoFisher, Canada) and viewed by BioRad Chemdoc™ imaging system. The membranes were subsequently blocked with 5% skim milk in TBS at room temperature for 1 hour with gentle agitation. The blots were then probed overnight at 4°C with primary antibodies at appropriate concentrations for PPAR γ (mouse monoclonal IgG, Cat: SC-7273), PKM2 (rabbit polyclonal IgG, Cat: SC-292640), α -SMA (mouse monoclonal IgG, Cat: 14-9760-82), ATF4 (rabbit polyclonal IgG, Cat: PA5-78832), CHOP (mouse monoclonal IgG, Cat: ab11419), Nrf2 (rabbit polyclonal IgG, Cat: 16396-1-AP) and β -actin (mouse monoclonal IgG, Cat: SC-47778). The next day, the blots were rinsed with TBS-tween (0.1%) and probed with the appropriate secondary antibodies for 1 hour at room temperature with gentle agitation. After washing, the chemiluminescent substrate was used for semi-quantification by BioRad Chemdoc™ imaging system. The results are expressed as ratios of integrated density values of corresponding protein bands from treated to untreated control cells. Statistical analysis was carried out by one-way

ANOVA, followed by Tukey test.

6.3 Objective 3: Whether flaxseed lignans exhibit antifibrotic effects in high-cholesterol diet-induced fatty liver rats.

6.3.1 Comparative oral PK study of purified SDG and SDG-enriched polymer complex in female Wistar rats

Twenty-four female Wistar rats around 300 g of body weight were surgically implanted with a jugular vein cannula at least 24 hours prior to the PK study. Rats were divided into four subgroups for two compounds with two sampling time frames per compound after one-week acclimatization. After full recovery from cannulation surgery, rats were fasted overnight, and pre-dose blood samples were collected *via* jugular vein cannulation before a single oral administration of purified SDG (purity: 96.1%) or SDG-enriched complex (both obtained from Prairie Tide Chemicals Inc. as a gift, Saskatoon, SK, Canada) at an SDG-equivalent dose of 40 mg/kg by oral gavage. Blood samples were collected *via* jugular vein cannulation at 15, 30, 45 min, and 1, 1.5, 2, 4, 8 h from one subgroup after dosing, and 12, 16, 20, 24, 32, 40, and 48 h from the second subgroup after dosing. Plasma samples were obtained with centrifugation after blood sampling into lithium heparinized microcentrifuge tubes (GE Healthcare Life Sciences Mississauga, ON, Canada). Rat blank plasma was obtained from rats under the UACC Animal & Tissue Share program. The plasma concentrations of SDG metabolites, including free and glucuronide conjugated forms of SECO, END, and ENL (purchased from Sigma, Oakville, ON, Canada), were measured using appropriate LC-MS/MS methods. This work was approved by the University of Saskatchewan's Animal Research Ethics Board and adhered to the Canadian Council on Animal Care guidelines for humane animal use (Appendix B – Certificate of Approval).

6.3.2 Comparative efficacy study of purified SDG and SDG-enriched polymer complex in female hypercholesterolemic Wistar rats

Thirty-five female Wistar rats were randomized to either standard diet (N=5), LabDiet® ProLab® RMH 5P00, or 1% high cholesterol diet (N=10 each treatment), Modified LabDiet® 5P00 with ~1% total cholesterol, throughout a one-week acclimatization period. Subsequently, rats in the 1% high cholesterol diet group were administered purified SDG (purity: 96.1%) or SDG-enriched polymer complex (SDG equivalent dose was 6 mg/kg, both

obtained from Prairie Tide Chemicals Inc. as a gift, Saskatoon, SK, Canada) in Ensure® Nutritional drinks (strawberry flavor, bought from Real Canadian Superstore, Saskatoon, SK, Canada) orally with syringes once daily for 3 weeks. Blood samples were collected under isoflurane anesthesia at 2 weeks after dosing *via* saphenous vein puncture and at 23 days *via* abdominal aorta puncture. Serum samples were obtained with centrifugation after the blood sampling. The body weight and liver weight were measured at the end of the study. ALT and AST levels in serum were detected to reflect liver function. Serum total cholesterol (TC), triglyceride (TG), high-density lipoprotein cholesterol (HDL-C) were detected after 14 days and 23 days of treatment with purified SDG and SDG polymer by using Stanbio Cholesterol LiquiColor® Test kit and Stanbio Triglycerides LiquiColor® Test kit, and Sigma HDL and LDL/VLDL Quantitation kit, respectively. LDL-C was calculated by these three parameters according to equation $[TC-TG/5-(HDL-C)]^{421}$. After 23 days of treatment, body and liver weight were measured to calculate the body weight gain and liver to body weight ratio. Liver tissues were collected into 10% formalin solution or RNAProtect Tissue Reagent (Cat No.: 76104, Qiagen, Hilden, Germany) for follow-up histology and molecular biological experiments, respectively. Histological changes in the liver tissue were observed by slicing the samples, which were stored in formalin with appropriate approach, and scoring was blinded and conducted by an independent pathologist according to the criteria in **Table 6.2**. From tissue samples stored in the RNAProtect Tissue Reagent, RNA and protein samples were isolated using Qiagen Midi RNase kit and ThermoFisher T-PER™ tissue protein extraction reagent according to the manuals for qPCR and western blot assays. The RNA samples underwent reverse transcription to cDNA and were diluted to the same concentration before qPCR analysis.

Table 6.2 The criteria used for histological scoring of the degree of severity of non-alcoholic fatty liver disease.

	Definition	Score
Steatosis	<5%	0
	5% - 33%	1
	33% - 66%	2
	>66%	3
Lobular inflammation	No foci	0
	<2 foci per 200×field	1
	2-4 foci per 200×field	2

	>4 foci per 200×field	3
Ballooning	None	1
	Few balloon cells	1
	Many cells/prominent ballooning	2

Note: NAS (NAFLD activity score) = steatosis + lobular inflammation + ballooning

6.3.3 Real-time PCR

Quantitative reverse transcription-polymerase chain reaction (qPCR) analysis for fibrotic biomarkers was evaluated in rat liver protein samples. After 30 days of high cholesterol diet with 23 days of SDG supplementation, the rat liver samples were collected into RNeasy Protect Tissue Reagent for qPCR and western blot assays. Total RNA was isolated from homogenized rat liver tissue samples using RNeasy Midi kit (Cat: 75144, Qiagen, Canada) according to the kit manual. The RNA concentration was measured at 260 and 280 nm using NanoVue Plus spectrophotometer (GE Lifescience, USA). After the total RNA was isolated, OneScript® Plus cDNA Synthesis Kit (Cat: G236, Applied Biological Materials (abm), Canada) was used for reverse transcription. cDNA was used for the real-time PCR reaction, using PowerUp SYBR™ Green PCR Master Mix (Cat: A25778, ThermoFisher, Canada). The primers were designed using IDT PrimerQuest Tool and PubMed gene database, the primers' sequence information is shown in **Table 6.3**. The Ct value was detected and analyzed using BioRad CFX96 Touch™ Real-Time PCR detection system, and the result was reported by comparing the $2^{(-\Delta\Delta Ct)}$ values to reflect the expression changes of the target genes, using Hrpt1 as reference gene for the normalization.

Table 6.3 Primer sequences used for rat liver samples in quantitative Polymerase Chain Reaction (qPCR)

Primers	Sequence (5' to 3')
Hrpt1	F: CAGTCCCAGCGTCGTGATTA
	R: GGCCTCCCATCTCCTTCATG
Collagen I α 1	F: CCAATGGTGCTCCTGGTATT
	R: GTTCACCACTGTTGCCTTTG
α -sma	F: GCTCCTCCAGAACGCAAATA
	R: CAGCTTCGTCATACTCCTGTTT
Timp-1	F: GATTTGTGCACCTGGCAATAC
	R: AGAGAAAGAAAGATGGAGGAAAGG

Mmp2 F: CACCAAGAACTTCCGACTATCC
 R: TCCAGTACCAGTGTCAGTATCA

Note: F – forward primer, R – reverse primer

6.3.4 Western blot

To assess possible antifibrotic effects of flaxseed lignans, changes in fibrotic protein targets, including collagen I, Mmp2, and Timp1 were measured by western blot. After the termination of treatment, rat liver samples were collected into RNeasy Protect Tissue Reagent for further study. Homogenized rat liver tissue samples were lysed in RNeasy lysis reagent with protease inhibitor according to manufacturer protocols. The samples were centrifuged at $14,000 \times g$ for 20 minutes to remove the debris. The supernatants were collected for further analysis. The protein concentrations were determined by Pierce™ BCA protein assay kit according to the manual. The samples were heated at 70°C for 10 minutes with Bolt LDS agent and electrophoresed in MES running buffer for 23 minutes at 200V through 4-12% SDS polyacrylamide gels at equal amount of protein, followed by the transference to nitrocellulose membranes at 10V for 60 minutes. Total protein was stained by SYPRO® Ruby protein blot stain and viewed by BioRad Chemdoc™ imaging system. The membranes were subsequently blocked with 5% skim milk in TBS at room temperature for 2 hours with gentle agitation. The blots were then probed overnight at 4°C with primary antibodies at appropriate concentrations of Collagen I (rabbit polyclonal IgG, Cat: PA1-26204), Mmp2 (rabbit recombinant monoclonal IgG, Cat: ab181286), and Timp1 (rabbit polyclonal IgG, Cat: ab61224). The next day, the blots were rinsed with TBS-tween (0.1%) and probed with appropriate secondary antibodies for 1 hour at room temperature with agitation. After washing, the chemiluminescent substrate was used for semi-quantification. The results are expressed as ratios of integrated density values of corresponding protein bands from treated to untreated control cells.

6.4 Statistical analysis

All data are reported as mean \pm SD (or mean \pm SEM for data from the animal study). Statistical analysis for the replicates on one occasion was carried out by one-way ANOVA or non-parametric one-way ANOVA for the histological score, or two-way ANOVA, followed by Dunnett or Tukey test. Differences were considered significant when

$P < 0.05$.

7. RESULTS

7.1 Objective 1: To determine whether TKIs and ENL are either full agonists or partial agonists of PPAR γ

A list of TKIs was reported with high binding affinities to PPAR γ similar to rosiglitazone using a computational docking model, which indicated a possibility that TKIs serve as PPAR γ agonists in many diseases¹³. Rather than detecting the conformational changes by direct binding assessment, the aim was determine the relative binding affinities of TKIs with the rosiglitazone binding site based upon the aforementioned *in silico* evidence using a competitive binding assay kit, followed by Guasch's methods in screening natural products as PPAR γ partial agonists¹⁸⁶.

The first objective was to experimentally corroborate the binding pattern to PPAR γ for three of the reported TKI's, ibrutinib, dabrafenib, and gefitinib, as well as the mammalian lignan, ENL. A competitive binding assay kit with rosiglitazone as a positive control was used to confirm the binding affinities of the tested compounds at the common binding site. In addition to the assessment of this competitive binding activity, the ability of the compounds to transactivate PPAR γ was necessary to confirm these compounds as agonists of PPAR γ . The ability of the compounds to transactivate PPAR γ was assessed using PPAR γ -transfected HepG2 cells, a commonly used cell line for transfection with PPAR γ and the Dual-Glo luciferase system. Based upon the PPAR γ binding affinity and transactivation activity of the tested compounds, these experiments would glean whether the compounds were possible full or partial agonists of PPAR γ . Biological functional assays were further used to confirm the pattern of agonism, following the screening method of Guasch's group¹⁸⁶. According to this screening method, PPAR γ -related biological functions are detected in differentiated 3T3-L1 mouse adipocytes to assess the compounds' abilities to modulate PPAR γ specific biological responses including adipogenesis and glucose uptake activity.

7.1.1 PPAR γ competitive binding assay

A PPAR γ competitive binding assay was applied to detect the competitive binding affinities of ibrutinib, dabrafenib, gefitinib, and ENL to PPAR γ using rosiglitazone and FMOC-L-Leu as positive controls. The relative binding affinities of the compounds were determined by measuring the shift of fluorescence value, and the relative IC₅₀ values of the compounds were determined from the binding plots by a non-linear regression model using

GraphPad Prism v6.0.

The relative IC₅₀ values of PPAR γ competitive binding assay for rosiglitazone and Fmoc-L-Leu were similar to values of 110 nM and 4.8 μ M, respectively, reported in the literature^{186, 422, 423} (**Table 7.1**). Ibrutinib showed a relative IC₅₀ value over 50 μ M, but solubility limitations precluded the ability to construct a complete cytotoxicity curve. The relative IC₅₀ value for dabrafenib was undetermined from the binding plot, while the relative IC₅₀ values for gefitinib and ENL were determinable, but similarly to dabrafenib without showing a binding saturation when the concentration approached 300 and 200 μ M, respectively (**Figure 7.1**).

Table 7.1 The competitive binding affinities, represented as relative IC₅₀ values, of the tyrosine kinase inhibitors and enterolactone (ENL).

Compounds	Rosiglitazone	Fmoc	Ibrutinib	Dabrafenib	Gefitinib	ENL
Relative IC ₅₀	111.3 nM	2 μ M	> 50 μ M	NA	> 50 μ M	> 50 μ M

Note: NA-not available. Fmoc: Fmoc-L-Leucine. ENL: enterolactone. Data shown as mean of six replicates, performed on three occasions.

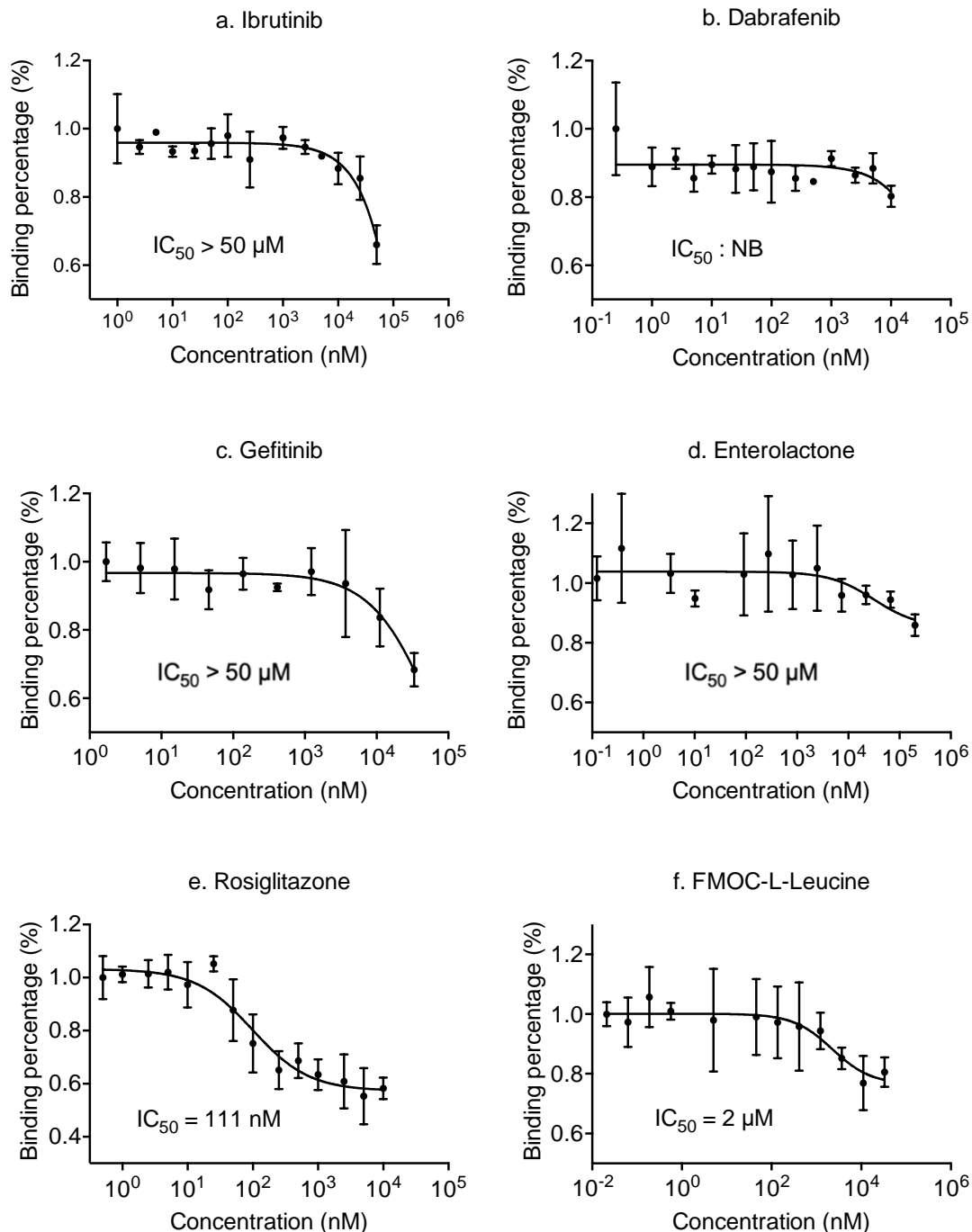


Figure 7.1 PPAR γ competitive binding assay results for ibrutinib (a), dabrafenib (b), gefitinib (c), enterolactone (ENL), (d), rosiglitazone (e), and FMOC-L-Leucine (FMOC, f), performed as binding percentage using the PolarScreenTM PPAR γ -Competitor Assay Kit. a: ibrutinib has a relative IC_{50} value over 50 μM calculated from the concentration range from 0.5 nM to 50,000 nM (could not go higher due to the solubility limitation); b: the relative IC_{50} value of dabrafenib is not available by the plot (no binding trend from the experimental data); c: gefitinib has a relative IC_{50} value of 62 μM ; d: ENL has a relative IC_{50} value of 117 μM ; e: rosiglitazone has a relative IC_{50} value of 111.3 nM as a known agonist of PPAR γ ; f: FMOC has a relative IC_{50} value of 2 μM . The data were analyzed by a nonlinear regression model of GraphPad Prism v6.0. The data are reported as mean \pm SD of six replicates, performed on three occasions.

7.1.2 PPAR γ transactivation assay

Following agonist binding to PPAR γ , the receptor interacts with its coactivators or corepressors to activate cellular transcriptional processes¹⁴². Hence, assessment of competitive binding affinity alone is not adequate to understand whether the tested compounds are agonists of PPAR γ , and subsequently the ability of the potential agonists to transactivate PPAR γ was confirmed. Dual-Glo® Luciferase reporter assay was performed to determine the transactivation of PPAR γ by ibrutinib, dabrafenib, gefitinib, and ENL in PPAR γ -transfected HepG2 cells, using rosiglitazone and FMOC-L-Leu as PPAR γ full and partial agonist controls, respectively. In this assay, rosiglitazone strongly increased the relative luciferase ratio (Firefly/Renilla) in PPAR γ -transfected HepG2 cells compared to untreated cells, and FMOC-L-Leu gave a moderate increase (**Table 7.2**). Ibrutinib and dabrafenib did not produce transactivation at concentrations of 200 nM or 2 μ M but dabrafenib produced moderate transactivation at a higher concentration (50 μ M) with statistical significance. Gefitinib and ENL also produced moderate transactivation at 50 μ M.

The higher concentrations (30 or 50 μ M) of ibrutinib, dabrafenib, gefitinib, and ENL were used to conduct a maximal transactivation measurement for those compounds. The relative transactivation potential (relative luciferase ratio to the negative control group) of rosiglitazone at the same concentration is about 20-times higher than ibrutinib, 3-times higher than dabrafenib and gefitinib, and 10-times and 8-times higher than ENL and known PPAR γ partial agonist FMOC-L-Leu, respectively ($P < 0.05$) (**Table 7.2**).

Table 7.2 The relative luciferase ratio for ibrutinib, dabrafenib, gefitinib, and enterolactone (ENL) in PPAR γ -transfected HepG2 cells.

Compounds	Concentration	Relative luciferase ratio	Compounds	Concentration	Relative luciferase ratio
Ibrutinib	200 nM	1.4 \pm 0.4	Gefitinib	50 μ M	8.5 \pm 0.6*
	2 μ M	1.1 \pm 0.0	ENL	50 μ M	10.7 \pm 0.6*
	30 μ M	2.4 \pm 0.8	FMOC-L-Leu	50 μ M	7.7 \pm 3.0*
Dabrafenib	200 nM	1.1 \pm 0.0	Rosiglitazone	100 nM	2.0 \pm 0.2
	2 μ M	1.1 \pm 0.2		30 μ M	47.6 \pm 2.0*
	50 μ M	7.4 \pm 2.6*			

Note: Transactivation of PPAR γ was assessed in PPAR γ -transfected HepG2 cells using rosiglitazone as a full agonist positive control and FMOC-L-Leucine (FMOC-L-Leu) as a partial agonist control. The ability of the compounds to transactivate PPAR γ was presented by the relative luciferase ratio normalized to the negative control provided within the kit. Data are reported as mean \pm SD, N=3, done on three occasions; * P <0.05 when compared with the vehicle control using one-way ANOVA followed by Dunnett test.

7.1.3 Adipogenesis and Glucose uptake assays

Although binding and transactivation assays suggested the potential of the tested compounds to act as PPAR γ partial agonists, the biological function of the compounds should be detected to confirm their effect on PPAR γ specific downstream biological processes, such as glucose uptake and adipogenesis activity. If the compounds have low to moderate binding affinity to PPAR γ but fail to stimulate adipogenesis yet enhance insulin-stimulated glucose uptake *in vitro*, then these compounds have the potential to be PPAR γ partial agonists¹⁸⁶.

To assess the possibility that the TKIs and ENL act as partial agonists, PPAR γ -mediated biological functional assays were conducted to confirm the ability of the compounds to modulate PPAR γ -related responses. Adipogenesis and glucose uptake assays were performed in mouse 3T3-L1 preadipocytes. These assays were conducted to distinguish partial and full agonists of PPAR γ according to the methods described by Guasch et al screening procedures¹⁸⁶.

As shown in **Figure 7.2**, adipogenic activity was increased to 1.9, 2.5, and 3.3 times of the vehicle control by 1, 20, and 50 μ M of rosiglitazone, respectively. The induction was higher when concentration increased. FMOC-L-Leu increased adipogenic activity by 34% and 38% of the vehicle control at 20 and 50 μ M, respectively. Dabrafenib increased adipogenesis by around 60%, 88%, and 135% of vehicle control at concentrations of 1, 20, and 50 μ M, respectively, with a similar concentration-related increase as rosiglitazone. Ibrutinib increased adipogenesis by approximately 136%, 175%, and 265% of the vehicle control at concentrations of 1, 20, and 50 μ M, respectively. ENL showed no induction on adipogenic activity, while gefitinib increased adipogenesis by 33%, 50 and 60% at 1, 20, and 50 μ M, respectively, similarly in pattern with FMOC-L-Leu.

After 3 days of treatment with the compounds, glucose uptake activity was significantly increased by 90% by 50 μ M of rosiglitazone and was not significantly changed by lower concentrations of rosiglitazone and FMOC-L-Leu. Ibrutinib increased glucose uptake activity by 70% and 72% at concentrations of 20 and 50 μ M, respectively. Gefitinib increased glucose uptake activity by 81% and 115% at concentrations of 20 and 50 μ M, respectively, while ENL increased glucose uptake activity by 89% only at 50 μ M. Dabrafenib gave the strongest effect and increased glucose uptake activity by 142%, 314%, and 401% at concentrations of 1, 20, and 50 μ M, respectively. (**Figure 7.3**).

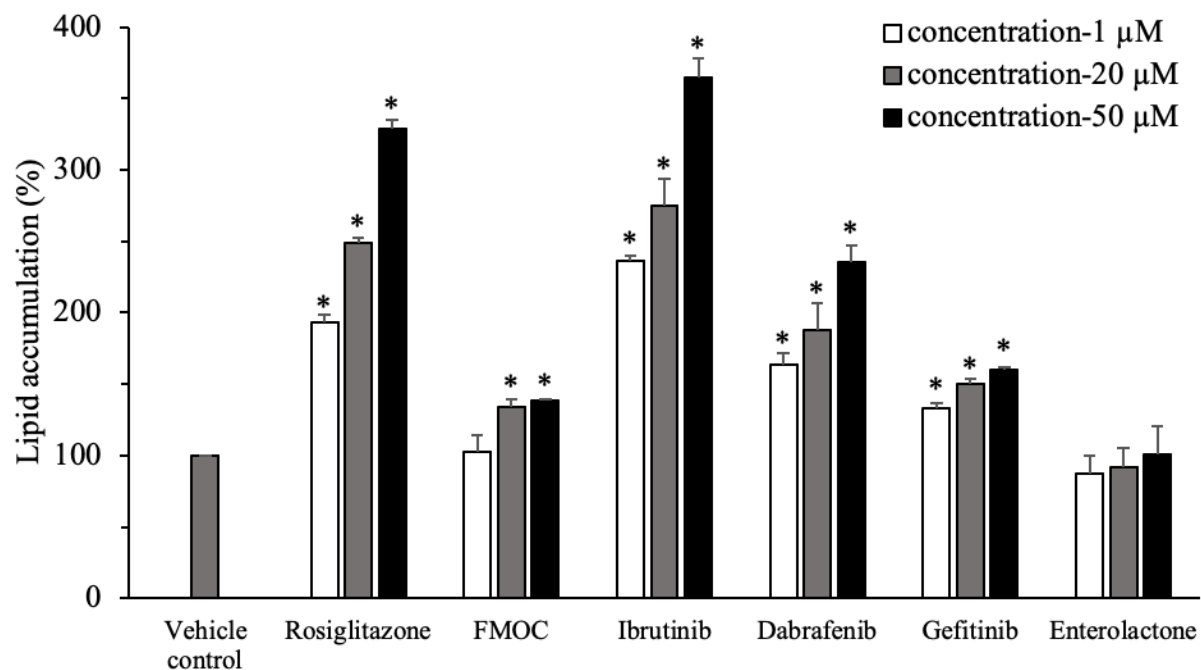


Figure 7.2 The adipogenesis assay was performed to detect PPAR γ -mediated biological functions of the compounds in mouse 3T3-L1 adipocytes. The adipogenic activities of different compounds at different concentrations (1 μ M, 20 μ M, and 50 μ M) were detected by absorbance measurement at 490 nm after extraction of the Oil Red staining, using the same concentrations of rosiglitazone as a full agonist positive control and FMOC-L-Leucine (FMOC) as a partial agonist control. The relative lipid accumulation to the vehicle control was plotted. Vehicle control (grey) used DMSO at a final concentration of 1%. Data were reported as mean + SD of six replicates; * P <0.05 when compared with vehicle control using two-way ANOVA followed by Dunnett test.

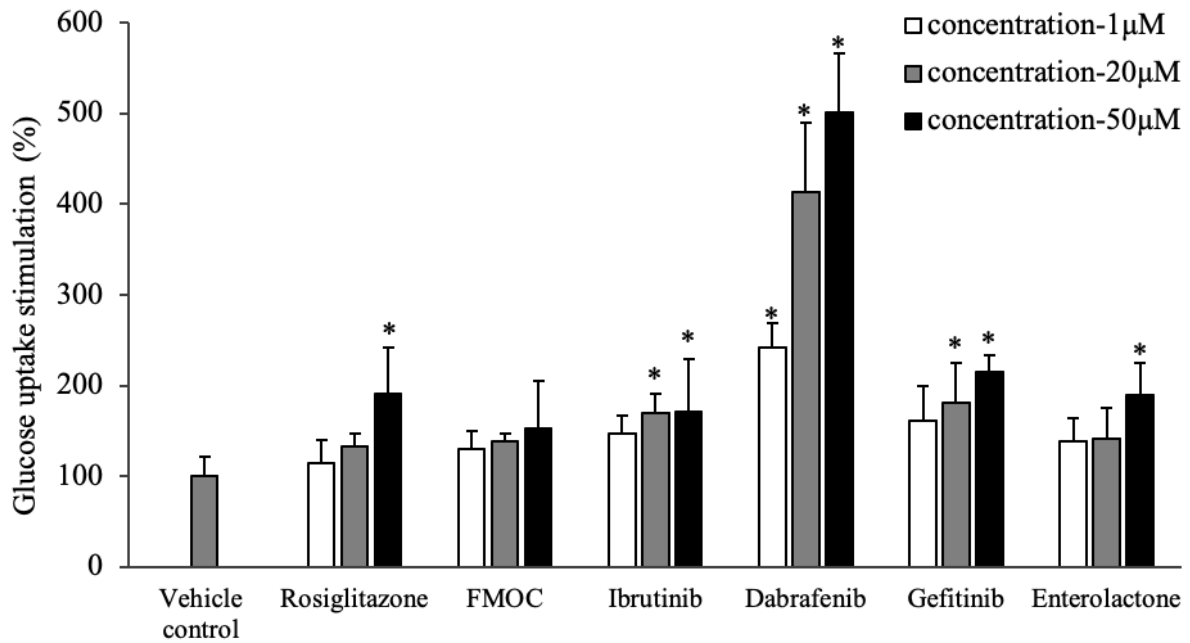


Figure 7.3 The glucose uptake assay was performed to detect PPAR γ -mediated biological functions of the compounds in mouse 3T3-L1 adipocytes. The glucose transport activities of different compounds at different concentrations (1 μ M, 20 μ M, and 50 μ M) for 3 days are shown by reading the fluorescence of 2-NBDG at (Ex/Em =485/528 nm) using same concentrations of rosiglitazone as a full agonist positive control and FMOC-L-Leucine (FMOC) as a partial agonist control. Vehicle control (grey) used DMSO at a final concentration of 1%. Data are shown as % of glucose uptake stimulation with vehicle control which was considered 100% insulin stimulation. Data are reported as mean + SD of six replicates; * P <0.05 compared with vehicle control using two-way ANOVA followed by Dunnett test.

7.2 Objective 2: To determine whether ENL and certain TKIs (ibrutinib, gefitinib, and dabrafenib) can suppress HSC activation in TGF- β 1-activated human HSCs (LX-2 cells).

As the tested TKIs and ENL might be PPAR γ agonists or partial agonists according to the first objective, they might suppress HSC activation through PPAR γ -related mechanisms. To confirm this, the next goal was to evaluate the suppression of fibrotic biomarkers in a cell culture model of hepatic fibrosis. A common-used human HSC cell line, LX-2 cell, was used and stimulated with one of the major stimuli of hepatic fibrosis, TGF- β 1, as the cell culture model to investigate the antifibrotic potential and possible mechanisms of the TKIs and/or ENL in hepatic fibrosis.

7.2.1 MTT and/or Calcein-AM assays for TKIs and ENL in TGF- β 1-stimulated LX-2 cells

7.2.1.1 MTT assay for TKIs in TGF- β 1-stimulated LX-2 cells

To identify appropriate concentrations for use in the assay systems, first, the effect of the three TKI drugs on activated LX-2 cell viability was assessed using the MTT assay. After LX-2 cells were seeded into 96-well plates, the cells were stimulated with TGF- β 1 at a concentration of 2.5 ng/mL at 24-hour post-seeding. Six hours after stimulation, the cells were treated with ibrutinib, gefitinib, and dabrafenib for 72 hours. The O.D. value at 570 nm was plotted against concentration. The relative IC₅₀ values for the test compounds were calculated from the plots by a nonlinear regression model using GraphPad Prism v6.0.

Ibrutinib gave a relative IC₅₀ value around 5 μ M in TGF- β 1-stimulated LX-2 cells, which is about 4 times lower than in the nonTGF- β -stimulated LX-2 cell (**Figure 7.4 plot a and b**); gefitinib had a relative IC₅₀ value around 13 μ M in the activated LX-2 cells (**Figure 7.4 plot c**); dabrafenib at the tested highest concentration of 100 μ M did not reach 50% of the maximum inhibitory effect on the cell viability; hence, the IC₅₀ value of dabrafenib was considered as over 100 μ M (**Figure 7.4 plot d**).

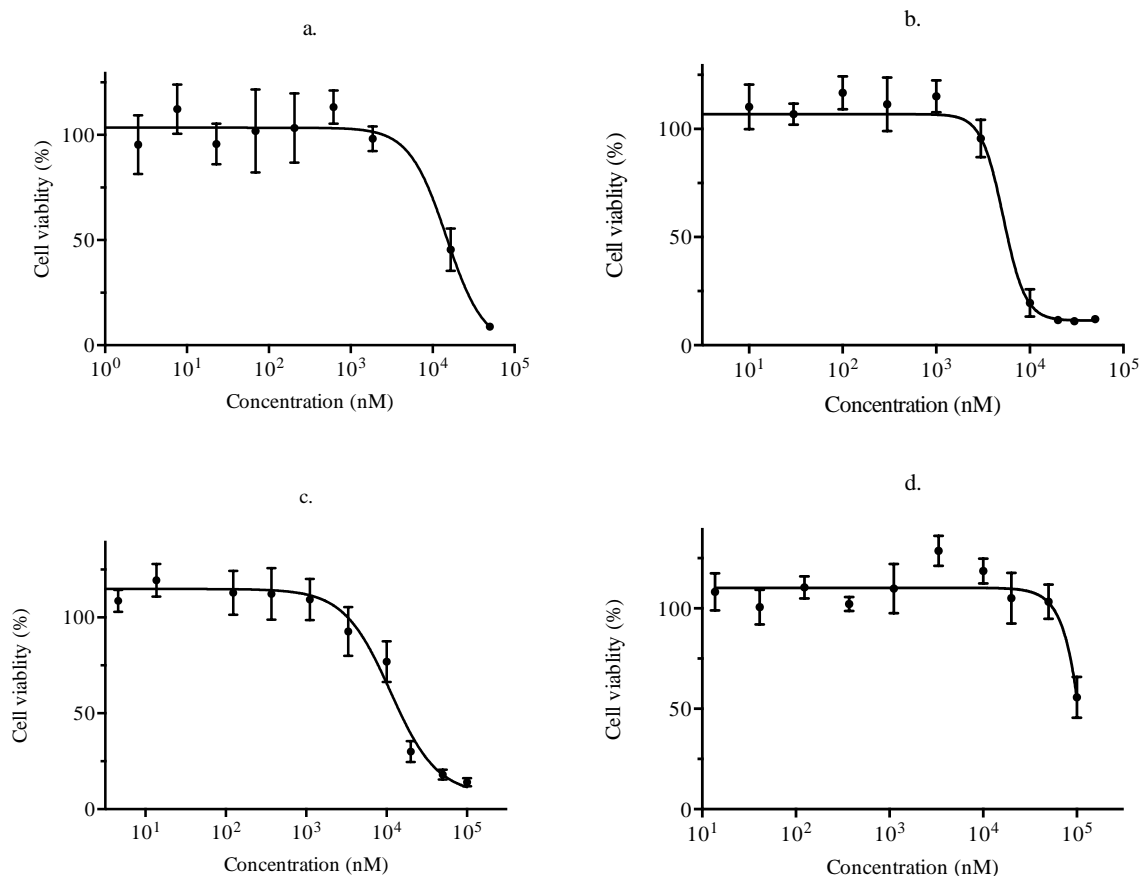


Figure 7.4 The effects of ibrutinib, gefitinib, and dabrafenib on cell viability in TGF-β1-activated LX-2 cells as determined by MTT assay. Cells were treated with compounds for 72 hours prior to the addition of MTT for cytotoxicity determination. The IC₅₀ values for the test compounds were calculated from the plots by a nonlinear regression model using GraphPad Prism v6.0. a) ibrutinib in nonTGF-β1-stimulated LX-2 cells, the IC₅₀ value calculated from this plot was 26 μM; plot b) ibrutinib in TGF-β1-stimulated LX-2 cells, the IC₅₀ value calculated from this plot was 5 μM; c) gefitinib in TGF-β1-stimulated LX-2 cells, the IC₅₀ value of gefitinib in activated LX-2 cells was 13 μM; d) dabrafenib in TGF-β1-stimulated LX-2 cells, the IC₅₀ value of dabrafenib in activated LX-2 cells was over 100 μM. The data were analyzed by a nonlinear regression model of GraphPad Prism v6.0. The data are reported as mean ± SD of six replicates (done on two occasions).

7.2.1.2 MTT and Calcein-AM assays for ENL in TGF- β 1-stimulated LX-2 cells

Previous work in the Alcorn laboratory suggested that lignans may interact with MTT reagent. Hence, both MTT and Calcein-AM assays were used to assess cell viability which work via different mechanisms using two different kinds of dyes. These assays were conducted to determine the cytotoxicity of ENL and FMOC-L-Leu in activated LX-2 cells⁴²⁴. After LX-2 cells were seeded to 96-well plates, the cells were stimulated with TGF- β 1 at a concentration of 2.5 ng/mL 24 hours later. Six hours after stimulation, the cells were treated with ENL and FMOC-L-Leu for 72 hours. The absorbance at 570 nm and fluorescence were read at the end of the treatment by MTT or Calcein-AM assay, respectively.

Both assays showed that even the highest concentrations of ENL (50 μ M) did little to impact cell viability of TGF- β 1-stimulated LX-2 cells (**Figure 7.5A**), suggesting ENL was not toxic to the activated LX-2 cells at high concentrations. FMOC-L-Leu, the known PPAR γ partial agonist, had a sharp decrease in cell viability when the concentration increased from 20 μ M to 50 μ M (**Figure 7.5B**).

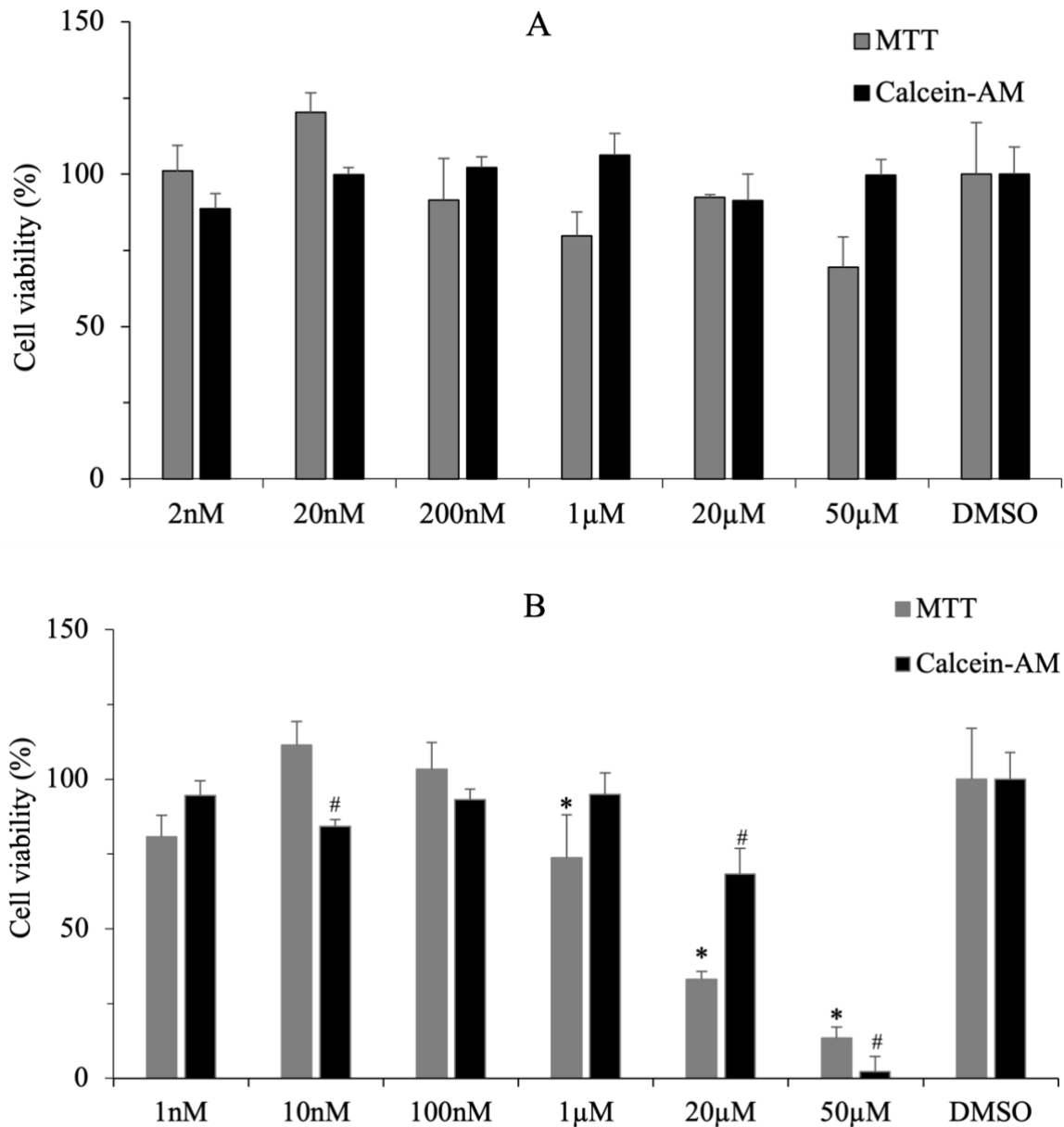


Figure 7.5 Cell viability of TGF- β 1-activated LX-2 cells following enterolactone (ENL) and FMOC-L-Leucine (FMOC, PPAR γ partial agonist control) treatment determined by MTT and Calcein-AM assays. A) ENL (concentrations from 2 nM to 50 μ M); B) FMOC (concentrations from 1 nM to 50 μ M). Cells were treated with the tested compounds for 72 hours prior to the addition of MTT or Calcein-AM for cytotoxicity determination. The data is reported as relative cell viability comparing with the 1% DMSO treated TGF- β 1-activated LX-2 cells, described as mean + SD of four replicates, done on two occasions. * for MTT assay and # for Calcein-AM assay $P < 0.05$ compared with each assay's vehicle control using one-way ANOVA followed by Tukey test.

7.2.2 Several factors impact gene expression of fibrotic biomarkers and PPAR γ in non-TGF- β 1 and TGF- β 1-activated LX-2 cells

Following determination of the cytotoxicity of the TKIs and ENL in activated LX-2 cells, preliminary studies were conducted to identify optimal assay conditions with respect to the concentration of TGF β 1 and stimulation time post cell seeding necessary to induce appropriate changes in the expression of the biomarkers of fibrosis, as well as treatment exposure times to the TKIs and ENL. Human recombinant TGF β 1 was used to activate quiescent the LX-2 cells to establish the *in vitro* model of hepatic fibrosis – the activated HSC. To optimize the time of TGF- β 1 stimulation as well as treatment exposure with the TKIs in LX-2 cells for assessment of changes in fibrotic biomarkers (collagen I α 1, α -SMA) and possible signaling mechanisms (PPAR γ), gene expression changes were assessed by qPCR using non-stimulated LX-2 cells as reference for the calculation. Difference was considered significant when the relative mRNA expression was beyond 2 or below 0.5.

7.2.2.1 The concentration of TGF- β 1 and the duration of cell-seeding and stimulation impacts the expression of fibrotic biomarkers.

When LX-2 cells were stimulated with human recombinant TGF- β 1 at different final concentrations (1, 2.5, and 5 ng/mL) 24 or 28 hours after plating, the expression of *COL1A1* and *ACTA2* were increased significantly except *ACTA2* with 12 hours stimulation at 1 ng/mL of TGF- β 1. Duration of cell plating before TGF- β 1 stimulation influenced the gene expression of fibrotic biomarkers. With a seeding time of 24h, TGF- β 1 stimulation showed greater changes in expression of fibrotic biomarkers as compared with a 28h post-seeding time, as shown in **Figure 7.6**.

The duration of TGF- β 1 stimulation and the concentration of TGF- β 1 influenced the fibrotic biomarkers as well. With treatment started at 24 hours after cell seeding, both *COL1A1* and *ACTA2* were increased at a final concentration of 2.5 ng/ml of TGF- β 1 with 24 hours stimulation (**Figure 7.6**).

Hence, 2.5 ng/mL of TGF- β 1 applied at 24 hours after cell seeding was used for subsequent evaluations. Taken *COL1A1* and *ACTA2* expression changes together into consideration, duration of stimulation of 24 hours seemed a better choice than shorter stimulation. This needed confirmation when treated with the tested compounds.

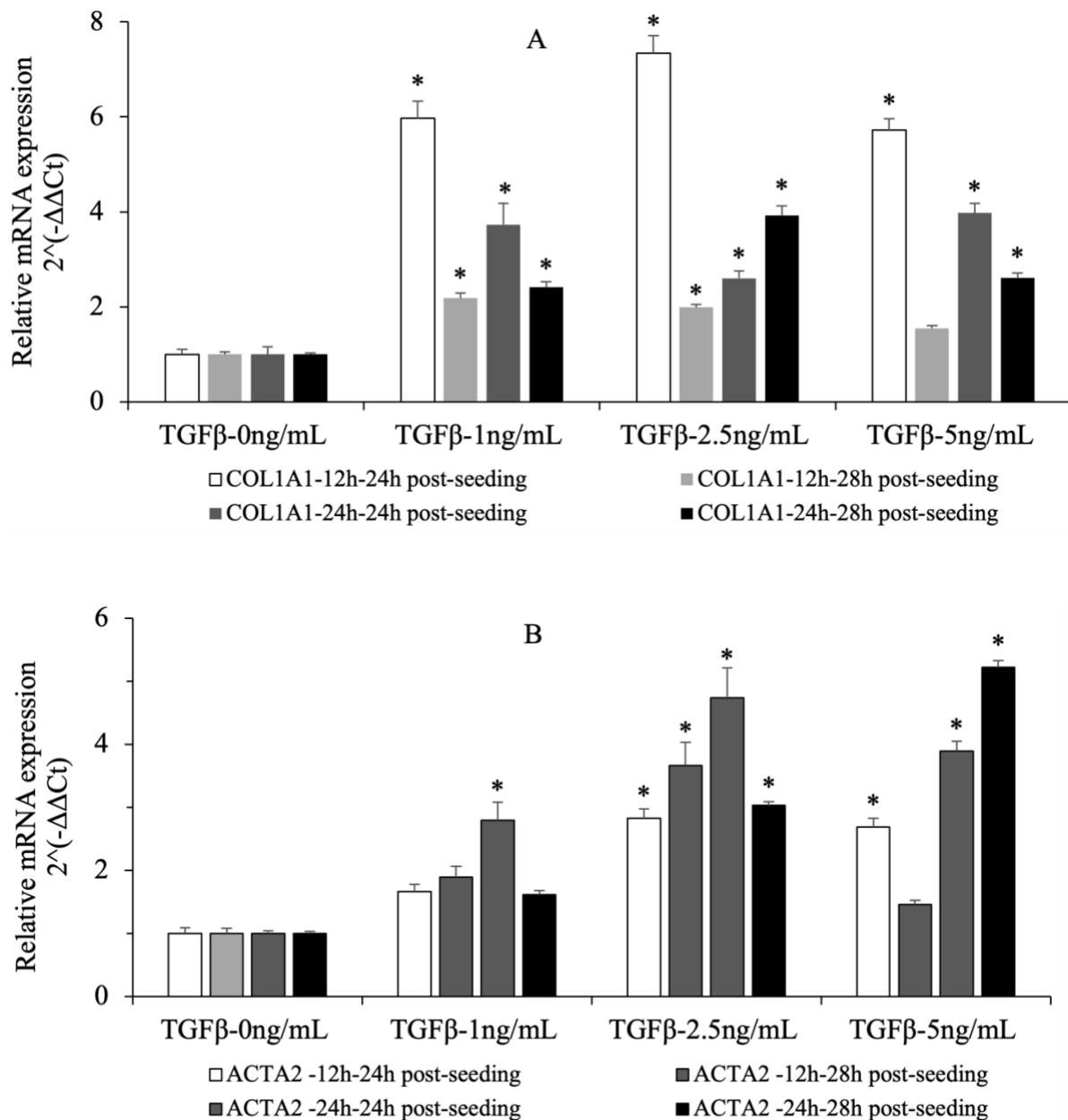


Figure 7.6 The mRNA expression of *COL1A1* (A) and *ACTA2* (B) in TGF- β 1-stimulated LX-2 cells. The final concentrations of TGF- β 1 were 5, 2.5, 1, and 0 ng/mL. 24 hours (12h/24h-24h) or 28 hours (12h/24h-28h) after seeding cells to 96-well plate, the cells were stimulated with TGF- β 1 for 12h and 24 h. The mRNA expression of *COL1A1* and *ACTA2* were measured by qPCR, using β -actin as reference gene for the calculation. The data are reported as mean + SD (N=3). * Induction or reduction when the relative mRNA expression beyond 2 or below 0.5, respectively.

7.2.2.2 mRNA expression changes of the fibrotic biomarkers in TGF- β 1-activated LX-2 cells

According to the results on the optimization of the duration of cell seeding and TGF- β 1 stimulation, other fibrotic biomarkers were detected to confirm the fibrogenic activity of TGF- β 1 in LX-2 cells. Activation of LX-2 cells with TGF- β 1 for 24 hours significantly upregulated mRNA expression of *COL1A1*, *MMP2*, and *TIMP1* relative to the non-TGF- β 1-stimulated LX-2 cells, while no significant increase was observed for α -SMA (**Figure 7.7**).

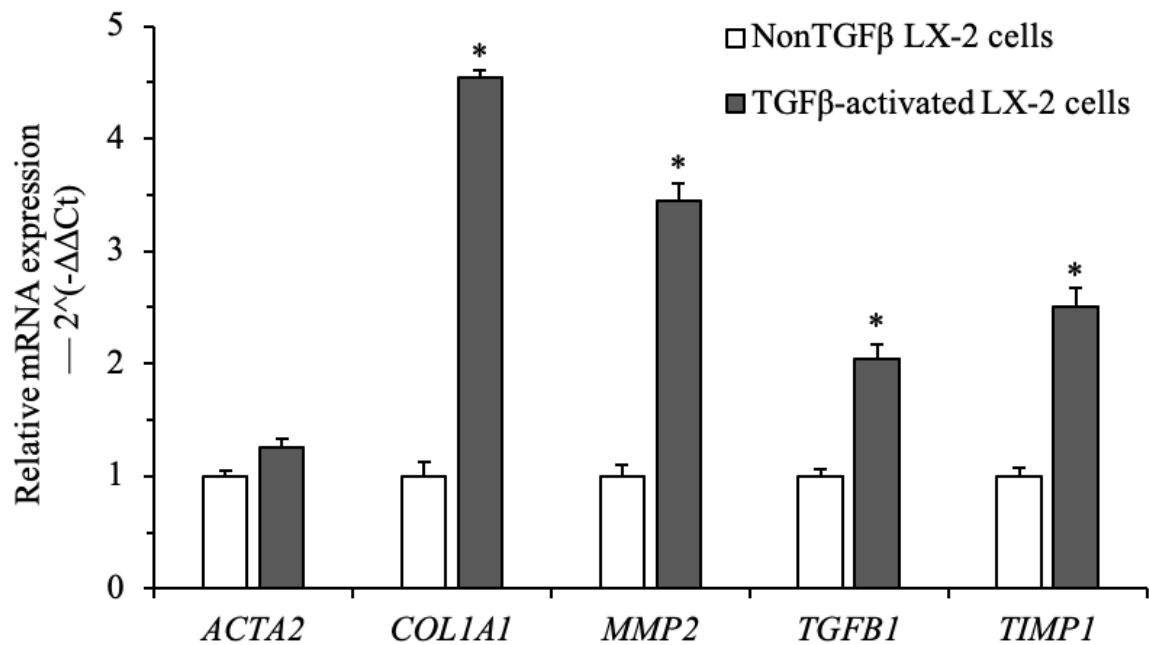


Figure 7.7 The mRNA expression changes of fibrotic biomarkers in nonTGF- β and TGF- β 1-activated LX-2 cells. The cells were stimulated with TGF- β 1 at a final concentration of 2.5 ng/mL for 24 hours. The mRNA expressions of *ACTA2*, *COL1A1*, *MMP2*, *TGFB1*, and *TIMP1* were detected by qPCR, using β -actin as reference gene for the calculation. The data are reported as mean + SD (N=3, performed on three occasions). *Induction or repression when the relative mRNA expression beyond 2 or below 0.5, respectively.

7.2.2.3 The time of administration of TKIs after stimulation impacts the expression of fibrotic biomarkers.

After cell seeding time and stimulation conditions were established as above, the treatment exposure time was then optimized using 2 and 10 μM of ibrutinib. The qPCR data indicated treatment with ibrutinib showed the best outcome when applied 6 hours after stimulation with TGF- β 1 in LX-2 cells. At 6 hours of exposure to TGF- β 1 before treatment caused an increase in *COL1A1* and *ACTA2* expression compared with nonTGF- β 1-activated LX-2 cells. Following treatment with 1 μM of rosiglitazone at 12 hours after TGF- β 1 stimulation, (rosiglitazone was used as a PPAR γ full agonist control for all treatment groups), the expression of *COL1A1* was decreased compared to the vehicle-treated TGF- β 1 activated LX-2 cells, while no changes were observed for *ACTA2* expression. Ibrutinib, at concentrations of 2 and 10 μM , decreased the expression of *COL1A1* further when was applied at 6 hours after TGF- β 1 stimulation than at 0 and 12 hours (**Figure 7.8**).

Consequently, the dosing time of TKI treatment was set to 6 hours after TGF- β 1 stimulation. Along with the concentration and duration of the stimulation, 24 hours of total stimulation with 2.5 ng/mL of TGF- β 1 and treatment applied 6 hours later seemed appropriate to investigate the ability of TKIs to suppress the biomarkers of hepatic fibrosis *in vitro*.

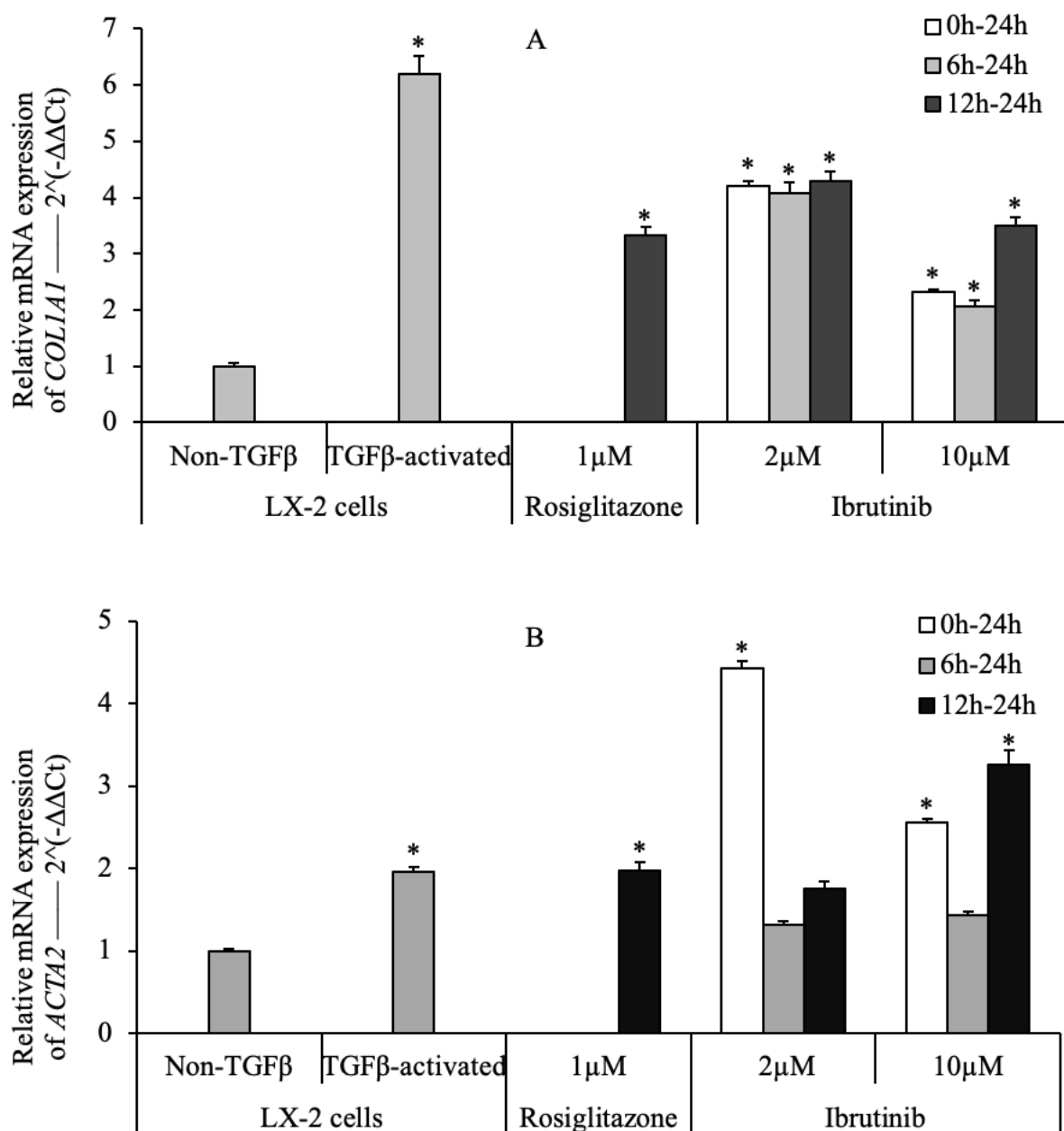


Figure 7.8 The mRNA expression of *COL1A1* (A) and *ACTA2* (B) after treatment with ibrutinib at different time points in TGF-β1-stimulated LX-2 cells. 2.5 ng/mL of TGF-β1 was applied to Non-TGF-β-stimulated LX-2 cells 24 hours after plating. Ibrutinib was applied at the same time with TGF-β1, 6 and 12 hours after TGF-β1 stimulation. The mRNA expression of *COL1A1* and *ACTA2* was measured by qPCR, using β-actin as reference gene for the calculation. The data are reported as mean + SD (N=3, performed on three occasions). *Induction or repression when the relative mRNA expression was beyond 2 or below 0.5, respectively.

7.2.3 Changes in fibrotic biomarkers in TGF- β 1-stimulated LX-2 cells

After the optimization of cell culture conditions necessary to stimulate the expression of biomarkers of hepatic fibrosis in activated LX-2 cells, the ability of TKI's and ENL to suppress the expression of the hepatic biomarkers was subsequently assessed in TGF- β 1-activated LX-2 cells in the absence and presence of TKI drugs and ENL using qPCR and Elisa. The key hepatic fibrotic biomarkers, including collagen I α 1, MMP2, TGF- β 1, and TIMP1, are highly expressed in TGF- β 1-activated LX-2 cells compared to non-TGF- β 1-stimulated LX-2 cells. As dabrafenib showed a significant induction of glucose uptake activity, it is believed that there might be other pathways involved in the modulation of PPAR γ -related mechanism. Thus, dabrafenib was excluded for further study on the antifibrotic effects of TKIs.

Both ibrutinib and gefitinib reduced collagen I α 1 expression in activated LX-2 cells at certain concentrations, especially for gefitinib (**Figure 7.9**). TGF- β 1 stimulation increased the expression of *COL1A1*, *MMP2*, *TGFB1*, and *TIMP1* compared with the non-TGF- β 1-stimulated LX-2 cells, while no differences were observed with *ACTA2* expression. Ibrutinib suppressed *ACTA2*, *COL1A1*, *MMP2*, *TGFB1*, and *TIMP1* at 0.5 μ M but increased *ACTA2*, *MMP2*, and *TIMP1* at 5 μ M, while no biological significant modulation was observed with the targets at other concentrations. Gefitinib considerably decreased the expression of *COL1A1* and *MMP2* in a concentration-dependent manner. *ACTA2* was increased by gefitinib to 2.2-fold at 1 μ M and remained similar to the vehicle control at 2 and 10 μ M. Gefitinib reduced *TGFB1* and *TIMP1* expression as well, but the concentration-response relationship is not as clear as *COL1A1* and *MMP2*. However, because TGF- β 1 is used as a stimulator for the hepatic fibrosis model, it might not be appropriate to use the expression of *TGFB1* as an indicator for antifibrotic effects of the compounds.

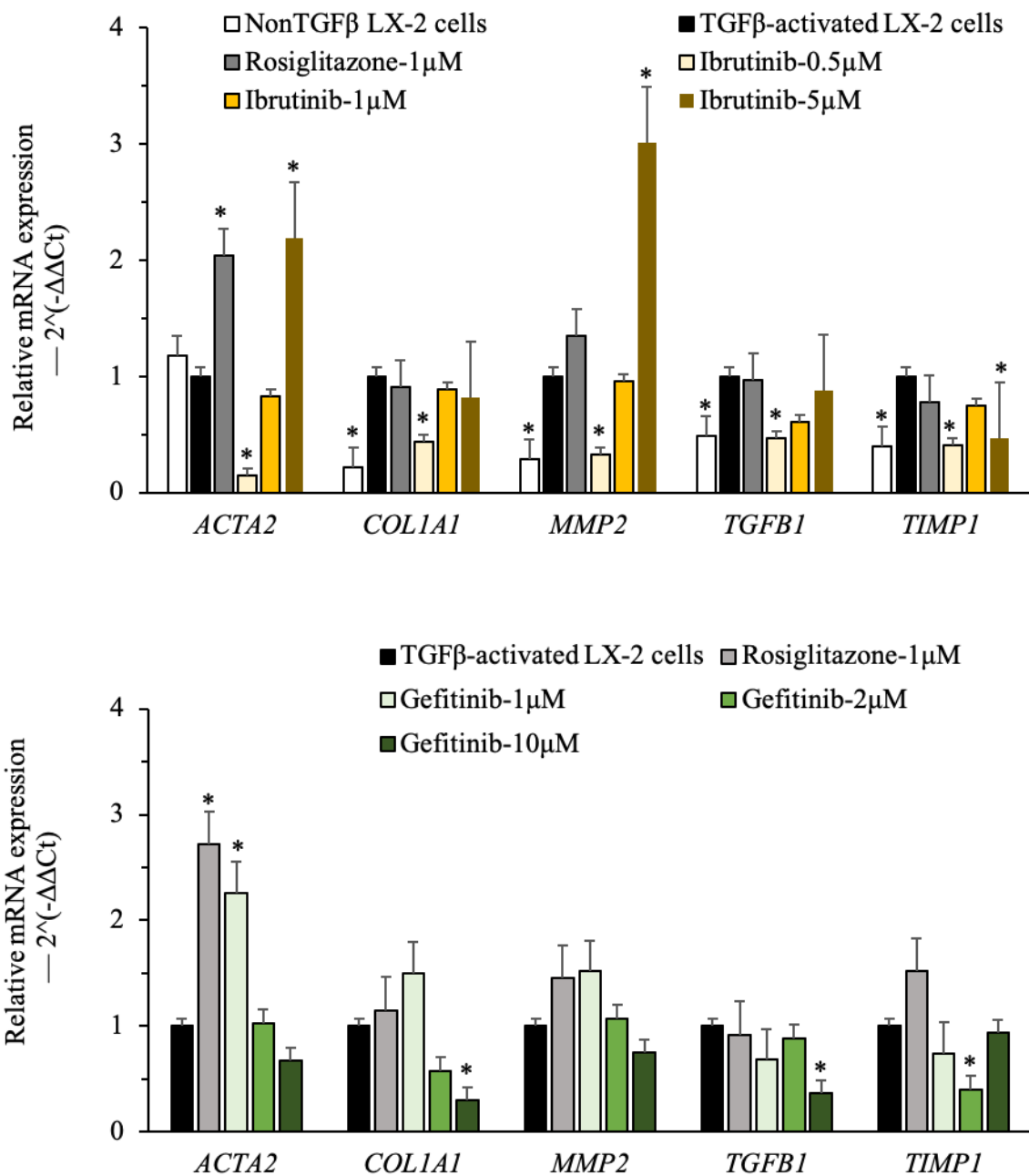


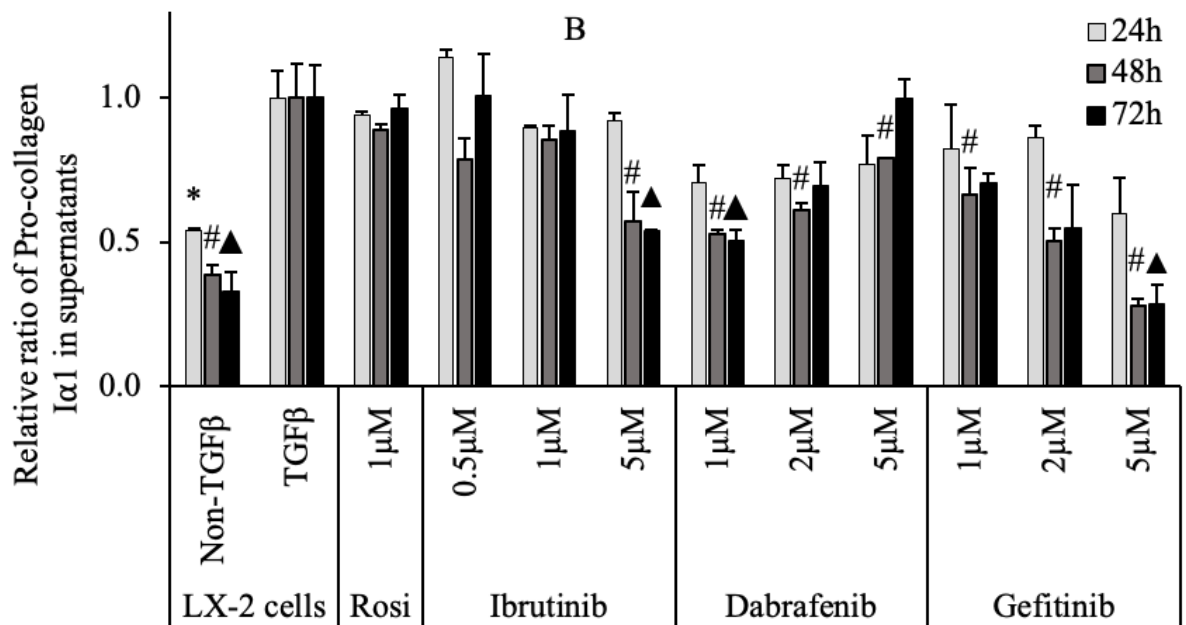
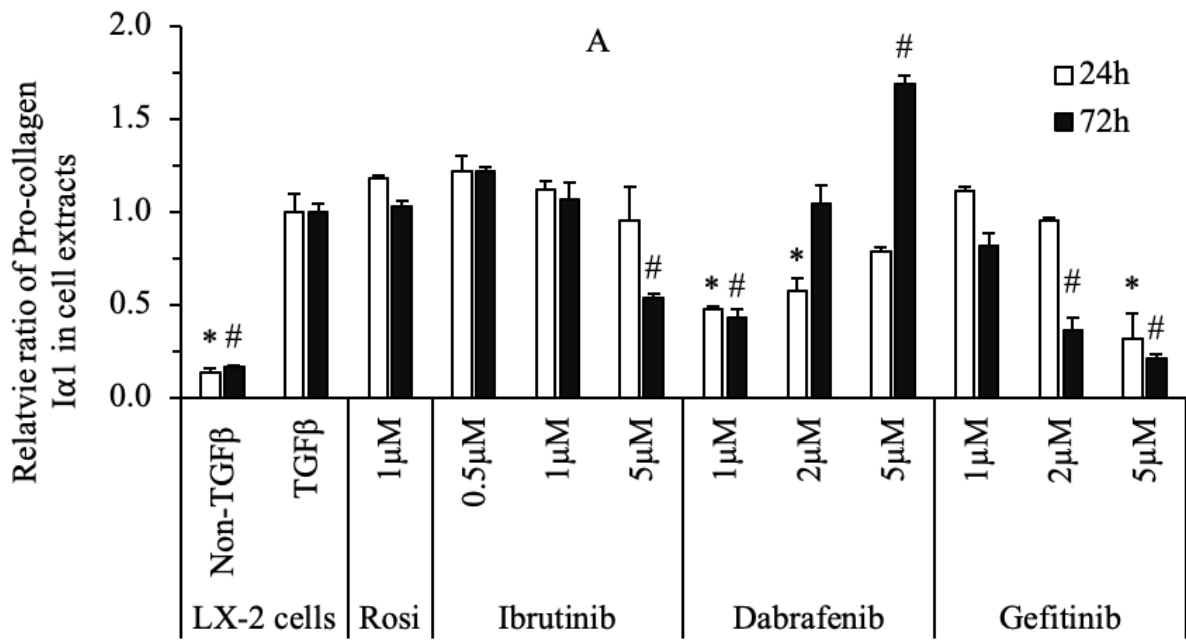
Figure 7.9 The relative mRNA expression of hepatic fibrotic biomarkers in TGF- β 1-stimulated LX-2 cells after treatment with ibrutinib (0.5, 1, 5 μ M) or gefitinib (1, 2, 10 μ M) for 24 hours (6 hours of stimulation with 18 hours of treatment with different concentrations of compounds), using β -actin as reference gene and the vehicle-treated activated LX-2 cells as control for the calculation. Rosiglitazone (1 μ M) was used as positive control. Data are presented as mean + SD of triplicates on three occasions. * significant induction or repression when the relative mRNA expression beyond 2 or below 0.5, respectively.

The secretion of ECM during fibrogenesis is one of the major characteristics of hepatic fibrosis. To understand the effects of TKIs and ENL on ECM production, ELISA was performed for collagen I α 1 and MMP9 in TGF- β 1-stimulated LX-2 cells after treatment with ibrutinib, dabrafenib, and gefitinib at different concentrations for 24h, 48h, and 72h (**Figure 7.10**). Pro-collagen I α 1 was detected in samples from the cell extracts as well as in the supernatants, while MMP9 was detected for the supernatant samples by the appropriate ELISA kits. The concentrations of the target proteins were determined by the corresponding standard curve, and the relative ratio of the different groups to the activated LX-2 cells at the same time point was reported.

TGF- β 1 induced the production and secretion of pro-collagen I α 1 and decreased the secretion of MMP9 in LX-2 cells when compared with nonTGF- β 1-treated LX-2 cells (**Figure 7.10**). TGF- β 1 stimulated the production of pro-collagen I α 1 in cell extracts at 24 and 72 hours after stimulation. The secretion of pro-collagen I α 1 in the supernatants was increased by the TGF- β 1 stimulation as well at 24, 48, and 72 hours. MMP9 was reduced by TGF- β 1 stimulation in supernatants at 48 and 72 hours. In TGF- β 1-stimulated LX-2 cells, rosiglitazone at 1 μ M showed no significant effect on pro-collagen I α 1 and MMP9 but caused an increasing trend on MMP9 at 24, 48 to 72 hours after treatment.

Ibrutinib decreased the production of pro-collagen I α 1 significantly in cell extracts only at 5 μ M after 72 hours of treatment. The secreted pro-collagen I α 1 was reduced while MMP9 was increased by 5 μ M of ibrutinib at both 48 and 72h. Gefitinib decreased protein production and secretion of pro-collagen I α 1 in both the cell extracts and supernatants in a concentration- and time-dependent pattern. Gefitinib also induced the production of MMP9 in the TGF- β 1-stimulated LX-2 cells at 5 μ M with 72 hours of treatment.

Dabrafenib also caused reduction of pro-collagen I α 1 protein expression at 1 μ M in a time-dependent manner in TGF- β 1-stimulated LX-2 cells. However, the pattern of expression changes changed at higher concentrations of dabrafenib, such that pro-collagen I α 1 protein induction occurred at 72h with 5 μ M of dabrafenib. This suggests that there might be multiple cellular signaling pathways involved in the modulation of fibrotic biomarkers in hepatic fibrotic processes, leading to different cellular responses. Further study should be performed to investigate possible mechanisms of the regulation of dabrafenib in hepatic fibrosis.



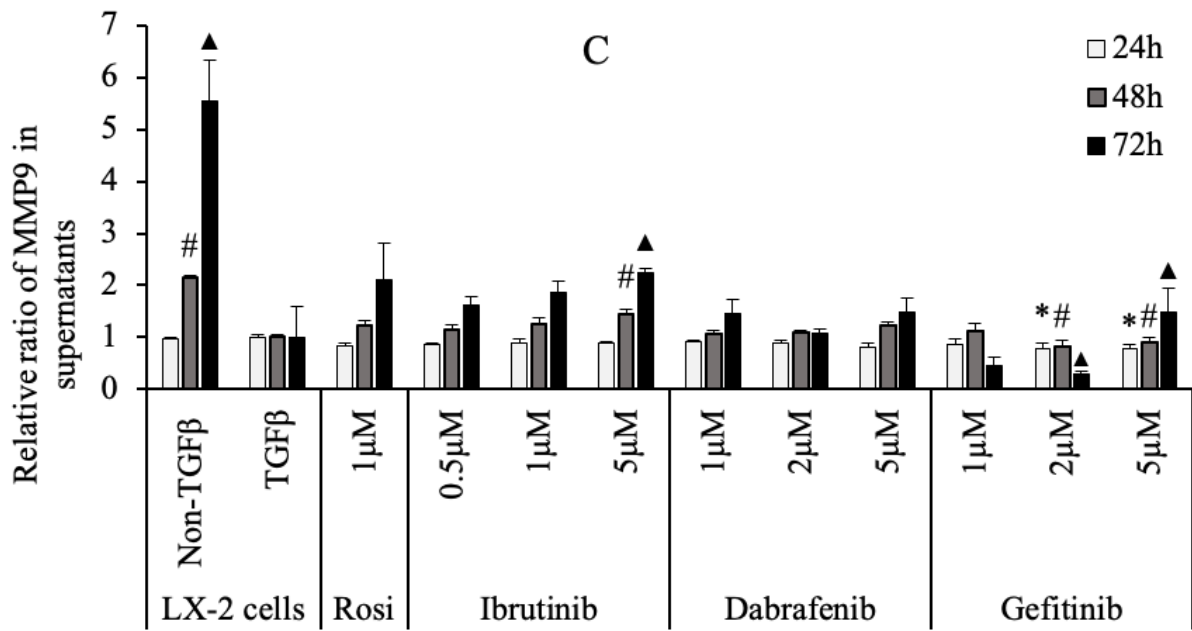


Figure 7.10 Protein expression changes of Pro-collagen I α 1 and MMP9 in TGF- β 1-activated LX-2 cells. The LX-2 cells were treated with or without ibrutinib, dabrafenib, and gefitinib for 24, 48, and 72 hours, using the vehicle-treated TGF- β 1-activated LX-2 as normalization reference and rosiglitazone at 1 μ M as a potential positive control. Pro-collagen I α 1 was detected in cell extract (A) and supernatants (B) at 24 h, 48h (not in cell extracts), and 72 h, while MMP9 was detected in the supernatants of the cell culture at 24 h, 48 h, and 72 h (C). Evaluations were performed in duplicate using TGF- β 1-activated LX-2 cells at the same time point as reference. (Rosi: rosiglitazone, at concentration of 1 μ M; ibrutinib, at concentrations of 0.5, 1, 5 μ M; dabrafenib, at concentrations of 1, 2, 5 μ M; gefitinib, at concentrations of 1, 2, 5 μ M). The data were reported as mean + SD of duplicates on two occasions. #, *, and ▲ means $P < 0.05$, compared with vehicle-treated TGF- β 1-stimulated LX-2 cells at the same time point using one-way ANOVA followed by Tukey test.

According to the gene and protein expression changes of the fibrotic markers in the TGF- β 1-stimulated LX-2 cells, gefitinib demonstrated the greatest ability to attenuate HSC activation and ECM production when compared with the other two TKIs. Thus, gefitinib was chosen as the TKI drug model for the next steps of investigation, along with the assessment on the combination with ENL in activated LX-2 cells. Although gefitinib downregulated the expression of *COL1A1*, *MMP2*, and *TIMP1* with a concentration-dependent trend in TGF- β 1-activated LX-2 cells, ENL showed no clear trend on those fibrotic biomarkers, and there were no biologically significant changes when the compounds were used alone (**Figure 7.11**). In combination, ENL and gefitinib decreased *COL1A1* and the reduction was stronger when the concentration of gefitinib increased, with significance at a high concentration of ENL. The combination caused modest downregulation of *MMP2* and *TIMP1*. However, the pattern of these changes was not observed at 10 μ M of gefitinib with 1 μ M of ENL. As minor changes to the cell culture conditions and the treatment may impact the expression of the fibrotic biomarkers (namely cell plating density and time when seeded qPCR results might differ on different occasions). Since a similar trend was observed, the mRNA expressional changes indicated that the combination of ENL and gefitinib improved fibrotic biomarker expression in TGF- β 1-activated LX-2 cells. Further study on the state of the LX-2 cells should be done to better understand this *in vitro* model in the investigation of hepatic fibrosis.

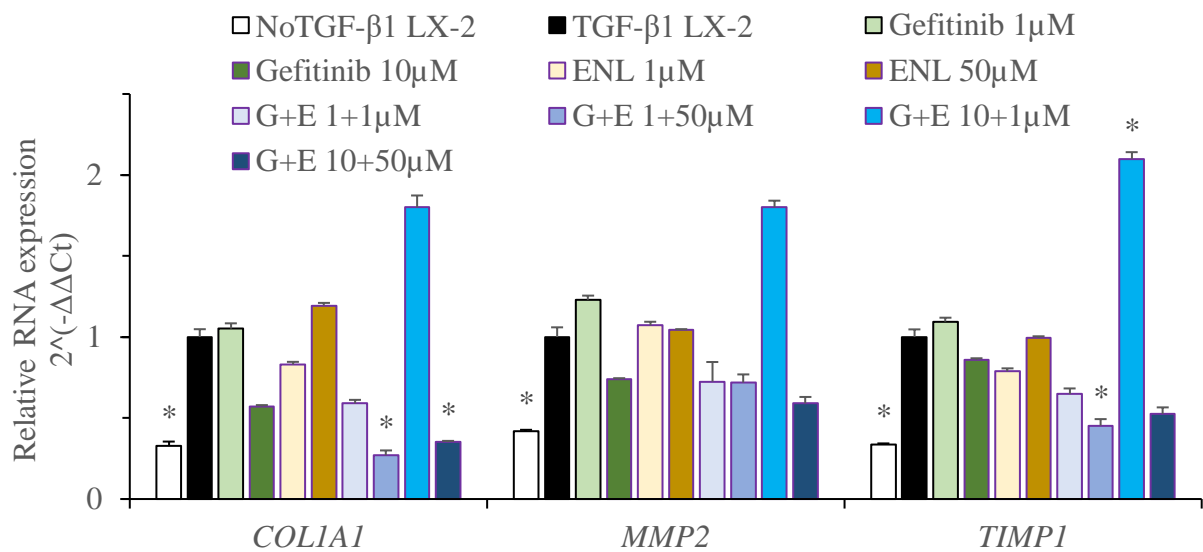


Figure 7.11 The relative mRNA expression of fibrotic biomarkers (collagen Iα1 (*COL1A1*), *MMP2*, and *TIMP1*) in TGF-β1 stimulated LX-2 cells after treatment with gefitinib (1 and 10 μM), enterolactone (ENL, 1 and 50 μM), and the combination of gefitinib (G, 1 and 10 μM) and ENL (E, 1 and 50 μM) for 24 hours (6 hours of stimulation with 18 hours of treatment with different concentrations of compounds), using β-actin as reference gene and TGF-β1-activated LX-2 cells as control for the calculation. Data are presented as mean + SD of triplicates on three occasions. *Induction or reduction when the relative mRNA expression beyond 2 or below 0.5, respectively.

At the protein level, gefitinib, at a concentration of 10 μ M, decreased the production and secretion of pro-collagen I α 1 protein in both the cell extracts and cell culture supernatants in TGF- β 1-stimulated LX-2 cells. The reduction was higher when the concentration increased or when the treatment was longer (**Figure 7.12**). ENL had little impact on the production of pro-collagen I α 1 protein in both cell extracts and supernatants when used alone. In combination, gefitinib with ENL decreased the production of pro-collagen I α 1 in cell extracts to a further extent than using gefitinib alone, a trend that was related to concentration and time. However, the secretion of pro-collagen I α 1 into the supernatants was increased by the combination of ENL with low concentrations of gefitinib to about 2 times of the vehicle control after 24 hours of treatment.

The protein expression changes of α -SMA, another fibrotic marker, were measured by western blot in TGF- β 1-activated LX-2 cells after treatment with gefitinib and/or ENL (**Figure 7.13**). After 24h treatment, α -SMA was decreased by ENL and its combination with gefitinib, but the changes caused by gefitinib were not significant. With longer treatment, gefitinib caused a reduction in α -SMA protein expression. ENL and the combination of ENL with gefitinib still showed a reduction, but the extent was lower than at 24h. There was no clear concentration-response relationship with respect to α -SMA modulation by the treatments.

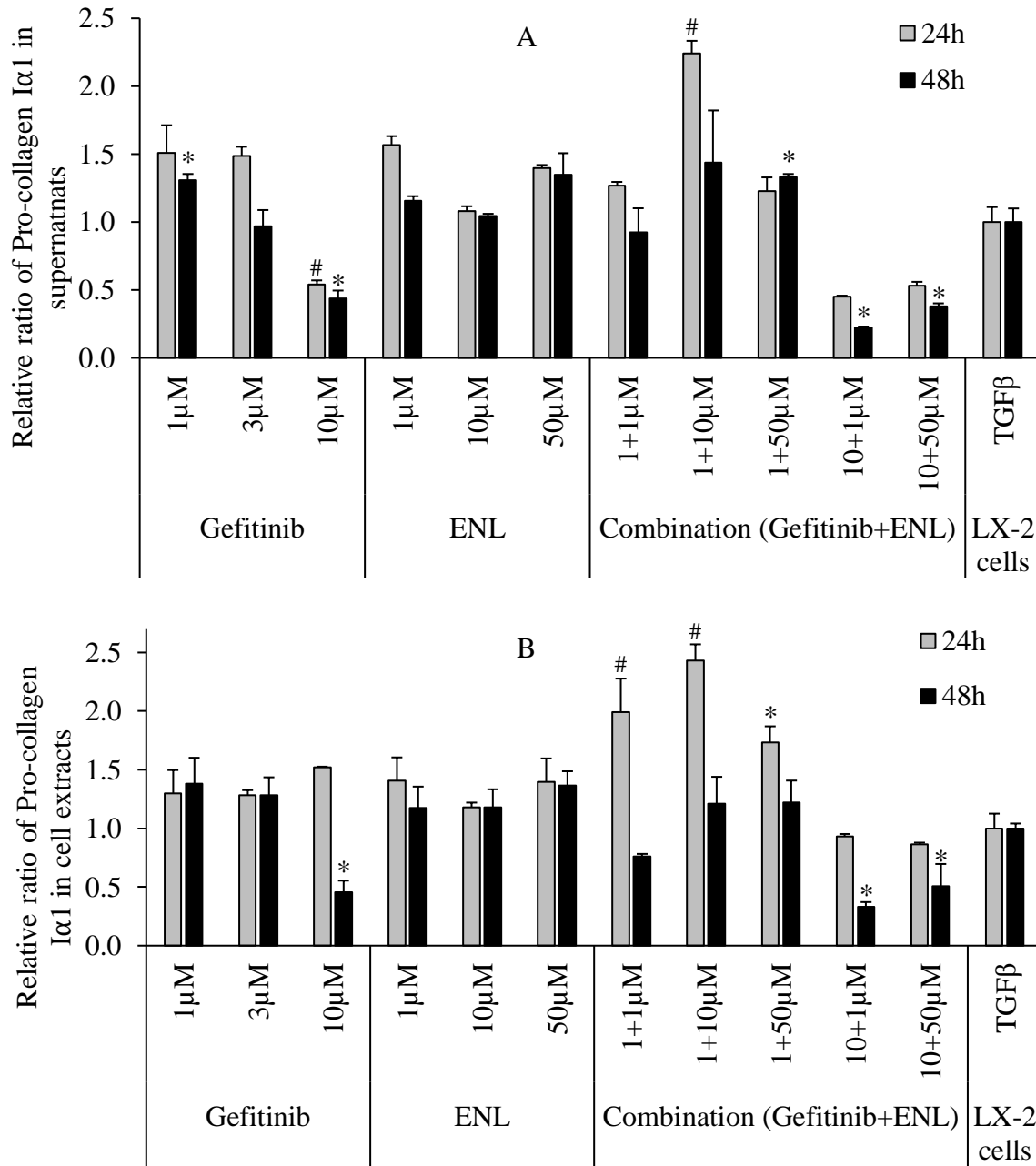


Figure 7.12 Protein expression changes of pro-collagen Iα1 in TGF-β1-stimulated LX-2 cells after treatment with gefitinib and/or enterolactone (ENL). LX-2 cells were stimulated for 6 hours before treatment with or without gefitinib and/or ENL at different concentrations for 24 and 48h, gefitinib at concentrations of 1, 3, and 10 μM; ENL at concentrations of 1, 10, and 50 μM; and combination of gefitinib (1 and 10 μM) and ENL (1, 10, and 50 μM). Pro-collagen Iα1 was measured in cell extracts (A) and supernatants (B), using TGF-β1-stimulated LX-2 cells at the same time point as normalization references. The data were reported as mean + SD of duplicates on three occasions. # * means $P < 0.05$, compared with the vehicle-treated TGF-β1-stimulated LX-2 cells at the same time point using two-way ANOVA followed by Tukey test.

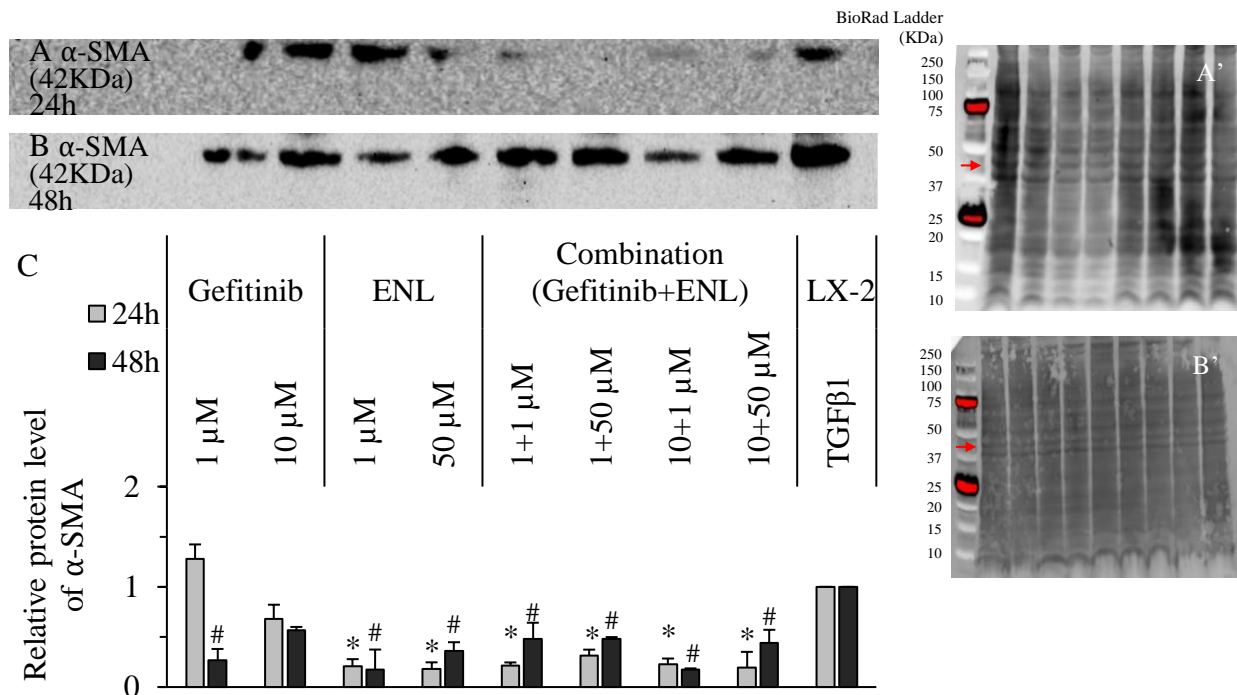


Figure 7.13 Protein expression of α -SMA in TGF- β 1-activated LX-2 cells after treatment with gefitinib and/or enterolactone (ENL). The LX-2 cells were stimulated for 6 hours before treatment with or without gefitinib and/or ENL at different concentrations for 18 and 42h. A and B) TGF- β 1-activated LX-2 cells were treated with gefitinib of 1 and 10 μ M (lanes 1 and 2) or ENL of 1 and 50 μ M (lanes 3 and 4); C and D) The TGF- β 1-activated LX-2 cells were treated with the combination of gefitinib (1 and 10 μ M) and ENL (1 and 50 μ M) (lanes 5, 6, 7, and 8), using vehicle-treated TGF- β 1-activated LX-2 cells as control (lane 9) and total protein stained by SYPRO Ruby blot stain reagent (A' and B' for A and B, respectively, protein ranges from 10 to 250 kDa according to BioRad Precision Plus Protein Dual Color Standards, where the dual-color bands were stained as the red in panel A' and B') as normalizing reference. The relative expression of α -SMA for each group was normalized to the TGF- β 1-activated LX-2 group, located at the red arrow on the blot. The data were reported as mean + SD of duplicates on two occasions. * and # mean $P < 0.05$, compared with the vehicle-treated TGF- β 1-stimulated LX-2 cells at the same time point using one-way ANOVA followed by Dunnett test.

7.2.4 Scratch wound healing assay for gefitinib and ENL in TGF- β 1-stimulated LX-2 cells

Hepatic fibrosis is characterized as a dynamic wound healing response of the liver, which is believed to be one therapeutic target to resolve fibrotic scars within the liver, making the recovery of hepatic fibrosis or even cirrhosis possible⁴²⁵. Since liver fibrosis is defined as a wound healing response, inhibition of cell migration by gefitinib and/or ENL was evaluated by the wound healing response assay. The width of the artificial wound was measured and performed as mean \pm SD for duplicates on three occasions measured by Image J according to Zoe imager (**Table 7.3**). Compared with TGF- β 1-stimulated LX-2 cells at 24 hours of treatment, gefitinib and ENL inhibited cell migration and the inhibition was increased when the concentration increased from 1 to 10 μ M, though ENL inhibition of migration was milder. In combination, gefitinib and ENL showed a greater inhibition on cell migration than each compound alone. Images were taken by Olympus due to their higher resolution (**Figure 7.14**).

Table 7.3 The width of the wound for three fields per well after treatment with gefitinib and/or enterolactone (ENL) for 24h in TGFβ1-stimulated LX-2 cells.

Treatment	Width
Before treatment (0h)	304.94 ± 42.46 μm
Non-TGF-β1-treated LX-2 cells	44.89 ± 2.08
TGF-β1-stimulated LX-2 cells	37.38 ± 4.11
Gefitinib - 1 μM	61.93 ± 7.57*
Gefitinib - 3 μM	148.89 ± 7.84*
Gefitinib - 10 μM	183.79 ± 6.33*
ENL - 1 μM	55.68 ± 1.19*
ENL - 10 μM	115.95 ± 8.86*
ENL - 100 μM	127.36 ± 1.98*
Gefitinib + ENL - 1+1 μM	71.28 ± 3.03*
Gefitinib + ENL - 1+10 μM	115.95 ± 8.86*
Gefitinib + ENL - 1+100 μM	154.33 ± 1.58*
Gefitinib + ENL - 10+1 μM	207.75 ± 4.94*
Gefitinib + ENL -10+100 μM	226.07± 5.61*

Note: * means P<0.05 when compared with the vehicle-treated TGF-β1-stimulated LX-2 cells at 24 hours after treatment with gefitinib and/or ENL using one-way ANOVA followed by Tukey test (data were shown as mean ± SD for duplicates, done in three occasions).



Figure 7.14 The wound healing assay endpoint images for gefitinib (G) and/or enterolactone (ENL or E) for 24 hours, using NonTGF- β -stimulated LX-2 and TGF- β 1-activated LX-2 as controls. LX-2 cells were seeded at appropriate density into 6-well plates for overnight attachment. A scraped gap was made by using a 10 μ L clear micropipette tip in each well right before the cells were stimulated with TGF- β 1 at 2.5 ng/mL 6 hours before treatment with gefitinib and/or ENL at different concentrations for 18 hours. The cell migration was observed and imaged by Olympus microscope, original magnification 400 \times . The gaps were indicated by two white lines, the inhibition on cell migration was revealed by the number of cells migrated to the gap after treatment, compared with the pre-treatment with both the nonTGF- β -stimulated and TGF- β -stimulated LX-2 cells after 24 hours.

7.2.5 Possible mechanisms of the attenuation of activated LX-2 cells by gefitinib and ENL

As indicated by the wound healing assay and the gene and protein expression changes of the key fibrotic biomarkers, gefitinib and ENL seem to exhibit antifibrotic potential in activated HSCs. As possible mechanisms of the suppression of HSC activation, PPAR γ , PKM2 as a potential downstream factor of PPAR γ , and key factors of the Wnt, Nrf2, and ER-stress related signaling pathways were assessed as a preliminary study. Markers including PPAR γ , Nrf2, and ATF4 and CHOP, as markers of ER-stress pathway, were chosen for this preliminary evaluation in TGF- β 1-stimulated LX-2 cells. All treatments with different TKIs and/or ENL were performed in TGF- β 1-stimulated LX-2 cells, TGF- β 1-stimulated LX-2 cells and/or non-TGF- β 1-stimulated LX-2 cells along with appropriate negative vehicle controls.

7.2.5.1 PPAR γ -related changes by gefitinib and ENL in LX-2 cells

7.2.5.1.1 PPARG mRNA expression changes by ibrutinib in Non-TGF- β 1-stimulated LX-2 cells

To confirm the involvement of PPAR γ in HSCs activation, the endogenous expression and the changes of *PPARG* after treatment with ibrutinib were first measured by qPCR in nonTGF- β 1-stimulated LX-2 cells. *PPARG* mRNA expression was low and relatively unchanged after treatments with ibrutinib and rosiglitazone for 12 hours, 24 hours, and 72 hours in nonTGF- β 1-stimulated LX-2 cells (**Figure 7.15**). The results indicated that cytokine activation should be applied to the LX-2 cells for PPAR γ study and evaluations should be conducted in TGF- β 1-stimulated LX-2 cells.

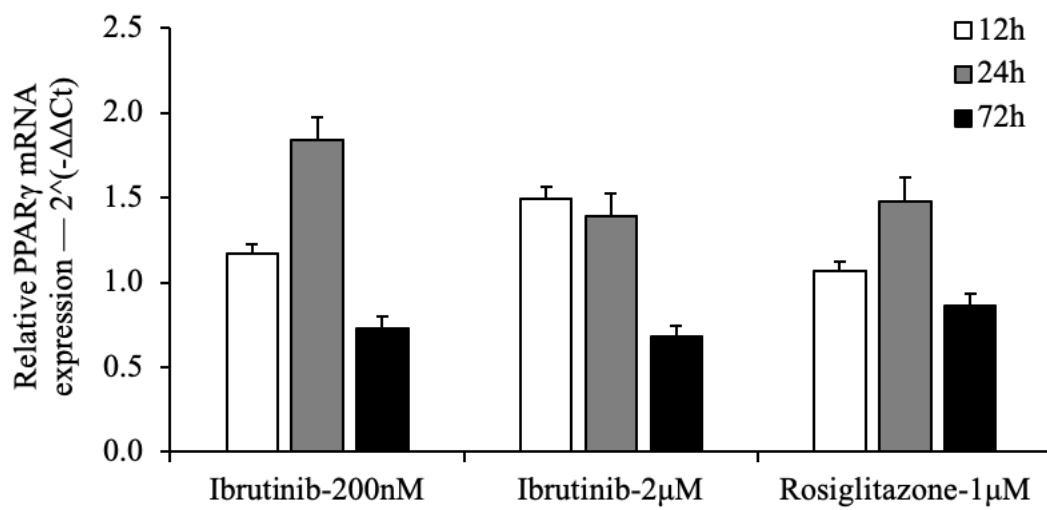


Figure 7.15 The relative *PPARG* mRNA expression in nonTGF- β 1-stimulated LX-2 cells after treatment with rosiglitazone and ibrutinib for 12h, 24h, and 72h (compared with the vehicle control group), using β -actin as reference gene for the calculation. Data are presented as mean + SD of triplicates on three occasions. It is considered significant induction or repression when the relative mRNA expression is beyond 2 or below 0.5, respectively.

7.2.5.1.2 *PPARG* and *PKM2* mRNA expression changes by TKIs in TGF- β 1-stimulated LX-2 cells

To confirm the involvement of *PKM2* as a downstream factor of *PPAR* γ , the expression changes of *PKM2* and *PPARG* was measured by qPCR in TGF- β 1-stimulated LX-2 cells after 18 hours of treatment with ibrutinib and gefitinib, using rosiglitazone at 1 μ M as positive control for *PPAR* γ . At 1 μ M, rosiglitazone showed no significant modulation of both *PPARG* and *PKM2*. *PKM2* mRNA expression was upregulated 3-fold by treatment of ibrutinib at concentration of 5 μ M and *PPARG* was downregulated 3-fold at the same concentration of ibrutinib in TGF- β 1-activated LX-2 cells. Gefitinib decreased the mRNA expression of *PKM2* in TGF- β 1-activated LX-2 cells by 2-fold while the impact on *PPARG* was mild at all concentrations of gefitinib for 18 hours (**Figure 7.16**).

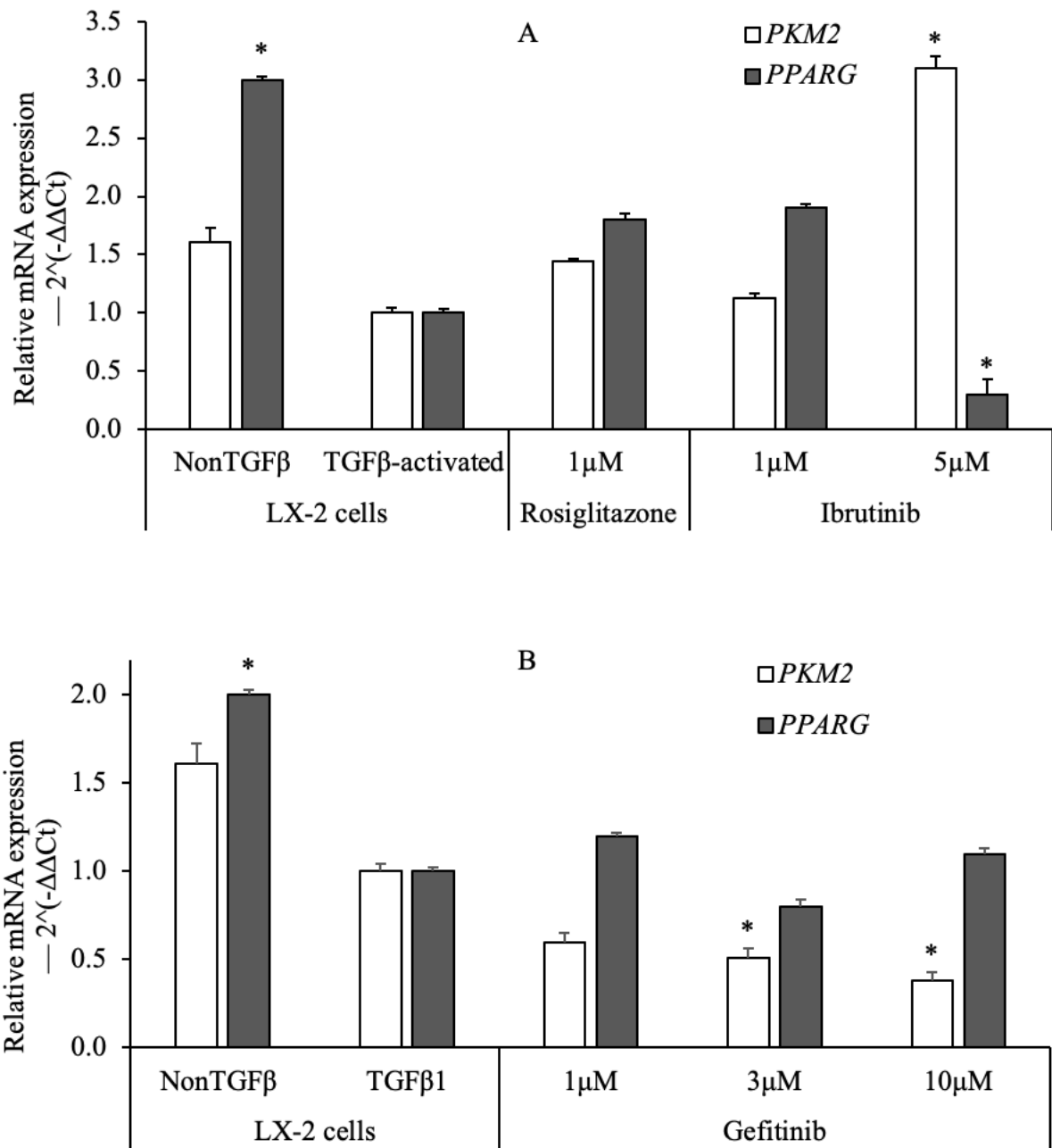


Figure 7.16 The relative *PPARG* and *PKM2* mRNA expression in TGF-β1-stimulated LX-2 cells with treatment of ibrutinib at 1 and 5 μM (A) and gefitinib at 1, 3, and 10 μM (B) for 18 hours), using β-actin as reference gene and TGF-β1-activated LX-2 cells as control for the calculation while rosiglitazone at 1 μM was used as a positive control. Data were presented as mean + SD of triplicates on three occasions. *Induction or reduction when the relative mRNA expression beyond 2 or below 0.5, respectively.

7.2.5.1.3 Protein changes of PPAR γ by gefitinib and ENL in TGF- β 1-stimulated LX-2 cells

To confirm the involvement of PPAR γ and PKM2 in the antifibrotic response of gefitinib and/or ENL, a preliminary study on the effects of test compounds on PPAR γ and PKM2 protein expression was conducted by western blot. Normalized to β -Actin, the result showed that low concentrations of ibrutinib had no impact on both PPAR γ and PKM2 while higher concentrations increased PPAR γ expression after 6 hours of TGF- β 1 stimulation with another 42 hours treatment (**Figure 7.17**). The expression of PPAR γ protein was not changed by TGF- β 1 stimulation in LX-2 cells and PKM2 was decreased by the stimulation. As well, rosiglitazone did little impact on both PPAR γ and PKM2 protein comparing with the vehicle control.

Based upon these results and other works in the Alcorn lab related to TKIs and ENL, the expression of β -actin fluctuated at the same loading amount, suggesting an effect on the β -actin protein by TGF- β 1 and the TKI treatments. Based upon the current results and the reported work of TKIs on housekeeping proteins, it is possible that the expression of common control proteins for western blot would be modified by TKIs and lignans. Because of the expression difference between reference genes within different treatments, the results were not appropriate for further investigation. Thus, normalization using total protein was used for subsequent western blot assays.

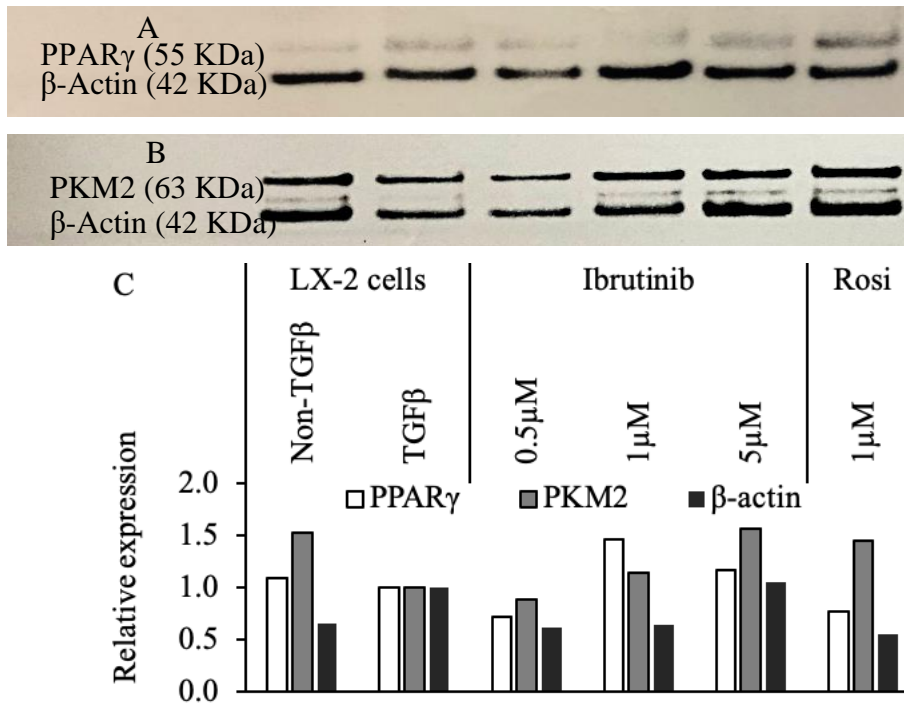


Figure 7.17 Preliminary study on the protein expression changes of PPAR γ and PKM2 as measured by western blot. The activated LX-2 cells were treated with different concentrations of ibrutinib for 42 hours, using rosiglitazone as positive control and non-TGF- β 1-stimulated LX-2 and TGF- β 1-activated LX-2 as negative controls. The relative expression of both PPAR γ (open), PKM2 (grey), and β -actin (dark) was calculated, using β -Actin as reference protein, and relative expression for each group was normalized to the PPAR γ or PKM2 protein levels of activated LX-2 group.

With a modification of the western blot protocol, PPAR γ protein expression was detected in TGF- β 1-activated LX-2 cells after treatment with the combination of gefitinib and ENL, using total protein as reference. Following 18 h of treatment with gefitinib and/or ENL after a 6 h TGF- β 1 stimulation period, gefitinib increased PPAR γ protein expression which was related to increases in concentration, while ENL failed to alter PPAR γ expression (**Figure 7.18 A and B**). The combination of gefitinib and ENL increased the induction of PPAR γ with increasing concentrations (**Figure 7.18 C and D**).

With longer treatment, PPAR γ expression increased further with gefitinib and/or ENL treatment (**Figure 7.19**). The combination increased PPAR γ expression to a further extent with a reverse relationship to concentration at 10 μ M of gefitinib, a concentration which approaches the IC₅₀ value of gefitinib in TGF- β 1-stimulated LX-2 cells. However, the combination of gefitinib and ENL caused a decreasing trend in the induction of PPAR γ with increasing concentrations and when gefitinib was at a high concentration (10 μ M), a concentration that approaches the IC₅₀ value obtained from the MTT assay.

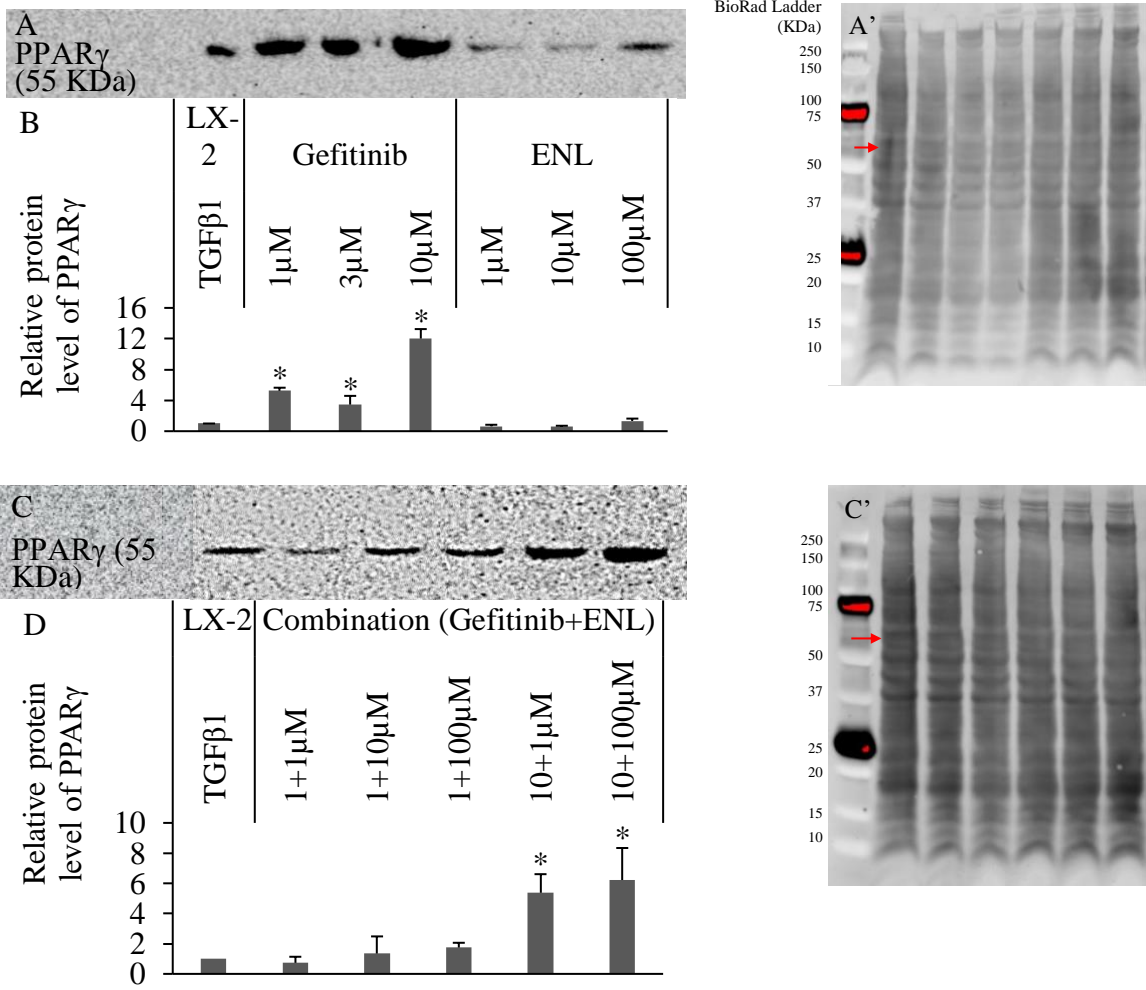


Figure 7.18 PPAR γ protein expression changes as measured by western blot in LX-2 cells stimulated with TGF- β 1 for 6 hours followed by treatment with gefitinib or enterolactone (ENL) or their combination for another 18 hours. A and B: The TGF- β 1-activated LX-2 cells were treated with gefitinib (1, 3, and 10 μ M) or ENL (1, 10, 100 μ M); C and D: The TGF- β 1-activated LX-2 cells were treated with the combination of gefitinib (1 and 10 μ M) and ENL (1, 10, and 100 μ M), using vehicle-treated TGF- β 1-activated LX-2 cells as control and total protein stained by SYPRO Ruby blot stain reagent (A' and C' for A and C, respectively, protein ranges from 10 to 250 kDa according to BioRad Precision Plus Protein Dual Color Standards, where the dual-color bands were stained as the red in panel A' and B') as normalizing reference. The relative expression of PPAR γ for each group was normalized to the TGF- β 1-activated LX-2 group, located at the red arrow on the blot. The data were reported as mean + SD of duplicates on two occasions. * means $P < 0.05$, compared with the vehicle-treated TGF- β 1-stimulated LX-2 cells using one-way ANOVA followed by Dunnett test.

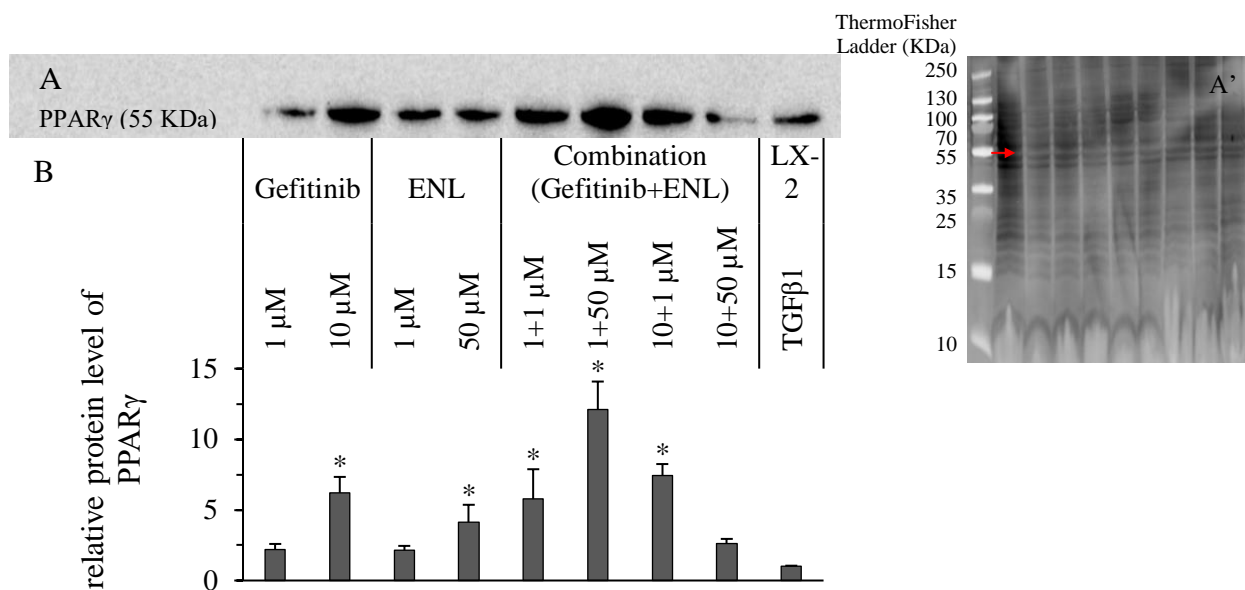


Figure 7.19 PPAR γ protein expression changes as measured by western blot in LX-2 cells stimulated with TGF- β 1 for 6 hours followed by treatment gefitinib or ENL or their combination for another 42 hours. The TGF- β 1-activated LX-2 cells were treated with gefitinib (1 and 10 μ M), ENL (1 and 50 μ M), or the combination of gefitinib (1 and 10 μ M) and ENL (1 and 50 μ M), using vehicle-treated TGF- β 1-activated LX-2 cells as control and total protein stained by SYPRO Ruby blot stain reagent (A', protein ranges from 10 to 250 kDa according to ThermoFisher PageRulerTM Plus Prestained Protein Ladder) as normalizing reference. The relative expression of PPAR γ for each group was normalized to the TGF- β 1-activated LX-2 group, located at the red arrow on the blot. The data were reported as mean + SD of duplicates on two occasions. * means $P < 0.05$, compared with the vehicle-treated TGF- β 1-stimulated LX-2 cells and # means $P < 0.05$, compared with the treatment of gefitinib at 1 μ M using one-way ANOVA followed by Tukey test.

7.2.5.2 Preliminary study on gene expression of Wnt pathway

To confirm the involvement of the Wnt pathway as a possible mechanism for the suppression of hepatic biomarkers of fibrosis in LX-2 cells, an initial qPCR study on β -catenin and several Wnt isoforms was performed in TGF- β 1-stimulated LX-2 cells, in the presence and absence of ENL and FMOC-L-Leu, along with the measurement on PPAR γ and collagen I (**Figure 7.20**). Comparison of activated LX-2 cells with the nonTGF- β 1-stimulated LX-2 cells suggested PPAR γ and Wnt pathways may be involved in the process of HSCs activation. For instance, *PPARG*, *AXIN2*, and *WNT1* expression were significantly decreased in TGF- β 1-activated LX-2 cells compared with nonTGF- β 1-activated LX-2 cells, while *COL1A1* and *WNT5A* expression was increased in the TGF- β 1-activated LX-2 cells. Mild resolution in some of the treatment groups occurred after 18-hour incubation including *PPARG*, *AXIN2*, and *WNT3* but without biologically significant changes, while *CTNNB1*, which codes for β -catenin, was decreased when treated with 10 μ M of FMOC-L-Leu, 1 and 10 μ M of ENL. As there was no pattern found in the gene expression changes for both canonical and non-canonical Wnt pathways, ENL may not work *via* the Wnt pathway primarily for potential antifibrotic effects. Further study at the protein level will need to be done in the future.

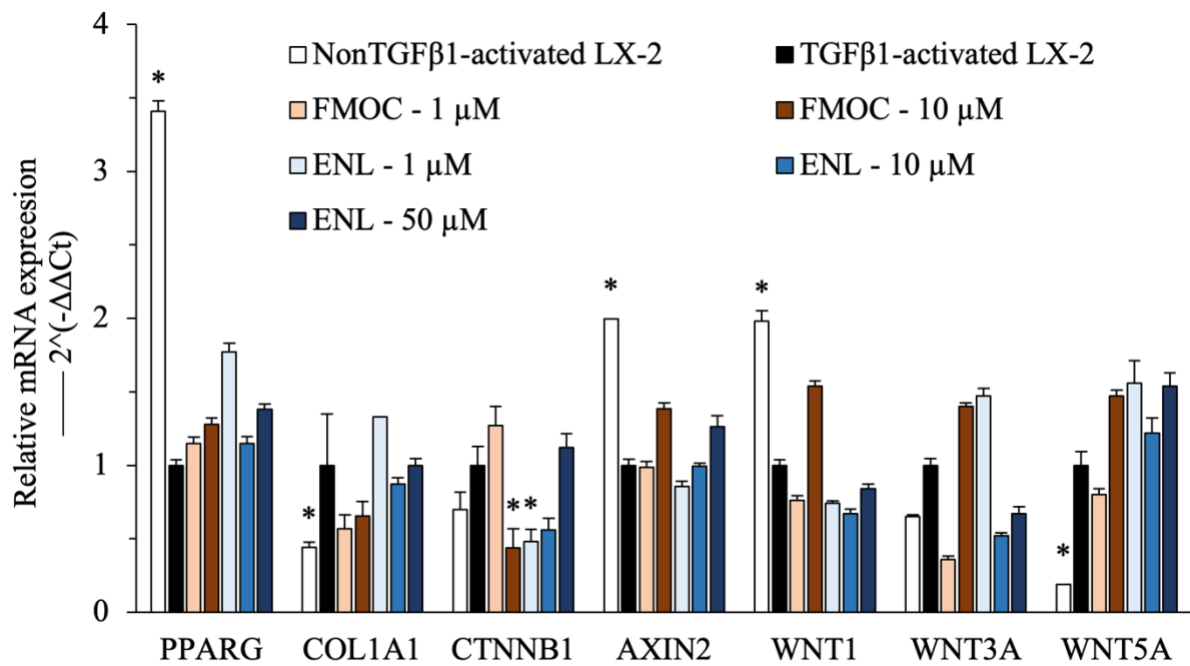


Figure 7.20 The relative mRNA expression of *PPARG*, *COL1A1*, and β -catenin/Wnt related targets in TGF- β 1-stimulated LX-2 cells with the treatment of FMOC-L-Leucine (FMOC) and enterolactone (ENL), using β -actin as reference gene and TGF- β 1-activated LX-2 cells as control for the calculation. Data are presented as mean + SD of triplicates on three occasions. *Induction or repression when the relative mRNA expression was beyond 2 or below 0.5, respectively.

7.2.5.3 Oxidative stress assay for gefitinib and ENL in TGF- β 1-activated LX-2 cells

7.2.5.3.1 Mitochondrial ROS production changes by gefitinib and ENL in TGF- β 1-activated LX-2 cells

Oxidative stress is indicated to play a role in the pathology of hepatic fibrosis and may serve as a therapeutic target for antifibrotic agents. TGF- β was reported to increase hydrogen peroxide production in rat HSCs¹³³. As mitochondrial production of ROS is related to the activation of HSCs and PPAR γ -related pathways, mitochondrial ROS production was measured using MitoSox Red mitochondrial superoxide indicator to reflect oxidative stress in TGF- β 1-activated LX-2 cells treated in the absence or presence of gefitinib and/or ENL.

As shown in **Figure 7.21**, TGF- β 1-stimulated LX-2 cells showed a greater superoxide production with 1 hour of treatment which is consistent with the literature¹³³, but there was no difference at the other time points. Gefitinib reduced superoxide production at 1 hour and the reduction became higher when the concentration increased from 1 to 10 μ M. ENL at 50 μ M mildly decreased superoxide production. The combination of gefitinib and ENL decreased the superoxide production earlier (i.e., at 0.5 h) and the attenuation generally increased when the concentration increased. All treatment groups showed no significant differences in superoxide production in activated LX-2 cells with a longer treatment at 3h, which agrees with the literature⁴²⁶. This is also confirmed with the antioxidant capacity assay, as the cell pellet samples were collected and homogenized by a hand-held vortex homogenizer, such that there was large variation for different groups (results of the total antioxidant capacity not shown).

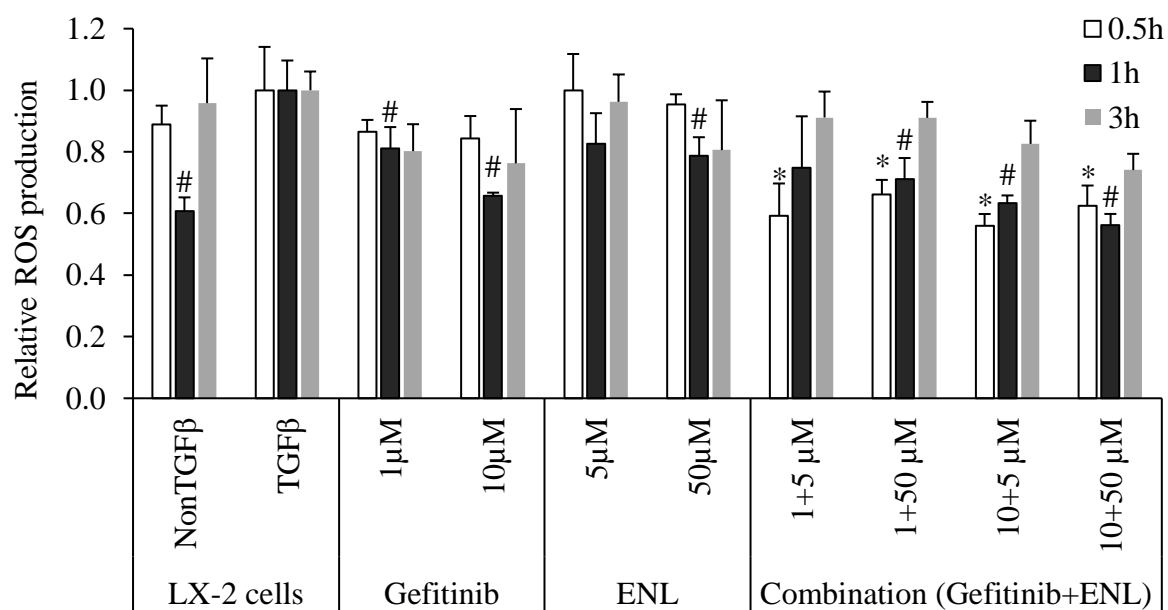


Figure 7.21 Mitochondrial superoxide production in TGF- β 1-stimulated LX-2 cells treated with gefitinib and enterolactone (ENL). LX-2 cells were stimulated with TGF- β 1 for 6 hours before treatment with gefitinib or ENL or their combination for another 0.5, 1, and 3 hours. The TGF- β -activated LX-2 cells were treated with gefitinib (1 and 10 μ M), ENL (5, 50 μ M), and the combination of gefitinib (1 and 10 μ M) and ENL (1 and 50 μ M), using non-TGF- β stimulated LX-2 cells as a negative control. Data are presented as mean + SD of triplicates on three occasions. * # means $P < 0.05$, comparing with the vehicle-treated TGF- β 1-stimulated LX-2 cells at the same time point, using two-way ANOVA followed by Tukey test.

7.2.5.3.2 Nrf2 protein changes by gefitinib and ENL in TGF- β 1-activated LX-2 cells

Since Nrf2 is believed to be involved in the antioxidant response and the ER stress-related pathway, protein expression changes of Nrf2 were determined after treatment with gefitinib and ENL in TGF- β 1-stimulated LX-2 cells. Nrf2 protein expression was decreased by half but with no significance in TGF- β 1-activated LX-2 cells when treated with gefitinib at both 0.5 h and 1 h following 6 hours of TGF- β 1 stimulation, when compared with vehicle-treated activated LX-2 cells (**Figure 7.22**). ENL showed a similar insignificant decrease at 0.5 h and returned to normal expression levels at 1 h. However, when combined, there was induction on Nrf2 at both 0.5 h and 1 h after treatment at the highest concentrations of gefitinib and ENL (i.e., 10 μ M of gefitinib with 50 μ M of ENL). At 3 h after treatment, all groups showed similar Nrf2 expression with the vehicle-treated group (data not shown).

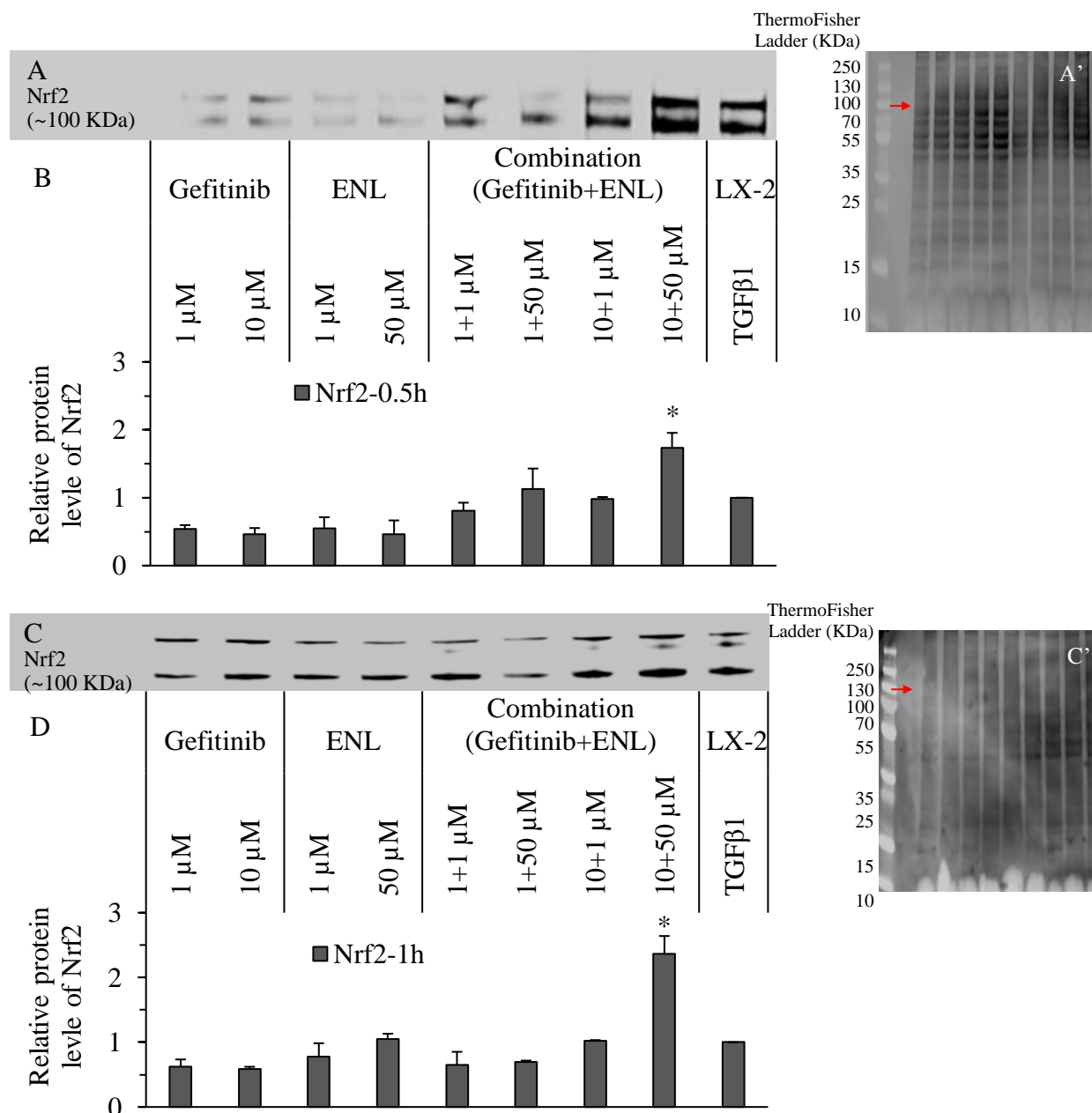


Figure 7.22 The expression changes of Nrf2 protein were measured by western blot. LX-2 cells were stimulated with TGF- β 1 for 6 hours before treatment with gefitinib, enterolactone (ENL), or their combination for another 0.5h (A) and 1h (C). The TGF- β 1-activated LX-2 cells were treated with gefitinib (1, and 10 μ M), ENL (1, and 50 μ M), or with the combination of gefitinib (1 and 10 μ M) and ENL (1 and 50 μ M), using vehicle-treated TGF- β 1-activated LX-2 cells as control and total protein stained by SYPRO Ruby blot stain reagent (A' and C' for A and C, respectively, protein ranges from 10 to 250 kDa according to ThermoFisher PageRuler™ Plus Prestained Protein Ladder) as normalizing reference. The relative expression of Nrf2 for each group was normalized to the TGF- β 1-activated LX-2 group (B and D), located at the red arrow on the blot. The data were reported as mean + SD of duplicates on two occasions. * means $P < 0.05$, compared with the vehicle-treated TGF- β 1-stimulated LX-2 cells and # means $P < 0.05$, compared with the treatment of gefitinib at 10 μ M using one-way ANOVA followed by Tukey test.

7.2.5.4 Apoptosis-related assays for gefitinib and ENL in TGF- β 1-stimulated LX-2 cells

As HSCs play a key role in the development of hepatic fibrosis, elimination of activated HSCs through induction of apoptosis of these cells in fibrotic liver might be an efficient therapeutic approach to treat hepatic fibrosis⁴²⁷. Thus, it is important to understand the effects of treatment on apoptosis of activated LX-2 cells in this study.

7.2.5.4.1 Caspase-3/7 apoptosis induction by gefitinib and ENL in TGF- β 1-activated LX-2 cells

According to the literature, a relationship may exist between oxidative stress and ER stress, and a potential target mechanism is ER stress-induced apoptosis to deplete activated myofibroblasts⁴²⁸. First, a caspase-3/7 apoptosis assay was conducted to assess whether gefitinib and ENL may cause apoptosis of TGF- β 1-stimulated LX-2 cells. Compared with vehicle control, gefitinib induced apoptosis at both 6 and 12 hours after treatment (longer treatments were optimized also but without further changes in the extent of apoptosis than 12-hour treatment, **Figure 7.23**). ENL also caused apoptosis but without a significant concentration-response relationship. Gefitinib and ENL in combination increased apoptosis of activated LX-2 cells in a trend related to concentration, and the induction effect of the combination was stronger than using gefitinib or ENL alone.

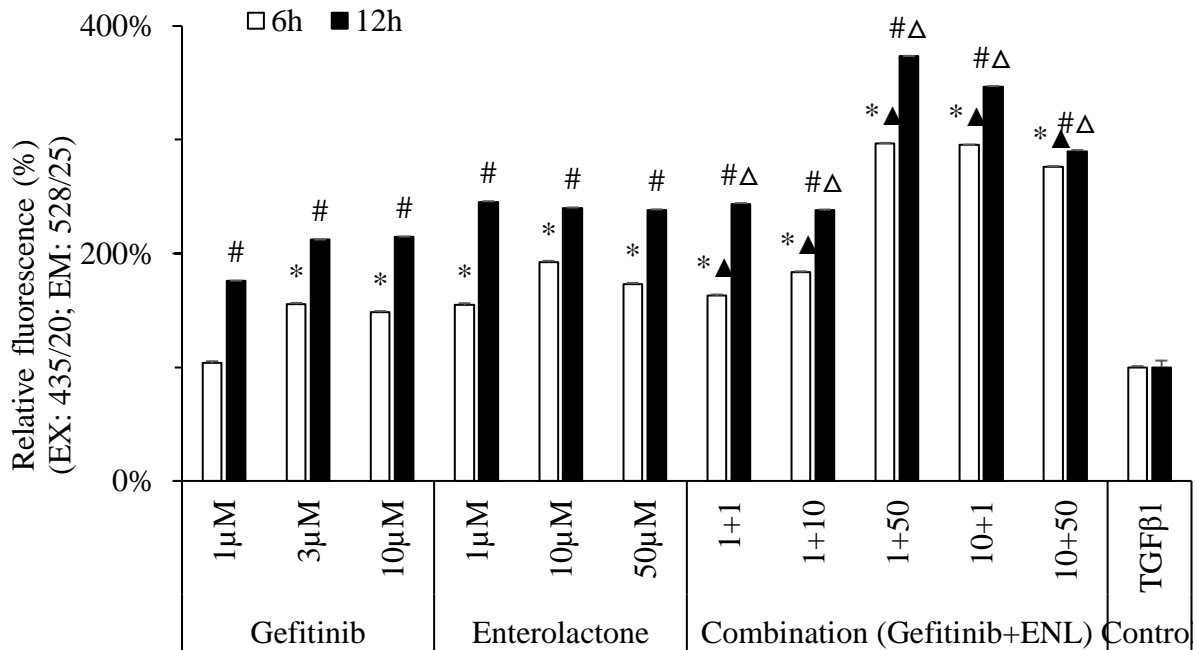


Figure 7.23 Caspase-3/7 apoptosis assay results of gefitinib and/or enterolactone (ENL) in TGF- β 1-stimulated LX-2 cells. LX-2 cells were seeded into 96-well plate at appropriate density for overnight attachment. The cells were stimulated with TGF- β 1 at 2.5 ng/mL for 6 hours before treatment with gefitinib (1, 3, and 10 μ M), ENL (1, 10, and 50 μ M), and the combination of gefitinib (1 and 10 μ M) and ENL (1, 10, and 50 μ M) for 6 and 12 hours. Caspase-3/7 caused apoptosis kit was used to detect the apoptosis following the kit manual. The relative fluorescence was calculated to reflect the apoptosis induced by the treatments, expressed as % of the vehicle-treated TGF- β 1-stimulated LX-2 cells as reference. Data were shown as mean + SD of duplicates on two occasions. * and # mean $P < 0.05$ when compared with the vehicle-treated control group at 24 and 48 h, respectively, while ▲ and Δ mean $P < 0.05$ when compared with the treatment of gefitinib at the same concentration at 24 and 48 h, respectively, using one-way ANOVA followed by Tukey test.

7.2.5.4.2 ER-stress related pathway

After confirmation of induction of apoptosis, ER stress was explored to determine its involvement in the induction of apoptosis⁴²⁹. ER stress is reported to be involved in the pathology of liver fibrosis and might serve as a mechanism for TKI and ENL suppression of HSC activation²⁶. ER stress-induced apoptosis might underscore the suppression of activated HSCs in liver fibrosis, leading to regression and resolution of fibrogenesis. To evaluate gefitinib- and ENL-mediated ER stress-induced apoptosis, the mRNA expression of three major biomarkers of ER stress branches was determined by qPCR and two of those were continued with protein detection by western blot.

Compared to nonTGF- β 1 stimulated LX-2 cells, TGF- β 1 dramatically decreased the mRNA expression of *CHOP*, *ATF4*, and *ATF6* in LX-2 cells, which indicated the involvement of ER stress-related pathways. ENL induced levels of the apoptotic marker, *CHOP*, by 2.5-fold at the highest concentration (100 μ M) (**Figure 7.24A**). At their highest concentrations, gefitinib and ENL also induced its upstream marker, *ATF4*. In combination, gefitinib and ENL significantly induced the expression of *ATF4* and *CHOP*, and the pattern depended upon the relative combination of ENL and gefitinib concentrations (**Figure 7.24B**).

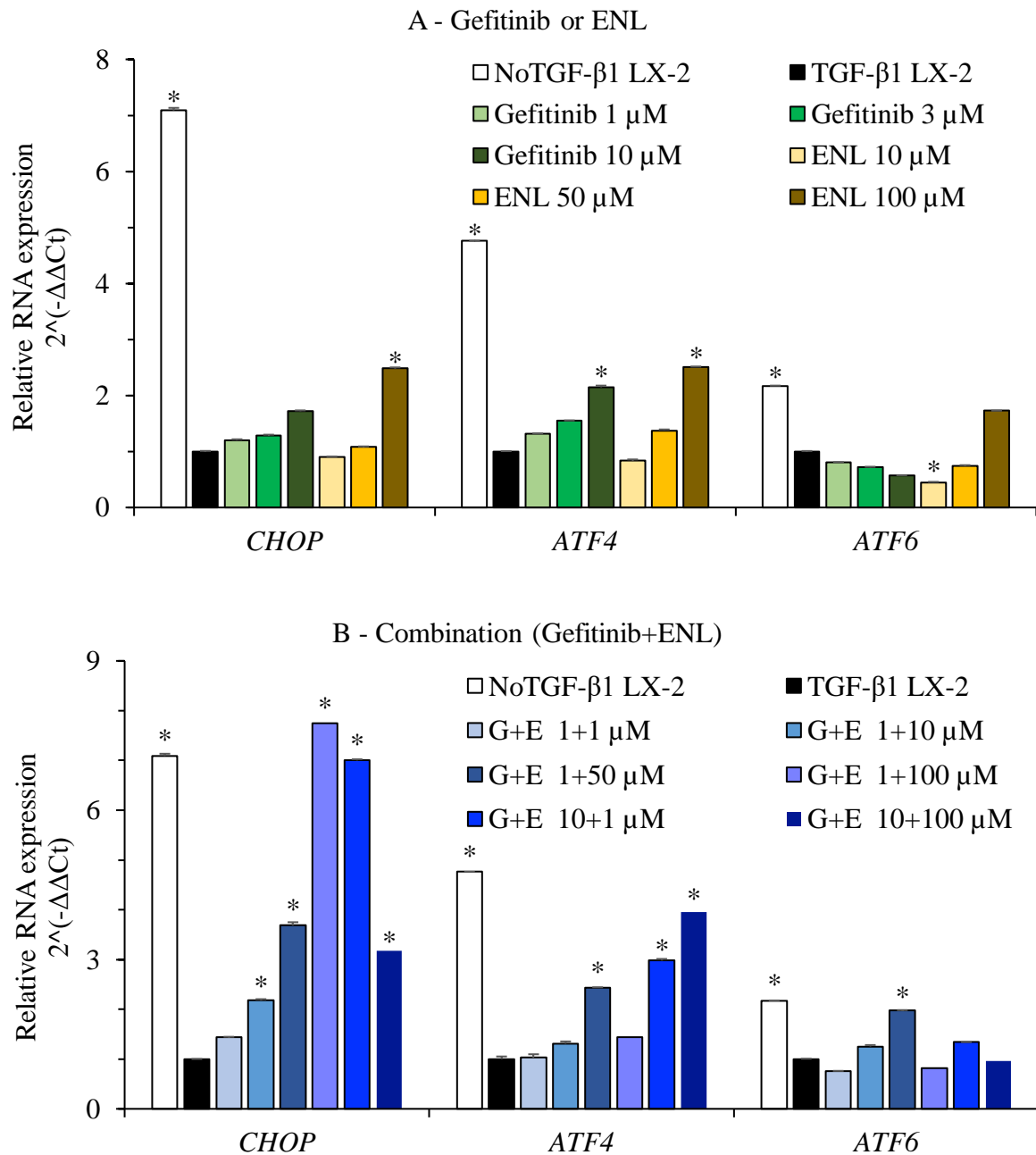


Figure 7.24 The relative mRNA expression of ER-stress related markers, including *CHOP*, *ATF4*, and *ATF6* in TGF-β1-stimulated LX-2 cells with treatment of gefitinib (1, 3, and 10 μM), ENL (10, 50, and 100 μM), and the combination of gefitinib (1 and 10 μM) and ENL (1, 10, 50, and 100 μM), using β-actin as reference gene and TGF-β1-activated LX-2 cells as control for the calculation (Data were presented as mean + SD of three replicates on three occasions). A) the TGF-β1 activated LX-2 cells were treated with gefitinib (1, 3, 10 μM) or ENL (10, 50, 100 μM) alone for 24 hours (6 hours of stimulation with 18 hours of treatment with different concentrations of compounds); B) the activated LX-2 cells were treated with the combination of gefitinib (1 or 10 μM) and ENL (1, 10, 50, or 100 μM) for 24 hours. Data were shown as mean + SD of triplicates on three occasions. *Induction or repression when the relative mRNA expression was beyond 2 or below 0.5, respectively.

After measurement of mRNA expression of the key ER stress-related apoptotic markers, protein expression of ATF4 and CHOP was assessed by western blot. Since ATF6 showed no significant changes at the mRNA level, protein expression of ATF6 was not monitored. ATF4 protein expression was measured in activated LX-2 cells with treatments of gefitinib and ENL, alone and in combination (**Figure 7.25**). Gefitinib increased ATF4 expression to 4 times of the vehicle control at 10 μ M with 48 hours of treatment. ENL did little to impact ATF4 protein expression when used alone. However, when treated with the combination of ENL and gefitinib, ATF4 expression was further induced, and the induction was higher when concentration increased.

CHOP protein was also induced by gefitinib at 10 μ M to about 3 times of the vehicle control at 72 hours of treatment (**Figure 7.26**). ENL had no significant effect on CHOP protein expression. The combination of gefitinib and ENL increased CHOP protein expression with a similar concentration-dependent trend, which is similar to the changes in PPAR γ at 48h after treatment.

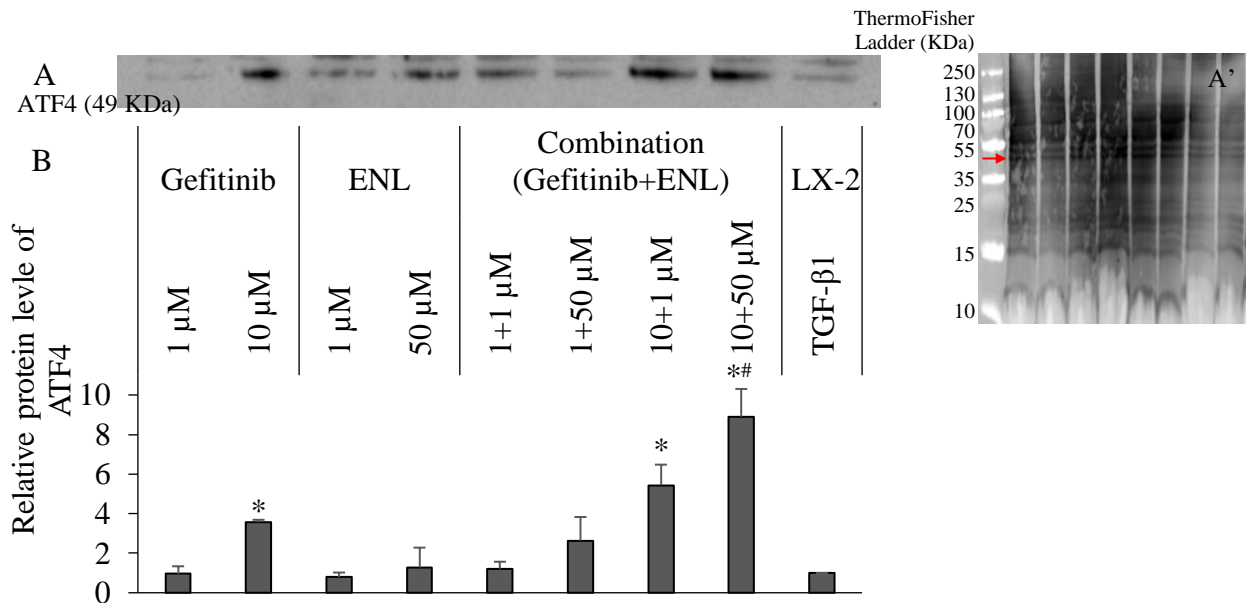


Figure 7.25 ATF4 protein expression changes were measured by western blot in gefitinib and/or enterolactone (ENL) treated LX-2 cells. LX-2 cells were stimulated with TGF- β 1 for 6 hours before the treatment for 42 hours (consider this as 48h treatment for results interpretation). The TGF- β 1-activated LX-2 cells were treated with gefitinib (1 and 10 μ M), ENL (1 and 50 μ M), or with the combination of gefitinib (1 and 10 μ M) and ENL (1 and 50 μ M), using vehicle-treated group as negative control and using total protein stained by SYPRO Ruby blot stain reagent (A', protein ranges from 10 to 250 kDa according to ThermoFisher PageRuler™ Plus Prestained Protein Ladder) as normalizing reference. The relative expression of ATF4 for each group was normalized to the TGF- β 1-activated LX-2 group (B), located at the red arrow on the blot. The data were reported as mean + SD of duplicates on two occasions. * means $P < 0.05$, compared with the vehicle-treated TGF- β 1-stimulated LX-2 cells, and # means $P < 0.05$, compared with the treatment of gefitinib at 10 μ M using one-way ANOVA followed by Tukey test.

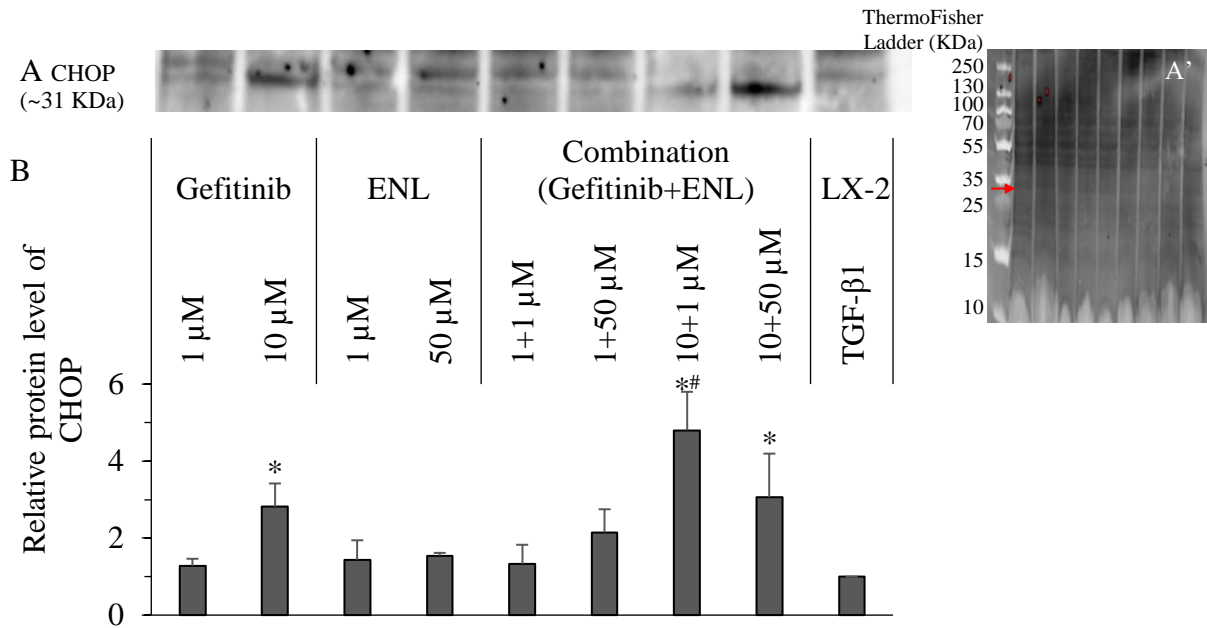


Figure 7.26 The changes in CHOP protein expression were measured by western blot in LX-2 cells. LX-2 cells were stimulated with TGF- β 1 for 6 hours before the treatment with gefitinib, enterolactone (ENL), or their combination for 66 hours (with a total treatment time of 72 hours). The TGF- β 1-activated LX-2 cells were treated with gefitinib (1 and 10 μ M), ENL (1, 10, 50 μ M), or with the combination of gefitinib (1 and 10 μ M) and ENL (1 and 50 μ M), using vehicle-treated group as negative control and total protein stained by SYPRO Ruby blot stain reagent (A', protein ranges from 10 to 250 kDa according to ThermoFisher PageRuler™ Plus Prestained Protein Ladder) as normalizing reference. The relative expression of CHOP for each group was normalized to the vehicle-treated TGF- β 1-activated LX-2 group (B), located at the red arrow on the blot. The data were reported as mean + SD of duplicates on two occasions. * means $P < 0.05$, compared with the vehicle-treated TGF- β 1-stimulated LX-2 cells, and # means $P < 0.05$, compared with the treatment of gefitinib at 10 μ M using one-way ANOVA followed by Tukey test.

7.3 Objective 3: Whether flaxseed lignans exhibit antifibrotic effects in fatty livers of high cholesterol diet-fed rats.

An opportunity arose to assess the potential of ENL, the mammalian lignan metabolite of SDG, to suppress markers of hepatic fibrosis in a non-alcoholic fatty liver rat model. In a study involving a comparative PK and efficacy analysis between purified SDG and SDG-enriched polymer complex in diet-induced hypercholesterolemic rats, the ability of flaxseed lignans to mitigate liver injury in non-alcoholic fatty liver disease was assessed by comparison of the expression of markers of hepatic fibrosis, as well as serum and liver lipid levels in control and SDG treated rats. A comparative oral PK study between the purified SDG and SDG-enriched polymer complex was furthermore conducted in attempts to relate serum ENL levels with changes in serum and hepatic lipids and markers of hepatic fibrosis.

7.3.1 Comparative oral PK study of purified SDG and SDG-enriched polymer complex in female Wistar rats

A comparative PK study in normal rats was conducted to support the efficacy analysis by identifying the major form of circulating lignans that may relate to the potential effects in hypercholesterolemia rats. Purified SDG and SDG polymer complex were administered orally to normal female Wistar rats and free and conjugated forms of the SDG metabolites, SECO, END, and ENL, were analyzed by LC-MS/MS. Area under curve (AUC), reflecting the exposure of lignans in rats, was calculated from the plasma concentration versus time (C-T) data using the linear trapezoidal method. The terminal slope of semi-logarithmic C-T profile provided an estimate of terminal rate constant, k , following a linear regression. Free forms of SECO, END, and ENL were rarely detectable in the rat plasma. Plasma concentrations of all samples for both free SECO and ENL were below the low level of quantification (LLOQ), only free END was quantifiable at 8- and 12-hour time points (data not shown here). Total SECO was sparsely detected before 4 hours of administration. Only the total level of END and ENL could be plotted and the area under curve of these two metabolites was calculated as shown in **Table 7.4** and **Figure 7.27**, respectively.

Similar exposures for total ENL and total END were found in both purified SDG and SDG polymer treated groups. Total ENL had an AUC of 2475.0 ± 183.1 in purified SDG group and 2480.4 ± 822.0 in SDG polymer group, while total END had an AUC of 1541.7 ± 1018.3 in purified SDG group and 1687.7 ± 709.1 in SDG polymer group, all without

significant differences according to two-way ANOVA followed by Tukey test.

Table 7.4 The area under curve (AUC) for enterolactone (ENL) and enterodiol (END) in 12 mg/kg secoisolariciresinol diglucoside (SDG) treated female Wistar rats after oral administration. AUC was determined for each individual rat in each subgroup and shown as mean \pm SD (N=5 for purified SDG and N=7 for SDG polymer). When $P < 0.05$, it suggests a significant difference between the groups using two-way ANOVA followed by Tukey test.

	Administered SDG	AUC _{0-12h}	AUC _{12-48h}	AUC _{last}	AUC _{inf}
ENL	purified SDG	432.1 \pm 81.8	1486.5 \pm 146.9	556.4 \pm 229.1	2475.0 \pm 183.1
	SDG polymer	422.1 \pm 99.0	1255.3 \pm 421.7	691.7 \pm 572.8	2480.4 \pm 822.0
END	purified SDG	1174.9 \pm 822.9	333.7 \pm 263.2	18.1 \pm 23.8	1541.7 \pm 1018.3
	SDG polymer	1257.2 \pm 454.3	615.7 \pm 440.8	24.3 \pm 29.8	1687.7 \pm 709.1

Note: AUC_{0-12h} is the area under curve from 0 to 12 hour; AUC_{12-48h} is the area under curve from 12 to 48 hour.

$$AUC_{last} = C_{last}/k.$$

$$AUC_{inf} = AUC_{0-12h} + AUC_{12-48h} + AUC_{last}.$$

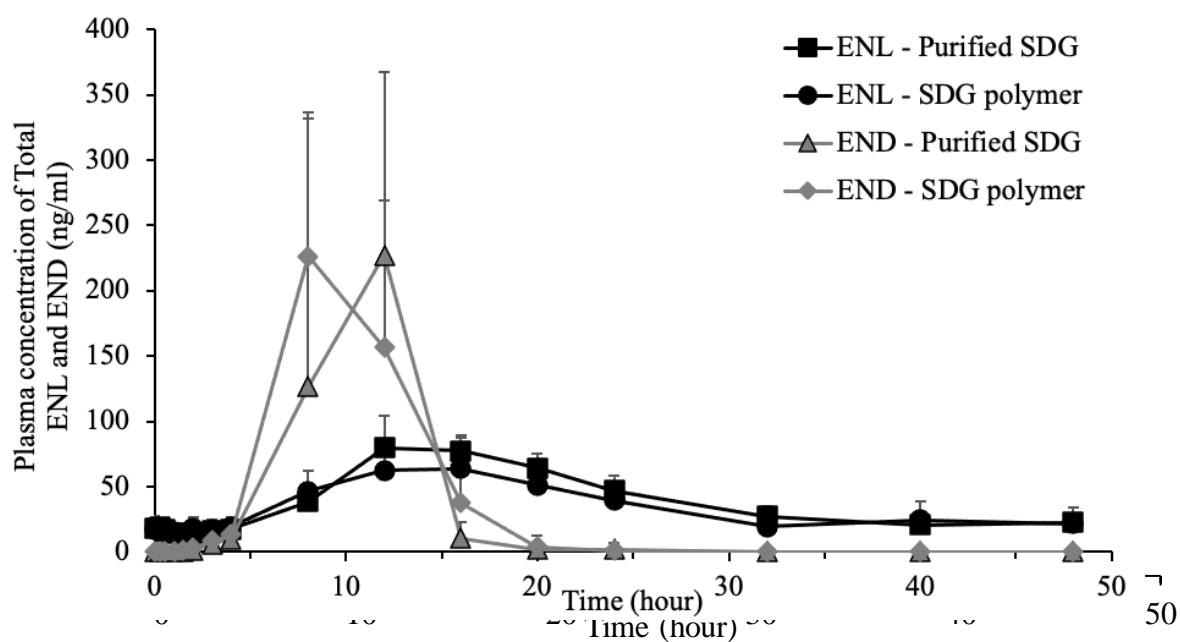


Figure 7.27 Plasma concentration versus time profile for total enterolactone (ENL) and enterodiol (END) in single oral dose pharmacokinetic study in female Wistar rats. Purified secoisolariciresinol diglucoside (SDG) or SDG polymer were administered orally at an equivalent dosage of 12 mg/kg into rats, and jugular blood samples were collected at 0, 15, 30 minutes, and 1, 1.5, 2, 3, 4, 8, 12, 16, 20, 24, 32, 40, and 48 hours from two subgroups of animals. The plasma concentrations of free and total secoisolariciresinol (SECO), END, and ENL were detected by appropriate LC-MS/MS methods. Data were shown as mean + SD of each group, N=5 for purified SDG and N=7 for SDG polymer.

7.3.2 Comparative efficacy of purified SDG and SDG-enriched polymer complex in female hypercholesterolemic Wistar rats

The liver protective effects of purified SDG and SDG polymer were investigated in female Wistar rats supplied with 1% high cholesterol diet. After 23 days of treatment with SDG enriched products, body and liver weights were measured before subsequent liver tissue sampling. The final body weight, body weight gain, liver weight, as well as the liver to body weight ratio of the high cholesterol diet groups (N=10) were normalized to the standard diet group (N=5). The liver to body weight ratio in purified SDG treated group was decreased by about 10% as compared with the vehicle-treated high cholesterol diet group, which was significantly different from the vehicle control (**Figure 7.28**). However, there were no other differences in both SDG-products treated groups when compared with the control group.

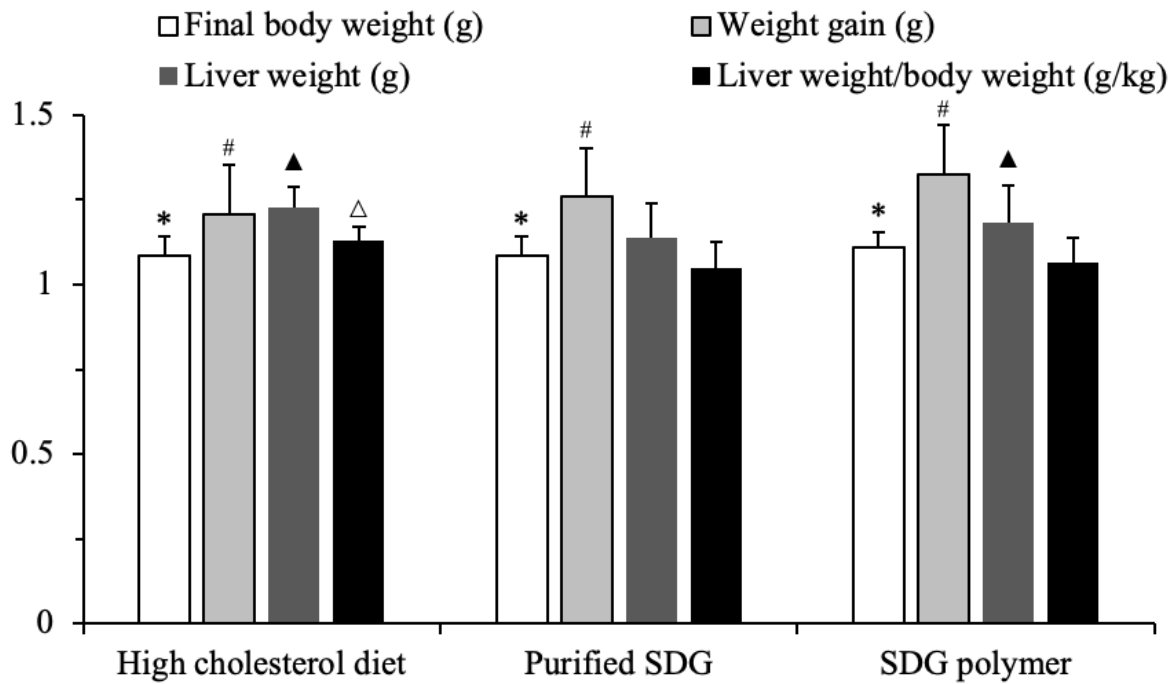


Figure 7.28 The relative final body weight, weight gain, liver weight, and liver body weight ratio of the purified secoisolariciresinol diglucoside (SDG) or SDG polymer treated female Wistar rats. The final body weight (open), weight gain (light grey), liver weight (dark grey), and liver to body weight ratio (black) were normalized to the standard diet group. Data were reported as mean + SD, N=10 (N=5 for the reference group). *, #, ▲, and △ $P < 0.05$ suggesting a significant difference from the normal diet group using one-way ANOVA followed by Tukey test.

The histological images of different treatment groups showed the presence of hepatic steatosis and lobular inflammation in the 1% high cholesterol diet rats. These histological changes were scored by a blinded pathologist. Although there was no significant difference between the different treatment groups, there was a slight reduction of lobular inflammation score (decreased from 1 to 0.7) in the purified SDG treated group, as well as the steatosis level, decreased from 1.8 in the vehicle control group to 1.3 in the purified SDG group. The non-alcoholic fatty liver disease activity score also was lower in the purified SDG treated group (with a score of 2) than the non-treated high cholesterol diet group (scored as 2.8) as indicated in **Figure 7.29** and **Table 7.5**.

Table 7.5 Hepatic histological scores for female Wistar rats fed a 1% cholesterol diet and treated with daily purified secoisolariciresinol diglucoside (SDG) or SDG-polymer for 23 days (Data shown as mean of each treatment group).

Group	Normal	1% cholesterol without treatment	1% cholesterol with purified SDG	1% cholesterol with SDG Polymer
Steatosis	0	1.8	1.3	1.4
Lobular inflammation	0.2	1	0.7	1
NAS (NAFLD activity score)	0.2	2.8	2	2.4

Note: Data were shown as mean of the histological score, which was scored according to standard pathological criteria in Table 2.

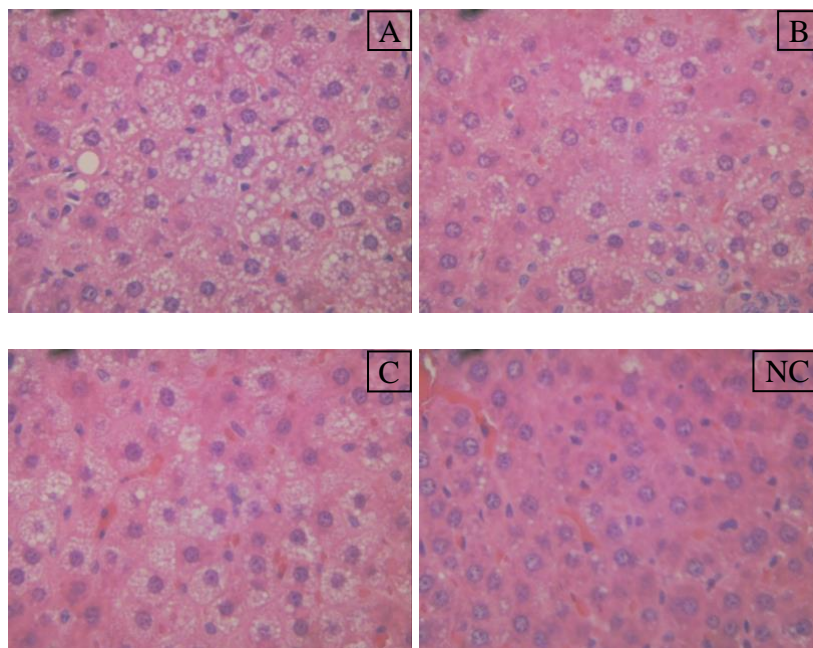


Figure 7.29 Liver histology with hematoxylin and eosin (H&E) staining of female Wistar rats fed 1% high cholesterol diet for 30 days and treated with oral doses of vehicle, purified secosolariciresinol diglucoside (SDG), or SDG polymer with equivalent SDG dose of 6 mg/kg or fed a standard diet for 30 days and treated with vehicle for 23 days. Liver samples were collected, and H&E stained after 23 days of vehicle control with 1% high cholesterol diet (A), treatment with purified SDG (B) or SDG polymer (C), and the standard diet control group (NC). Representative images are presented at 40X.

The effects of purified SDG and SDG polymer on cholesterol and lipid homeostasis were also measured by determination of serum lipid parameters including total cholesterol (TC), triglycerides (TG), and HDL-C after 14 and 23 days of treatment. LDL was calculated by subtracting HDL-C and very low-density lipoprotein cholesterol (VLDL-C) (calculated as one-fifth the level of TG) from TC. The normalized levels of these four serum lipid parameters to the standard diet are indicated in **Figure 7.30**. The high cholesterol diet had little impact on the TG level but increased TC and LDL to 2.5 and 5.5 times of the normal diet group at 14 days of treatment and after 23 days remained at around 2 and 3 times of the normal control. Both SDG-enriched products showed a limited impact on TC at both 14 and 23 days after treatment, or on TG at 23 days. After 14 days of treatment, SDG polymer showed a 40% increase in TG. Although with no significant changes, LDL showed a trend towards reduction with both purified SDG and SDG polymer treated groups in a treatment duration-dependent manner. The high cholesterol diet caused a reduction in HDL in rats to about 60% of the normal diet rats. At 14 days of treatment, SDG polymer increased the HDL level to around 80% of the normal diet group, but at end of treatment both SDG treated groups showed no difference in HDL when compared with the high cholesterol diet group.

Alanine aminotransferase (ALT) and aspartate aminotransferase (AST) levels were measured to reflect liver damage after 23 days of treatment with purified SDG and SDG polymer. Purified SDG had no effect on ALT and AST levels, while SDG polymer significantly increased the ALT/AST ratio compared to the high-cholesterol diet control (**Figure 7.31**).

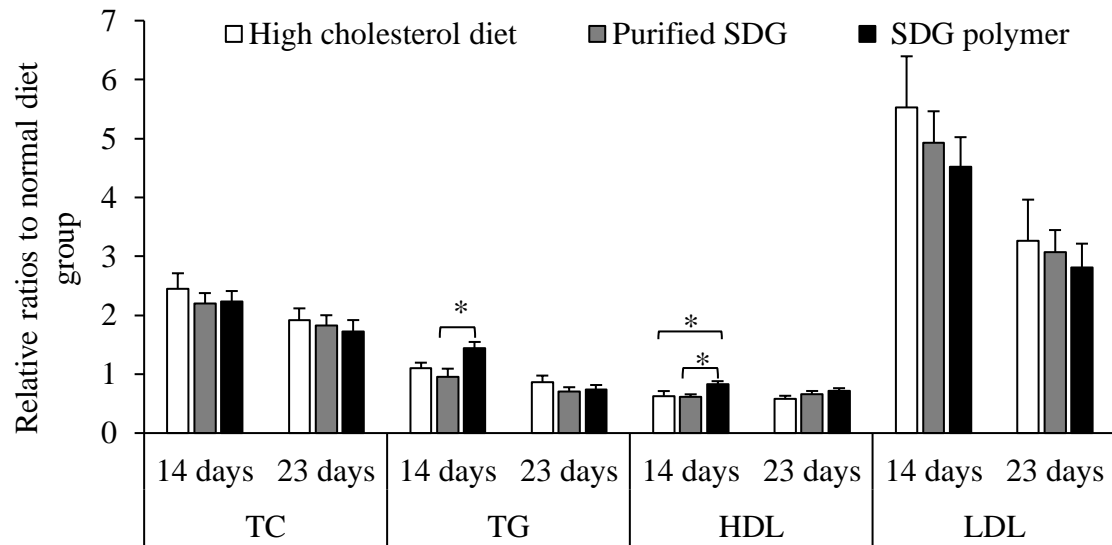


Figure 7.30 The relative levels of total cholesterol (TC), triglyceride (TG), high-density lipoprotein cholesterol (HDL-C), and low-density lipoprotein (LDL) in purified secoisolariciresinol diglucoside (SDG) or SDG polymer treated female Wistar rats. All four parameters are the measured levels compared to the normal diet group, the high-cholesterol diet group without lignan treatment applied as control (open), high-cholesterol diet with purified SDG labeled as purified SDG (grey), while high-cholesterol diet with SDG polymer labeled as SDG polymer (black). Data were reported as mean + SEM (N=10 for the high cholesterol diet group, N=5 for the normal diet group), * $P < 0.05$ indicates a significant difference between the groups indicated using two-way ANOVA followed by Tukey test.

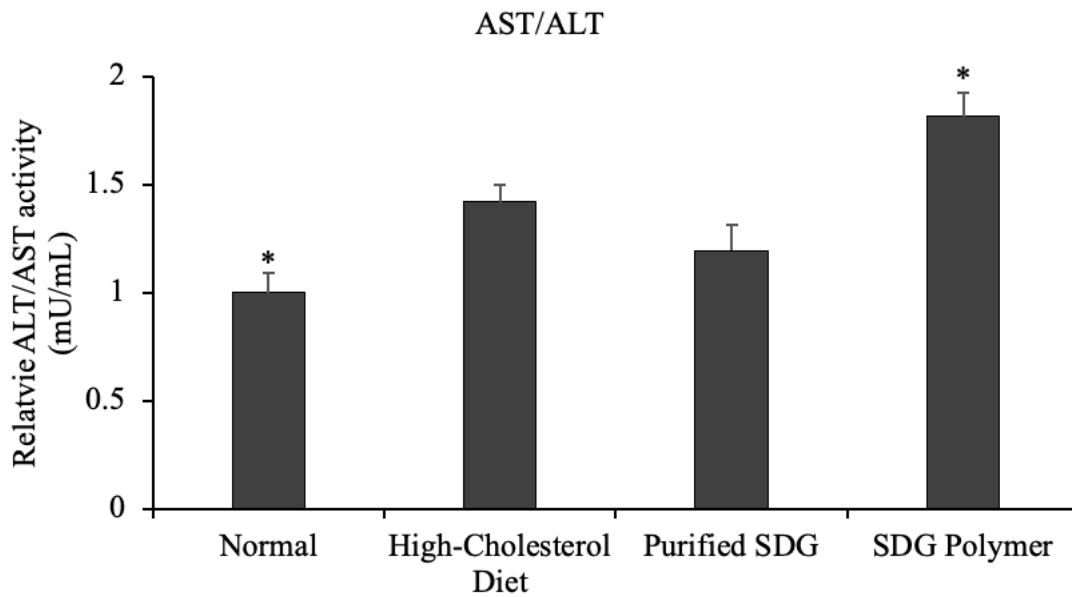


Figure 7.31 The AST/ALT ratio of 23-day purified secoisolariciresinol diglucoside (SDG) and SDG polymer treated female Wistar rats. The AST and ALT activities were detected and normalized to the standard diet group. Data were shown as mean + SEM (N=10 for fatty liver groups and N=5 for normal diet group). *indicates a significant difference ($P < 0.05$) from the High-Cholesterol Diet group using one-way ANOVA followed by Dunnett test.

7.3.3 The gene and protein expression changes in the rat liver from SDG treated group

The antifibrotic potential of the flaxseed lignans *in vivo* was evaluated by qPCR and western blot assessment of fibrotic biomarkers in rat liver in rats treated with or without purified SDG in 1% high cholesterol diet fed Wistar rats (**Figure 7.32**). *Coll1a1* was slightly increased in hypercholesterolemic rat liver but with no biological significance and was not changed by SDG treatment. However, the expressions of *Mmp2*, *Timp1*, and *Acta2* were decreased by the high cholesterol diet. The expression of *Mmp2* was increased slightly but not significantly by purified SDG. *Timp1* expression was not significantly affected by the purified SDG compared to the high cholesterol diet group. The expression of *Acta2* was increased by purified SDG to 2.6-fold of the high cholesterol diet group.

The expression of Collagen I protein was decreased by purified SDG treatment. In pooled rat liver samples, Collagen I expression in the whole rat liver sample was increased in the 1% high cholesterol diet group, and purified SDG decreased the Collagen I protein in the fatty liver (shown in **Figure 7.33A and B**). This was also observed in the individual samples, but the low purity of the protein samples derived from the fatty liver made it difficult to get clear bands of Collagen I protein and quantify on the western blot (**Figure A1, Appendix A**).

The expression of Mmp2 protein was increased in the high cholesterol diet control group to 3-fold of the normal control (**Figure A2, Appendix A**) which is consistent with the higher production of Collagen I (**Figure A1**). The expression of Mmp2 was reduced non-significantly by SDG to 0.7-fold of the high cholesterol diet group (**Figure A2, Appendix A**). The expression of Timp1 was increased to 5-fold of normal control in the high cholesterol diet group, while purified SDG slightly reduced the protein expression of Timp1 in the fatty liver samples with no statistical significance (**Figure A3, Appendix A**).

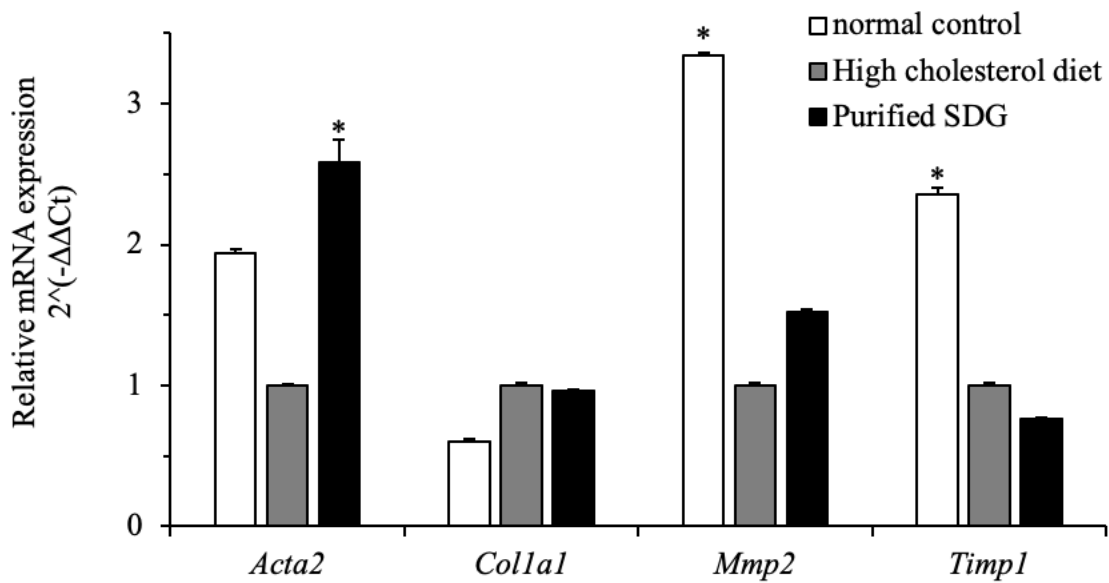


Figure 7.32 The relative mRNA expression of hepatic fibrotic biomarkers (*Acta2*, *Colla1*, *Mmp2*, and *Timp1*) in the liver tissue of purified secoisolariciresinol diglucoside (SDG) and SDG polymer treated female hypercholesterolaemic Wistar rats. The 1% high cholesterol diet group was used as control and β -actin was used as reference gene for the calculation. Data are presented as mean + SD of triplicates. *Induction or repression when the relative mRNA expression was beyond 2 or below 0.5, respectively.

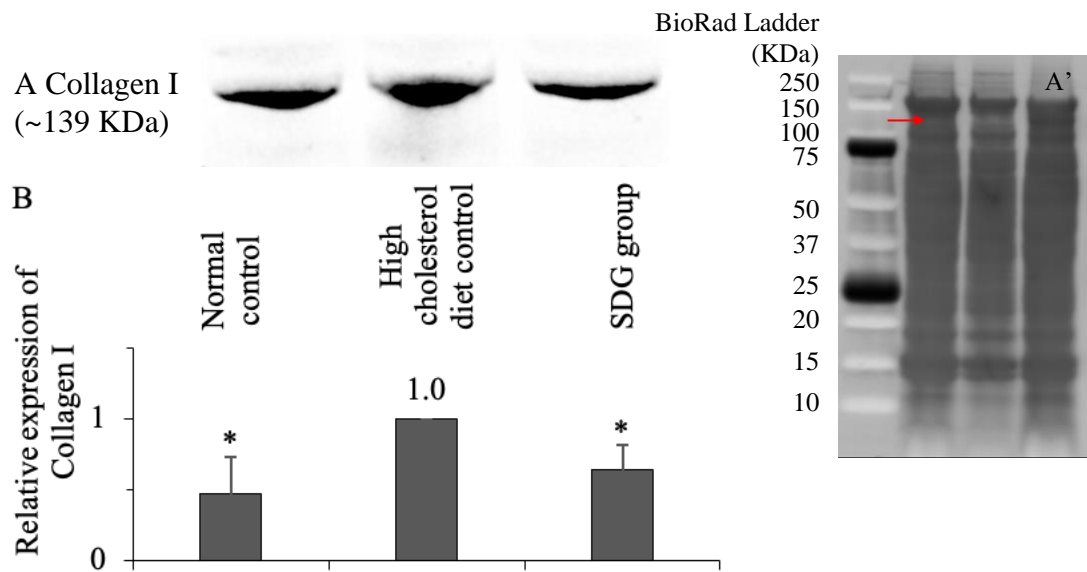


Figure 7.33 The relative expression of Collagen I in rat liver tissue after treatment with purified secoisolariciresinol diglucoside (SDG) in high cholesterol diet induced Wistar rats. The expression of Collagen I in pooled rat liver (A) and the relative expression for each group were normalized to the 1% high cholesterol diet group (B), using total protein stained by SYPRO Ruby blot stain reagent (A', protein ranges from 10 to 250 kDa according to BioRad Precision Plus Protein Dual Color Standards where the dual-color bands were stained dark in panel A') as normalizing reference. Data were shown as mean + SD of the relative expression of Collagen I protein (N=5 for the normal control group and N=10 for high cholesterol diet and SDG groups), located at the red arrow on the blot. * means $P < 0.05$ when comparing with the high cholesterol diet group using one-way ANOVA followed by Tukey test.

8. DISCUSSION

Hepatic fibrosis results from most chronic liver injuries and is a clinical challenge globally⁴²⁵. Treatment options for hepatic fibrosis, especially its end-stage cirrhosis, are still limited at present. Both TKI drugs and flaxseed lignans are reported as multi-target compounds that may have antifibrotic potential in attenuating hepatic fibrotic biomarkers^{330, 430}. Furthermore, the combination of the two may favorably modulate hepatic antifibrotic biomarkers to a further extent than using each compound alone. In the past decades, great progress has been made in understanding the cellular mechanisms of liver fibrosis with the recognition of the central role of HSCs in fibrotic response⁴³¹. This dissertation research aimed to confirm the antifibrotic effects of the combination of selected TKI drugs and the bioactive mammalian lignan, ENL, and to explore possible cellular mechanisms including PPAR γ , oxidative stress, and ER stress-induced apoptosis, using an *in vitro* hepatic fibrosis model. Three TKIs, including ibrutinib, dabrafenib, and gefitinib, were used for the screening of both antifibrotic response and PPAR γ agonism, and gefitinib alone and in combination with ENL was chosen for further evaluation of the antifibrotic response and mechanisms involved in hepatic fibrosis. Furthermore, an opportunity was presented to evaluate the antifibrotic effect of flaxseed lignans *in vivo* in a diet-induced hypercholesterolemic rat model of NAFLD. The results of this current work provides some experimental evidence for the application of the combination of bioactive mammalian lignan and TKI drugs as therapeutic alternatives in hepatic fibrosis.

8.1 PPAR γ agonism of the tested compounds

PPAR γ is well known as a treatment for type 2 diabetes and metabolic disorders and has drawn increasing interest as a potential therapeutic target for proliferative dysfunction diseases⁴³². Upon either full or partial activation by ligands, PPAR γ elicits transcription of a variety of genes in many tissues involving metabolism and cell proliferation⁴³³. However, the unwanted side effects of PPAR γ full agonists limit their therapeutic application⁴³⁴. Recent literature evidence indicated that PPAR γ partial activation offers a potential improvement of the balance between efficacy and safety as such compounds exhibit similar biological functions devoid of the disappointing adverse effects associated with full agonists⁴³⁵. A list of repurposing TKI drugs has been studied in fibrotic diseases, and many natural products have shown PPAR γ activation via agonism in many proliferation dysfunction diseases. Thus, we aimed to study the possibility of compounds from these two groups as agonists or partial

agonists of PPAR γ . Based upon these findings, we planned to proceed with further evaluations of the potential of TKI's and natural products in hepatic fibrosis as PPAR γ plays a key role in HSC activation and regression⁴³⁶.

In-silico docking modeling demonstrated that several marketed anti-cancer TKI drugs including ibrutinib, dabrafenib, and gefitinib have similar binding affinities to PPAR γ as rosiglitazone, a known PPAR γ full agonist¹³. Such compounds may have the potential to mitigate the dysfunction in cellular proliferation associated with many fibrotic diseases⁹⁻¹¹. However, these tyrophostin compounds also associate with non-negligible toxicity at their common doses in cancer therapy, which might limit their repurposing to other diseases involving dysfunction in cell proliferation¹⁴. Natural products also have been studied for their potential to activate PPAR γ , beyond their traditional medical and dietary usage²². The plant lignans have shown promising anti-proliferative effects with a good safety profile, and ENL, one of the major bioactive flaxseed lignan metabolites, was reported to modulate PPAR γ -related responses⁴³⁷⁻⁴³⁹. Thus current study aimed to experimentally confirm the PPAR γ agonism pattern of three TKI compounds, ibrutinib, dabrafenib, and gefitinib, as well as the mammalian lignan, ENL, to allow future investigations into their anti-proliferative mechanisms and potential to combine ENL with TKIs to improve their safety and efficacy in hepatic fibrosis.

The data suggest that gefitinib and ENL are potential PPAR γ partial agonists. Based upon the current screening pipelines for novel PPAR γ ligands, transactivation assay combined with a PPAR γ binding assay are considered the well-established and commonly used methods⁴⁴⁰. Guasch and colleagues used Polarscreen PPAR γ competitive assay, Dual-Luciferase reporter assay in HepG2 cells, and adipogenesis and glucose uptake assays in 3T3-L1 preadipocytes after computational analysis to identify PPAR γ partial agonists of natural products¹⁸⁶. As well, other researchers applied one or more of the three assays in the identification of partial agonists of PPAR γ , combined with *in silico* docking models⁴⁴¹⁻⁴⁴³. Such studies provided the support to proceed with our exploratory experimental evaluations of ibrutinib, dabrafenib, and gefitinib, as well as the lignan, ENL, as putative ligands of PPAR γ .

The competitive binding affinity and transactivation activity to PPAR γ of the three TKIs and ENL was compared to known full and partial agonists of PPAR γ , rosiglitazone and FMOC-L-Leu, respectively. In a PPAR γ competitive binding affinity assay, ibrutinib, dabrafenib, and gefitinib illustrated weak binding to the rosiglitazone's PPAR γ binding site. Using a cell-based transactivation assay in PPAR γ -overexpressed HepG2 cells, the tested

TKI compounds and ENL also showed limited ability to transactivate PPAR γ . Based upon the low binding affinity and more limited ability to transactivate PPAR γ relative to the full agonist, rosiglitazone, it seemed these compounds exhibited characteristics of PPAR γ partial agonism because partial agonists are known to bind differently to the ligand-binding domain of PPAR γ and exhibit weaker binding properties that lead to lowered transcriptional activity of this nuclear receptor¹⁸⁶. This was in strong contrast to the results reported from the computational docking model in the literature, which suggested high affinity to PPAR γ ¹³. This lack of experimental consistency with *in silico* computation methods was not surprising since all binding affinity estimation methods have important limitations, and the success of the docking programs is usually system dependent and relies on the quality of the underlying scoring functions⁴⁴⁴. Lack of corroboration between *in silico* computational analysis and experimental verification studies is not uncommon in the literature. Furthermore, it was shown that flaxseed lignans act as weak PPAR γ agonists and ENL induces PPAR γ binding activity, which is consistent with the binding characteristics of lignans in the literature^{343, 445}. The experimental data agreed with the literature in that ENL exhibited weak binding and ability to transactivate to PPAR γ similar to other partial agonists.

To support the competitive binding and transactivation studies, the biological function of the compounds was assessed since PPAR γ partial agonists are also reported to stimulate glucose uptake in adipocytes, but typically are unable to induce adipogenesis in preadipocyte cells^{186, 446}. Ibrutinib, gefitinib, and ENL stimulated glucose uptake in differentiated mouse preadipocytes with a similar pattern as rosiglitazone and FMOC-L-Leu, while gefitinib and ENL showed limited adipogenic activity in mouse adipocytes similar to FMOC-L-Leu. Thus, the PPAR γ -mediated biological function of the tested compounds is suggested to be similar to the known partial agonist indicating that gefitinib and ENL are possibly partial agonists of PPAR γ . This is supported by the literature where PPAR γ partial agonists may have considerable anti-diabetic activity as full agonists but may exhibit weak anti-obesity potency⁴⁴⁷. Collectively, the binding, transactivation, and biological activity assays suggest ENL and gefitinib are potential PPAR γ partial agonists, while possibly having a limited effect on adipogenesis.

Interestingly, dabrafenib was detected with weak binding and a poor ability to transactivate PPAR γ , yet increased glucose uptake at higher concentrations at levels considerably greater than rosiglitazone. Ibrutinib and dabrafenib also demonstrated ability to stimulate adipogenesis where increasing concentrations caused greater stimulation of

adipogenesis in a pattern similar to rosiglitazone. Although it cannot be ruled out that ibrutinib and dabrafenib are partial agonists of PPAR γ , the marked increase in glucose uptake by dabrafenib and induction of adipogenesis suggests other binding sites or mechanisms beyond PPAR γ . The *in silico* docking model of the literature suggested that ibrutinib and dabrafenib form a single hydrogen bond at Tyr-327 and Ser342 with a similar total binding energy with rosiglitazone¹³. The weak competitive binding affinity and transactivation activity of dabrafenib to PPAR γ suggested a partial PPAR γ agonism pattern of dabrafenib, while the glucose uptake activity of ibrutinib was similar to the control compounds as well as the tested compounds. However, the stimulation of glucose uptake activity of dabrafenib and the adipogenic activity of both ibrutinib and dabrafenib were stronger than other compounds. This induction of adipogenesis by ibrutinib and dabrafenib and the increase of glucose uptake by dabrafenib might be due to its ability to bind to alternative binding sites on PPAR γ or by crosstalk with PPAR γ by dabrafenib's target cell signaling. Other than the common binding sites of PPAR γ full agonists, ibrutinib binds to other amino acids including the main binding sites for PPAR γ partial agonists, for instance, Ser-342, Leu-330, and Leu-333¹³. Ibrutinib, as a multi-target TKI with high selectivity for Bruton's tyrosine kinase, may also suppress AKT and MAPK pathways in certain cell lines, which are believed to interact with PPAR γ pathways^{162, 448}. Dabrafenib, as a second BRAF kinase inhibitor on both the wild type BRAF and the mutant BRAF V600E, is now suggested to target other kinases which may also lead to a modulation of glucose uptake activity via PPAR γ and other pathways^{449, 450}. For instance, as a BRAF kinase inhibitor, dabrafenib might have an impact on the expression and phosphorylation of PPAR γ via MEK/ERK pathway and subsequently affect glucose uptake activity^{451, 452}. Based upon the current data on the binding and transactivation of ibrutinib and dabrafenib on PPAR γ , it is likely that ibrutinib and dabrafenib are potential partial agonists, but the significant induction on adipogenesis with ibrutinib and dabrafenib as well as increased glucose uptake with higher exposure of dabrafenib suggests further study should be performed to confirm the PPAR γ agonism of ibrutinib and dabrafenib as well as the mechanisms through which ibrutinib and dabrafenib enhances adipogenesis and how dabrafenib modulates glucose uptake.

As the goal was to focus on the downstream effects of PPAR γ agonism rather than focus on the confirmation of their exact binding interaction with PPAR γ , it is clear that pitfalls existed with the exploratory examination of the TKI's and ENL as agonists of PPAR γ , although the methods used are common and well-established. For instance, PPAR γ is known to have multiple binding sites, and use of a competitive binding kit specifically for

rosiglitazone's binding site might overlook the possible interaction of the tested compounds with alternative PPAR γ binding sites^{147, 453}. The focus remained on the rosiglitazone binding site due to the results reported from *in silico* docking analysis of the TKIs with rosiglitazone's binding site on PPAR γ ¹³. It is possible that there are other binding sites or conformational changes for one or all of the tested compounds as indicated in the literature, and further assessments are necessary to verify the exact binding pattern of the compounds to PPAR γ ^{182, 454}.

Alternatively, ibrutinib, dabrafenib, gefitinib, as well as ENL may regulate PPAR γ through ligand-independent mechanisms. As a phosphoprotein, PPAR γ 's transcriptional activity depends on the relative interplay of kinases and phosphatases⁴⁵⁵. Inhibition of phosphorylation of ser273 on PPAR γ can decrease the activation of PPAR γ ⁴⁴⁷. Hence, the TKIs, as kinase inhibitors, may block the phosphorylation of PPAR γ , thereby lowering its transcriptional activity. In proliferative cancer cells, ENL also can decrease the phosphorylation of key kinase pathways, which might suggest an ability to inhibit PPAR γ phosphorylation^{456, 457}. For both the TKIs and ENL, ligand-independent mechanisms involving inhibition of PPAR γ phosphorylation as a mechanism to explain the improved insulin sensitivity and glucose uptake in preadipocytes warrants further investigation.

In conclusion, ENL and gefitinib are potential partial agonists of PPAR γ based on their poor PPAR γ binding affinities and limited ability to transactivate PPAR γ while stimulating glucose uptake without an ability to induce adipogenesis. Although the actual structural transformation caused by the partial agonism should be clarified, all but ibrutinib and dabrafenib may be partial agonists. Given that multi-target TKIs and the flaxseed lignan metabolites are known to inhibit kinase function, ligand-independent mechanisms involving inhibition of PPAR γ phosphorylation may have a role and warrant further investigation.

8.2 The antifibrotic potential and possible mechanisms of PPAR γ -related TKIs with

ENL

Hepatic fibrosis remains a severe global health problem caused by various liver injuries and is characterized by the accumulation of proliferative HSCs and ECM⁴⁵⁸. Based upon the significant progress made in our understanding of the role of HSCs in fibrogenesis, recent studies have indicated the potential to target HSC activation as well as promote matrix degradation and HSC apoptosis as an approach to mitigate and even reverse hepatic fibrosis,

particularly during early disease development⁴⁵⁹. Suppression of transdifferentiated HSCs has been applied as antifibrotic therapeutic options, possibly via TGF- β inactivation, AMPK activation, inhibition of NF- κ B, or activation of p53, and when the activation and proliferation of HSCs are suppressed and apoptosis of HSCs stimulated, the progression of hepatic fibrosis can be inhibited or reversed⁴⁶⁰⁻⁴⁶². Several TKIs have shown antifibrotic effects in several organ systems. For instance, gefitinib and imatinib show antifibrotic effects in the lung, while ibrutinib and sorafenib demonstrated antifibrotic effects in the pancreas and liver, respectively, suggesting that certain TKIs may serve as antifibrotic agents in hepatic fibrosis^{11, 281, 294-296}. Similarly, natural products have gained increasing interest as antifibrotic agents promising long-term safety, and possibly working through inhibition of HSC activation or suppression of ECM deposition⁴⁶³.

Based on the literature suggesting antifibrotic effects of the TKIs and lignans in other organ systems, exploratory studies of the possible role of these compounds were conducted in an *in vitro* model of hepatic fibrosis. Ibrutinib, gefitinib, and ENL applied alone were able to suppress the expression of the major fibrotic biomarkers within a modest range of concentrations in TGF- β 1-stimulated LX-2 cells. Since dabrafenib showed no significant ability to suppress the biomarkers of fibrosis, it was not continued with further evaluation in combination studies with ENL. As well, Ibrutinib, with a relative IC₅₀ value of about 5 μ M in TGF- β 1-stimulated LX-2 cells, caused no significant reductions in fibrotic biomarkers at 1 μ M, although higher but toxic concentrations did result in a modest response. Consequently, ibrutinib was also removed from consideration for further investigations involving the combination of ENL with the TKIs. With the *in vitro* evidence of reduction in biomarkers of fibrosis for gefitinib, subsequent studies evaluating the combination of TKIs and ENL focused only on gefitinib. This focus was supported by literature evidence of the ability of gefitinib to modulate cell migration in non-small cell lung cancers, inhibit the proliferation of hepatic biliary epithelial cells, and increase the rate of hepatic cellular apoptosis in rats^{464, 465}. As a known EGFR inhibitor, gefitinib may have antifibrotic effects through direct suppression of HSC activation via inhibition of EGFR and TGF- β 1; however, the mechanism of EGFR and its ligands in fibrosis remains unclear⁴⁶⁶. This current work confirmed that gefitinib may inhibit the migration and expression of fibrotic markers of HSCs and induce the apoptosis of HSCs. As a potential PPAR γ partial agonist, gefitinib might influence hepatic fibrosis beyond direct inhibition of EGFR.

According to the results, the combination of ENL with gefitinib further attenuated the

expression of the hepatic fibrotic biomarkers than using gefitinib alone *in vitro*. Furthermore, the combination of ENL with gefitinib caused greater suppression of HSC migration and induced apoptosis to a greater extent than using gefitinib alone. The ability of ENL to enhance gefitinib's effects is consistent with the literature of other proliferative diseases such as cancer⁴⁶⁷. Studies have shown that natural products may serve as anti-cancer agents through inhibition of EGFR, PDGFR, or other tyrosine kinase receptors signaling⁴⁶⁸. ENL may enhance gefitinib's activity through similar mechanisms but needs confirmation in future analyses.

Although alone ENL weakly inhibited the migration of HSC, it further enhanced the ability of gefitinib to prevent the migration of activated HSC as compared to gefitinib alone. Since the motility of the activated HSCs partially determines the wound healing response, the ability to inhibit the migration of activated HSCs is an important mechanism in preventing or resolving hepatic fibrosis⁴⁶⁹. The flavonolignan, silibinin, was shown to inhibit the migration of HSCs possibly related to its induction of PPAR γ expression⁴⁷⁰. In this study, gefitinib also upregulated the protein level of PPAR γ when used alone and further increased PPAR γ protein expression in combination with ENL in a concentration- and time-related manner. Hence, as partial agonists of PPAR γ and ability to induce PPAR γ expression, the inhibition of HSC migration by gefitinib and ENL may, in part, act through the PPAR γ pathway. This was shown with ergosterol, an active natural product, which attenuated HSCs activation and ROS production by upregulating PPAR γ ⁴⁷¹. Further, studies have shown that PPAR γ expression in quiescent HSCs in the normal liver is higher than in proliferative HSCs, and ligands of PPAR γ have the ability to reverse the activation of collagen production by HSCs⁴⁷². Finally, PPAR γ agonists have been reported to have antifibrotic effects in different hepatic fibrosis models, so it is possible that gefitinib and ENL may exert antifibrotic effects *via* PPAR γ -related pathways^{473, 474}. This assertion is supported by studies that have shown the PPAR γ pathway can be a therapeutic target for hepatic fibrosis by reversing HSC activation, and mediate anti-proliferative and antifibrotic effects involving either PPAR γ -dependent or -independent pathways^{79, 475-477}. It was attempted to provide further supportive evidence of the involvement of PPAR γ through assessment of PKM2, a common downstream factor of PPAR γ . Gefitinib did modulate the mRNA expression level of PKM2 in activated HSC cells, but PKM2 expression changes were different when gefitinib was combined with ENL. Possibly other cell signaling pathways are involved in the modulation of PKM2, indicating that PKM2 is not a specific downstream factor of PPAR γ .

Research has shown that the TGF- β /Smad pathway plays a pivotal role in hepatic

fibrogenesis⁴⁷⁸. It has been reported that TKIs and natural products have antifibrotic action via modulation of the TGF- β pathway^{15, 330}. For instance, active EGFR was reported to promote proliferation and survival of hepatic progenitors and was associated with the apoptotic process induced by TGF- β in these cells⁴⁶⁶. Kaerophyllin, one kind of lignan, was reported to inhibit TGF- β 1 induced LX-2 activation⁴⁷⁹. Unfortunately, the involvement of this pathway could not be assessed as TGF- β 1 was used to stimulate the LX-2 cells, as activated HSCs was the primary focus for evaluating the potential of TKIs and ENL in attenuating biomarkers of hepatic fibrosis. This is an important limitation of the work and further studies should be conducted to address the role of TGF- β in the antifibrotic effects of TKIs and ENL in hepatic fibrosis. For instance, LPS could be used to stimulate HSCs, followed by measurement on the TGF- β pathway, or a co-culture cellular system including immunocytes with HSCs can be used to study the role of TGF- β in fibrogenic and antifibrotic processes⁴⁸⁰.

Recent investigations suggest several cellular signaling pathways might be involved in the antifibrotic effects of PPAR γ agonists. Rosiglitazone, a known PPAR γ full agonist, is reported to inhibit TGF- β 1 mediated fibrosis *via* Smad2 pathway in autosomal dominant polycystic kidney disease animal model⁴⁸¹. Activation of PPAR γ may also repress the PDGF β receptor and subsequently attenuate HSC mobility and angiogenesis probably *via* interference with other transcription factors such as NF- κ B and PI3K-Akt-mTOR pathways^{482, 483}. Other than the better-known signaling pathways that might be involved in the antifibrotic response of PPAR γ agonists, TLR-4-related pathway is considered a novel mechanism *via* which a PPAR γ agonist relieves fibrosis in nutrition deficient diet-induced non-alcoholic fibrotic steatohepatitis mice⁴⁷⁴. Free cholesterol accumulation was believed an important promotor of TLR4 signal transduction and the HSCs became more sensitive to profibrotic stimulators⁴⁸⁴. Previous work of the Alcorn lab found that ENL modulated the expression of PPAR γ , and also improved key markers of free cholesterol accumulation including SREBP-1 and INSIG-1 in Caco-2 cells³⁸⁵. Thus, it is possible that PPAR γ partial agonism may help modulate free cholesterol accumulation and adipogenic activity in HSCs, to reduce the fibrosis within the liver. This should be confirmed by assessing those cholesterol-related biomarkers both *in vitro* and *in vivo* in hepatic fibrosis models in the future.

The results also indicate that there might be enhanced apoptosis of activated HSCs with the combination of gefitinib and ENL, suggesting promise to resolve hepatic fibrosis by depleting HSCs, the key player in the process of fibrogenesis. The combination of gefitinib

and ENL showed time- and concentration-related effects on stellate cell migration and apoptosis. Gefitinib induced the expression of ATF4 and CHOP, accordingly, at both gene and protein levels. In combination with ENL, the expression of both markers were induced to a further extent in a concentration-related manner. This indicates an involvement of ER stress-induced apoptosis in the potential antifibrotic effects of the treatment in human HSCs. According to the literature, although deactivation of HSCs results in decreased proliferation as well as production of fibrotic markers, HSC deactivation is not adequate for reversal of hepatic fibrosis, because the deactivated HSCs are more likely to be reactivated than the quiescent type⁸¹. Thus, the depletion of activated HSCs by apoptosis becomes critical to reverse hepatic fibrogenesis⁴⁸⁵. Different cellular signaling pathways were reported to be involved in the apoptosis of HSCs, among those possible apoptosis-related proteins, one major pathway to cause apoptosis is cellular stress²⁶.

ER stress is considered an important contributor to hepatic fibrosis and the therapeutic targeting of ER stress in HSCs is an attractive target in antifibrotic therapy²⁶. With the ER stress response, the IRE1 α and PERK branches would be activated by autophosphorylation, while ATF6 might be induced by proteolytic processing, leading to an ER stress response^{486, 487}. The IRE1 α pathway, as the most conserved branch of the three, is responsible for both the activation and the autophagy of HSCs depending on the p38 MAPK pathway and its blockage reduced the fibrotic response of mouse HSCs⁴²⁸. In CCl₄-induced fibrosis of rat and cultured HSCs, the Ire1 pathway regulated the expression of TGF- β expression and α -sma⁴⁸⁸. Clear examples of the involvement of ER stress in HSC apoptosis include etoposide, a chemotherapy agent, which induced apoptosis of activated human HSCs through ER stress and caspase-dependent mitochondrial pathways⁴⁸⁹. As well, caffeine activated IRE1 α in HSCs with concomitant increases in CHOP and cytosolic calcium, suggesting that ER stress-induced apoptosis might be involved in caffeine's effect⁴⁹⁰. ATF6 α is likely to play a role in HSC activation, as in cardiac fibrosis, where activation of ATF6 α promoted ECM protein production and inhibition of ATF6 α suppressed HSC activation to stimuli^{491, 492}.

Among the three branches, the PERK pathway plays a key role in modulating both proapoptotic and antioxidant response and PERK activation would upregulate proapoptotic ATF4/CHOP signaling, which could serve as an antifibrotic strategy⁴⁹³. The potential for gefitinib and ENL to induce ER stress was investigated by evaluating the expression of several key markers of ER stress-related pathways including ATF6 at mRNA level, CHOP and ATF4 at both mRNA and protein levels. The results suggested ER stress-induced

apoptosis may be involved in the suppression of activated HSCs by treatment with the combination of gefitinib and ENL. However, studies have suggested that CHOP, although is necessary, alone would not be sufficient to fully induce cell death, which usually requires cooperation between CHOP with ATF4⁴⁹⁴. This is consistent with our results on the expression changes of ATF4 and CHOP at both mRNA and protein levels in the TGF- β 1-activated LX-2 cells. Thus, ATF4/CHOP signaling might be involved in the possible effects of gefitinib and ENL.

Another important role of PERK is its effect on antioxidant responses through the activation of Nrf2. This transcription factor provides a protective effect at the onset of ER stress by increasing the production of phase II detoxifying enzymes and antioxidants such as GSH⁴⁹⁵. Moreover, Nrf2 is reported to dimerize with ATF4 to regulate the oxidative stress-response⁴⁹⁶. However, as both Nrf2 and ATF4/CHOP are downstream signaling pathways of PERK, Nrf2 might perform as a negative regulator of CHOP expression directly or indirectly, yet the mechanism is not clear⁴⁹⁷. Of note, although the mechanism of the relationship between oxidative stress and ER stress is yet not clear, it is believed that chronic ER stress may initiate oxidative stress *via* release of calcium from the ER to induce ROS production in mitochondria^{497, 498}. In turn, mitochondrially produced ROS contributes to the sensitivity of the cells to ER stress-induced apoptosis^{497, 498}. In this current study, the MitoSox red reagent indicated that there was higher ROS production within TGF- β 1-stimulated LX-2 cells, and treatment with gefitinib and ENL reduced ROS production at an earlier stage of LX-2 activation. This may be related to the increased expression of Nrf2 within the cells, possibly *via* PERK signaling⁴⁹⁹. With prolonged stimulation, ER stress-induced cell apoptosis may occur possibly *via* the ATF4/CHOP pathway. Further assessment is required to identify the relationship between the two pathways and to determine if PERK is the same upstream factor of the two pathways.

There is still controversy regarding the role of ER stress in hepatic fibrosis. The UPR has a protective role, and activation of UPR in HSCs would facilitate the removal of damaged organelles or fibrotic cells. However, sustained ER stress response can be detrimental^{500, 501}. As far as it is known, prolonged ER stress in hepatocytes may lead to hepatocellular damage or apoptosis, which may lead to fibrogenesis by causing activation of HSCs^{490, 502}. The tight interrelationship between TGF- β /SMAD and UPR signaling contributes to the HSC activation during fibrogenesis *via* IRE1 α signaling⁴⁸⁸. Upregulation of SMAD2 was also reported to be involved in PERK-mediated fibrogenesis in mice HSCs⁵⁰³. Thus, a better understanding of the function of ER stress and ER stress-induced apoptosis in hepatic fibrosis

has become an emerging research area of interest.

Oxidative stress is another possible mechanism involved in the antifibrotic effects of potential antifibrotic compounds in HSCs. In this study, TGF- β 1 induced ROS production in LX-2 cells, which is consistent with the literature⁹⁶. Oxidative stress is a common feature of chronic liver disease and is involved in the etiology of hepatic fibrosis by activating HSCs, and recent studies indicated oxidative stress could be pro-apoptotic irrespective of the liver injury^{504, 505}. In an arsenic-induced hepatic fibrosis mouse model, chronic arsenic exposure results in oxidative stress and activation of HSCs, leading to the development of liver fibrosis¹³¹. TGF- β is reported to induce the expression of several NADPH oxidases (Noxs) in different types of cells to produce ROS, and among the Nox enzymes, Nox4 was found to be associated with ER and mitochondria, mediating fibrogenic responses⁵⁰⁶. Gefitinib and a high concentration of ENL reduced ROS production at one hour, while the combination of gefitinib and ENL reduced the ROS production further and earlier. This suggests the involvement of decreased oxidative stress in the combination effect of gefitinib and ENL in this *in vitro* fibrosis model. Besides the oxidative stress-dependent modulation, PERK-dependent induction of the nuclear translocation of Nrf2 is also a possible mechanism of Nrf2-mediated cyto-protection effects⁴⁹⁹.

Based upon the current results and the literature evidence, the expression of Nrf2 was evaluated to determine whether it had a role in the antioxidant activity with the combination of gefitinib and ENL. The literature indicates an ability of Nrf2 to suppress the expression of genes involved in lipogenesis, inflammation, oxidative stress, and fibrosis⁴⁹⁸. (+)-Lariciresinol, an active lignan derived from *Rubia pholippinensis*, exhibits antioxidant potential through upregulation of Nrf2-mediated heme oxygenase-1 expression⁵⁰⁷. Although there is little evidence for TKIs' direct modulation of Nrf2, in cancer cell lines, EGFR-TKIs possibly inhibit the PI3K/AKT/mTOR pathway which leads to an imbalance between mitochondrial ROS production and antioxidant defense by Nrf2⁵⁰⁸. The crosstalk between Nrf2 and PERK/ATF4 pathways was also supportive evidence for us to speculate the influence of Nrf2 expression. The current results indicated that treatment with the combination of gefitinib and ENL induces Nrf2 protein expression in activated LX-2 cells, suggesting that Nrf2 might play a role in the antioxidant response of the combination of gefitinib with ENL. Further studies are needed to identify the dimerization and the phosphorylation of Nrf2 and ATF4, as well as the changes of PERK to define the roles of PERK-Nrf2 and PERK-ATF4-CHOP pathways.

In summary, PPAR γ , oxidative stress, and ER stress pathways are possibly involved in

the attenuation of biomarkers of hepatic fibrosis, and there might be underlying crosstalk between these three possible pathways (**Figure 8.1**). Further investigations are needed to confirm their inter-relationship, for instance, the relationship between oxidative stress and ER-stress-induced apoptosis in activated HSCs. Other possible key mechanisms involved in liver fibrosis, for example, inflammatory responses, are additionally believed to be involved in the process, since fibrogenesis can be initiated by inflammation⁵⁰⁹.

The ability of ENL to enhance gefitinib's effects on the suppression of biomarkers of hepatic fibrosis suggests a possibility of reducing the dose of gefitinib when co-administered with ENL if applied therapeutically in the context of hepatic fibrosis. Dose reductions can reduce the risk of dose-limiting side effects in the treatment of chronic disease. The cytotoxicity assays in this study showed that gefitinib had an acceptable range of non-toxic concentrations, while ENL exhibited no cytotoxicity in activated LX-2 cells. At lower concentrations of gefitinib with higher concentrations of ENL, the combination caused the attenuation of fibrotic biomarkers. ENL may help reduce the potential toxicity of gefitinib as a therapeutic measure in hepatic fibrosis by helping to reduce the dose of gefitinib required to therapeutically manage hepatic fibrosis.

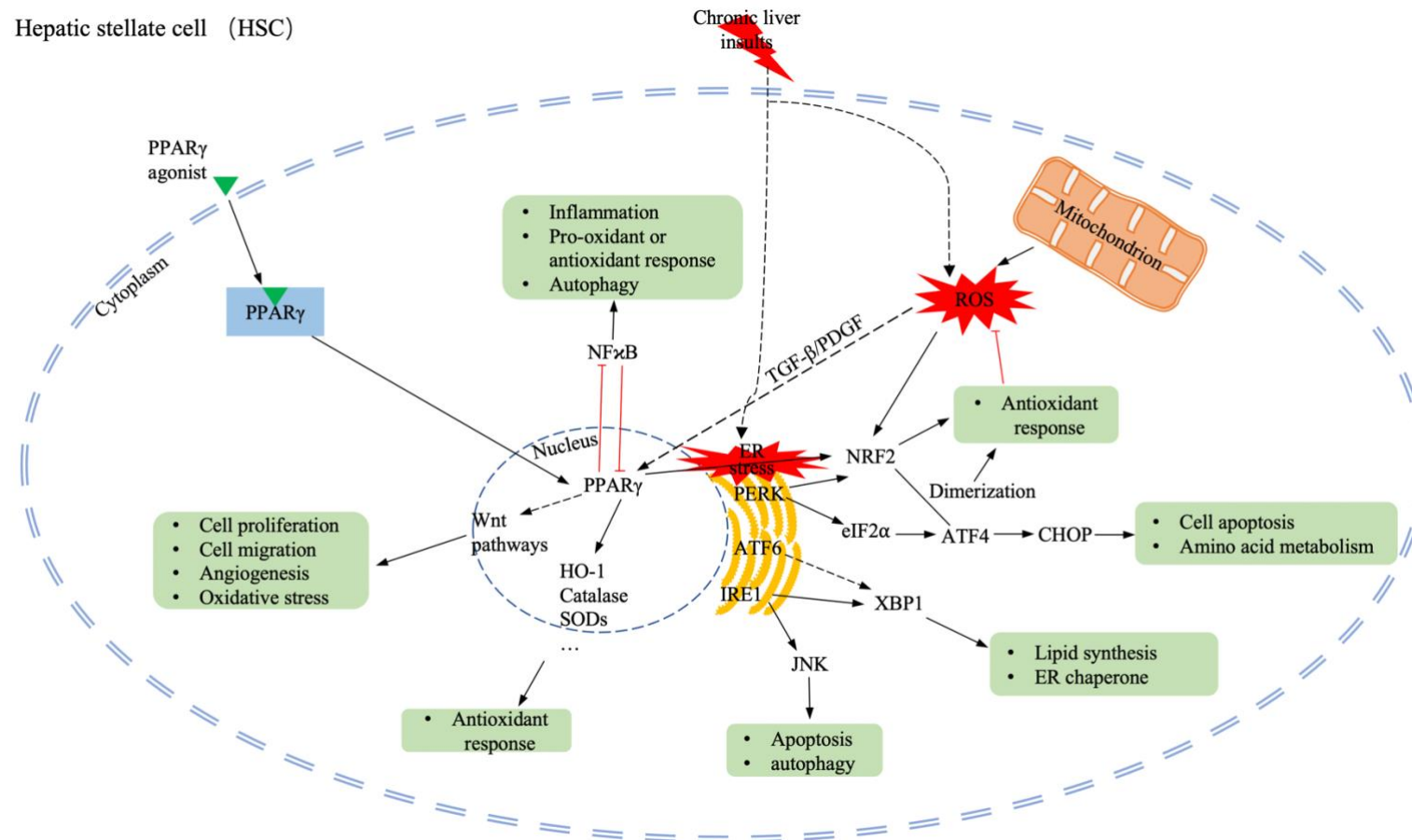


Figure 8.1 A schematic model of the possible mechanisms involved in the antifibrotic effects of the combination of gefitinib and enterolactone (ENL) related to PPAR γ , oxidative stress, and ER stress. With chronic liver insults, hepatic stellate cells (HSCs) would be activated possibly involving processes like oxidative stress and ER stress. PPAR γ would play a central role in the potential antifibrotic effects of antifibrotic agents. Possible agonists may activate PPAR γ which in turn would transcriptionally activate fibrotic downstream factors, including Wnt pathways, antioxidant response, and ER stress-related pathways. These potential mechanisms may cause inhibition of cellular oxidative stress, cell proliferation, and migration as well as induction of apoptosis and antioxidant responses in the fibrotic HSCs.

8.3 Other possible antifibrotic mechanisms of TKIs with ENL

TKIs, as multitarget kinase inhibitors, are known to inhibit the phosphorylation of protein targets at tyrosine and serine sites. Such inhibition might have some direct effects on elevated tyrosine kinase activity^{449, 510}. In this current work three different subtypes of TKIs were chosen including the EGFR inhibitor, gefitinib, the multitarget TKI, ibrutinib, and a non-EGFR-TKI, dabrafenib. Based on our results, many of the subsequent experiments focused on gefitinib. EGFR, as an important RTK, is a therapeutic agent for cancer treatment³⁰⁴. The latest research suggests that myofibroblasts express EGFR, which may be involved in cell proliferation, and administration of an EGFR inhibitor could mitigate the proliferation of myofibroblasts in BDL mice via reducing the phosphorylation of EGFR⁵¹¹. Tumor necrosis factor-like weak inducer of apoptosis was found to promote HSC migration and collagen production by upregulating the phosphorylation of EGFR/Src and PI3K/AKT pathways, while inhibition of the PI3K/AKT pathway attenuated the expression of MMP9⁵¹². Recent evidence also showed that reductions in EGFR levels in eIF2 α phosphorylation-deficient hepatocytes were critical for cell susceptibility to oxidative stress, which supports this current work regarding the relationship between oxidative stress and ER stress in the *in vitro* hepatic fibrosis model – gefitinib and ENL treated activated LX-2 cells⁵¹³. Although collective evidence showed that an EGFR inhibitor prevented fibrogenesis in HSCs by reducing the phosphorylation of EGFR, yet EGFR deletion in HSCs alone or all liver cells showed no effect on the progression and resolution of CCl₄-induced hepatic fibrosis⁴⁶⁶. Taken together, EGFR-mediated pathway and its inhibitor may play a role in the progression of liver fibrosis, and EGFR could be a therapeutic target for liver diseases including liver fibrosis. In this current study, the potential antifibrotic effect of gefitinib may be related to an EGFR-related mechanism. Furthermore, there might also be direct inhibition of other cellular signaling factors, such as PERK and Wnt pathways, but further studies are needed to confirm the involvement of EGFR-related pathways and other possible mechanisms.

Lignans have been reported to demonstrate antioxidant and anti-inflammatory effects, as well as antifibrotic effects^{514, 515}. Polyphenolic compounds including lignans can target inflammatory mediators via TLR-4/NF- κ B signaling pathways in neuroinflammatory disease⁵¹⁶. Schisandrin, another kind of active lignan, induced HO-1 expression to result in an anti-inflammatory response in macrophages related to Nrf-2, PI3K/Akt, and ERK activation⁵¹⁷. In carbon tetrachloride-induced rats, sesamin showed protective effects against hepatic fibrosis through antioxidant and anti-inflammatory effects⁵⁰⁵. Flaxseed lignan

complex supplementation for more than three months is also reported to reduce inflammation and LDL oxidation in diabetic obese people, and SDG decreased local inflammation likely via NF- κ B activity in mice^{518, 519}. Taken all these together, it is possible that flaxseed lignans may exert antifibrotic effects related to anti-inflammatory and antioxidant responses.

In activated HSCs, both canonical and noncanonical Wnt signaling pathways were reported to be induced⁵²⁰. Elevation of canonical Wnt signaling caused alteration of cell morphology and cell proliferation in fibroblasts, and the canonical Wnt antagonism was reported to inhibit HSC activation^{520, 521}. In rat HSCs, non-canonical Wnt was found to be involved in the activation of HSC or Kupffer cells and HSC apoptosis⁵²². In this study, a preliminary study on the Wnt/ β -catenin pathway at the mRNA expression level showed that β -catenin and several Wnt subtypes might be involved in the activation of HSCs, which is consistent with the literature²³¹. From the limited data on mRNA, there seems to be a close linkage between PPAR γ and Wnt/ β -catenin pathway with regards to the suppression of fibrotic biomarkers. Thus, it is possible that PPAR γ and Wnt/ β -catenin pathways are involved in the activation of HSCs in hepatic fibrogenesis and can be therapeutic targets for hepatic fibrosis. However, ENL showed no significant modulation of either the canonical and non-canonical Wnt pathways; thus, further investigations of the Wnt signaling pathways at protein level in the *in vitro* hepatic fibrosis model are warranted to make confirm that Wnt signaling pathways play a role in the antifibrotic response of gefitinib and ENL.

8.4 The antifibrotic potential of SDG in hypercholesterolemia rats

Patients with NAFLD or NASH and progressive hepatic fibrosis are at the highest risk for severe liver disease⁵²³. NAFLD, paralleling the epidemic of type 2 diabetes and obesity, is the most prevalent form of chronic liver disease with a global prevalence of 25%^{524, 525}. NAFLD has become the leading cause of morbidity and mortality related to the liver within recent decades^{524, 525}. NAFLD, with a wide spectrum of pathologies ranging from non-inflammatory lipid accumulation to NASH, is also recognized as a common cause of fibrosis resulting eventually in cirrhosis and hepatocellular carcinoma^{526, 527}. Lifestyle diseases including hypercholesterolemia and hypertriglyceridemia are associated with NASH and free cholesterol accumulation in HSCs is involved in the pathogenesis of hepatic fibrosis⁴⁸⁴. Diets high in cholesterol are believed to contribute to the pathogenesis of non-alcoholic fatty liver with fibrotic steatohepatitis, due to increases in TC, LDL, and the LDL to HDL ratio, lipid accumulation, as well as activation of inflammatory signaling such as NF- κ B and MAPK and

attenuation of antioxidant signaling like Nrf2⁵²⁸. To manage hypercholesterolemia and hypertriglyceridemia, lifestyle changes including healthy diet, physical exercise, and drug treatment, such as statins, are applied^{529, 530}. In the evolution of NAFLD, steatosis and steatohepatitis represent different stages, and insulin resistance might be a factor in the progression from steatosis to steatohepatitis with fibrosis⁵²⁶. A previous study of our laboratory suggested ENL may alter cholesterol trafficking with Caco-2 epithelial cells and can suppress the expression of LDLR and HMG-CoA reductase, which are involved in cholesterol synthesis and uptake in hepatocytes, at both RNA and protein levels^{364, 385, 531}.

Given the evidence for the role of lignans to reduce hepatic lipidosis, the ability of lignans to reduce biomarkers of hepatic fibrosis was explored in an animal model of diet-induced hypercholesterolemia. In a study that replicated a previous study design in the Alcorn laboratory a comparative analysis of the PK and efficacy of purified SDG and SDG enriched product was conducted³⁶⁴. The results confirmed the ability of SDG to modulate cholesterol homeostasis. The LDL level was reduced in both purified SDG and SDG polymer treated groups, and purified SDG showed a greater effect on TG and HDL modulation than SDG polymer. This is consistent with the previous work in the Alcorn laboratory and results reported on the ability of flaxseed lignans to modulate cholesterol both preclinically and clinically^{385, 395, 417}. These data suggest that oral supplementation with SDG helps improve the lipid profile in non-alcoholic fatty liver disease rats, possibly playing a role in lipid homeostasis. Purified SDG caused modest reductions in hepatic steatosis and lobular inflammation of non-alcoholic fatty liver in high cholesterol diet-fed rats, and mild improvements in the ALT/AST ratio with 23 days of daily oral SDG administration. This indicates that SDG supplementation might help improve the fatty liver condition. In a previous study in the laboratory, SDG and its metabolites including ENL were shown to improve hepatic lipid accumulation and lipid metabolism in an animal model⁴³⁰. In the current study, an important limitation of the study was inadequate induction of hypercholesterolemia and fatty liver in high cholesterol diet fed rats due to a shortage in the supply of a high cholesterol diet. This, in turn, led to a shorter treatment period with SDG relative to the previously reported study in the Alcorn lab. Further studies should be done to confirm the hepatic protective effects of SDG-enriched products in non-alcoholic fatty liver disease *in vivo*.

It is reported that elevated plasma cholesterol levels in NAFLD and NASH patients are associated with oxidative stress and ER stress because free cholesterol might be stored in the liver by accumulating LDL with triglycerides and apolipoproteins followed by secretion of

lipoproteins into the systemic circulation⁵³². In this study, the HDL level at 14 days of administration of SDG polymer was increased, but no significant changes occurred in other lipoprotein levels. This is consistent with a pioglitazone trial, which indicated that HDL increased with NASH resolution, but no significant changes were observed for LDL and other lipoprotein levels⁵³³. As pioglitazone is a PPAR γ agonist, this literature evidence suggests that PPAR γ agonists may modulate cholesterol levels in NASH patients. In the NASH rabbit model associated with metabolic syndrome, inhibition of NASH development and adipose tissue function were accompanied by enhanced mitochondrial function and insulin sensitivity⁵³⁴. This indicates that PPAR γ , which may modulate adipogenesis and insulin sensitivity, may play a role in mitochondrial function and metabolism in NASH patients. Such effects might have important consequences in the antifibrotic effects of such therapeutic agents.

Subsequently, we evaluated mRNA and protein levels of fibrotic biomarkers in the liver tissues of rats administered purified SDG to determine whether SDG treatment suppressed biomarker expression. The mRNA expression of *Acta2* showed an unexpected change in the rat liver samples, which is hard to explain with the current results of the study. First, the expression of *Acta2* in whole rat liver remains unclear in fatty liver as there are different cell types in the liver that can produce α -sma. Second, the sample area of the study may be critical for the monitoring of fibrotic α -sma. These were also observed in the preliminary western blot study which makes the outcome hard to interpret. Thus, α -sma protein expression in the rat liver samples was not used as a marker of fibrosis. The hepatic production of Collagen I protein was reduced in the purified SDG treated group, and *Mmp2* and *Timp1* expression were changed in accordance with Collagen I expression at both gene and protein levels in the liver samples. As an inhibitor of *Mmp2*, the changes in the expression of *Timp1* agrees with changes in Collagen I and *Mmp2* expression, which suggests that purified SDG has modest effects on the expression of fibrotic biomarkers in this high-cholesterol diet-induced NAFLD rat model. This is consistent with the literature which indicated that dietary flaxseed lignan components mitigated pulmonary fibrosis by decreasing the collagen deposition in lung tissues and reduced lung inflammation and oxidative stress response⁴⁰⁸. Increased degradation of Collagen I protein caused by the increased level of collagenase might result in the overall decrease of Collagen I protein in the SDG-treated hypercholesterolemic rats. It is also reported that flaxseed and flaxseed oil helped to decrease the expression of EGFR and HER2 in breast cancer models with changes in the membrane

phospholipid fatty acid profile⁵³⁵. The limited literature along with the *in vivo* study suggest that SDG and its metabolites have potential to mitigate liver fibrosis. The exact mechanisms involved in the possible antifibrotic effects of flaxseed lignans are unclear but may involve cholesterol modulation, insulin sensitivity, and mitochondrial ROS. This is agreeable with the *in vitro* study in human HSCs, yet further study should be done to confirm the antifibrotic effects of SDG or its metabolites and to identify the possible mechanism(s) of antifibrotic modulation *in vivo*.

A PK analysis was conducted in attempt to relate plasma concentrations to the observed effects. The lignan metabolites, SECO, END, and ENL undergo extensive glucuronidation (and some sulfate conjugation) and exist mostly as conjugates (of glucuronic acid and sulfate)^{27, 364}. Unconjugated lignan metabolite was barely detectable requiring the assessment of total area under the plasma concentration versus time curve (AUC) (conjugate plus unconjugated) of the lignan metabolites. The total AUC of END was higher than the ENL AUC in the SDG polymer group but lower than ENL in the purified SDG group. Based upon the known PK properties of flaxseed lignans, orally administered SDG would be converted to SECO completely within 20 hours; however, SDG was not detected in plasma and urine and SECO is partially absorbed into systemic circulation^{536, 537}. SECO is then converted into END and ENL, which are absorbed into systemic circulation in small amounts and can be metabolized to its conjugates^{27, 364}. Furthermore, the literature indicates that END and ENL accumulate in liver, testes, and prostate in a dose-dependent pattern in male rats with the majority of lignan metabolites found in the liver in rats^{380, 382}. In this study, total END was detected between 2 h and 24 h, and total ENL was detected in almost all blood samples including pre-dose samples, which is consistent with the literature and is due to the abundance of lignans in foods³⁷⁴. Since ENL and its glucuronide form are believed to be the most bioactive form of mammalian lignans and lignan metabolites accumulate in the liver, it is possible that the higher levels of total ENL associated with purified SDG administration, resulted in greater improvements in serum and hepatic lipids and changes in biomarkers of hepatic fibrosis as observed with the purified SDG form relative to the SDG enriched complex. Further study is needed to identify the possible antifibrotic effects of lignan administration alone and in conjunction with the TKI, gefitinib, and how efficacy relates to the relative dose and blood concentrations of lignan metabolites and gefitinib.

9. SUMMARY AND CONCLUSIONS

In conclusion, we suggest gefitinib and mammalian lignan, ENL, are potential partial agonists of PPAR γ because of their weak PPAR γ binding affinities and limited ability to transactivate PPAR γ while stimulating glucose uptake without an ability to induce adipogenesis. Although PPAR γ partial agonism requires confirmation with specific conformational and functional studies, we believe this potential PPAR γ partial agonism could explain, in part, their possible therapeutic role in fibroproliferative diseases.

As well, the *in vitro* work suggests that gefitinib has a mild antifibrotic response in activated LX-2 cells, while the *in vivo* study suggests lignans, in particular ENL, may attenuate hepatic lipidosis and fibrotic markers in the NAFLD rat model, along with modulation of serum cholesterol levels. In combinatory studies, the *in vitro* work also suggests ENL enhances gefitinib's ability to attenuate the biomarkers of hepatic fibrosis. PPAR γ , oxidative stress, and ER stress pathways are possibly involved in the attenuation of fibrotic biomarkers *in vitro*, and there might be underlying crosstalk between these three possible pathways. Co-administration of ENL with gefitinib has potential to lead to dose reductions of gefitinib, and hence greater safety, in the treatment of hepatic fibrosis. With further study, the roles and crosstalk of these pathways would be clarified and used as putative therapeutic targets for hepatic fibrosis.

10. FUTURE WORK

This current study demonstrates that gefitinib and ENL might be PPAR γ partial agonists according to the binding, transactivation, and biological activity on PPAR γ . But the binding of these compounds with PPAR γ was not clarified in terms of direct binding to PPAR γ . This is a shortcoming since this PPAR γ agonism-like response can involve PPAR γ ligand-independent modulation or crosstalk with other cell signaling pathways. Further study on the veritable structural modification following binding by the compounds should be confirmed to support the possibility that these compounds are PPAR γ partial agonists. These studies can involve surface plasmon resonance and/or X-ray crystallization and structure determination, using known full and partial agonists as positive controls and known antagonists as negative controls. The ability of the compounds to alter phosphorylation of PPAR γ also needs assessment to verify the actual mechanism of how the compounds modulate PPAR γ , and linkage of other cell signaling mechanisms on PPAR γ -related response should be investigated to confirm the PPAR γ -related function of these compounds, especially ibrutinib and dabrafenib.

During the course of this study, many factors were discovered to impact the state of the human hepatic stellate cell line, LX-2 cells. Further work is required to identify stable cell culture conditions and optimal stimulation with TGF- β 1 to ensure consistent outcomes when using this system as an *in vitro* hepatic fibrosis model. Furthermore, TGF- β 1 is a key stimulator for hepatic fibrosis, but it is not sufficient to only use TGF- β 1 to reflect the complexity of all kinds of chronic liver insults. To better mimic fibrogenesis *in vitro*, a co-culture system with certain types of hepatic cells such as Kupffer cells, hepatocytes, and HSCs can be utilized. Appropriate co-culture systems would consider the different pathophysiological responses of hepatic fibrogenesis and, therefore, would allow a greater understanding of the antifibrotic mechanisms of potential therapeutic agents.

Since inflammation plays an essential role in the pathological process of hepatic fibrosis regardless of etiology, the anti-inflammatory response of the combination of TKIs and lignans may be the next goal. The involvement of inflammatory factors in the fibrogenesis of HSCs and the anti-inflammatory response of gefitinib and ENL would be assessed by measuring the expression of key inflammatory biomarkers at both mRNA and protein levels in mono-cellular culture system, such as activated LX-2 cells, and also in a co-culture system with HSCs, immune cells, and hepatocytes. The relationship between anti-inflammatory properties and other mechanisms, including PPAR γ , antioxidant, and ER

stress-related apoptosis pathways, would also be evaluated by assessing changes in the expression of the markers of these pathways at both gene and protein levels in the aforementioned cellular systems. Co-culture system for this investigation could involve Kupffer cells, as the main immune cells during the fibrosis process, with HSCs and hepatocytes. Also, a non-alcoholic fatty liver disease rat model could be used to define the role of inflammation in fatty liver.

As the preliminary western blot assay on PKM2 suggested that PPAR γ is not a unique upstream factor of PKM2, other more specific PPAR γ downstream factors should be considered to confirm the mechanism of PPAR γ 's role in the resolution of hepatic fibrosis. Also, the relationship of PPAR γ with other pathways should be clarified further, for instance, the relationship between PPAR γ and ER-stress induced apoptosis, as well as PPAR γ with oxidative stress. These relationships should be evaluated for a better understanding on the role of these important pathways. To study this, *in vitro* studies would be performed in human HSCs, the mRNA and protein expression changes in the aforementioned signaling pathways would be detected after treatment with the tested compounds, with or without PPAR γ antagonist, or using siRNA in the cell system. Furthermore, the involvement and the possible role of PPAR γ in animal models should be assessed to confirm the mechanisms of potential antifibrotic agents.

As discussed above, PPAR γ might modulate Wnt pathways in fibrogenic HSCs, which might contribute to the antifibrotic effects in hepatic fibrosis. However, the involvement of Wnt pathways in the antifibrotic response of the TKIs and ENL in LX-2 cells could not be defined due to limited mRNA expression changes with application of the combination of gefitinib and ENL. Canonical- and/or non-canonical-Wnt pathways at protein level or biological level should be assessed to verify the involvement of Wnt pathways in the resolution of liver fibrosis by the combination of gefitinib and ENL, as well as the relationship between canonical and non-canonical Wnt pathways in the possible antifibrotic effects. If Wnt signaling is indeed involved, the relationship of Wnt pathways with PPAR γ and other pathways should be further evaluated.

A better understanding of the relationship between oxidative stress and ER stress is also necessary. Currently, evaluations on PERK-related pathways, namely, Nrf2 and ATF4 signaling, and the dimerization between Nrf2 and ATF4 should be assessed. With clarification of the relationship between Nrf2 and PERK/ATF4, there may be more supportive evidence for depletion of a key player of hepatic fibrosis – myofibroblasts. Besides, we are also investigating the role of mitochondrial ROS and the relationship

between oxidative stress and ER stress-related pathways in HSCs related with activation. This would result in the linkage of this project to another project investigating TKIs and ENL combinations in cancer in the Alcorn lab, which will lead to a broader understanding of the role of TKIs and ENL in proliferation dysfunction diseases.

Another important mechanism of gefitinib might be through inhibition of phosphorylation of EGFR or other cellular signaling pathways. In the future, the role of EGFR-mediated pathways in the attenuation of HSCs related with activation should be evaluated to identify the major mechanism(s) of the antifibrotic effects of gefitinib and the relationship between the major cellular signaling pathways by using EGFR inhibitor or EGFR siRNA in the cell culture model with treatment with gefitinib and/or ENL. This would involve assessments of changes in the biomarkers of fibrosis and the potential cellular pathways that might be involved. Although the focus was on gefitinib, another goal would be to define more general evidence for potential-PPAR γ -agonist TKIs that can be applied in hepatic fibrosis. More PPAR γ -related TKIs could be screened in liver fibrosis models to gain a better understanding of the repurposing potential of TKIs in liver fibrosis.

Evidence from the Alcorn lab indicates that ENL and ENL glucuronide modulates cholesterol homeostasis. This suggests a greater focus should be placed on the glucuronic acid conjugate of ENL in future *in vitro* evaluations of the potential of ENL to suppress HSC activation and the mechanisms through which ENL-glucuronide may mediate these effects including the role of PPAR γ , oxidative stress, ER stress-induced apoptosis-related pathways. The next step then would be the assessment on the antifibrotic ability and mechanisms of the combination of ENL or its conjugates with gefitinib *in vivo* to preclinically determine the antifibrotic effects and toxicity. Although this study started with the speculation that PPAR γ -related mechanisms are involved in the antifibrotic effects, the complexity of the pathology and the resolution of hepatic fibrosis suggests that other signaling pathways are likely involved in the effects of gefitinib and ENL in hepatic fibrosis. Our results provide an impetus for further study into the therapeutic potential of these compounds alone and in combination for hepatic fibrosis.

In summary, an overall aim will be to generally map out the antifibrotic and anti-proliferative mechanisms of PPAR γ -related TKIs and mammalian lignans in fibroproliferative diseases both *in vitro* and *in vivo*, providing necessary evidence for further drug discovery research for liver disease, especially for hepatic fibrosis.

REFERENCES

1. Lotersztajn, S.; Julien, B.; Teixeira-Clerc, F.; Grenard, P.; Mallat, A., Hepatic fibrosis: molecular mechanisms and drug targets. *Annu Rev Pharmacol Toxicol* **2005**, *45*, 605-28.
2. Bataller, R.; Brenner, D. A., Liver fibrosis. *J Clin Invest* **2005**, *115* (2), 209-218.
3. Rockey, D. C., Antifibrotic therapy in chronic liver disease. *Clin Gastroenterol Hepatol* **2005**, *3* (2), 95-107.
4. Czaja, A. J., Hepatic inflammation and progressive liver fibrosis in chronic liver disease. *World J Gastroenterol* **2014**, *20* (10), 2515-32.
5. Friedman, S. L., Liver fibrosis – from bench to bedside. *J Hepatol* **2003**, *38*, 38-53.
6. Skripinova, S.; Trainer, T. D.; Krawitt, E. L.; Blaszyk, H., Variability of grade and stage in simultaneous paired liver biopsies in patients with hepatitis C. *J Clin Pathol* **2007**, *60* (3), 321-4.
7. Lee, U. E.; Friedman, S. L., Mechanisms of hepatic fibrogenesis. *Best Pract Res Clin Gastroenterol* **2011**, *25* (2), 195-206.
8. Friedman, S. L., Mechanisms of hepatic fibrogenesis. *Gastroenterology* **2008**, *134* (6), 1655-69.
9. Prakash, J.; de Borst, M. H.; van Loenen-Weemaes, A. M.; Lacombe, M.; Opdam, F.; van Goor, H.; Meijer, D. K.; Moolenaar, F.; Poelstra, K.; Kok, R. J., Cell-specific delivery of a transforming growth factor-beta type I receptor kinase inhibitor to proximal tubular cells for the treatment of renal fibrosis. *Pharm Res* **2008**, *25* (10), 2427-39.
10. Wollin, L.; Maillet, I.; Quesniaux, V.; Holweg, A.; Ryffel, B., Antifibrotic and anti-inflammatory activity of the tyrosine kinase inhibitor nintedanib in experimental models of lung fibrosis. *J Pharmacol Exp Ther* **2014**, *349* (2), 209-20.
11. Masso-Valles, D.; Jauset, T.; Serrano, E.; Sodir, N. M.; Pedersen, K.; Affara, N. I.; Whitfield, J. R.; Beaulieu, M. E.; Evan, G. I.; Elias, L.; Arribas, J.; Soucek, L., Ibrutinib exerts potent antifibrotic and antitumor activities in mouse models of pancreatic adenocarcinoma. *Cancer Res* **2015**, *75* (8), 1675-81.
12. Wei, J.; Bhattacharyya, S.; Jain, M.; Varga, J., Regulation of Matrix Remodeling by Peroxisome Proliferator-Activated Receptor-gamma: A Novel Link Between Metabolism and Fibrogenesis. *Open Rheumatol J* **2012**, *6*, 103-15.
13. Mazumder, M.; Ponnann, P.; Das, U.; Gourinath, S.; Khan, H.; Yang, J.; Sakharkar, M. K., Investigations on binding pattern of kinase inhibitors with PPAR γ : Molecular docking, molecular dynamic simulations and free energy calculation studies. *PPAR Res* **2017**, *11*.
14. Sakao, S.; Tatsumi, K., Molecular mechanisms of lung-specific toxicity induced by epidermal growth factor receptor tyrosine kinase inhibitors. *Oncol Lett* **2012**, *4* (5), 865-867.
15. Chen, S. R.; Chen, X. P.; Lu, J. J.; Wang, Y.; Wang, Y. T., Potent natural products and herbal medicines for treating liver fibrosis. *Chin Med* **2015**, *10*, 7.
16. Weiskirchen, R., Hepatoprotective and Anti-fibrotic Agents: It's Time to Take the Next Step. *Front Pharmacol* **2015**, *6*, 303.
17. Zhang, A.; Sun, H.; Wang, X., Recent advances in natural products from plants for treatment of liver diseases. *Eur J Med Chem* **2013**, *63*, 570-7.
18. Meng, X.; Li, S.; Li, Y.; Gan, R. Y.; Li, H. B., Gut Microbiota's Relationship with Liver Disease and Role in Hepatoprotection by Dietary Natural Products and Probiotics. *Nutrients* **2018**, *10* (10).
19. Quang, T. H.; Nguyen, T. T. N.; Minh, C. V.; Van Kiem, P.; Nhiem, N. X.; Tai, B. H.; Thao, N. P.; Bui, T. T. L.; Song, S. B.; Kim, Y. H., Anti-inflammatory and PPAR

- Subtypes Transactivational Activities of Phenolics and Lignans from the Stem Bark of *Kalopanax pictus*. *B Korean Chem Soc* **2011**, *32* (11), 4049-4054.
20. Leong, P. K.; Ko, K. M., Schisandrin B: A Double-Edged Sword in Nonalcoholic Fatty Liver Disease. *Oxid Med Cell Longev* **2016**, *2016*, 6171658.
 21. Turowski, J. B.; Pietrofesa, R. A.; Lawson, J. A.; Christofidou-Solomidou, M.; Hadjiliadis, D., Flaxseed modulates inflammatory and oxidative stress biomarkers in cystic fibrosis: a pilot study. *BMC Complement Altern Med* **2015**, *15*, 148.
 22. Wang, L.; Waltenberger, B.; Pferschy-Wenzig, E. M.; Blunder, M.; Liu, X.; Malainer, C.; Blazevic, T.; Schwaiger, S.; Rollinger, J. M.; Heiss, E. H.; Schuster, D.; Kopp, B.; Bauer, R.; Stuppner, H.; Dirsch, V. M.; Atanasov, A. G., Natural product agonists of peroxisome proliferator-activated receptor gamma (PPARgamma): a review. *Biochem Pharmacol* **2014**, *92* (1), 73-89.
 23. Wang, C. Y.; Liu, Q.; Huang, Q. X.; Liu, J. T.; He, Y. H.; Lu, J. J.; Bai, X. Y., Activation of PPAR gamma is required for hydroxysafflor yellow A of *Carthamus tinctorius* to attenuate hepatic fibrosis induced by oxidative stress. *Phytomedicine* **2013**, *20* (7), 592-599.
 24. Zhang, Z.; Zhao, S.; Yao, Z.; Wang, L.; Shao, J.; Chen, A.; Zhang, F.; Zheng, S., Autophagy regulates turnover of lipid droplets via ROS-dependent Rab25 activation in hepatic stellate cell. *Redox Biol* **2017**, *11*, 322-334.
 25. Dara, L.; Ji, C.; Kaplowitz, N., The contribution of endoplasmic reticulum stress to liver diseases. *Hepatology* **2011**, *53* (5), 1752-63.
 26. De Minicis, S.; Candelaresi, C.; Agostinelli, L.; Taffetani, S.; Saccomanno, S.; Rychlicki, C.; Trozzi, L.; Marzioni, M.; Benedetti, A.; Svegliati-Baroni, G., Endoplasmic Reticulum stress induces hepatic stellate cell apoptosis and contributes to fibrosis resolution. *Liver Int* **2012**, *32* (10), 1574-84.
 27. Di, Y.; Jones, J.; Mansell, K.; Whiting, S.; Fowler, S.; Thorpe, L.; Billinsky, J.; Viveky, N.; Cheng, P. C.; Almousa, A.; Hadjistavropoulos, T.; Alcorn, J., Influence of Flaxseed Lignan Supplementation to Older Adults on Biochemical and Functional Outcome Measures of Inflammation. *J Am Coll Nutr* **2017**, *36* (8), 646-653.
 28. Honigberg, L. A.; Smith, A. M.; Sirisawad, M.; Verner, E.; Loury, D.; Chang, B.; Li, S.; Pan, Z.; Thamm, D. H.; Miller, R. A.; Buggy, J. J., The Bruton tyrosine kinase inhibitor PCI-32765 blocks B-cell activation and is efficacious in models of autoimmune disease and B-cell malignancy. *Proc Natl Acad Sci U S A* **2010**, *107* (29), 13075-80.
 29. Xu, Z. H.; Hang, J. B.; Hu, J. A.; Gao, B. L., Gefitinib, an EGFR tyrosine kinase inhibitor, activates autophagy through AMPK in human lung cancer cells. *J Buon* **2014**, *19* (2), 466-473.
 30. Mittapalli, R. K.; Vaidhyanathan, S.; Dudek, A. Z.; Elmquist, W. F., Mechanisms limiting distribution of the threonine-protein kinase B-RaF(V600E) inhibitor dabrafenib to the brain: implications for the treatment of melanoma brain metastases. *J Pharmacol Exp Ther* **2013**, *344* (3), 655-64.
 31. Wynn, T. A., Common and unique mechanisms regulate fibrosis in various fibroproliferative diseases. *J Clin Invest* **2007**, *117* (3), 524-529.
 32. Pinzani, M., Welcome to fibrogenesis & tissue repair. *Fibrogenesis Tissue Repair* **2008**, *1* (1), 1.
 33. Kochanek, K. D.; Murphy, S. L.; Xu, J.; Tejada-Vera, B., Deaths: Final Data for 2014. *Natl Vital Stat Rep* **2016**, *65* (4), 1-122.
 34. Younossi, Z. M.; Blissett, D.; Blissett, R.; Henry, L.; Stepanova, M.; Younossi, Y.; Racila, A.; Hunt, S.; Beckerman, R., The economic and clinical burden of nonalcoholic fatty liver disease in the United States and Europe. *Hepatology* **2016**, *64* (5), 1577-1586.

35. Zhou, W. C.; Zhang, Q. B.; Qiao, L., Pathogenesis of liver cirrhosis. *World J Gastroenterol* **2014**, *20* (23), 7312-24.
36. Brenner, D. A., Molecular pathogenesis of liver fibrosis. *Trans Am Clin Climatol Assoc* **2009**, *120*, 361-8.
37. Pellicoro, A.; Ramachandran, P.; Iredale, J. P.; Fallowfield, J. A., Liver fibrosis and repair: immune regulation of wound healing in a solid organ. *Nat Rev Immunol* **2014**, *14* (3), 181-94.
38. Nanthakumar, C. B.; Hatley, R. J.; Lemma, S.; Gauldie, J.; Marshall, R. P.; Macdonald, S. J., Dissecting fibrosis: therapeutic insights from the small-molecule toolbox. *Nat Rev Drug Discov* **2015**, *14* (10), 693-720.
39. Hernandez-Gea, V.; Friedman, S. L., Pathogenesis of liver fibrosis. *Annu Rev Pathol* **2011**, *6*, 425-56.
40. Zhubanchaliyev, A.; Temirbekuly, A.; Kongrtay, K.; Wanshura, L. C.; Kunz, J., Targeting Mechanotransduction at the Transcriptional Level: YAP and BRD4 Are Novel Therapeutic Targets for the Reversal of Liver Fibrosis. *Front Pharmacol* **2016**, *7*, 462.
41. Mallat, A.; Lotersztajn, S., Cellular mechanisms of tissue fibrosis. 5. Novel insights into liver fibrosis. *Am J Physiol Cell Physiol* **2013**, *305* (8), C789-99.
42. Thompson, A. I.; Conroy, K. P.; Henderson, N. C., Hepatic stellate cells: central modulators of hepatic carcinogenesis. *BMC Gastroenterol* **2015**, *15*, 63.
43. Reeves, H. L., Activation of hepatic stellate cells - a key issue in liver fibrosis. *Front. Biosci* **2002**, *7* (1-3).
44. Tang, W.; Jiang, Y. F.; Ponnusamy, M.; Diallo, M., Role of Nrf2 in chronic liver disease. *World J Gastroenterol* **2014**, *20* (36), 13079-87.
45. Purohit, V.; Brenner, D. A., Mechanisms of alcohol-induced hepatic fibrosis: a summary of the Ron Thurman Symposium. *Hepatology* **2006**, *43* (4), 872-8.
46. Zhang, C. Y.; Yuan, W. G.; He, P.; Lei, J. H.; Wang, C. X., Liver fibrosis and hepatic stellate cells: Etiology, pathological hallmarks and therapeutic targets. *World J Gastroenterol* **2016**, *22* (48), 10512-10522.
47. Rehermann, B., Pathogenesis of chronic viral hepatitis: differential roles of T cells and NK cells. *Nat Med* **2013**, *19* (7), 859-68.
48. Friedman, S. L., Hepatic fibrosis -- overview. *Toxicology* **2008**, *254* (3), 120-9.
49. Ramachandran, P.; Iredale, J. P., Liver fibrosis: a bidirectional model of fibrogenesis and resolution. *QJM* **2012**, *105* (9), 813-7.
50. Van de Bovenkamp, M.; Groothuis, G. M.; Meijer, D. K.; Olinga, P., Liver fibrosis in vitro: cell culture models and precision-cut liver slices. *Toxicol In Vitro* **2007**, *21* (4), 545-57.
51. Bataller, R.; Brenner, D. A., Hepatic stellate cells as a target for the treatment of liver fibrosis. *Semin Liver Dis* **2001**, *21* (3), 437-451.
52. Bansal, R.; van Baarlen, J.; Storm, G.; Prakash, J., The interplay of the Notch signaling in hepatic stellate cells and macrophages determines the fate of liver fibrogenesis. *Sci Rep* **2015**, *5*, 18272.
53. Friedman, S. L., Hepatic stellate cells: protean, multifunctional, and enigmatic cells of the liver. *Physiol Rev* **2008**, *88* (1), 125-72.
54. Geerts, A., History, heterogeneity, developmental biology, and functions of quiescent hepatic stellate cells. *Semin Liver Dis* **2001**, *21* (3), 311-35.
55. Borthwick, L. A.; Wynn, T. A.; Fisher, A. J., Cytokine mediated tissue fibrosis. *Biochim Biophys Acta* **2013**, *1832* (7), 1049-60.
56. Weiner, F. R.; Shah, A.; Biempica, L.; Zern, M. A.; Czaja, M. J., The effects of hepatic fibrosis on Ito cell gene expression. *Matrix* **1992**, *12* (1), 36-43.

57. Duval, F.; Moreno-Cuevas, J. E.; Gonzalez-Garza, M. T.; Rodriguez-Montalvo, C.; Cruz-Vega, D. E., Liver fibrosis and protection mechanisms action of medicinal plants targeting apoptosis of hepatocytes and hepatic stellate cells. *Adv Pharmacol Sci* **2014**, *2014*, 373295.
58. Knittel, T.; Mehde, M.; Kobold, D.; Saile, B.; Dinter, C.; Ramadori, G., Expression patterns of matrix metalloproteinases and their inhibitors in parenchymal and non-parenchymal cells of rat liver: regulation by TNF-alpha and TGF-beta 1. *J Hepatol* **1999**, *30* (1), 48-60.
59. Lua, I.; Li, Y.; Zagory, J. A.; Wang, K. S.; French, S. W.; Seigny, J.; Asahina, K., Characterization of hepatic stellate cells, portal fibroblasts, and mesothelial cells in normal and fibrotic livers. *J Hepatol* **2016**, *64* (5), 1137-1146.
60. Koyama, Y.; Brenner, D. A., New therapies for hepatic fibrosis. *Clin Res Hepatol Gastroenterol* **2015**, *39 Suppl 1*, S75-9.
61. Guyot, C.; Lepreux, S.; Combe, C.; Doudnikoff, E.; Bioulac-Sage, P.; Balabaud, C.; Desmouliere, A., Hepatic fibrosis and cirrhosis: the (myo)fibroblastic cell subpopulations involved. *Int J Biochem Cell Biol* **2006**, *38* (2), 135-51.
62. Xu, J.; Cong, M.; Park, T. J.; Scholten, D.; Brenner, D. A.; Kisseleva, T., Contribution of bone marrow-derived fibrocytes to liver fibrosis. *Hepatobiliary Surg Nutr* **2015**, *4* (1), 34-47.
63. Nwosu, Z. C.; Alborzinia, H.; Wolfl, S.; Dooley, S.; Liu, Y., Evolving Insights on Metabolism, Autophagy, and Epigenetics in Liver Myofibroblasts. *Front Physiol* **2016**, *7*, 191.
64. Li, H.; You, H.; Fan, X.; Jia, J., Hepatic macrophages in liver fibrosis: pathogenesis and potential therapeutic targets. *BMJ Open Gastroenterol* **2016**, *3* (1), e000079.
65. Henderson, N. C.; Mackinnon, A. C.; Farnworth, S. L.; Poirier, F.; Russo, F. P.; Iredale, J. P.; Haslett, C.; Simpson, K. J.; Sethi, T., Galectin-3 regulates myofibroblast activation and hepatic fibrosis. *Proc Natl Acad Sci U S A* **2006**, *103* (13), 5060-5.
66. Miao, C. G.; Yang, Y. Y.; He, X.; Huang, C.; Huang, Y.; Zhang, L.; Lv, X. W.; Jin, Y.; Li, J., Wnt signaling in liver fibrosis: progress, challenges and potential directions. *Biochimie* **2013**, *95* (12), 2326-35.
67. Jadeja, R. N.; Upadhyay, K. K.; Devkar, R. V.; Khurana, S., Naturally Occurring Nrf2 Activators: Potential in Treatment of Liver Injury. *Oxid Med Cell Longev* **2016**, *2016*, 3453926.
68. Sahani, D. V.; Kalva, S. P., Imaging the liver. *Oncologist* **2004**, *9* (4), 385-97.
69. Shin, S. M.; Yang, J. H.; Ki, S. H., Role of the Nrf2-ARE pathway in liver diseases. *Oxid Med Cell Longev* **2013**, *2013*, 763257.
70. Elpek, G. O., Cellular and molecular mechanisms in the pathogenesis of liver fibrosis: An update. *World J Gastroenterol* **2014**, *20* (23), 7260-76.
71. Malhi, H.; Gores, G. J., Cellular and molecular mechanisms of liver injury. *Gastroenterology* **2008**, *134* (6), 1641-54.
72. Heymann, F.; Tacke, F., Immunology in the liver--from homeostasis to disease. *Nat Rev Gastroenterol Hepatol* **2016**, *13* (2), 88-110.
73. Koyama, Y.; Taura, K.; Hatano, E.; Tanabe, K.; Yamamoto, G.; Nakamura, K.; Yamanaka, K.; Kitamura, K.; Narita, M.; Nagata, H.; Yanagida, A.; Iida, T.; Iwaisako, K.; Fujinawa, H.; Uemoto, S., Effects of oral intake of hydrogen water on liver fibrogenesis in mice. *Hepatol Res* **2014**, *44* (6), 663-677.
74. Foo, N. P.; Lin, S. H.; Lee, Y. H.; Wu, M. J.; Wang, Y. J., alpha-Lipoic acid inhibits liver fibrosis through the attenuation of ROS-triggered signaling in hepatic stellate cells activated by PDGF and TGF-beta. *Toxicology* **2011**, *282* (1-2), 39-46.

75. Akhmetshina, A.; Venalis, P.; Dees, C.; Busch, N.; Zwerina, J.; Schett, G.; Distler, O.; Distler, J. H., Treatment with imatinib prevents fibrosis in different preclinical models of systemic sclerosis and induces regression of established fibrosis. *Arthritis Rheum* **2009**, *60* (1), 219-24.
76. Osna, N. A.; Donohue, T. M.; Kharbanda, K. K., Alcoholic Liver Disease: Pathogenesis and Current Management. *Alcohol Res-Curr Rev* **2017**, *38* (2), 147-161.
77. Friedman, S. L., Molecular mechanisms of hepatic fibrosis and principles of therapy. *J Gastroenterol* **1997**, *32* (3), 424-430.
78. Friedman, S. L.; Sheppard, D.; Duffield, J. S.; Violette, S., Therapy for fibrotic diseases: nearing the starting line. *Science translational medicine* **2013**, *5* (167), 167sr1.
79. Zhang, F.; Lu, Y.; Zheng, S., Peroxisome proliferator-activated receptor-gamma cross-regulation of signaling events implicated in liver fibrogenesis. *Cell Signal* **2012**, *24* (3), 596-605.
80. Friedman, S. L., Evolving challenges in hepatic fibrosis. *Nat Rev Gastroenterol Hepatol* **2010**, *7* (8), 425-36.
81. Kisseleva, T.; Cong, M.; Paik, Y.; Scholten, D.; Jiang, C.; Benner, C.; Iwaisako, K.; Moore-Morris, T.; Scott, B.; Tsukamoto, H.; Evans, S. M.; Dillmann, W.; Glass, C. K.; Brenner, D. A., Myofibroblasts revert to an inactive phenotype during regression of liver fibrosis. *Proc Natl Acad Sci U S A* **2012**, *109* (24), 9448-53.
82. Barcena, C.; Stefanovic, M.; Tutusaus, A.; Joannas, L.; Menendez, A.; Garcia-Ruiz, C.; Sancho-Bru, P.; Marii, M.; Caballeria, J.; Rothlin, C. V.; Fernandez-Checa, J. C.; de Frutos, P. G.; Morales, A., Gas6/Axl pathway is activated in chronic liver disease and its targeting reduces fibrosis via hepatic stellate cell inactivation. *J Hepatol* **2015**, *63* (3), 670-678.
83. Huang, Y.; Li, X.; Wang, Y.; Wang, H.; Huang, C.; Li, J., Endoplasmic reticulum stress-induced hepatic stellate cell apoptosis through calcium-mediated JNK/P38 MAPK and Calpain/Caspase-12 pathways. *Mol Cell Biochem* **2014**, *394* (1-2), 1-12.
84. Lim, M. P.; Devi, L. A.; Rozenfeld, R., Cannabidiol causes activated hepatic stellate cell death through a mechanism of endoplasmic reticulum stress-induced apoptosis. *Cell Death Dis* **2011**, *2*.
85. Tabas, I.; Ron, D., Integrating the mechanisms of apoptosis induced by endoplasmic reticulum stress. *Nat Cell Biol* **2011**, *13* (3), 184-90.
86. Zheng, S. Z.; Chen, A. P., Activation of PPARgamma is required for curcumin to induce apoptosis and to inhibit the expression of extracellular matrix genes in hepatic stellate cells in vitro. *Biochem J* **2004**, *384*, 149-157.
87. Iredale, J. P.; Benyon, R. C.; Pickering, J.; McCullen, M.; Northrop, M.; Pawley, S.; Hovell, C.; Arthur, M. J. P., Mechanisms of spontaneous resolution of rat liver fibrosis - Hepatic stellate cell apoptosis and reduced hepatic expression of metalloproteinase inhibitors. *J Clin Invest* **1998**, *102* (3), 538-549.
88. Massague, J.; Cheifetz, S.; Laiho, M.; Ralph, D. A.; Weis, F. M.; Zentella, A., Transforming growth factor-beta. *Cancer Surv* **1992**, *12*, 81-103.
89. Kajdaniuk, D.; Marek, B.; Borgiel-Marek, H.; Kos-Kudla, B., Transforming growth factor beta1 (TGFbeta1) in physiology and pathology. *Endokrynol Pol* **2013**, *64* (5), 384-96.
90. Bissell, D. M.; Roulot, D.; George, J., Transforming growth factor beta and the liver. *Hepatology* **2001**, *34* (5), 859-67.
91. Chang, X. H.; Zhu, A.; Liu, F. F.; Zou, L. Y.; Su, L.; Liu, S. K.; Zhou, H. H.; Sun, Y. Y.; Han, A. J.; Sun, Y. F.; Li, S.; Li, J.; Sun, Y. B., Nickel oxide nanoparticles induced pulmonary fibrosis via TGF-beta1 activation in rats. *Hum Exp Toxicol* **2016**.

92. Zhang, M.; Cao, S. R.; Zhang, R.; Jin, J. L.; Zhu, Y. F., The inhibitory effect of salvianolic acid B on TGF-beta1-induced proliferation and differentiation in lung fibroblasts. *Exp Lung Res* **2014**, *40* (4), 172-85.
93. Tandon, A.; Tovey, J. C.; Sharma, A.; Gupta, R.; Mohan, R. R., Role of transforming growth factor Beta in corneal function, biology and pathology. *Curr Mol Med* **2010**, *10* (6), 565-78.
94. Andrianifahanana, M.; Wilkes, M. C.; Gupta, S. K.; Rahimi, R. A.; Repellin, C. E.; Edens, M.; Wittenberger, J.; Yin, X.; Maidl, E.; Becker, J.; Leof, E. B., Profibrotic TGFbeta responses require the cooperative action of PDGF and ErbB receptor tyrosine kinases. *FASEB J* **2013**, *27* (11), 4444-54.
95. Meng, X. M.; Nikolic-Paterson, D. J.; Lan, H. Y., TGF-beta: the master regulator of fibrosis. *Nat Rev Nephrol* **2016**, *12* (6), 325-38.
96. Dewidar, B.; Meyer, C.; Dooley, S.; Meindl-Beinker, A. N., TGF-beta in Hepatic Stellate Cell Activation and Liver Fibrogenesis-Updated 2019. *Cells* **2019**, *8* (11).
97. Sun, K.; Wang, Q.; Huang, X. H., PPAR gamma inhibits growth of rat hepatic stellate cells and TGF beta-induced connective tissue growth factor expression. *Acta Pharmacol Sin* **2006**, *27* (6), 715-23.
98. Shah, R.; Reyes-Gordillo, K.; Arellanes-Robledo, J.; Lechuga, C. G.; Hernandez-Nazara, Z.; Cotty, A.; Rojkind, M.; Lakshman, M. R., TGF-beta1 up-regulates the expression of PDGF-beta receptor mRNA and induces a delayed PI3K-, AKT-, and p70(S6K) -dependent proliferative response in activated hepatic stellate cells. *Alcohol Clin Exp Res* **2013**, *37* (11), 1838-48.
99. Qian, J.; Niu, M.; Zhai, X.; Zhou, Q.; Zhou, Y., beta-Catenin pathway is required for TGF-beta1 inhibition of PPARgamma expression in cultured hepatic stellate cells. *Pharmacol Res* **2012**, *66* (3), 219-25.
100. Kim, M. J.; Park, S. A.; Kim, C. H.; Park, S. Y.; Kim, J. S.; Kim, D. K.; Nam, J. S.; Sheen, Y. Y., TGF-beta Type I Receptor Kinase Inhibitor EW-7197 Suppresses Cholestatic Liver Fibrosis by Inhibiting HIF1alpha-Induced Epithelial Mesenchymal Transition. *Cell Physiol Biochem* **2016**, *38* (2), 571-88.
101. Varga, J.; Rosenbloom, J.; Jimenez, S. A., Transforming Growth-Factor-Beta (Tgf-Beta) Causes a Persistent Increase in Steady-State Amounts of Type-I and Type-Iii Collagen and Fibronectin Messenger-Rnas in Normal Human Dermal Fibroblasts. *Biochemical Journal* **1987**, *247* (3), 597-604.
102. Eickelberg, O., Endless healing: TGF-beta, SMADs, and fibrosis. *FEBS Letters* **2001**, *506* (1), 11-4.
103. Gressner, A. M.; Weiskirchen, R.; Breitkopf, K.; Dooley, S., Roles of TGF-beta in hepatic fibrosis. *Front Biosci* **2002**, *7*, d793-807.
104. Bujak, M.; Frangogiannis, N. G., The role of TGF-beta signaling in myocardial infarction and cardiac remodeling. *Cardiovasc Res* **2007**, *74* (2), 184-95.
105. Dooley, S.; Delvoux, B.; Lahme, B.; Mangasser-Stephan, K.; Gressner, A. M., Modulation of transforming growth factor beta response and signaling during transdifferentiation of rat hepatic stellate cells to myofibroblasts. *Hepatology* **2000**, *31* (5), 1094-1106.
106. Cheng, K.; Yang, N.; Mahato, R. I., TGF-beta1 gene silencing for treating liver fibrosis. *Mol Pharm* **2009**, *6* (3), 772-9.
107. Borkham-Kamphorst, E.; Weiskirchen, R., The PDGF system and its antagonists in liver fibrosis. *Cytokine Growth Factor Rev* **2016**, *28*, 53-61.
108. Liu, Y.; Wang, Z.; Kwong, S. Q.; Lui, E. L. H.; Friedman, S. L.; Li, F. R.; Lam, R. W. C.; Zhang, G. C.; Zhang, H.; Ye, T., Inhibition of PDGF, TGF-beta, and Abl

- signaling and reduction of liver fibrosis by the small molecule Bcr-Abl tyrosine kinase antagonist Nilotinib. *J Hepatol* **2011**, *55* (3), 612-625.
109. Beyer, C.; Distler, J. H.; Distler, O., Are tyrosine kinase inhibitors promising for the treatment of systemic sclerosis and other fibrotic diseases? *Swiss Med Wkly* **2010**, *140*, w13050.
110. Wu, J.; Zern, M. A., Hepatic stellate cells: a target for the treatment of liver fibrosis. *J Gastroenterol* **2000**, *35* (9), 665-72.
111. Akhmetshina, A.; Palumbo, K.; Dees, C.; Bergmann, C.; Venalis, P.; Zerr, P.; Horn, A.; Kireva, T.; Beyer, C.; Zwerina, J.; Schneider, H.; Sadowski, A.; Riener, M. O.; MacDougald, O. A.; Distler, O.; Schett, G.; Distler, J. H., Activation of canonical Wnt signalling is required for TGF-beta-mediated fibrosis. *Nat Commun* **2012**, *3*, 735.
112. Verrecchia, F.; Mauviel, A., Transforming growth factor-beta and fibrosis. *World J Gastroenterol* **2007**, *13* (22), 3056-3062.
113. Leask, A., Potential therapeutic targets for cardiac fibrosis: TGFbeta, angiotensin, endothelin, CCN2, and PDGF, partners in fibroblast activation. *Circ Res* **2010**, *106* (11), 1675-80.
114. Poli, G., Pathogenesis of liver fibrosis: role of oxidative stress. *Mol Aspects Med* **2000**, *21* (3), 49-98.
115. Betteridge, D. J., What is oxidative stress? *Metabolism* **2000**, *49* (2 Suppl 1), 3-8.
116. Halliwell, B., Antioxidants and human disease: a general introduction. *Nutr Rev* **1997**, *55* (1 Pt 2), S44-9; discussion S49-52.
117. Dos Santos, J. M.; de Oliveira, D. S.; Moreli, M. L.; Benite-Ribeiro, S. A., The role of mitochondrial DNA damage at skeletal muscle oxidative stress on the development of type 2 diabetes. *Mol Cell Biochem* **2018**, *449* (1-2), 251-255.
118. Valko, M.; Leibfritz, D.; Moncol, J.; Cronin, M. T.; Mazur, M.; Telser, J., Free radicals and antioxidants in normal physiological functions and human disease. *Int J Biochem Cell Biol* **2007**, *39* (1), 44-84.
119. Starkov, A. A., The role of mitochondria in reactive oxygen species metabolism and signaling. *Ann N Y Acad Sci* **2008**, *1147*, 37-52.
120. Finaud, J.; Lac, G.; Filaire, E., Oxidative stress : relationship with exercise and training. *Sports Med* **2006**, *36* (4), 327-58.
121. Cadenas, E., Basic mechanisms of antioxidant activity. *Biofactors* **1997**, *6* (4), 391-7.
122. Filaire, E.; Dupuis, C.; Galvaing, G.; Aubreton, S.; Laurent, H.; Richard, R.; Filaire, M., Lung cancer: What are the links with oxidative stress, physical activity and nutrition. *Lung Cancer* **2013**, *82* (3), 383-389.
123. Pandey, K. B.; Rizvi, S. I., Plant polyphenols as dietary antioxidants in human health and disease. *Oxid Med Cell Longev* **2009**, *2* (5), 270-8.
124. Phull, A. R.; Nasir, B.; Haq, I. U.; Kim, S. J., Oxidative stress, consequences and ROS mediated cellular signaling in rheumatoid arthritis. *Chemico-biological interactions* **2018**, *281*, 121-136.
125. Murphy, M. P., Mitochondrial dysfunction indirectly elevates ROS production by the endoplasmic reticulum. *Cell Metab* **2013**, *18* (2), 145-6.
126. Sanchez-Valle, V.; Chavez-Tapia, N. C.; Uribe, M.; Mendez-Sanchez, N., Role of oxidative stress and molecular changes in liver fibrosis: a review. *Curr Med Chem* **2012**, *19* (28), 4850-60.
127. Zhang, X.; Han, X.; Yin, L.; Xu, L.; Qi, Y.; Xu, Y.; Sun, H.; Lin, Y.; Liu, K.; Peng, J., Potent effects of dioscin against liver fibrosis. *Sci Rep* **2015**, *5*, 9713.
128. Friedman, S. L., Molecular regulation of hepatic fibrosis, an integrated cellular response to tissue injury. *J Biol Chem* **2000**, *275* (4), 2247-50.

129. Gebhardt, R., Oxidative stress, plant-derived antioxidants and liver fibrosis. *Planta Med* **2002**, *68* (4), 289-96.
130. Parola, M.; Robino, G., Oxidative stress-related molecules and liver fibrosis. *J Hepatol* **2001**, *35* (2), 297-306.
131. Ghatak, S.; Biswas, A.; Dhali, G. K.; Chowdhury, A.; Boyer, J. L.; Santra, A., Oxidative stress and hepatic stellate cell activation are key events in arsenic induced liver fibrosis in mice. *Toxicol Appl Pharmacol* **2011**, *251* (1), 59-69.
132. Galli, A.; Svegliati-Baroni, G.; Ceni, E.; Milani, S.; Ridolfi, F.; Salzano, R.; Tarocchi, M.; Grappone, C.; Pellegrini, G.; Benedetti, A.; Surrenti, C.; Casini, A., Oxidative stress stimulates proliferation and invasiveness of hepatic stellate cells via a MMP2-mediated mechanism. *Hepatology* **2005**, *41* (5), 1074-1084.
133. De Bleser, P. J.; Xu, G. X.; Rombouts, K.; Rogiers, V.; Geerts, A., Glutathione levels discriminate between oxidative stress and transforming growth factor-beta signaling in activated rat hepatic stellate cells. *J Biol Chem* **1999**, *274* (48), 33881-33887.
134. Aleksunes, L. M.; Manautou, J. E., Emerging role of Nrf2 in protecting against hepatic and gastrointestinal disease. *Toxicol Pathol* **2007**, *35* (4), 459-73.
135. Digaleh, H.; Kiaei, M.; Khodagholi, F., Nrf2 and Nrf1 signaling and ER stress crosstalk: implication for proteasomal degradation and autophagy. *Cellular and molecular life sciences : CMLS* **2013**, *70* (24), 4681-94.
136. Cuadrado, A.; Manda, G.; Hassan, A.; Alcaraz, M. J.; Barbas, C.; Daiber, A.; Ghezzi, P.; Leon, R.; Lopez, M. G.; Oliva, B.; Pajares, M.; Rojo, A. I.; Robledinos-Anton, N.; Valverde, A. M.; Guney, E.; Schmidt, H. H. H. W., Transcription Factor NRF2 as a Therapeutic Target for Chronic Diseases: A Systems Medicine Approach. *Pharmacol Rev* **2018**, *70* (2), 348-383.
137. Ohtsuji, M.; Katsuoka, F.; Kobayashi, A.; Aburatani, H.; Hayes, J. D.; Yamamoto, M., Nrf1 and Nrf2 play distinct roles in activation of antioxidant response element-dependent genes. *J Biol Chem* **2008**, *283* (48), 33554-62.
138. Chigurupati, S.; Dhanaraj, S. A.; Balakumar, P., A step ahead of PPARgamma full agonists to PPARgamma partial agonists: therapeutic perspectives in the management of diabetic insulin resistance. *Eur J Pharmacol* **2015**, *755*, 50-7.
139. Varga, T.; Czimmerer, Z.; Nagy, L., PPARs are a unique set of fatty acid regulated transcription factors controlling both lipid metabolism and inflammation. *Biochim Biophys Acta* **2011**, *1812* (8), 1007-22.
140. Wilding, J. P., PPAR agonists for the treatment of cardiovascular disease in patients with diabetes. *Diabetes Obes Metab* **2012**, *14* (11), 973-82.
141. Kota, B. P.; Huang, T. H.; Roufogalis, B. D., An overview on biological mechanisms of PPARs. *Pharmacol Res* **2005**, *51* (2), 85-94.
142. Berger, J. P.; Akiyama, T. E.; Meinke, P. T., PPARs: therapeutic targets for metabolic disease. *Trends Pharmacol Sci* **2005**, *26* (5), 244-51.
143. Wahli, W.; Michalik, L., PPARs at the crossroads of lipid signaling and inflammation. *Trends Endocrinol Metab* **2012**, *23* (7), 351-63.
144. Choi, S. S.; Park, J.; Choi, J. H., Revisiting PPAR gamma as a target for the treatment of metabolic disorders. *BMB Rep* **2014**, *47* (11), 599-608.
145. Liu, Y. Y.; Feng, X. Y.; Jia, W. Q.; Jing, Z.; Xu, W. R.; Cheng, X. C., Virtual identification of novel PPARalpha/gamma dual agonists by 3D-QSAR, molecule docking and molecular dynamics studies. *J Biomol Struct Dyn* **2019**, 1-14.
146. Lewis, S. N.; Bassaganya-Riera, J.; Bevan, D. R., Virtual Screening as a Technique for PPAR Modulator Discovery. *PPAR Res* **2010**.

147. Hughes, T. S.; Giri, P. K.; de Vera, I. M.; Marciano, D. P.; Kuruvilla, D. S.; Shin, Y.; Blayo, A. L.; Kamenecka, T. M.; Burris, T. P.; Griffin, P. R.; Kojetin, D. J., An alternate binding site for PPAR γ ligands. *Nat Commun* **2014**, *5*, 3571.
148. Waku, T.; Shiraki, T.; Oyama, T.; Maebara, K.; Nakamori, R.; Morikawa, K., The nuclear receptor PPAR γ individually responds to serotonin- and fatty acid-metabolites. *EMBO J* **2010**, *29* (19), 3395-407.
149. Michalik, L.; Auwerx, J.; Berger, J. P.; Chatterjee, V. K.; Glass, C. K.; Gonzalez, F. J.; Grimaldi, P. A.; Kadowaki, T.; Lazar, M. A.; O'Rahilly, S.; Palmer, C. N.; Plutzky, J.; Reddy, J. K.; Spiegelman, B. M.; Staels, B.; Wahli, W., International Union of Pharmacology. LXI. Peroxisome proliferator-activated receptors. *Pharmacol Rev* **2006**, *58* (4), 726-41.
150. Vasaturo, M.; Fiengo, L.; De Tommasi, N.; Sabatino, L.; Ziccardi, P.; Colantuoni, V.; Bruno, M.; Cerchia, C.; Novellino, E.; Lupo, A.; Lavecchia, A.; Piaz, F. D., A compound-based proteomic approach discloses 15-ketoatractyligenin methyl ester as a new PPAR γ partial agonist with anti-proliferative ability. *Sci Rep* **2017**, *7*, 41273.
151. Moore, J. T.; Collins, J. L.; Pearce, K. H., The nuclear receptor superfamily and drug discovery. *ChemMedChem* **2006**, *1* (5), 504-23.
152. Hughes, T. S.; Chalmers, M. J.; Novick, S.; Kuruvilla, D. S.; Chang, M. R.; Kamenecka, T. M.; Rance, M.; Johnson, B. A.; Burris, T. P.; Griffin, P. R.; Kojetin, D. J., Ligand and receptor dynamics contribute to the mechanism of graded PPAR γ agonism. *Structure* **2012**, *20* (1), 139-50.
153. Guasch, L.; Sala, E.; Valls, C.; Blay, M.; Mulero, M.; Arola, L.; Pujadas, G.; Garcia-Vallve, S., Structural insights for the design of new PPAR γ partial agonists with high binding affinity and low transactivation activity. *J Comput Aided Mol Des* **2011**, *25* (8), 717-28.
154. Einstein, M.; Akiyama, T. E.; Castriota, G. A.; Wang, C. F.; McKeever, B.; Mosley, R. T.; Becker, J. W.; Moller, D. E.; Meinke, P. T.; Wood, H. B.; Berger, J. P., The differential interactions of peroxisome proliferator-activated receptor gamma ligands with Tyr473 is a physical basis for their unique biological activities. *Mol Pharmacol* **2008**, *73* (1), 62-74.
155. Ohashi, M.; Oyama, T.; Miyachi, H., Different structures of the two peroxisome proliferator-activated receptor gamma (PPAR γ) ligand-binding domains in homodimeric complex with partial agonist, but not full agonist. *Bioorg Med Chem Lett* **2015**, *25* (13), 2639-44.
156. Panasyuk, G.; Espeillac, C.; Chauvin, C.; Pradelli, L. A.; Horie, Y.; Suzuki, A.; Annicotte, J. S.; Fajas, L.; Foretz, M.; Verdeguer, F.; Pontoglio, M.; Ferre, P.; Scoazec, J. Y.; Birnbaum, M. J.; Ricci, J. E.; Pende, M., PPAR γ contributes to PKM2 and HK2 expression in fatty liver. *Nat Commun* **2012**, *3*, 672.
157. Lee, N. J.; Oh, J. H.; Ban, J. O.; Shim, J. H.; Lee, H. P.; Jung, J. K.; Ahn, B. W.; Yoon, D. Y.; Han, S. B.; Ham, Y. W.; Hong, J. T., 4-O-methylhonokiol, a PPAR γ agonist, inhibits prostate tumour growth: p21-mediated suppression of NF-kappaB activity. *Br J Pharmacol* **2013**, *168* (5), 1133-45.
158. Zurlo, D.; Ziccardi, P.; Votino, C.; Colangelo, T.; Cerchia, C.; Dal Piaz, F.; Dallavalle, S.; Moricca, S.; Novellino, E.; Lavecchia, A.; Colantuoni, V.; Lupo, A., The antiproliferative and proapoptotic effects of cladospirals A and B are related to their different binding mode as PPAR γ ligands. *Biochem Pharmacol* **2016**, *108*, 22-35.
159. Yi, W.; Shi, J.; Zhao, G.; Zhou, X. E.; Suino-Powell, K.; Melcher, K.; Xu, H. E., Identification of a novel selective PPAR γ ligand with a unique binding mode and improved therapeutic profile in vitro. *Sci Rep* **2017**, *7*, 41487.

160. Zhang, J.; Liu, X.; Wang, S. Q.; Liu, G. Y.; Xu, W. R.; Cheng, X. C.; Wang, R. L., Identification of dual ligands targeting angiotensin II type 1 receptor and peroxisome proliferator-activated receptor-gamma by core hopping of telmisartan. *J Biomol Struct Dyn* **2017**, *35* (12), 2665-2680.
161. Zhang, F.; Kong, D.; Lu, Y.; Zheng, S., Peroxisome proliferator-activated receptor-gamma as a therapeutic target for hepatic fibrosis: from bench to bedside. *Cell Mol Life Sci* **2013**, *70* (2), 259-76.
162. Kelly, D. P., The pleiotropic nature of the vascular PPAR gene regulatory pathway. *Circ Res* **2001**, *89* (11), 935-7.
163. Attia, Y. M.; Elalkamy, E. F.; Hammam, O. A.; Mahmoud, S. S.; El-Khatib, A. S., Telmisartan, an AT1 receptor blocker and a PPAR gamma activator, alleviates liver fibrosis induced experimentally by *Schistosoma mansoni* infection. *Parasit Vectors* **2013**, *6*, 199.
164. Chang, F.; Jaber, L. A.; Berlie, H. D.; O'Connell, M. B., Evolution of peroxisome proliferator-activated receptor agonists. *Ann Pharmacother* **2007**, *41* (6), 973-83.
165. Zhang, J.; Liu, X.; Xie, X. B.; Cheng, X. C.; Wang, R. L., Multitargeted bioactive ligands for PPARs discovered in the last decade. *Chem Biol Drug Des* **2016**, *88* (5), 635-663.
166. Feldman, P. L.; Lambert, M. H.; Henke, B. R., PPAR modulators and PPAR pan agonists for metabolic diseases: the next generation of drugs targeting peroxisome proliferator-activated receptors? *Curr Top Med Chem* **2008**, *8* (9), 728-49.
167. Liu, X.; Lian, J.; Hu, C. H.; Deng, C., Betahistine co-treatment ameliorates dyslipidemia induced by chronic olanzapine treatment in rats through modulation of hepatic AMPKalpha-SREBP-1 and PPARalpha-dependent pathways. *Pharmacol Res* **2015**, *100*, 36-46.
168. Papi, A.; De Carolis, S.; Bertoni, S.; Storci, G.; Sceberas, V.; Santini, D.; Ceccarelli, C.; Taffurelli, M.; Orlandi, M.; Bonafe, M., PPARgamma and RXR ligands disrupt the inflammatory cross-talk in the hypoxic breast cancer stem cells niche. *J Cell Physiol* **2014**, *229* (11), 1595-606.
169. Bays, H.; Stein, E. A., Pharmacotherapy for dyslipidaemia--current therapies and future agents. *Expert Opin Pharmacother* **2003**, *4* (11), 1901-38.
170. Ebdrup, S.; Pettersson, I.; Rasmussen, H. B.; Deussen, H. J.; Frost Jensen, A.; Mortensen, S. B.; Fleckner, J.; Pridal, L.; Nygaard, L.; Sauerberg, P., Synthesis and biological and structural characterization of the dual-acting peroxisome proliferator-activated receptor alpha/gamma agonist ragaglitazar. *J Med Chem* **2003**, *46* (8), 1306-17.
171. Chevalier, S.; Roberts, R. A., Perturbation of rodent hepatocyte growth control by nongenotoxic hepatocarcinogens: mechanisms and lack of relevance for human health (review). *Oncol Rep* **1998**, *5* (6), 1319-27.
172. Dong, Z.; Su, L.; Esmaili, S.; Iseli, T. J.; Ramezani-Moghadam, M.; Hu, L.; Xu, A.; George, J.; Wang, J., Adiponectin attenuates liver fibrosis by inducing nitric oxide production of hepatic stellate cells. *J Mol Med (Berl)* **2015**, *93* (12), 1327-39.
173. Kostadinova, R.; Montagner, A.; Gouranton, E.; Fleury, S.; Guillou, H.; Dombrowicz, D.; Desreumaux, P.; Wahli, W., GW501516-activated PPARbeta/delta promotes liver fibrosis via p38-JNK MAPK-induced hepatic stellate cell proliferation. *Cell & bioscience* **2012**, *2* (1), 34.
174. Van der Veen, J. N.; Lingrell, S.; Gao, X.; Quiroga, A. D.; Takawale, A.; Armstrong, E. A.; Yager, J. Y.; Kassiri, Z.; Lehner, R.; Vance, D. E.; Jacobs, R. L., Pioglitazone attenuates hepatic inflammation and fibrosis in phosphatidylethanolamine N-methyltransferase-deficient mice. *Am J Physiol Gastrointest Liver Physiol* **2016**, *310* (7), G526-38.
175. Wang, L. H.; Yang, X. Y.; Zhang, X.; Huang, J.; Hou, J.; Li, J.; Xiong, H.; Mihalic, K.; Zhu, H.; Xiao, W.; Farrar, W. L., Transcriptional inactivation of STAT3 by

- PPARgamma suppresses IL-6-responsive multiple myeloma cells. *Immunity* **2004**, *20* (2), 205-18.
176. Ohashi, M.; Gamo, K.; Tanaka, Y.; Waki, M.; Beniyama, Y.; Matsuno, K.; Wada, J.; Tenta, M.; Eguchi, J.; Makishima, M.; Matsuura, N.; Oyama, T.; Miyachi, H., Structural design and synthesis of arylalkynyl amide-type peroxisome proliferator-activated receptor gamma (PPARgamma)-selective antagonists based on the helix12-folding inhibition hypothesis. *Eur J Med Chem* **2015**, *90*, 53-67.
177. Burgermeister, E.; Schnoebelen, A.; Flament, A.; Benz, J.; Stihle, M.; Gsell, B.; Rufer, A.; Ruf, A.; Kuhn, B.; Marki, H. P.; Mizrahi, J.; Sebkova, E.; Niesor, E.; Meyer, M., A novel partial agonist of peroxisome proliferator-activated receptor-gamma (PPARgamma) recruits PPARgamma-coactivator-1alpha, prevents triglyceride accumulation, and potentiates insulin signaling in vitro. *Mol Endocrinol* **2006**, *20* (4), 809-30.
178. Hsu, W. H.; Lee, B. H.; Hsu, Y. W.; Pan, T. M., Peroxisome proliferator-activated receptor-gamma activators monascin and rosiglitazone attenuate carboxymethyllysine-induced fibrosis in hepatic stellate cells through regulating the oxidative stress pathway but independent of the receptor for advanced glycation end products signaling. *J Agric Food Chem* **2013**, *61* (28), 6873-9.
179. Bilik, D.; McEwen, L. N.; Brown, M. B.; Selby, J. V.; Karter, A. J.; Marrero, D. G.; Hsiao, V. C.; Tseng, C. W.; Mangione, C. M.; Lasser, N. L.; Crosson, J. C.; Herman, W. H., Thiazolidinediones, cardiovascular disease and cardiovascular mortality: translating research into action for diabetes (TRIAD). *Pharmacoepidemiol Drug Saf.* **2010**, *19* (7), 715-21.
180. Nissen, S. E., The rise and fall of rosiglitazone. *Eur Heart J* **2010**, *31* (7), 773-6.
181. Yoshida, H.; Tshuhako, R.; Atsumi, T.; Narumi, K.; Watanabe, W.; Sugita, C.; Kurokawa, M., Naringenin interferes with the anti-diabetic actions of pioglitazone via pharmacodynamic interactions. *J Nat Med* **2016**.
182. Ohashi, M.; Gamo, K.; Oyama, T.; Miyachi, H., Peroxisome proliferator-activated receptor gamma (PPARgamma) has multiple binding points that accommodate ligands in various conformations: Structurally similar PPARgamma partial agonists bind to PPARgamma LBD in different conformations. *Bioorg Med Chem Lett* **2015**, *25* (14), 2758-62.
183. Milton, F. A.; Cvorovic, A.; Amato, A. A.; Sieglaff, D. H.; Filgueira, C. S.; Arumanayagam, A. S.; de Lima Mdo, C.; Pitta, I. R.; de Assis Rocha Neves, F.; Webb, P., PPARgamma partial agonist GQ-16 strongly represses a subset of genes in 3T3-L1 adipocytes. *Biochem Biophys Res Commun* **2015**, *464* (3), 718-23.
184. Choi, J. H.; Banks, A. S.; Kamenecka, T. M.; Busby, S. A.; Chalmers, M. J.; Kumar, N.; Kuruvilla, D. S.; Shin, Y.; He, Y.; Bruning, J. B.; Marciano, D. P.; Cameron, M. D.; Laznik, D.; Jurczak, M. J.; Schurer, S. C.; Vidovic, D.; Shulman, G. I.; Spiegelman, B. M.; Griffin, P. R., Antidiabetic actions of a non-agonist PPARgamma ligand blocking Cdk5-mediated phosphorylation. *Nature* **2011**, *477* (7365), 477-81.
185. Montanari, R.; Saccoccia, F.; Scotti, E.; Crestani, M.; Godio, C.; Gilardi, F.; Loiodice, F.; Fracchiolla, G.; Laghezza, A.; Tortorella, P.; Lavecchia, A.; Novellino, E.; Mazza, F.; Aschi, M.; Pochetti, G., Crystal Structure of the Peroxisome Proliferator-Activated Receptor gamma (PPAR gamma) Ligand Binding Domain Complexed with a Novel Partial Agonist: A New Region of the Hydrophobic Pocket Could Be Exploited for Drug Design. *J Med Chem* **2008**, *51* (24), 7768-7776.
186. Guasch, L.; Sala, E.; Castell-Auvi, A.; Cedo, L.; Liedl, K. R.; Wolber, G.; Muehlbacher, M.; Mulero, M.; Pinent, M.; Ardevol, A.; Valls, C.; Pujadas, G.; Garcia-Vallve, S., Identification of PPARgamma partial agonists of natural origin (I): development of a virtual screening procedure and in vitro validation. *PLoS One* **2012**, *7* (11), e50816.

187. Lakatos, H. F.; Thatcher, T. H.; Kottmann, R. M.; Garcia, T. M.; Phipps, R. P.; Sime, P. J., The Role of PPARs in Lung Fibrosis. *PPAR Res* **2007**, *2007*, 71323.
188. Zheng, S.; Chen, A., Disruption of transforming growth factor-beta signaling by curcumin induces gene expression of peroxisome proliferator-activated receptor-gamma in rat hepatic stellate cells. *Am J Physiol Gastrointest Liver Physiol* **2007**, *292* (1), G113-23.
189. Ghosh, A. K.; Wei, J.; Wu, M.; Varga, J., Constitutive Smad signaling and Smad-dependent collagen gene expression in mouse embryonic fibroblasts lacking peroxisome proliferator-activated receptor-gamma. *Biochem Biophys Res Commun* **2008**, *374* (2), 231-6.
190. Israelsen, W. J.; Vander Heiden, M. G., Pyruvate kinase: Function, regulation and role in cancer. *Semin Cell Dev Biol* **2015**, *43*, 43-51.
191. Gupta, V.; Bamezai, R. N., Human pyruvate kinase M2: a multifunctional protein. *Protein Sci* **2010**, *19* (11), 2031-44.
192. Spoden, G. A.; Rostek, U.; Lechner, S.; Mitterberger, M.; Mazurek, S.; Zwerschke, W., Pyruvate kinase isoenzyme M2 is a glycolytic sensor differentially regulating cell proliferation, cell size and apoptotic cell death dependent on glucose supply. *Exp Cell Res* **2009**, *315* (16), 2765-74.
193. Dong, G.; Mao, Q.; Xia, W.; Xu, Y.; Wang, J.; Xu, L.; Jiang, F., PKM2 and cancer: The function of PKM2 beyond glycolysis. *Oncol Lett* **2016**, *11* (3), 1980-1986.
194. Chiavarina, B.; Whitaker-Menezes, D.; Martinez-Outschoorn, U. E.; Witkiewicz, A. K.; Birbe, R.; Howell, A.; Pestell, R. G.; Smith, J.; Daniel, R.; Sotgia, F.; Lisanti, M. P., Pyruvate kinase expression (PKM1 and PKM2) in cancer-associated fibroblasts drives stromal nutrient production and tumor growth. *Cancer Biol Ther* **2011**, *12* (12), 1101-13.
195. Wang, X. L.; Jia, D. W.; Liu, H. Y.; Yan, X. F.; Ye, T. J.; Hu, X. D.; Li, B. Q.; Chen, Y. L.; Liu, P., Effect of Yiguanjian decoction on cell differentiation and proliferation in CCl₄-treated mice. *World J Gastroenterol* **2012**, *18* (25), 3235-49.
196. Nault, R.; Fader, K. A.; Kirby, M. P.; Ahmed, S.; Matthews, J.; Jones, A. D.; Lunt, S. Y.; Zacharewski, T. R., Pyruvate Kinase Isoform Switching and Hepatic Metabolic Reprogramming by the Environmental Contaminant 2,3,7,8-Tetrachlorodibenzo-p-Dioxin. *Toxicol Sci* **2016**, *149* (2), 358-71.
197. Yang, W.; Lu, Z., Pyruvate kinase M2 at a glance. *J. Cell. Sci.* **2015**, *128* (9), 1655-1660.
198. Oakley, F.; Meso, M.; Iredale, J. P.; Green, K.; Marek, C. J.; Zhou, X.; May, M. J.; Millward-Sadler, H.; Wright, M. C.; Mann, D. A., Inhibition of inhibitor of kappaB kinases stimulates hepatic stellate cell apoptosis and accelerated recovery from rat liver fibrosis. *Gastroenterology* **2005**, *128* (1), 108-20.
199. Oakley, F.; Teoh, V.; Ching, A. S. G.; Bataller, R.; Colmenero, J.; Jonsson, J. R.; Eliopoulos, A. G.; Watson, M. R.; Manas, D.; Mann, D. A., Angiotensin II activates I kappaB kinase phosphorylation of RelA at Ser 536 to promote myofibroblast survival and liver fibrosis. *Gastroenterology* **2009**, *136* (7), 2334-2344 e1.
200. Gehrke, N.; Worns, M. A.; Mann, A.; Huber, Y.; Hoefelmeyer, N.; Longrich, T.; Waisman, A.; Galle, P. R.; Schattenberg, J. M., Hepatic B cell leukemia-3 suppresses chemically-induced hepatocarcinogenesis in mice through altered MAPK and NF-kappaB activation. *Oncotarget* **2016**.
201. Xiao, C.; Ghosh, S., NF-kappaB, an evolutionarily conserved mediator of immune and inflammatory responses. *Adv Exp Med Biol* **2005**, *560*, 41-5.
202. Shu, M.; Huang, D. D.; Hung, Z. A.; Hu, X. R.; Zhang, S., Inhibition of MAPK and NF-kappaB signaling pathways alleviate carbon tetrachloride (CCl₄)-induced liver fibrosis in Toll-like receptor 5 (TLR5) deficiency mice. *Biochem Biophys Res Commun* **2016**, *471* (1), 233-9.

203. Xu, P.; Zhang, Y.; Liu, Y.; Yuan, Q.; Song, L.; Liu, M.; Liu, Z.; Yang, Y.; Li, J.; Li, D.; Ren, G., Fibroblast growth factor 21 attenuates hepatic fibrogenesis through TGF-beta/smad2/3 and NF-kappaB signaling pathways. *Toxicol Appl Pharmacol* **2016**, *290*, 43-53.
204. Zhang, F.; Sodroski, C.; Cha, H.; Li, Q.; Liang, T. J., Infection of Hepatocytes With HCV Increases Cell Surface Levels of Heparan Sulfate Proteoglycans, Uptake of Cholesterol and Lipoprotein, and Virus Entry by Up-regulating SMAD6 and SMAD7. *Gastroenterology* **2017**, *152* (1), 257-270 e7.
205. Bai, T.; Lian, L. H.; Wu, Y. L.; Wan, Y.; Nan, J. X., Thymoquinone attenuates liver fibrosis via PI3K and TLR4 signaling pathways in activated hepatic stellate cells. *Int Immunopharmacol* **2013**, *15* (2), 275-81.
206. Hong, S. Y.; Yu, F. X.; Luo, Y.; Hagen, T., Oncogenic activation of the PI3K/Akt pathway promotes cellular glucose uptake by downregulating the expression of thioredoxin-interacting protein. *Cell Signal* **2016**, *28* (5), 377-83.
207. Reif, S.; Lang, A.; Lindquist, J. N.; Yata, Y.; Gabele, E.; Scanga, A.; Brenner, D. A.; Rippe, R. A., The role of focal adhesion kinase-phosphatidylinositol 3-kinase-akt signaling in hepatic stellate cell proliferation and type I collagen expression. *J Biol Chem* **2003**, *278* (10), 8083-90.
208. Son, M. K.; Ryu, Y. L.; Jung, K. H.; Lee, H.; Lee, H. S.; Yan, H. H.; Park, H. J.; Ryu, J. K.; Suh, J. K.; Hong, S.; Hong, S. S., HS-173, a novel PI3K inhibitor, attenuates the activation of hepatic stellate cells in liver fibrosis. *Sci Rep* **2013**, *3*, 3470.
209. Fang, L.; Zhan, S.; Huang, C.; Cheng, X.; Lv, X.; Si, H.; Li, J., TRPM7 channel regulates PDGF-BB-induced proliferation of hepatic stellate cells via PI3K and ERK pathways. *Toxicol Appl Pharmacol* **2013**, *272* (3), 713-25.
210. Kim, J. E.; Chen, J., Regulation of peroxisome proliferator-activated receptor-gamma activity by mammalian target of rapamycin and amino acids in adipogenesis. *Diabetes* **2004**, *53* (11), 2748-56.
211. Cnop, M.; Foufelle, F.; Velloso, L. A., Endoplasmic reticulum stress, obesity and diabetes. *Trends Mol Med* **2012**, *18* (1), 59-68.
212. Romero, Y.; Bueno, M.; Ramirez, R.; Alvarez, D.; Sembrat, J. C.; Goncharova, E. A.; Rojas, M.; Selman, M.; Mora, A. L.; Pardo, A., mTORC1 activation decreases autophagy in aging and idiopathic pulmonary fibrosis and contributes to apoptosis resistance in IPF fibroblasts. *Aging Cell* **2016**, *15*, pp1103-1112.
213. Tapia-Abellan, A.; Ruiz-Alcaraz, A. J.; Anton, G.; Miras-Lopez, M.; Frances, R.; Such, J.; Martinez-Esparza, M.; Garcia-Penarrubia, P., Regulatory role of PI3K-protein kinase B on the release of interleukin-1beta in peritoneal macrophages from the ascites of cirrhotic patients. *Clin Exp Immunol* **2014**, *178* (3), 525-36.
214. Planaguma, A.; Claria, J.; Miquel, R.; Lopez-Parra, M.; Titos, E.; Masferrer, J. L.; Arroyo, V.; Rodes, J., The selective cyclooxygenase-2 inhibitor SC-236 reduces liver fibrosis by mechanisms involving non-parenchymal cell apoptosis and PPARgamma activation. *FASEB J* **2005**, *19* (9), 1120-2.
215. Galli, A.; Crabb, D. W.; Ceni, E.; Salzano, R.; Mello, T.; Svegliati-Baroni, G.; Ridolfi, F.; Trozzi, L.; Surrenti, C.; Casini, A., Antidiabetic thiazolidinediones inhibit collagen synthesis and hepatic stellate cell activation in vivo and in vitro. *Gastroenterology* **2002**, *122* (7), 1924-1940.
216. Sano, R.; Reed, J. C., ER stress-induced cell death mechanisms. *Biochimica et Biophysica Acta* **2013**, *1833* (12), 3460-70.
217. Boyce, M.; Yuan, J., Cellular response to endoplasmic reticulum stress: a matter of life or death. *Cell Death Differ* **2006**, *13* (3), 363-73.

218. Kaufman, R. J., Stress signaling from the lumen of the endoplasmic reticulum: coordination of gene transcriptional and translational controls. *Genes Dev* **1999**, *13* (10), 1211-33.
219. Zhang, K., Integration of ER stress, oxidative stress and the inflammatory response in health and disease. *Int J Clin Exp Med* **2010**, *3* (1), 33-40.
220. Schroder, M.; Kaufman, R. J., ER stress and the unfolded protein response. *Mutat Res* **2005**, *569* (1-2), 29-63.
221. Haze, K.; Yoshida, H.; Yanagi, H.; Yura, T.; Mori, K., Mammalian transcription factor ATF6 is synthesized as a transmembrane protein and activated by proteolysis in response to endoplasmic reticulum stress. *Mol Biol Cell* **1999**, *10* (11), 3787-99.
222. Sovolyova, N.; Healy, S.; Samali, A.; Logue, S. E., Stressed to death - mechanisms of ER stress-induced cell death. *Biol Chem* **2014**, *395* (1), 1-13.
223. Lee, A. H.; Iwakoshi, N. N.; Glimcher, L. H., XBP-1 regulates a subset of endoplasmic reticulum resident chaperone genes in the unfolded protein response. *Mol Cell Biol* **2003**, *23* (21), 7448-59.
224. Szegezdi, E.; Herbert, K. R.; Kavanagh, E. T.; Samali, A.; Gorman, A. M., Nerve growth factor blocks thapsigargin-induced apoptosis at the level of the mitochondrion via regulation of Bim. *J Cell Mol Med* **2008**, *12* (6A), 2482-96.
225. Gupta, S.; Cuffe, L.; Szegezdi, E.; Logue, S. E.; Neary, C.; Healy, S.; Samali, A., Mechanisms of ER Stress-Mediated Mitochondrial Membrane Permeabilization. *Int J Cell Biol* **2010**, *2010*, 170215.
226. Feng, B.; Yao, P. M.; Li, Y. K.; Devlin, C. M.; Zhang, D. J.; Harding, H. P.; Sweeney, M.; Rong, J. X.; Kuriakose, G.; Fisher, E. A.; Marks, A. R.; Ron, D.; Tabas, I., The endoplasmic reticulum is the site of cholesterol-induced cytotoxicity in macrophages. *Nature Cell Biology* **2003**, *5* (9), 781-792.
227. Szegezdi, E.; Duffy, A.; O'Mahoney, M. E.; Logue, S. E.; Mylotte, L. A.; O'Brien, T.; Samali, A., ER stress contributes to ischemia-induced cardiomyocyte apoptosis. *Biochem Biophys Res Commun* **2006**, *349* (4), 1406-11.
228. Gong, J.; Wang, X. Z.; Wang, T.; Chen, J. J.; Xie, X. Y.; Hu, H.; Yu, F.; Liu, H. L.; Jiang, X. Y.; Fan, H. D., Molecular signal networks and regulating mechanisms of the unfolded protein response. *J Zhejiang Univ Sci B* **2017**, *18* (1), 1-14.
229. Healy, S. J.; Gorman, A. M.; Mousavi-Shafaei, P.; Gupta, S.; Samali, A., Targeting the endoplasmic reticulum-stress response as an anticancer strategy. *Eur J Pharmacol* **2009**, *625* (1-3), 234-46.
230. Rojo de la Vega, M.; Chapman, E.; Zhang, D. D., NRF2 and the Hallmarks of Cancer. *Cancer Cell* **2018**, *34* (1), 21-43.
231. Ge, W. S.; Wang, Y. J.; Wu, J. X.; Fan, J. G.; Chen, Y. W.; Zhu, L., beta-catenin is overexpressed in hepatic fibrosis and blockage of Wnt/beta-catenin signaling inhibits hepatic stellate cell activation. *Mol Med Rep* **2014**, *9* (6), 2145-51.
232. Clevers, H.; Nusse, R., Wnt/beta-catenin signaling and disease. *Cell* **2012**, *149* (6), 1192-205.
233. Niehrs, C., The complex world of WNT receptor signalling. *Nat Rev Mol Cell Biol* **2012**, *13* (12), 767-79.
234. Kahn, M., Can we safely target the WNT pathway? *Nat Rev Drug Discov* **2014**, *13* (7), 513-32.
235. De, A., Wnt/Ca²⁺ signaling pathway: a brief overview. *Acta Biochim Biophys Sin (Shanghai)* **2011**, *43* (10), 745-56.
236. Myung, S. J.; Yoon, J. H.; Gwak, G. Y.; Kim, W.; Lee, J. H.; Kim, K. M.; Shin, C. S.; Jang, J. J.; Lee, S. H.; Lee, S. M.; Lee, H. S., Wnt signaling enhances the activation and survival of human hepatic stellate cells. *FEBS Lett* **2007**, *581* (16), 2954-8.

237. Xiong, W. J.; Hu, L. J.; Jian, Y. C.; Wang, L. J.; Jiang, M.; Li, W.; He, Y., Wnt5a participates in hepatic stellate cell activation observed by gene expression profile and functional assays. *World J Gastroenterol* **2012**, *18* (15), 1745-52.
238. Zhu, N. L.; Wang, J.; Tsukamoto, H., The Necdin-Wnt pathway causes epigenetic peroxisome proliferator-activated receptor gamma repression in hepatic stellate cells. *J Biol Chem* **2010**, *285* (40), 30463-71.
239. Sheng, R.; Kim, H.; Lee, H.; Xin, Y.; Chen, Y.; Tian, W.; Cui, Y.; Choi, J. C.; Doh, J.; Han, J. K.; Cho, W., Cholesterol selectively activates canonical Wnt signalling over non-canonical Wnt signalling. *Nat Commun* **2014**, *5*, 4393.
240. Li, W.; Zhu, C.; Chen, X.; Li, Y.; Gao, R.; Wu, Q., Pokeweed antiviral protein down-regulates Wnt/beta-catenin signalling to attenuate liver fibrogenesis in vitro and in vivo. *Dig Liver Dis* **2011**, *43* (7), 559-66.
241. Subramaniam, N.; Sherman, M. H.; Rao, R.; Wilson, C.; Coulter, S.; Atkins, A. R.; Evans, R. M.; Liddle, C.; Downes, M., Metformin-Mediated Bambi Expression in Hepatic Stellate Cells Induces Prosurvival Wnt/beta-Catenin Signaling. *Cancer Prev Res* **2012**, *5* (4), 553-561.
242. van der Meer, J. H.; van der Poll, T.; van 't Veer, C., TAM receptors, Gas6, and protein S: roles in inflammation and hemostasis. *Blood* **2014**, *123* (16), 2460-9.
243. Mann, D. A.; Marra, F., Fibrogenic signalling in hepatic stellate cells. *J Hepatol* **2010**, *52* (6), 949-50.
244. Fallowfield, J. A., Therapeutic targets in liver fibrosis. *Am J Physiol Gastrointest Liver Physiol* **2011**, *300* (5), G709-15.
245. Popov, Y.; Schuppan, D., Targeting liver fibrosis: strategies for development and validation of antifibrotic therapies. *Hepatology* **2009**, *50* (4), 1294-306.
246. Wang, Y.; Zhang, X.; Yang, Y.; Yang, X.; Ye, B., Study on the Antifibrotic Effects of Recombinant Shark Hepatical Stimulator Analogue (r-sHSA) in Vitro and in Vivo. *Mar Drugs* **2015**, *13* (8), 5201-18.
247. Cales, P.; Boursier, J.; Chaigneau, J.; Oberti, F.; Rousselet, M. C., Treatment of liver fibrosis: clinical aspects. *Gastroenterol Clin Biol* **2009**, *33* (10-11), 958-66.
248. Crespo Yanguas, S.; Cogliati, B.; Willebrords, J.; Maes, M.; Colle, I.; van den Bossche, B.; de Oliveira, C. P.; Andraus, W.; Alves, V. A.; Leclercq, I.; Vinken, M., Experimental models of liver fibrosis. *Arch Toxicol* **2016**, *90* (5), 1025-48.
249. Blachier, M.; Leleu, H.; Peck-Radosavljevic, M.; Valla, D. C.; Roudot-Thoraval, F., The burden of liver disease in Europe: a review of available epidemiological data. *J Hepatol* **2013**, *58* (3), 593-608.
250. Gaça, M. D. A.; Zhou, X.; Issa, R.; Kiriella, K.; Iredale, J. P.; Benyon, R. C., Basement membrane-like matrix inhibits proliferation and collagen synthesis by activated rat hepatic stellate cells: evidence for matrix-dependent deactivation of stellate cells. *Matrix Biol* **2003**, *22* (3), 229-239.
251. Friedman, S. L.; Yamasaki, G.; Wong, L., Modulation of transforming growth factor beta receptors of rat lipocytes during the hepatic wound healing response. Enhanced binding and reduced gene expression accompany cellular activation in culture and in vivo. *J Biol Chem* **1994**, *269* (14), 10551-8.
252. Shang, L.; Hosseini, M.; Liu, X.; Kisseleva, T.; Brenner, D. A., Human hepatic stellate cell isolation and characterization. *J Gastroenterol* **2018**, *53* (1), 6-17.
253. Xu, L.; Hui, A. Y.; Albanis, E.; Arthur, M. J.; O'Byrne, S. M.; Blaner, W. S.; Mukherjee, P.; Friedman, S. L.; Eng, F. J., Human hepatic stellate cell lines, LX-1 and LX-2: new tools for analysis of hepatic fibrosis. *Gut* **2005**, *54* (1), 142-51.

254. Weiskirchen, R.; Weimer, J.; Meurer, S. K.; Kron, A.; Seipel, B.; Vater, I.; Arnold, N.; Siebert, R.; Xu, L.; Friedman, S. L.; Bergmann, C., Genetic characteristics of the human hepatic stellate cell line LX-2. *PLoS One* **2013**, *8* (10), e75692.
255. Meurer, S. K.; Tihaa, L.; Borkham-Kamphorst, E.; Weiskirchen, R., Expression and functional analysis of endoglin in isolated liver cells and its involvement in fibrogenic Smad signalling. *Cell Signal* **2011**, *23* (4), 683-699.
256. He, H.; Mennone, A.; Boyer, J. L.; Cai, S. Y., Combination of retinoic acid and ursodeoxycholic acid attenuates liver injury in bile duct-ligated rats and human hepatic cells. *Hepatology* **2011**, *53* (2), 548-57.
257. Melgar-Lesmes, P.; Casals, G.; Pauta, M.; Ros, J.; Reichenbach, V.; Bataller, R.; Morales-Ruiz, M.; Jimenez, W., Apelin mediates the induction of profibrogenic genes in human hepatic stellate cells. *Endocrinology* **2010**, *151* (11), 5306-14.
258. Shi, Y. F.; Fong, C. C.; Zhang, Q.; Cheung, P. Y.; Tzang, C. H.; Wu, R. S.; Yang, M., Hypoxia induces the activation of human hepatic stellate cells LX-2 through TGF-beta signaling pathway. *FEBS Lett* **2007**, *581* (2), 203-10.
259. Herrmann, J.; Gressner, A. M.; Weiskirchen, R., Immortal hepatic stellate cell lines: useful tools to study hepatic stellate cell biology and function? *J Cell Mol Med* **2007**, *11* (4), 704-22.
260. Schon, H. T.; Bartneck, M.; Borkham-Kamphorst, E.; Nattermann, J.; Lammers, T.; Tacke, F.; Weiskirchen, R., Pharmacological Intervention in Hepatic Stellate Cell Activation and Hepatic Fibrosis. *Front Pharmacol* **2016**, *7*, 33.
261. Fourcot, A.; Couchie, D.; Chobert, M. N.; Zafrani, E. S.; Mavier, P.; Laperche, Y.; Brouillet, A., Gas6 deficiency prevents liver inflammation, steatohepatitis, and fibrosis in mice. *Am J Physiol Gastrointest Liver Physiol* **2011**, *300* (6), G1043-53.
262. George, J.; Pera, N.; Phung, N.; Leclercq, I.; Yun Hou, J.; Farrell, G., Lipid peroxidation, stellate cell activation and hepatic fibrogenesis in a rat model of chronic steatohepatitis. *J Hepatol* **2003**, *39* (5), 756-64.
263. Krause, P.; Saghatolislam, F.; Koenig, S.; Unthan-Fechner, K.; Probst, I., Maintaining hepatocyte differentiation in vitro through co-culture with hepatic stellate cells. *In Vitro Cell Dev-An* **2009**, *45* (5-6), 205-212.
264. Giraudi, P. J.; Becerra, V. J.; Marin, V.; Chavez-Tapia, N. C.; Tiribelli, C.; Rosso, N., The importance of the interaction between hepatocyte and hepatic stellate cells in fibrogenesis induced by fatty accumulation. *Exp Mol Pathol* **2015**, *98* (1), 85-92.
265. Chen, W.; Wu, J.; Shi, H.; Wang, Z.; Zhang, G.; Cao, Y.; Jiang, C.; Ding, Y., Hepatic stellate cell coculture enables sorafenib resistance in Huh7 cells through HGF/c-Met/Akt and Jak2/Stat3 pathways. *Biomed Res Int* **2014**, *2014*, 764981.
266. Alabraba, E. B.; Lai, V.; Boon, L.; Wigmore, S. J.; Adams, D. H.; Afford, S. C., Coculture of human liver macrophages and cholangiocytes leads to CD40-dependent apoptosis and cytokine secretion. *Hepatology* **2008**, *47* (2), 552-62.
267. Nieto, N., Oxidative-stress and IL-6 mediate the fibrogenic effects of [corrected] Kupffer cells on stellate cells. *Hepatology* **2006**, *44* (6), 1487-501.
268. Wirz, W.; Antoine, M.; Tag, C. G.; Gressner, A. M.; Korff, T.; Hellerbrand, C.; Kiefer, P., Hepatic stellate cells display a functional vascular smooth muscle cell phenotype in a three-dimensional co-culture model with endothelial cells. *Differentiation* **2008**, *76* (7), 784-94.
269. Akil, A.; Endsley, M.; Shanmugam, S.; Saldarriaga, O.; Somasunderam, A.; Spratt, H.; Stevenson, H. L.; Utay, N. S.; Ferguson, M.; Yi, M., Fibrogenic Gene Expression in Hepatic Stellate Cells Induced by HCV and HIV Replication in a Three Cell Co-Culture Model System. *Sci Rep* **2019**, *9* (1), 568.

270. Ries, K.; Krause, P.; Solsbacher, M.; Schwartz, P.; Unthan-Fechner, K.; Christ, B.; Markus, P. M.; Probst, I., Elevated expression of hormone-regulated rat hepatocyte functions in a new serum-free hepatocyte-stromal cell coculture model. *In Vitro Cell Dev Biol Anim* **2000**, *36* (8), 502-12.
271. Bader, A.; Knop, E.; Kern, A.; Boker, K.; Fruhauf, N.; Crome, O.; Esselmann, H.; Pape, C.; Kempka, G.; Sewing, K. F., 3-D coculture of hepatic sinusoidal cells with primary hepatocytes-design of an organotypical model. *Exp Cell Res* **1996**, *226* (1), 223-33.
272. Fisher, R. L.; Vickers, A. E., Preparation and culture of precision-cut organ slices from human and animal. *Xenobiotica* **2013**, *43* (1), 8-14.
273. Westra, I. M.; Oosterhuis, D.; Groothuis, G. M.; Olinga, P., Precision-cut liver slices as a model for the early onset of liver fibrosis to test antifibrotic drugs. *Toxicol Appl Pharmacol* **2014**, *274* (2), 328-38.
274. Pham, B. T.; van Haaften, W. T.; Oosterhuis, D.; Nieken, J.; de Graaf, I. A.; Olinga, P., Precision-cut rat, mouse, and human intestinal slices as novel models for the early-onset of intestinal fibrosis. *Physiol Rep* **2015**, *3* (4).
275. Michalik, L.; Wahli, W., Involvement of PPAR nuclear receptors in tissue injury and wound repair. *J Clin Invest* **2006**, *116* (3), 598-606.
276. Tsukamoto, H.; Towner, S. J.; Ciofalo, L. M.; French, S. W., Ethanol-induced liver fibrosis in rats fed high fat diet. *Hepatology* **1986**, *6* (5), 814-22.
277. Jeftic, I.; Jovicic, N.; Pantic, J.; Arsenijevic, N.; Lukic, M. L.; Pejnovic, N., Galectin-3 Ablation Enhances Liver Steatosis, but Attenuates Inflammation and IL-33-Dependent Fibrosis in Obesogenic Mouse Model of Nonalcoholic Steatohepatitis. *Mol Med* **2015**, *21*, 453-65.
278. Andreola, F.; Calvisi, D. F.; Elizondo, G.; Jakowlew, S. B.; Mariano, J.; Gonzalez, F. J.; De Luca, L. M., Reversal of liver fibrosis in aryl hydrocarbon receptor null mice by dietary vitamin A depletion. *Hepatology* **2004**, *39* (1), 157-166.
279. Kawaguchi, K.; Sakaida, I.; Tsuchiya, M.; Omori, K.; Takami, T.; Okita, K., Pioglitazone prevents hepatic steatosis, fibrosis, and enzyme-altered lesions in rat liver cirrhosis induced by a choline-deficient L-amino acid-defined diet. *Biochem Biophys Res Commun* **2004**, *315* (1), 187-195.
280. Chu, X.; Wang, H.; Jiang, Y. M.; Zhang, Y. Y.; Bao, Y. F.; Zhang, X.; Zhang, J. P.; Guo, H.; Yang, F.; Luan, Y. C.; Dong, Y. S., Ameliorative effects of tannic acid on carbon tetrachloride-induced liver fibrosis in vivo and in vitro. *J Pharmacol Sci* **2016**, *130* (1), 15-23.
281. Wang, Y.; Gao, J. C.; Zhang, D.; Zhang, J. A.; Ma, J. J.; Jiang, H. Q., New insights into the antifibrotic effects of sorafenib on hepatic stellate cells and liver fibrosis. *J Hepatol* **2010**, *53* (1), 132-144.
282. Tsukamoto, H.; Matsuoka, M.; French, S. W., Experimental models of hepatic fibrosis: a review. *Semin Liver Dis* **1990**, *10* (1), 56-65.
283. Zhang, Y.; Huang, D.; Gao, W.; Yan, J.; Zhou, W.; Hou, X.; Liu, M.; Ren, C.; Wang, S.; Shen, J., Lack of IL-17 signaling decreases liver fibrosis in murine schistosomiasis japonica. *Int Immunol* **2015**, *27* (7), 317-25.
284. McCaffrey, A. P.; Nakai, H.; Pandey, K.; Huang, Z.; Salazar, F. H.; Xu, H.; Wieland, S. F.; Marion, P. L.; Kay, M. A., Inhibition of hepatitis B virus in mice by RNA interference. *Nat Biotechnol* **2003**, *21* (6), 639-44.
285. Tag, C. G.; Sauer-Lehnen, S.; Weiskirchen, S.; Borkham-Kamphorst, E.; Tolba, R. H.; Tacke, F.; Weiskirchen, R., Bile duct ligation in mice: induction of inflammatory liver injury and fibrosis by obstructive cholestasis. *J Vis Exp* **2015**, (96).
286. Liedtke, C.; Luedde, T.; Sauerbruch, T.; Scholten, D.; Streetz, K.; Tacke, F.; Tolba, R.; Trautwein, C.; Trebicka, J.; Weiskirchen, R., Experimental liver fibrosis

research: update on animal models, legal issues and translational aspects. *Fibrogenesis Tissue Repair* **2013**, *6* (1), 19.

287. Hayashi, H.; Sakai, T., Animal models for the study of liver fibrosis: new insights from knockout mouse models. *Am J Physiol Gastrointest Liver Physiol* **2011**, *300* (5), G729-38.
288. Sakai, K.; Jawaid, S.; Sasaki, T.; Bou-Gharios, G.; Sakai, T., Transforming growth factor-beta-independent role of connective tissue growth factor in the development of liver fibrosis. *Am J Pathol* **2014**, *184* (10), 2611-7.
289. Weber, S.; Gressner, O. A.; Hall, R.; Grunhage, F.; Lammert, F., Genetic determinants in hepatic fibrosis: from experimental models to fibrogenic gene signatures in humans. *Clin Liver Dis* **2008**, *12* (4), 747-57, vii.
290. Bostrom, N., Drugs can be used to treat more than disease. *Nature* **2008**, *451* (7178), 520-520.
291. Schlessinger, J., Cell signaling by receptor tyrosine kinases. *Cell* **2000**, *103* (2), 211-25.
292. Grimminger, F.; Gunther, A.; Vancheri, C., The role of tyrosine kinases in the pathogenesis of idiopathic pulmonary fibrosis. *Eur Respir J* **2015**, *45* (5), 1426-33.
293. Beyer, C.; Distler, J. H., Tyrosine kinase signaling in fibrotic disorders: Translation of basic research to human disease. *Biochim Biophys Acta* **2013**, *1832* (7), 897-904.
294. Ishii, Y.; Fujimoto, S.; Fukuda, T., Gefitinib prevents bleomycin-induced lung fibrosis in mice. *Am J Respir Crit Care Med* **2006**, *174* (5), 550-6.
295. Daniels, C. E.; Wilkes, M. C.; Edens, M.; Kottom, T. J.; Murphy, S. J.; Limper, A. H.; Leof, E. B., Imatinib mesylate inhibits the profibrogenic activity of TGF-beta and prevents bleomycin-mediated lung fibrosis. *J Clin Invest* **2004**, *114* (9), 1308-16.
296. Yoshiji, H.; Noguchi, R.; Kuriyama, S.; Ikenaka, Y.; Yoshii, J.; Yanase, K.; Namisaki, T.; Kitade, M.; Masaki, T.; Fukui, H., Imatinib mesylate (STI-571) attenuates liver fibrosis development in rats. *Am J Physiol Gastrointest Liver Physiol* **2005**, *288* (5), G907-13.
297. Deng, J.; Shao, J.; Markowitz, J. S.; An, G., ABC transporters in multi-drug resistance and ADME-Tox of small molecule tyrosine kinase inhibitors. *Pharm Res* **2014**, *31* (9), 2237-55.
298. Bhullar, K. S.; Lagaron, N. O.; McGowan, E. M.; Parmar, I.; Jha, A.; Hubbard, B. P.; Rupasinghe, H. P. V., Kinase-targeted cancer therapies: progress, challenges and future directions. *Mol Cancer* **2018**, *17* (1), 48.
299. Hubbard, S. R.; Miller, W. T., Receptor tyrosine kinases: mechanisms of activation and signaling. *Curr Opin Cell Biol* **2007**, *19* (2), 117-23.
300. Robinson, D. R.; Wu, Y. M.; Lin, S. F., The protein tyrosine kinase family of the human genome. *Oncogene* **2000**, *19* (49), 5548-57.
301. Lemmon, M. A.; Schlessinger, J., Cell signaling by receptor tyrosine kinases. *Cell* **2010**, *141* (7), 1117-34.
302. Baselga, J.; Swain, S. M., Novel anticancer targets: revisiting ERBB2 and discovering ERBB3. *Nat Rev Cancer* **2009**, *9* (7), 463-75.
303. Arteaga, C. L.; Engelman, J. A., ERBB receptors: from oncogene discovery to basic science to mechanism-based cancer therapeutics. *Cancer Cell* **2014**, *25* (3), 282-303.
304. Ciardiello, F.; Tortora, G., EGFR antagonists in cancer treatment. *N ENGL J MED* **2008**, *358* (11), 1160-74.
305. Fornaro, L.; Lucchesi, M.; Caparello, C.; Vasile, E.; Caponi, S.; Ginocchi, L.; Masi, G.; Falcone, A., Anti-HER agents in gastric cancer: from bench to bedside. *Nat Rev Gastroenterol Hepatol* **2011**, *8* (7), 369-83.

306. Makinoshima, H.; Takita, M.; Saruwatari, K.; Umemura, S.; Obata, Y.; Ishii, G.; Matsumoto, S.; Sugiyama, E.; Ochiai, A.; Abe, R.; Goto, K.; Esumi, H.; Tsuchihara, K., Signaling through the Phosphatidylinositol 3-Kinase (PI3K)/Mammalian Target of Rapamycin (mTOR) Axis Is Responsible for Aerobic Glycolysis mediated by Glucose Transporter in Epidermal Growth Factor Receptor (EGFR)-mutated Lung Adenocarcinoma. *J Biol Chem* **2015**, *290* (28), 17495-17504.
307. Yamane, K.; Ihn, H.; Tamaki, K., Epidermal growth factor up-regulates expression of transforming growth factor beta receptor type II in human dermal fibroblasts by phosphoinositide 3-kinase/Akt signaling pathway: Resistance to epidermal growth factor stimulation in scleroderma fibroblasts. *Arthritis Rheum* **2003**, *48* (6), 1652-66.
308. Vallath, S.; Hynds, R. E.; Succony, L.; Janes, S. M.; Giangreco, A., Targeting EGFR signalling in chronic lung disease: therapeutic challenges and opportunities. *Eur Respir J* **2014**, *44* (2), 513-22.
309. Nethery, D. E.; Moore, B. B.; Minowada, G.; Carroll, J.; Faress, J. A.; Kern, J. A., Expression of mutant human epidermal receptor 3 attenuates lung fibrosis and improves survival in mice. *J Appl Physiol (1985)* **2005**, *99* (1), 298-307.
310. Li, Q.; Zhang, D.; Chen, X.; He, L.; Li, T.; Xu, X.; Li, M., Nuclear PKM2 contributes to gefitinib resistance via upregulation of STAT3 activation in colorectal cancer. *Sci Rep* **2015**, *5*, 16082.
311. Hong, S.; Gu, Y.; Gao, Z.; Guo, L.; Guo, W.; Wu, X.; Shen, Y.; Sun, Y.; Wu, X.; Xu, Q., EGFR inhibitor-driven endoplasmic reticulum stress-mediated injury on intestinal epithelial cells. *Life Sci* **2014**, *119* (1-2), 28-33.
312. Wang, Z.; Du, T.; Dong, X.; Li, Z.; Wu, G.; Zhang, R., Autophagy inhibition facilitates erlotinib cytotoxicity in lung cancer cells through modulation of endoplasmic reticulum stress. *Int J Oncol* **2016**, *48* (6), 2558-66.
313. Suh, D. H.; Kim, M. K.; Kim, H. S.; Chung, H. H.; Song, Y. S., Unfolded protein response to autophagy as a promising druggable target for anticancer therapy. *Ann Ny Acad Sci* **2012**, *1271*, 20-32.
314. Harding, H. P.; Zhang, Y. H.; Bertolotti, A.; Zeng, H. Q.; Ron, D., Perk is essential for translational regulation and cell survival during the unfolded protein response. *Mol Cell* **2000**, *5* (5), 897-904.
315. Qu, K.; Liu, T.; Lin, T.; Zhang, X.; Cui, R.; Liu, S.; Meng, F.; Zhang, J.; Tai, M.; Wan, Y.; Liu, C., Tyrosine kinase inhibitors: friends or foe in treatment of hepatic fibrosis? *Oncotarget* **2016**, *41*, 67650-67660.
316. Fu, J. J.; Xia, A.; Qi, X., Identification of novel peptoid agonists of fibroblast growth factor receptors using microarray-based screening. *Medchemcomm* **2016**, *7* (6), 1183-1189.
317. Beenken, A.; Mohammadi, M., The FGF family: biology, pathophysiology and therapy. *Nat Rev Drug Discov* **2009**, *8* (3), 235-53.
318. Tiseo, M.; Gelsomino, F.; Alfieri, R.; Cavazzoni, A.; Bozzetti, C.; De Giorgi, A. M.; Petronini, P. G.; Ardizzoni, A., FGFR as potential target in the treatment of squamous non small cell lung cancer. *Cancer Treat Rev* **2015**, *41* (6), 527-539.
319. Chow, L. Q.; Eckhardt, S. G., Sunitinib: from rational design to clinical efficacy. *J Clin Oncol* **2007**, *25* (7), 884-96.
320. Maurer, B.; Distler, A.; Suliman, Y. A.; Gay, R. E.; Michel, B. A.; Gay, S.; Distler, J. H.; Distler, O., Vascular endothelial growth factor aggravates fibrosis and vasculopathy in experimental models of systemic sclerosis. *Ann Rheum Dis* **2014**, *73* (10), 1880-7.
321. Hakrroush, S.; Moeller, M. J.; Theilig, F.; Kaissling, B.; Sijmonsma, T. P.; Jugold, M.; Akeson, A. L.; Traykova-Brauch, M.; Hosser, H.; Hahnel, B.; Grone, H. J.; Koesters, R.; Kriz, W., Effects of Increased Renal Tubular Vascular Endothelial Growth Factor

- (VEGF) on Fibrosis, Cyst Formation, and Glomerular Disease. *Am J Pathol* **2009**, *175* (5), 1883-1895.
322. Holmes, D. I.; Zachary, I., The vascular endothelial growth factor (VEGF) family: angiogenic factors in health and disease. *Genome Biol* **2005**, *6* (2), 209.
323. Dvorak, H. F.; Brown, L. F.; Detmar, M.; Dvorak, A. M., Vascular permeability factor/vascular endothelial growth factor, microvascular hyperpermeability, and angiogenesis. *Am J Pathol* **1995**, *146* (5), 1029-39.
324. Jiang, G.; Dallas-Yang, Q.; Biswas, S.; Li, Z.; Zhang, B. B., Rosiglitazone, an agonist of peroxisome-proliferator-activated receptor gamma (PPARgamma), decreases inhibitory serine phosphorylation of IRS1 in vitro and in vivo. *Biochem J* **2004**, *377* (Pt 2), 339-46.
325. Prost, S.; Relouzat, F.; Spentchian, M.; Ouzegdouh, Y.; Saliba, J.; Massonnet, G.; Beressi, J. P.; Verhoeyen, E.; Raggiueanu, V.; Maneglier, B.; Castaigne, S.; Chomienne, C.; Chretien, S.; Rousselot, P.; Leboulch, P., Erosion of the chronic myeloid leukaemia stem cell pool by PPARgamma agonists. *Nature* **2015**, *525* (7569), 380-3.
326. Lokes, D.; Szadvari, I.; Krizanova, O.; Lopusna, K.; Rezuchova, I.; Novakova, M.; Novakova, Z.; Parak, T.; Babula, P., Nilotinib induces ER stress and cell death in H9c2 cells. *Physiol Res* **2016**, *65* (Supplementum 4), S505-S514.
327. Xia, Y.; Fang, H.; Zhang, J.; Du, Y., Endoplasmic reticulum stress-mediated apoptosis in imatinib-resistant leukemic K562-r cells triggered by AMN107 combined with arsenic trioxide. *Experimental biology and medicine* **2013**, *238* (8), 932-42.
328. Urano, F.; Wang, X.; Bertolotti, A.; Zhang, Y.; Chung, P.; Harding, H. P.; Ron, D., Coupling of stress in the ER to activation of JNK protein kinases by transmembrane protein kinase IRE1. *Science* **2000**, *287* (5453), 664-6.
329. Tournier, C.; Hess, P.; Yang, D. D.; Xu, J.; Turner, T. K.; Nimmual, A.; Bar-Sagi, D.; Jones, S. N.; Flavell, R. A.; Davis, R. J., Requirement of JNK for stress-induced activation of the cytochrome c-mediated death pathway. *Science* **2000**, *288* (5467), 870-4.
330. Qu, K.; Huang, Z. C.; Lin, T.; Liu, S. N.; Chang, H. L.; Yan, Z. Y.; Zhang, H. X.; Liu, C., New Insight into the Anti-liver Fibrosis Effect of Multitargeted Tyrosine Kinase Inhibitors: From Molecular Target to Clinical Trials. *Front Pharmacol* **2016**, *6*.
331. Paul, B.; Trovato, J. A.; Thompson, J., Lapatinib: a dual tyrosine kinase inhibitor for metastatic breast cancer. *Am J Health Syst Pharm* **2008**, *65* (18), 1703-10.
332. Distler, J. H.; Distler, O., Cardiotoxicity of imatinib mesylate: an extremely rare phenomenon or a major side effect? *Ann Rheum Dis* **2007**, *66* (6), 836.
333. Park, S.; Kim, D. S.; Kang, S., A high lignan fraction of Fructus Schisandrae improves hepatic insulin sensitivity in in vitro and in vivo studies. *FASEB J* **2011**, *25*.
334. Mishra, B. B.; Tiwari, V. K., Natural products: An evolving role in future drug discovery. *Eur J Med Chem* **2011**, *46* (10), 4769-4807.
335. Cheuka, P. M.; Mayoka, G.; Mutai, P.; Chibale, K., The Role of Natural Products in Drug Discovery and Development against Neglected Tropical Diseases. *Molecules* **2016**, *22* (1), 58.
336. Zhang, C.; Wang, Y.; Chen, H.; Yang, G.; Wang, S.; Jiang, M.; Cong, L.; Yuan, L.; Li, H.; Jia, Y., Protective effect of the herbal medicine Ganfukang against carbon tetrachloride-induced liver fibrosis in rats. *Mol Med Rep* **2013**, *8* (3), 954-62.
337. Gullo, V. P.; McAlpine, J.; Lam, K. S.; Baker, D.; Petersen, F., Drug discovery from natural products. *J Ind Microbiol Biotechnol* **2006**, *33* (7), 523-31.
338. Cufi, S.; Vazquez-Martin, A.; Oliveras-Ferraros, C.; Martin-Castillo, B.; Joven, J.; Menendez, J. A., Metformin against TGFbeta-induced epithelial-to-mesenchymal transition (EMT): from cancer stem cells to aging-associated fibrosis. *Cell Cycle* **2010**, *9* (22), 4461-8.

339. Pari, L.; Tewas, D.; Eckel, J., Role of curcumin in health and disease. *Arch Physiol Biochem* **2008**, *114* (2), 127-49.
340. Shen, B., A New Golden Age of Natural Products Drug Discovery. *Cell* **2015**, *163* (6), 1297-300.
341. Thompson, L. U.; Boucher, B. A.; Liu, Z.; Cotterchio, M.; Kreiger, N., Phytoestrogen content of foods consumed in Canada, including isoflavones, lignans, and coumestan. *Nutr Cancer* **2006**, *54* (2), 184-201.
342. Zhang, J.; Chen, J. J.; Liang, Z. Z.; Zhao, C. Q., New Lignans and Their Biological Activities. *Chem Biodivers* **2014**, *11* (1), 1-54.
343. Fukumitsu, S.; Aida, K.; Ueno, N.; Ozawa, S.; Takahashi, Y.; Kobori, M., Flaxseed lignan attenuates high-fat diet-induced fat accumulation and induces adiponectin expression in mice. *Br J Nutr* **2008**, *100* (3), 669-76.
344. Teponno, R. B.; Kusari, S.; Spitteller, M., Recent advances in research on lignans and neolignans. *Nat Prod Rep* **2016**, *33* (9), 1044-92.
345. Pan, J. Y.; Chen, S. L.; Yang, M. H.; Wu, J.; Sinkkonen, J.; Zou, K., An update on lignans: natural products and synthesis. *Nat Prod Rep* **2009**, *26* (10), 1251-92.
346. Saleem, M.; Kim, H. J.; Ali, M. S.; Lee, Y. S., An update on bioactive plant lignans. *Nat Prod Rep* **2005**, *22* (6), 696-716.
347. Kuijsten, A.; Arts, I. C.; van't Veer, P.; Hollman, P. C., The relative bioavailability of enterolignans in humans is enhanced by milling and crushing of flaxseed. *J Nutr* **2005**, *135* (12), 2812-6.
348. Muir, A. D.; Westcott, N. D., Flax: the genus *Linum*. *CRC Press* **2003**.
349. Priy, R.; Katoch, M.; Kumar, A.; Csk, V.; Pradesh, H.; Vishwavidyalya, K., *Flaxseed-composition and its health benefits*. *Res. Environ. Life Sci*: **2017**; Vol. 9.
350. Goyal, A.; Sharma, V.; Upadhyay, N.; Gill, S.; Sihag, M., Flax and flaxseed oil: an ancient medicine & modern functional food. *J Food Sci Technol* **2014**, *51* (9), 1633-53.
351. Covington, M. B., Omega-3 fatty acids. *Am Fam Physician* **2004**, *70* (1), 133-40.
352. Kristensen, M.; Jensen, M. G.; Aarestrup, J.; Petersen, K. E.; Sondergaard, L.; Mikkelsen, M. S.; Astrup, A., Flaxseed dietary fibers lower cholesterol and increase fecal fat excretion, but magnitude of effect depend on food type. *Nutr Metab (Lond)* **2012**, *9*, 8.
353. Opyd, P. M.; Jurgonski, A.; Juskiewicz, J.; Fotschki, B.; Koza, J., Comparative Effects of Native and Defatted Flaxseeds on Intestinal Enzyme Activity and Lipid Metabolism in Rats Fed a High-Fat Diet Containing Cholic Acid. *Nutrients* **2018**, *10* (9).
354. Khalatbari Soltani, S.; Jamaluddin, R.; Tabibi, H.; Mohd Yusof, B. N.; Atabak, S.; Loh, S. P.; Rahmani, L., Effects of flaxseed consumption on systemic inflammation and serum lipid profile in hemodialysis patients with lipid abnormalities. *Hemodial Int* **2013**, *17* (2), 275-81.
355. Mukker, J. K.; Singh, R. S.; Muir, A. D.; Krol, E. S.; Alcorn, J., Comparative pharmacokinetics of purified flaxseed and associated mammalian lignans in male Wistar rats. *Br J Nutr* **2015**, *113* (5), 749-57.
356. Di, Y.; Ji, S.; Wolf, P.; Krol, E. S.; Alcorn, J., Enterolactone glucuronide and beta-glucuronidase in antibody directed enzyme prodrug therapy for targeted prostate cancer cell treatment. *AAPS PharmSciTech* **2017**, *18* (6), 2336-2345.
357. Mukker, J. K.; Michel, D.; Muir, A. D.; Krol, E. S.; Alcorn, J., Permeability and conjugative metabolism of flaxseed lignans by Caco-2 human intestinal cells. *J Nat Prod* **2014**, *77* (1), 29-34.
358. Shim, Y. Y.; Gui, B.; Arnison, P. G.; Wang, Y.; Reaney, M. J. T., Flaxseed (*Linum usitatissimum* L.) bioactive compounds and peptide nomenclature: A review. *Trends Food Sci Technol* **2014**, *38* (1), 5-20.

359. Chen, J.; Saggar, J. K.; Corey, P.; Thompson, L. U., Flaxseed and pure secoisolariciresinol diglucoside, but not flaxseed hull, reduce human breast tumor growth (MCF-7) in athymic mice. *J Nutr* **2009**, *139* (11), 2061-6.
360. Lin, X.; Switzer, B. R.; Demark-Wahnefried, W., Effect of mammalian lignans on the growth of prostate cancer cell lines. *Anticancer Res* **2001**, *21* (6A), 3995-9.
361. Boccardo, F.; Lunardi, G.; Guglielmini, P.; Parodi, M.; Murialdo, R.; Schettini, G.; Rubagotti, A., Serum enterolactone levels and the risk of breast cancer in women with palpable cysts. *Eur J Cancer* **2004**, *40* (1), 84-9.
362. Pietinen, P.; Stumpf, K.; Mannisto, S.; Kataja, V.; Uusitupa, M.; Adlercreutz, H., Serum enterolactone and risk of breast cancer: a case-control study in eastern Finland. *Cancer Epidemiol Biomarkers Prev* **2001**, *10* (4), 339-44.
363. Kitts, D. D.; Yuan, Y. V.; Wijewickreme, A. N.; Thompson, L. U., Antioxidant activity of the flaxseed lignan secoisolariciresinol diglycoside and its mammalian lignan metabolites enterodiol and enterolactone. *Mol Cell Biochem* **1999**, *202* (1-2), 91-100.
364. Felmlee, M. A.; Woo, G.; Simko, E.; Krol, E. S.; Muir, A. D.; Alcorn, J., Effects of the flaxseed lignans secoisolariciresinol diglucoside and its aglycone on serum and hepatic lipids in hyperlipidaemic rats. *Br J Nutr* **2009**, *102* (3), 361-9.
365. Lee, J. C.; Krochak, R.; Blouin, A.; Kanterakis, S.; Chatterjee, S.; Arguiri, E.; Vachani, A.; Solomides, C. C.; Cengel, K. A.; Christofidou-Solomidou, M., Dietary flaxseed prevents radiation-induced oxidative lung damage, inflammation and fibrosis in a mouse model of thoracic radiation injury. *Cancer Biol Ther* **2009**, *8* (1), 47-53.
366. Prasad, K., Suppression of phosphoenolpyruvate carboxykinase gene expression by secoisolariciresinol diglucoside (SDG), a new antidiabetic agent. *Int J Angiol* **2002**, *11* (02), 107-109.
367. Vanharanta, M.; Voutilainen, S.; Rissanen, T. H.; Adlercreutz, H.; Salonen, J. T., Risk of cardiovascular disease-related and all-cause death according to serum concentrations of enterolactone: Kuopio Ischaemic Heart Disease Risk Factor Study. *Arch Intern Med* **2003**, *163* (9), 1099-104.
368. Vanharanta, M.; Voutilainen, S.; Lakka, T. A.; van der Lee, M.; Adlercreutz, H.; Salonen, J. T., Risk of acute coronary events according to serum concentrations of enterolactone: a prospective population-based case-control study. *The Lancet* **1999**, *354* (9196), 2112-2115.
369. Hasler, C. M.; Kundrat, S.; Wool, D., Functional foods and cardiovascular disease. *Curr Atheroscler Rep* **2000**, *2* (6), 467-75.
370. Spence, J. D.; Thornton, T.; Muir, A. D.; Westcott, N. D., The effect of flax seed cultivars with differing content of alpha-linolenic acid and lignans on responses to mental stress. *J Am Coll Nutr* **2003**, *22* (6), 494-501.
371. Heinonen, S.; Nurmi, T.; Liukkonen, K.; Poutanen, K.; Wahala, K.; Deyama, T.; Nishibe, S.; Adlercreutz, H., In vitro metabolism of plant lignans: new precursors of mammalian lignans enterolactone and enterodiol. *J Agric Food Chem* **2001**, *49* (7), 3178-86.
372. Wang, L. Q.; Meselhy, M. R.; Li, Y.; Qin, G. W.; Hattori, M., Human intestinal bacteria capable of transforming secoisolariciresinol diglucoside to mammalian lignans, enterodiol and enterolactone. *Chem Pharm Bull (Tokyo)* **2000**, *48* (11), 1606-10.
373. Saxena, S.; Katare, C., Evaluation of flaxseed formulation as a potential therapeutic agent in mitigation of dyslipidemia. *Biomed J* **2014**, *37* (6), 386-90.
374. Kuijsten, A.; Arts, I. C.; Vree, T. B.; Hollman, P. C., Pharmacokinetics of enterolignans in healthy men and women consuming a single dose of secoisolariciresinol diglucoside. *J Nutr* **2005**, *135* (4), 795-801.
375. Bach Knudsen, K. E.; Serena, A.; Kjaer, A. K.; Tetens, I.; Heinonen, S. M.; Nurmi, T.; Adlercreutz, H., Rye bread in the diet of pigs enhances the formation of

- enterolactone and increases its levels in plasma, urine and feces. *J Nutr* **2003**, *133* (5), 1368-75.
376. Yang, T.; Liu, S.; Zheng, T. H.; Tao, Y. Y.; Liu, C. H., Comparative pharmacokinetics and tissue distribution profiles of lignan components in normal and hepatic fibrosis rats after oral administration of Fuzheng Huayu recipe. *J Ethnopharmacol* **2015**, *166*, 305-12.
377. Clavel, T.; Dore, J.; Blaut, M., Bioavailability of lignans in human subjects. *Nutr Res Rev* **2006**, *19* (2), 187-96.
378. Zhang, W.; Wang, X.; Liu, Y.; Tian, H.; Flickinger, B.; Empie, M. W.; Sung, S. Z., Dietary flaxseed lignan extract lowers plasma cholesterol and glucose concentrations in hypercholesterolaemic subjects. *Br J Nutr* **2008**, *99* (6), 1301-1309.
379. Rickard, S. E.; Thompson, L. U., Chronic exposure to secoisolariciresinol diglycoside alters lignan disposition in rats. *J Nutr* **1998**, *128* (3), 615-23.
380. Saarinen, N. M.; Thompson, L. U., Prolonged administration of secoisolariciresinol diglycoside increases lignan excretion and alters lignan tissue distribution in adult male and female rats. *Br J Nutr* **2010**, *104* (6), 833-41.
381. Schottner, M.; Gansser, D.; Spiteller, G., Lignans from the roots of *Urtica dioica* and their metabolites bind to human sex hormone binding globulin (SHBG). *Planta Med* **1997**, *63* (6), 529-532.
382. Murray, T.; Kang, J.; Astheimer, L.; Price, W. E., Tissue distribution of lignans in rats in response to diet, dose-response, and competition with isoflavones. *J Agric Food Chem* **2007**, *55* (12), 4907-12.
383. Niemeyer, H. B.; Honig, D. M.; Kulling, S. E.; Metzler, M., Studies on the metabolism of the plant lignans secoisolariciresinol and matairesinol. *J Agric Food Chem* **2003**, *51* (21), 6317-25.
384. Chaojie, L.; Ed, S. K.; Jane, A., The Comparison of Rat and Human Intestinal and Hepatic Glucuronidation of Enterolactone Derived from Flaxseed Lignans. *Nat Prod J* **2013**, *3* (3), 159-171.
385. Almousa, A. A.; University of Saskatchewan College of Graduate Studies and Research., Local effects of Linoorbittides and enterolactone On intestinal epithelial functions. **2017**. <http://hdl.handle.net/10388/7781>.
386. Quartieri, A.; Garcia-Villalba, R.; Amaretti, A.; Raimondi, S.; Leonardi, A.; Rossi, M.; Tomas-Barberan, F., Detection of novel metabolites of flaxseed lignans in vitro and in vivo. *Mol Nutr Food Res* **2016**, *60* (7), 1590-601.
387. Frische, E. J.; Hutchins, A. M.; Martini, M. C.; Thomas, W.; Slavin, J. L., Effect of flaxseed and wheat bran on serum hormones and lignan excretion in premenopausal women. *J Am Coll Nutr* **2003**, *22* (6), 550-4.
388. Kurzer, M. S.; Lampe, J. W.; Martini, M. C.; Adlercreutz, H., Fecal Lignan and Isoflavonoid Excretion in Premenopausal Women Consuming Flaxseed Powder. *Cancer Epidem Biomar* **1995**, *4* (4), 353-358.
389. Toure, A.; Xu, X. M., Flaxseed Lignans: Source, Biosynthesis, Metabolism, Antioxidant Activity, Bio-Active Components, and Health Benefits. *Compr Rev Food Sci F* **2010**, *9* (3), 261-269.
390. Kulling, S. E.; Jacobs, E.; Pfeiffer, E.; Metzler, M., Studies on the genotoxicity of the mammalian lignans enterolactone and enterodiol and their metabolic precursors at various endpoints in vitro. *Mutat Res-Gen Tox En* **1998**, *416* (1-2), 115-124.
391. Billinsky, J.; Glew, R. A.; Cornish, S. M.; Whiting, S. J.; Thorpe, L. U.; Alcorn, J.; Paus-Jenssen, L.; Hadjistavropoulos, T.; Chilibeck, P. D., No evidence of hypoglycemia or hypotension in older adults during 6 months of flax lignan supplementation in a randomized controlled trial: A safety evaluation. *Pharm Biol* **2013**, *51* (6), 778-782.

392. Viveky, N.; Thorpe, L.; Alcorn, J.; Hadjistavropoulos, T.; Whiting, S. J., Safety evaluation of flaxseed lignan supplementation in older adults residing in long-term care homes. *J Nurs Home Res Sci* **2015**, *1*, 84-88.
393. Miura, K.; Satoh, M.; Kinouchi, M.; Yamamoto, K.; Hasegawa, Y.; Kakugawa, Y.; Kawai, M.; Uchimi, K.; Aizawa, H.; Ohnuma, S.; Kajiwara, T.; Sakurai, H.; Fujiya, T., The use of natural products in colorectal cancer drug discovery. *Expert Opin Drug Discov* **2015**, *10* (4), 411-26.
394. Chun, J. N.; Cho, M.; So, I.; Jeon, J. H., The protective effects of Schisandra chinensis fruit extract and its lignans against cardiovascular disease: a review of the molecular mechanisms. *Fitoterapia* **2014**, *97*, 224-33.
395. Adolphe, J. L.; Whiting, S. J.; Juurlink, B. H.; Thorpe, L. U.; Alcorn, J., Health effects with consumption of the flax lignan secoisolariciresinol diglucoside. *Br J Nutr* **2010**, *103* (7), 929-38.
396. Chen, Y. C.; Liaw, C. C.; Cheng, Y. B.; Lin, Y. C.; Chen, C. H.; Huang, Y. T.; Liou, S. S.; Chen, S. Y.; Chien, C. T.; Lee, G. C.; Shen, Y. C., Anti-liver fibrotic lignans from the fruits of Schisandra arisanensis and Schisandra sphenanthera. *Bioorg Med Chem Lett* **2013**, *23* (3), 880-5.
397. Imran, M.; Ahmad, N.; Anjum, F. M.; Khan, M. K.; Mushtaq, Z.; Nadeem, M.; Hussain, S., Potential protective properties of flax lignan secoisolariciresinol diglucoside. *Nutr J* **2015**, *14*, 71.
398. Abarzua, S.; Serikawa, T.; Szewczyk, M.; Richter, D. U.; Piechulla, B.; Briese, V., Antiproliferative activity of lignans against the breast carcinoma cell lines MCF 7 and BT 20. *Arch Gynecol Obstet* **2012**, *285* (4), 1145-51.
399. Bhatia, A. L.; Sharma, A.; Patni, S.; Sharma, A. L., Prophylactic effect of flaxseed oil against radiation-induced hepatotoxicity in mice. *Phytother Res* **2007**, *21* (9), 852-9.
400. Almousa, A. A.; Meurens, F.; Krol, E. S.; Alcorn, J., Linoorbittides and enterolactone mitigate inflammation-induced oxidative stress and loss of intestinal epithelial barrier integrity. *Int Immunopharmacol* **2018**, *64*, 42-51.
401. Zhang, F.; Zhang, Z.; Chen, L.; Kong, D.; Zhang, X.; Lu, C.; Lu, Y.; Zheng, S., Curcumin attenuates angiogenesis in liver fibrosis and inhibits angiogenic properties of hepatic stellate cells. *J Cell Mol Med* **2014**, *18* (7), 1392-406.
402. Liu, N.; Wu, C.; Sun, L.; Zheng, J.; Guo, P., Sesamin enhances cholesterol efflux in RAW264.7 macrophages. *Molecules* **2014**, *19* (6), 7516-27.
403. Quang, T. H.; Ngan, N. T.; Minh, C. V.; Kiem, P. V.; Tai, B. H.; Thao, N. P.; Song, S. B.; Kim, Y. H., Anti-inflammatory and PPAR transactivational effects of secondary metabolites from the roots of *Asarum sieboldii*. *Bioorg Med Chem Lett* **2012**, *22* (7), 2527-33.
404. Dong, X. Y.; Tang, S. Q.; Chen, J. D., Dual functions of Insig proteins in cholesterol homeostasis. *Lipids Health Dis* **2012**, *11*, 173.
405. Scharinger, B.; Messner, B.; Turkcan, A.; Schuster, D.; Vuorinen, A.; Pitterl, F.; Heinz, K.; Arnhard, K.; Laufer, G.; Grimm, M.; Stuppner, H.; Oberacher, H.; Eller, P.; Ritsch, A.; Bernhard, D., Leoligin, the major lignan from Edelweiss, inhibits 3-hydroxy-3-methyl-glutaryl-CoA reductase and reduces cholesterol levels in ApoE^{-/-} mice. *J Mol Cell Cardiol* **2016**, *99*, 35-46.
406. Wang, Z.; Xu, J. P.; Zheng, Y. C.; Chen, W.; Sun, Y. W.; Wu, Z. Y.; Luo, M., Peroxisome proliferator-activated receptor gamma inhibits hepatic fibrosis in rats. *Hepatobiliary Pancreat Dis Int* **2011**, *10* (1), 64-71.
407. Kulkarni, A. A.; Thatcher, T. H.; Olsen, K. C.; Maggirwar, S. B.; Phipps, R. P.; Sime, P. J., PPAR-gamma ligands repress TGFbeta-induced myofibroblast differentiation by

- targeting the PI3K/Akt pathway: implications for therapy of fibrosis. *PLoS One* **2011**, *6* (1), e15909.
408. Pietrofesa, R.; Turowski, J.; Tyagi, S.; Dukes, F.; Arguiri, E.; Busch, T. M.; Gallagher-Colombo, S. M.; Solomides, C. C.; Cengel, K. A.; Christofidou-Solomidou, M., Radiation mitigating properties of the lignan component in flaxseed. *BMC Cancer* **2013**, *13*, 179.
409. Lee, J. H.; Jang, E. J.; Seo, H. L.; Ku, S. K.; Lee, J. R.; Shin, S. S.; Park, S. D.; Kim, S. C.; Kim, Y. W., Sauchinone attenuates liver fibrosis and hepatic stellate cell activation through TGF-beta/Smad signaling pathway. *Chemico-biological interactions* **2014**, *224*, 58-67.
410. Zhao, M.; Zheng, S.; Yang, J.; Wu, Y.; Ren, Y.; Kong, X.; Li, W.; Xuan, J., Suppression of TGF-beta1/Smad signaling pathway by sesamin contributes to the attenuation of myocardial fibrosis in spontaneously hypertensive rats. *PLoS One* **2015**, *10* (3), e0121312.
411. Park, J. H.; Yoon, J., Schizandrin inhibits fibrosis and epithelial-mesenchymal transition in transforming growth factor-beta1-stimulated AML12 cells. *Int Immunopharmacol* **2015**, *25* (2), 276-84.
412. Gu, Y.; Sun, X. X.; Ye, J. M.; He, L.; Yan, S. S.; Zhang, H. H.; Hu, L. H.; Yuan, J. Y.; Yu, Q., Arctigenin alleviates ER stress via activating AMPK. *Acta Pharmacol Sin* **2012**, *33* (7), 941-52.
413. Wu, Y. F.; Cao, M. F.; Gao, Y. P.; Chen, F.; Wang, T.; Zumbika, E. P.; Qian, K. X., Down-modulation of heat shock protein 70 and up-modulation of Caspase-3 during schisandrin B-induced apoptosis in human hepatoma SMMC-7721 cells. *World J Gastroenterol* **2004**, *10* (20), 2944-8.
414. De Silva, F.; Yang, X.; Almousa, A.; Hawsawai, A.; Alcorn, J., Lignan enterolactone modulates cellular lipid and cholesterol homeostasis linking diverse molecular mechanisms. *DMPK* **2019**, *34* (1, Supplement), S33.
415. Majdalawieh, A. F.; Ro, H. S., The anti-atherogenic properties of sesamin are mediated via improved macrophage cholesterol efflux through PPARgamma1-LXRalpha and MAPK signaling. *Int J Vitam Nutr Res* **2014**, *84* (1-2), 79-91.
416. Xu, X.; Li, Q.; Pang, L.; Huang, G.; Huang, J.; Shi, M.; Sun, X.; Wang, Y., Arctigenin promotes cholesterol efflux from THP-1 macrophages through PPAR-gamma/LXR-alpha signaling pathway. *Biochem Biophys Res Commun* **2013**, *441* (2), 321-6.
417. Edel, A. L.; Rodriguez-Leyva, D.; Maddaford, T. G.; Caligiuri, S. P.; Austria, J. A.; Weighell, W.; Guzman, R.; Aliani, M.; Pierce, G. N., Dietary flaxseed independently lowers circulating cholesterol and lowers it beyond the effects of cholesterol-lowering medications alone in patients with peripheral artery disease. *J Nutr* **2015**, *145* (4), 749-57.
418. Li, A.; Wang, J.; Zhu, D.; Zhang, X.; Pan, R.; Wang, R., Arctigenin suppresses transforming growth factor-beta1-induced expression of monocyte chemoattractant protein-1 and the subsequent epithelial-mesenchymal transition through reactive oxygen species-dependent ERK/NF-kappaB signaling pathway in renal tubular epithelial cells. *Free Radic Res* **2015**, *49* (9), 1095-113.
419. Lin, C. H.; Shen, M. L.; Kao, S. T.; Wu, D. C., The effect of sesamin on airway fibrosis in vitro and in vivo. *Int Immunopharmacol* **2014**, *22* (1), 141-50.
420. Farmer, S. R., Regulation of PPARgamma activity during adipogenesis. *Int J Obes (Lond)* **2005**, *29 Suppl 1*, S13-6.
421. Friedewald, W. T.; Levy, R. I.; Fredrickson, D. S., Estimation of the concentration of low-density lipoprotein cholesterol in plasma, without use of the preparative ultracentrifuge. *Clin Chem* **1972**, *18* (6), 499-502.

422. Nakano, R.; Kurosaki, E.; Yoshida, S.; Yokono, M.; Shimaya, A.; Maruyama, T.; Shibasaki, M., Antagonism of peroxisome proliferator-activated receptor gamma prevents high-fat diet-induced obesity in vivo. *Biochem Pharmacol* **2006**, *72* (1), 42-52.
423. Rocchi, S.; Picard, F.; Vamecq, J.; Gelman, L.; Potier, N.; Zeyer, D.; Dubuquoy, L.; Bac, P.; Champy, M. F.; Plunket, K. D.; Leesnitzer, L. M.; Blanchard, S. G.; Desreumaux, P.; Moras, D.; Renaud, J. P.; Auwerx, J., A unique PPARgamma ligand with potent insulin-sensitizing yet weak adipogenic activity. *Mol Cell* **2001**, *8* (4), 737-47.
424. Mueller, H.; Kassack, M. U.; Wiese, M., Comparison of the usefulness of the MTT, ATP, and calcein assays to predict the potency of cytotoxic agents in various human cancer cell lines. *J Biomol Screen* **2004**, *9* (6), 506-15.
425. Benyon, R. C.; Iredale, J. P., Is liver fibrosis reversible? *Gut* **2000**, *46* (4), 443-446.
426. Yang, J. H.; Kim, S. C.; Kim, K. M.; Jang, C. H.; Cho, S. S.; Kim, S. J.; Ku, S. K.; Cho, I. J.; Ki, S. H., Isorhamnetin attenuates liver fibrosis by inhibiting TGF-beta/Smad signaling and relieving oxidative stress. *Eur J Pharmacol* **2016**, *783*, 92-102.
427. Issa, R.; Williams, E.; Trim, N.; Kendall, T.; Arthur, M. J. P.; Reichen, J.; Benyon, R. C.; Iredale, J. P., Apoptosis of hepatic stellate cells: involvement in resolution of biliary fibrosis and regulation by soluble growth factors. *Gut* **2001**, *48* (4), 548.
428. Hernandez-Gea, V.; Hilscher, M.; Rozenfeld, R.; Lim, M. P.; Nieto, N.; Werner, S.; Devi, L. A.; Friedman, S. L., Endoplasmic reticulum stress induces fibrogenic activity in hepatic stellate cells through autophagy. *J Hepatol* **2013**, *59* (1), 98-104.
429. Apostolova, N.; Gomez-Sucerquia, L. J.; Alegre, F.; Funes, H. A.; Victor, V. M.; Barrachina, M. D.; Blas-Garcia, A.; Esplugues, J. V., ER stress in human hepatic cells treated with Efavirenz: Mitochondria again. *J Hepatol* **2013**, *59* (4), 780-789.
430. Davis, J. E.; Cain, J.; Small, C.; Hales, D. B., Therapeutic effect of flax-based diets on fatty liver in aged laying hens. *Poult Sci* **2016**, *95* (11), 2624-2632.
431. Albanis, E.; Friedman, S. L., Hepatic fibrosis. Pathogenesis and principles of therapy. *Clin Liver Dis* **2001**, *5* (2), 315-34, v-vi.
432. Nagao, S.; Yamaguchi, T., PPAR-gamma agonists in polycystic kidney disease with frequent development of cardiovascular disorders. *Curr Mol Pharmacol* **2012**, *5* (2), 292-300.
433. Henriksen, K.; Byrjalsen, I.; Qvist, P.; Beck-Nielsen, H.; Hansen, G.; Riis, B. J.; Perrild, H.; Svendsen, O. L.; Gram, J.; Karsdal, M. A.; Christiansen, C.; Investigators, B. T., Efficacy and safety of the PPARgamma partial agonist balaglitazone compared with pioglitazone and placebo: a phase III, randomized, parallel-group study in patients with type 2 diabetes on stable insulin therapy. *Diabetes Metab Res Rev* **2011**, *27* (4), 392-401.
434. Ahmadian, M.; Suh, J. M.; Hah, N.; Liddle, C.; Atkins, A. R.; Downes, M.; Evans, R. M., PPARgamma signaling and metabolism: the good, the bad and the future. *Nat Med* **2013**, *19* (5), 557-66.
435. Balakumar, P.; Kathuria, S., Submaximal PPARgamma activation and endothelial dysfunction: new perspectives for the management of cardiovascular disorders. *Br J Pharmacol* **2012**, *166* (7), 1981-92.
436. Wu, L.; Guo, C.; Wu, J., Therapeutic potential of PPARgamma natural agonists in liver diseases. *J Cell Mol Med* **2020**, *24* (5), 2736-2748.
437. Azrad, M.; Vollmer, R. T.; Madden, J.; Dewhirst, M.; Polascik, T. J.; Snyder, D. C.; Ruffin, M. T.; Moul, J. W.; Brenner, D. E.; Demark-Wahnefried, W., Flaxseed-Derived Enterolactone Is Inversely Associated with Tumor Cell Proliferation in Men with Localized Prostate Cancer. *J Med Food* **2013**, *16* (4), 357-360.
438. Zanella, I.; Biasiotto, G.; Holm, F.; di Lorenzo, D., Cereal Lignans, Natural Compounds of Interest for Human Health? *Nat Prod Commun* **2017**, *12* (1), 139-146.

439. Mali, A. V.; Padhye, S. B.; Anant, S.; Hegde, M. V.; Kadam, S. S., Anticancer and antimetastatic potential of enterolactone: Clinical, preclinical and mechanistic perspectives. *Eur J Pharmacol* **2019**, *852*, 107-124.
440. Ribeiro Filho, H. V.; Bernardi Videira, N.; Bridi, A. V.; Tittanegro, T. H.; Helena Batista, F. A.; de Carvalho Pereira, J. G.; de Oliveira, P. S. L.; Bajgelman, M. C.; Le Maire, A.; Figueira, A. C. M., Screening for PPAR Non-Agonist Ligands Followed by Characterization of a Hit, AM-879, with Additional No-Adipogenic and cdk5-Mediated Phosphorylation Inhibition Properties. *Front Endocrinol (Lausanne)* **2018**, *9*, 11.
441. Chen, R.; Wan, J.; Song, J.; Qian, Y.; Liu, Y.; Gu, S., Rational screening of peroxisome proliferator-activated receptor-gamma agonists from natural products: potential therapeutics for heart failure. *Pharm Biol* **2017**, *55* (1), 503-509.
442. Gregoire, F. M.; Zhang, F.; Clarke, H. J.; Gustafson, T. A.; Sears, D. D.; Favellyukis, S.; Lenhard, J.; Rentzeperis, D.; Clemens, L. E.; Mu, Y.; Lavan, B. E., MBX-102/JNJ39659100, a novel peroxisome proliferator-activated receptor-ligand with weak transactivation activity retains antidiabetic properties in the absence of weight gain and edema. *Mol Endocrinol* **2009**, *23* (7), 975-88.
443. Porskjaer Christensen, L.; Bahij El-Houri, R., Development of an In Vitro Screening Platform for the Identification of Partial PPARgamma Agonists as a Source for Antidiabetic Lead Compounds. *Molecules* **2018**, *23* (10).
444. Kairys, V.; Baranauskiene, L.; Kazlauskiene, M.; Matulis, D.; Kazlauskas, E., Binding affinity in drug design: experimental and computational techniques. *Expert Opin Drug Discov* **2019**, *14* (8), 755-768.
445. Ukiya, M.; Sato, D.; Kimura, H.; Koketsu, M.; Phay, N.; Nishina, A., (-)-O-Methylcubebin from *Vitex trifolia* Enhanced Adipogenesis in 3T3-L1 Cells via the Inhibition of ERK1/2 and p38MAPK Phosphorylation. *Molecules* **2019**, *25* (1).
446. Oberfield, J. L.; Collins, J. L.; Holmes, C. P.; Goreham, D. M.; Cooper, J. P.; Cobb, J. E.; Lenhard, J. M.; Hull-Ryde, E. A.; Mohr, C. P.; Blanchard, S. G.; Parks, D. J.; Moore, L. B.; Lehmann, J. M.; Plunket, K.; Miller, A. B.; Milburn, M. V.; Kliewer, S. A.; Willson, T. M., A peroxisome proliferator-activated receptor gamma ligand inhibits adipocyte differentiation. *Proc Natl Acad Sci U S A* **1999**, *96* (11), 6102-6.
447. Choi, J. H.; Banks, A. S.; Estall, J. L.; Kajimura, S.; Bostrom, P.; Laznik, D.; Ruas, J. L.; Chalmers, M. J.; Kamenecka, T. M.; Bluher, M.; Griffin, P. R.; Spiegelman, B. M., Anti-diabetic drugs inhibit obesity-linked phosphorylation of PPARgamma by Cdk5. *Nature* **2010**, *466* (7305), 451-6.
448. Grabinski, N.; Ewald, F., Ibrutinib (ImbruvicaTM) potently inhibits ErbB receptor phosphorylation and cell viability of ErbB2-positive breast cancer cells. *Invest New Drugs* **2014**, *32* (6), 1096-104.
449. Kannaiyan, R.; Mahadevan, D., A comprehensive review of protein kinase inhibitors for cancer therapy. *Expert Rev Anticancer Ther* **2018**, *18* (12), 1249-1270.
450. Klaeger, S.; Heinzlmeir, S.; Wilhelm, M.; Polzer, H.; Vick, B.; Koenig, P. A.; Reinecke, M.; Ruprecht, B.; Petzoldt, S.; Meng, C.; Zecha, J.; Reiter, K.; Qiao, H.; Helm, D.; Koch, H.; Schoof, M.; Canevari, G.; Casale, E.; Depaolini, S. R.; Feuchtinger, A.; Wu, Z.; Schmidt, T.; Rueckert, L.; Becker, W.; Huenges, J.; Garz, A. K.; Gohlke, B. O.; Zolg, D. P.; Kayser, G.; Vooder, T.; Preissner, R.; Hahne, H.; Tonisson, N.; Kramer, K.; Gotze, K.; Bassermann, F.; Schlegl, J.; Ehrlich, H. C.; Aiche, S.; Walch, A.; Greif, P. A.; Schneider, S.; Felder, E. R.; Ruland, J.; Medard, G.; Jeremias, I.; Spiekermann, K.; Kuster, B., The target landscape of clinical kinase drugs. *Science* **2017**, *358* (6367).
451. Yang, S. M.; Park, Y. K.; Kim, J. I.; Lee, Y. H.; Lee, T. Y.; Jang, B. C., LY3009120, a pan-Raf kinase inhibitor, inhibits adipogenesis of 3T3-L1 cells by controlling

- the expression and phosphorylation of C/EBP-alpha, PPAR-gamma, STAT3, FAS, ACC, perilipin A, and AMPK. *Int J Mol Med* **2018**, *42* (6), 3477-3484.
452. Bellevicine, C.; Sgariglia, R.; Migliatico, I.; Vigliar, E.; D'Anna, M.; Nacchio, M. A.; Serra, N.; Malapelle, U.; Bongiovanni, M.; Troncone, G., Different qualifiers of AUS/FLUS thyroid FNA have distinct BRAF, RAS, RET/PTC, and PAX8/PPAR γ alterations. *Cancer Cytopathol* **2018**, *126* (5), 317-325.
453. Hughes, T. S.; Shang, J.; Brust, R.; de Vera, I. M.; Fuhrmann, J.; Ruiz, C.; Cameron, M. D.; Kamenecka, T. M.; Kojetin, D. J., Probing the Complex Binding Modes of the PPAR γ Partial Agonist 2-Chloro-N-(3-chloro-4-((5-chlorobenzo[d]thiazol-2-yl)thio)phenyl)-4-(trifluoromethyl)benzenesulfonamide (T2384) to Orthosteric and Allosteric Sites with NMR Spectroscopy. *J Med Chem* **2016**, *59* (22), 10335-10341.
454. Bruning, J. B.; Chalmers, M. J.; Prasad, S.; Busby, S. A.; Kamenecka, T. M.; He, Y.; Nettles, K. W.; Griffin, P. R., Partial agonists activate PPAR γ using a helix 12 independent mechanism. *Structure* **2007**, *15* (10), 1258-71.
455. Burns, K. A.; Vanden Heuvel, J. P., Modulation of PPAR activity via phosphorylation. *Biochim Biophys Acta* **2007**, *1771* (8), 952-60.
456. Chen, L. H.; Fang, J.; Sun, Z.; Li, H.; Wu, Y.; Demark-Wahnefried, W.; Lin, X., Enterolactone inhibits insulin-like growth factor-1 receptor signaling in human prostatic carcinoma PC-3 cells. *J Nutr* **2009**, *139* (4), 653-9.
457. Chikara, S.; Lindsey, K.; Borowicz, P.; Christofidou-Solomidou, M.; Reindl, K. M., Enterolactone alters FAK-Src signaling and suppresses migration and invasion of lung cancer cell lines. *BMC Complement Altern Med* **2017**, *17* (1), 30.
458. Wei, Y.; Kang, X. L.; Wang, X., The peripheral cannabinoid receptor 1 antagonist VD60 efficiently inhibits carbon tetrachloride-intoxicated hepatic fibrosis progression. *Experimental biology and medicine* **2014**, *239* (2), 183-92.
459. Albanis, E.; Friedman, S. L., Antifibrotic agents for liver disease. *Am J Transplant* **2006**, *6* (1), 12-9.
460. Dooley, S.; Hamzavi, J.; Breitkopf, K.; Wiercinska, E.; Said, H. M.; Lorenzen, J.; Ten Dijke, P.; Gressner, A. M., Smad7 prevents activation of hepatic stellate cells and liver fibrosis in rats. *Gastroenterology* **2003**, *125* (1), 178-191.
461. Fujii, M.; Yoneda, A.; Takei, N.; Sakai-Sawada, K.; Kosaka, M.; Minomi, K.; Yokoyama, A.; Tamura, Y., Endoplasmic reticulum oxidase 1 alpha is critical for collagen secretion from and membrane type 1-matrix metalloproteinase levels in hepatic stellate cells. *J Biol Chem* **2017**, *292* (38), 15649-15660.
462. Huang, Y.; Deng, X.; Liang, J., Modulation of hepatic stellate cells and reversibility of hepatic fibrosis. *Exp Cell Res* **2017**, *352* (2), 420-426.
463. Duval, F.; Moreno-Cuevas, J. E.; Gonzalez-Garza, M. T.; Rodriguez-Montalvo, C.; Cruz-Vega, D. E., Protective mechanisms of medicinal plants targeting hepatic stellate cell activation and extracellular matrix deposition in liver fibrosis. *Chin Med* **2014**, *9* (1), 27.
464. Sato, Y.; Harada, K.; Furubo, S.; Kizawa, K.; Sanzen, T.; Yasoshima, M.; Ozaki, S.; Isse, K.; Sasaki, M.; Nakanuma, Y., Inhibition of intrahepatic bile duct dilation of the polycystic kidney rat with a novel tyrosine kinase inhibitor gefitinib. *Am J Pathol* **2006**, *169* (4), 1238-50.
465. Garofalo, M.; Romano, G.; Di Leva, G.; Nuovo, G.; Jeon, Y. J.; Ngankeu, A.; Sun, J.; Lovat, F.; Alder, H.; Condorelli, G.; Engelman, J. A.; Ono, M.; Rho, J. K.; Cascione, L.; Volinia, S.; Nephew, K. P.; Croce, C. M., EGFR and MET receptor tyrosine kinase-altered microRNA expression induces tumorigenesis and gefitinib resistance in lung cancers. *Nature medicine* **2012**, *18* (1), 74-82.
466. Komposch, K.; Sibilica, M., EGFR Signaling in Liver Diseases. *Int J Mol Sci* **2015**, *17* (1).

467. Chamberlin, S. R.; Blucher, A.; Wu, G.; Shinto, L.; Choonoo, G.; Kulesz-Martin, M.; McWeeney, S., Natural Product Target Network Reveals Potential for Cancer Combination Therapies. *Front. Pharmacol.* **2019**, *10* (557).
468. Yin, B.; Fang, D.-M.; Zhou, X.-L.; Gao, F., Natural products as important tyrosine kinase inhibitors. *Eur. J. Med. Chem.* **2019**, *182*, 111664.
469. Kershenobich Stalnikowitz, D.; Weissbrod, A. B., Liver fibrosis and inflammation. A review. *Ann Hepatol* **2003**, *2* (4), 159-63.
470. Ezhilarasan, D.; Evraerts, J.; Brice, S.; Buc-Calderon, P.; Karthikeyan, S.; Sokal, E.; Najimi, M., Silibinin Inhibits Proliferation and Migration of Human Hepatic Stellate LX-2 Cells. *J Clin Exp Hepatol* **2016**, *6* (3), 167-174.
471. Tai, C. J.; Choong, C. Y.; Lin, Y. C.; Shi, Y. C.; Tai, C. J., The anti-hepatic fibrosis activity of ergosterol depended on upregulation of PPARgamma in HSC-T6 cells. *Food Funct* **2016**, *7* (4), 1915-23.
472. Miyahara, T.; Schrum, L.; Rippe, R.; Xiong, S.; Yee, H. F., Jr.; Motomura, K.; Anania, F. A.; Willson, T. M.; Tsukamoto, H., Peroxisome proliferator-activated receptors and hepatic stellate cell activation. *J Biol Chem* **2000**, *275* (46), 35715-22.
473. Rockey, D. C., Current and future anti-fibrotic therapies for chronic liver disease. *Clin Liver Dis* **2008**, *12* (4), 939-62, xi.
474. Du, J.; Niu, X.; Wang, R.; Zhao, S.; Kong, L.; Zhang, Y.; Nan, Y., TLR4dependent signaling pathway modulation: A novel mechanism by which pioglitazone protects against nutritional fibrotic steatohepatitis in mice. *Mol Med Rep* **2016**, *13* (3), 2159-66.
475. Lin, Q.; Fang, L. P.; Zhou, W. W.; Liu, X. M., Rosiglitazone inhibits migration, proliferation, and phenotypic differentiation in cultured human lung fibroblasts. *Exp Lung Res* **2010**, *36* (2), 120-8.
476. Zhao, C.; Chen, W.; Yang, L.; Chen, L.; Stimpson, S. A.; Diehl, A. M., PPARgamma agonists prevent TGFbeta1/Smad3-signaling in human hepatic stellate cells. *Biochem Biophys Res Commun* **2006**, *350* (2), 385-91.
477. Yu, J.; Zhang, S.; Chu, E. S.; Go, M. Y.; Lau, R. H.; Zhao, J.; Wu, C. W.; Tong, L.; Zhao, J.; Poon, T. C.; Sung, J. J., Peroxisome proliferator-activated receptors gamma reverses hepatic nutritional fibrosis in mice and suppresses activation of hepatic stellate cells in vitro. *Int J Biochem Cell Biol* **2010**, *42* (6), 948-57.
478. Breitkopf, K.; Godoy, P.; Ciuculan, L.; Singer, M. V.; Dooley, S., TGF-beta/Smad signaling in the injured liver. *Z Gastroenterol* **2006**, *44* (1), 57-66.
479. Lee, T. F.; Lin, Y. L.; Huang, Y. T., Kaerophyllin inhibits hepatic stellate cell activation by apoptotic bodies from hepatocytes. *Liver Int* **2011**, *31* (5), 618-29.
480. Lopez-Sanchez, I.; Dunkel, Y.; Roh, Y. S.; Mittal, Y.; De Minicis, S.; Muranyi, A.; Singh, S.; Shanmugam, K.; Aroonsakool, N.; Murray, F.; Ho, S. B.; Seki, E.; Brenner, D. A.; Ghosh, P., GIV/Girdin is a central hub for profibrogenic signalling networks during liver fibrosis. *Nat Commun* **2014**, *5*, 4451.
481. Liu, Y.; Dai, B.; Xu, C.; Fu, L.; Hua, Z.; Mei, C., Rosiglitazone inhibits transforming growth factor-beta1 mediated fibrogenesis in ADPKD cyst-lining epithelial cells. *PLoS One* **2011**, *6* (12), e28915.
482. Zhang, F.; Kong, D.; Chen, L.; Zhang, X.; Lian, N.; Zhu, X.; Lu, Y.; Zheng, S., Peroxisome proliferator-activated receptor-gamma interrupts angiogenic signal transduction by transrepression of platelet-derived growth factor-beta receptor in hepatic stellate cells. *J Cell Sci* **2014**, *127* (Pt 2), 305-14.
483. Yang, H.; Zhao, L. F.; Zhao, Z. F.; Wang, Y.; Zhao, J. J.; Zhang, L., Heme oxygenase-1 prevents liver fibrosis in rats by regulating the expression of PPARgamma and NF-kappaB. *World J Gastroenterol* **2012**, *18* (14), 1680-8.

484. Tomita, K.; Teratani, T.; Suzuki, T.; Shimizu, M.; Sato, H.; Narimatsu, K.; Okada, Y.; Kurihara, C.; Irie, R.; Yokoyama, H.; Shimamura, K.; Usui, S.; Ebinuma, H.; Saito, H.; Watanabe, C.; Komoto, S.; Kawaguchi, A.; Nagao, S.; Sugiyama, K.; Hokari, R.; Kanai, T.; Miura, S.; Hibi, T., Free cholesterol accumulation in hepatic stellate cells: mechanism of liver fibrosis aggravation in nonalcoholic steatohepatitis in mice. *Hepatology* **2014**, *59* (1), 154-69.
485. Fu, M. Y.; He, Y. J.; Lv, X.; Liu, Z. H.; Shen, Y.; Ye, G. R.; Deng, Y. M.; Shu, J. C., Transforming growth factorbeta1 reduces apoptosis via autophagy activation in hepatic stellate cells. *Mol Med Rep* **2014**, *10* (3), 1282-8.
486. Oikawa, D.; Kimata, Y.; Kohno, K.; Iwawaki, T., Activation of mammalian IRE1alpha upon ER stress depends on dissociation of BiP rather than on direct interaction with unfolded proteins. *Exp Cell Res* **2009**, *315* (15), 2496-504.
487. Bertolotti, A.; Zhang, Y.; Hendershot, L. M.; Harding, H. P.; Ron, D., Dynamic interaction of BiP and ER stress transducers in the unfolded-protein response. *Nat Cell Biol* **2000**, *2* (6), 326-32.
488. Liu, Z. K.; Li, C.; Kang, N. L.; Malhi, H.; Shah, V. H.; Maiers, J. L., Transforming growth factor (TGF) cross-talk with the unfolded protein response is critical for hepatic stellate cell activation. *J Biol Chem* **2019**, *294* (9), 3137-3151.
489. Wang, C.; Zhang, F.; Cao, Y.; Zhang, M.; Wang, A.; Xu, M.; Su, M.; Zhang, M.; Zhuge, Y., Etoposide Induces Apoptosis in Activated Human Hepatic Stellate Cells via ER Stress. *Sci Rep* **2016**, *6*, 34330.
490. Li, Y. J.; Chen, Y. Y.; Huang, H. Y.; Shi, M. M.; Yang, W. P.; Kuang, J.; Yan, J. Q., Autophagy mediated by endoplasmic reticulum stress enhances the caffeine-induced apoptosis of hepatic stellate cells. *Int J Mol Med* **2017**, *40* (5), 1405-1414.
491. Shih, Y. C.; Chen, C. L.; Zhang, Y.; Mellor, R. L.; Kanter, E. M.; Fang, Y.; Wang, H. C.; Hung, C. T.; Nong, J. Y.; Chen, H. J.; Lee, T. H.; Tseng, Y. S.; Chen, C. N.; Wu, C. C.; Lin, S. L.; Yamada, K. A.; Nerbonne, J. M.; Yang, K. C., Endoplasmic Reticulum Protein TXNDC5 Augments Myocardial Fibrosis by Facilitating Extracellular Matrix Protein Folding and Redox-Sensitive Cardiac Fibroblast Activation. *Circ Res* **2018**, *122* (8), 1052-1068.
492. Groenendyk, J.; Lee, D.; Jung, J.; Dyck, J. R.; Lopaschuk, G. D.; Agellon, L. B.; Michalak, M., Inhibition of the Unfolded Protein Response Mechanism Prevents Cardiac Fibrosis. *PLoS One* **2016**, *11* (7), e0159682.
493. Maiers, J. L.; Malhi, H., Endoplasmic Reticulum Stress in Metabolic Liver Diseases and Hepatic Fibrosis. *Semin Liver Dis* **2019**, *39* (2), 235-248.
494. Han, J.; Back, S. H.; Hur, J.; Lin, Y. H.; Gildersleeve, R.; Shan, J.; Yuan, C. L.; Krokowski, D.; Wang, S.; Hatzoglou, M.; Kilberg, M. S.; Sartor, M. A.; Kaufman, R. J., ER-stress-induced transcriptional regulation increases protein synthesis leading to cell death. *Nat Cell Biol* **2013**, *15* (5), 481-90.
495. Cullinan, S. B.; Zhang, D.; Hannink, M.; Arvisais, E.; Kaufman, R. J.; Diehl, J. A., Nrf2 is a direct PERK substrate and effector of PERK-dependent cell survival. *Mol Cell Biol* **2003**, *23* (20), 7198-209.
496. Nagelkerke, A.; Bussink, J.; Sweep, F. C.; Span, P. N., The unfolded protein response as a target for cancer therapy. *Biochim Biophys Acta* **2014**, *1846* (2), 277-84.
497. Cullinan, S. B.; Diehl, J. A., PERK-dependent activation of Nrf2 contributes to redox homeostasis and cell survival following endoplasmic reticulum stress. *J Biol Chem* **2004**, *279* (19), 20108-17.
498. Sharma, R. S.; Harrison, D. J.; Kisielowski, D.; Cassidy, D. M.; McNeilly, A. D.; Gallagher, J. R.; Walsh, S. V.; Honda, T.; McCrimmon, R. J.; Dinkova-Kostova, A. T.; Ashford, M. L. J.; Dillon, J. F.; Hayes, J. D., Experimental Nonalcoholic Steatohepatitis and

- Liver Fibrosis Are Ameliorated by Pharmacologic Activation of Nrf2 (NF-E2 p45-Related Factor 2). *Cell Mol Gastroenterol Hepatol* **2018**, 5 (3), 367-398.
499. Cullinan, S. B.; Diehl, J. A., Coordination of ER and oxidative stress signaling: the PERK/Nrf2 signaling pathway. *Int J Biochem Cell Biol* **2006**, 38 (3), 317-32.
500. Ji, C., Dissection of endoplasmic reticulum stress signaling in alcoholic and non-alcoholic liver injury. *J Gastroenterol Hepatol* **2008**, 23 Suppl 1, S16-24.
501. Cinaroglu, A.; Gao, C.; Imrie, D.; Sadler, K. C., Activating transcription factor 6 plays protective and pathological roles in fatty liver disease due to endoplasmic reticulum stress. *Hepatology* **2011**, 54 (2), 495-508.
502. Iracheta-Vellve, A.; Petrasek, J.; Gyongyosi, B.; Satishchandran, A.; Lowe, P.; Kodys, K.; Catalano, D.; Calenda, C. D.; Kurt-Jones, E. A.; Fitzgerald, K. A.; Szabo, G., Endoplasmic Reticulum Stress-induced Hepatocellular Death Pathways Mediate Liver Injury and Fibrosis via Stimulator of Interferon Genes. *J Biol Chem* **2016**, 291 (52), 26794-26805.
503. Koo, J. H.; Lee, H. J.; Kim, W.; Kim, S. G., Endoplasmic Reticulum Stress in Hepatic Stellate Cells Promotes Liver Fibrosis via PERK-Mediated Degradation of HNRNPA1 and Up-regulation of SMAD2. *Gastroenterology* **2016**, 150 (1), 181-193 e8.
504. Tsuchida, T.; Friedman, S. L., Mechanisms of hepatic stellate cell activation. *Nat Rev Gastroenterol Hepatol* **2017**, 14 (7), 397-411.
505. Chen, X.; Ying, X.; Chen, L.; Zhang, W.; Zhang, Y., Protective effects of sesamin on liver fibrosis through antioxidative and anti-inflammatory activities in rats. *Immunopharmacol Immunotoxicol* **2015**, 37 (5), 465-72.
506. Liu, R. M.; Desai, L. P., Reciprocal regulation of TGF-beta and reactive oxygen species: A perverse cycle for fibrosis. *Redox Biol* **2015**, 6, 565-77.
507. Bajpai, V. K.; Alam, M. B.; Quan, K. T.; Kwon, K. R.; Ju, M. K.; Choi, H. J.; Lee, J. S.; Yoon, J. I.; Majumder, R.; Rather, I. A.; Kim, K.; Lee, S. H.; Na, M., Antioxidant efficacy and the upregulation of Nrf2-mediated HO-1 expression by (+)-lariciresinol, a lignan isolated from *Rubia philippinensis*, through the activation of p38. *Sci Rep-Uk* **2017**, 7.
508. Mukai, S.; Moriya, S.; Hiramoto, M.; Kazama, H.; Kokuba, H.; Che, X. F.; Yokoyama, T.; Sakamoto, S.; Sugawara, A.; Sunazuka, T.; Omura, S.; Handa, H.; Itoi, T.; Miyazawa, K., Macrolides sensitize EGFR-TKI-induced non-apoptotic cell death via blocking autophagy flux in pancreatic cancer cell lines. *Int J Oncol* **2016**, 48 (1), 45-54.
509. Ouyang, X.; Ghani, A.; Mehal, W. Z., Inflammasome biology in fibrogenesis. *Biochim Biophys Acta* **2013**, 1832 (7), 979-88.
510. Radha, V.; Nambirajan, S.; Swarup, G., Association of Lyn tyrosine kinase with the nuclear matrix and cell-cycle-dependent changes in matrix-associated tyrosine kinase activity. *Eur J Biochem* **1996**, 236 (2), 352-9.
511. Xu, H.; Liu, L.; Cong, M.; Liu, T.; Sun, S.; Ma, H.; You, H.; Jia, J.; Wang, P., EGF neutralization antibodies attenuate liver fibrosis by inhibiting myofibroblast proliferation in bile duct ligation mice. *Histochem Cell Biol* **2020**.
512. Zhang, F.; Xu, M.; Yin, X.; Guo, H.; Zhang, B.; Wang, Y.; Xiao, J.; Zou, X.; Zhang, M.; Zhuge, Y., TWEAK promotes hepatic stellate cell migration through activating EGFR/Src and PI3K/AKT pathways. *Cell Biol Int* **2019**.
513. Kim, M. J.; Choi, W. G.; Ahn, K. J.; Chae, I. G.; Yu, R.; Back, S. H., Reduced EGFR Level in eIF2alpha Phosphorylation Deficient Hepatocytes Is Responsible for Susceptibility to Oxidative Stress. *Mol Cells* **2020**, 43 (3), 264-275.
514. Jeng, K. C.; Hou, R. C.; Wang, J. C.; Ping, L. I., Sesamin inhibits lipopolysaccharide-induced cytokine production by suppression of p38 mitogen-activated protein kinase and nuclear factor-kappaB. *Immunol Lett* **2005**, 97 (1), 101-6.

515. Zhang, Z.; Guo, Y.; Zhang, S.; Zhang, Y.; Wang, Y.; Ni, W.; Kong, D.; Chen, W.; Zheng, S., Curcumin modulates cannabinoid receptors in liver fibrosis in vivo and inhibits extracellular matrix expression in hepatic stellate cells by suppressing cannabinoid receptor type-1 in vitro. *Eur J Pharmacol* **2013**, *721* (1-3), 133-40.
516. Rahimifard, M.; Maqbool, F.; Moeini-Nodeh, S.; Niaz, K.; Abdollahi, M.; Braidy, N.; Nabavi, S. M.; Nabavi, S. F., Targeting the TLR4 signaling pathway by polyphenols: A novel therapeutic strategy for neuroinflammation. *Ageing Res Rev* **2017**, *36*, 11-19.
517. Park, S. Y.; Park, D. J.; Kim, Y. H.; Kim, Y.; Kim, S. G.; Shon, K. J.; Choi, Y. W.; Lee, S. J., Upregulation of heme oxygenase-1 via PI3K/Akt and Nrf-2 signaling pathways mediates the anti-inflammatory activity of Schisandrin in Porphyromonas gingivalis LPS-stimulated macrophages. *Immunol Lett* **2011**, *139* (1-2), 93-101.
518. Barre, D. E.; Mizier-Barre, K. A.; Stelmach, E.; Hobson, J.; Griscti, O.; Rudiuk, A.; Muthuthavar, D., Flaxseed lignan complex administration in older human type 2 diabetics manages central obesity and prothrombosis-an invitation to further investigation into polypharmacy reduction. *J Nutr Metab* **2012**, *2012*, 585170.
519. Bowers, L. W.; Lineberger, C. G.; Ford, N. A.; Rossi, E. L.; Punjala, A.; Camp, K. K.; Kimler, B. K.; Fabian, C. J.; Hursting, S. D., The flaxseed lignan secoisolariciresinol diglucoside decreases local inflammation, suppresses NFkappaB signaling, and inhibits mammary tumor growth. *Breast Cancer Res Treat* **2019**, *173* (3), 545-557.
520. Cheng, J. H.; She, H.; Han, Y. P.; Wang, J.; Xiong, S.; Asahina, K.; Tsukamoto, H., Wnt antagonism inhibits hepatic stellate cell activation and liver fibrosis. *Am J Physiol Gastrointest Liver Physiol* **2008**, *294* (1), G39-49.
521. Young, C. S.; Kitamura, M.; Hardy, S.; Kitajewski, J., Wnt-1 induces growth, cytosolic beta-catenin, and Tcf/Lef transcriptional activation in Rat-1 fibroblasts. *Mol Cell Biol* **1998**, *18* (5), 2474-85.
522. Corbett, L.; Mann, J.; Mann, D. A., Non-Canonical Wnt Predominates in Activated Rat Hepatic Stellate Cells, Influencing HSC Survival and Paracrine Stimulation of Kupffer Cells. *PLoS One* **2015**, *10* (11), e0142794.
523. Angulo, P.; Hui, J. M.; Marchesini, G.; Bugianesi, E.; George, J.; Farrell, G. C.; Enders, F.; Saksena, S.; Burt, A. D.; Bida, J. P.; Lindor, K.; Sanderson, S. O.; Lenzi, M.; Adams, L. A.; Kench, J.; Therneau, T. M.; Day, C. P., The NAFLD fibrosis score: A noninvasive system that identifies liver fibrosis in patients with NAFLD. *Hepatology* **2007**, *45* (4), 846-854.
524. Calzadilla Bertot, L.; Adams, L. A., The Natural Course of Non-Alcoholic Fatty Liver Disease. *Int J Mol Sci* **2016**, *17* (5).
525. Maurice, J.; Manousou, P., Non-alcoholic fatty liver disease. *Clin Med (Lond)* **2018**, *18* (3), 245-250.
526. McPherson, S.; Hardy, T.; Henderson, E.; Burt, A. D.; Day, C. P.; Anstee, Q. M., Evidence of NAFLD progression from steatosis to fibrosing-steatohepatitis using paired biopsies: implications for prognosis and clinical management. *J Hepatol* **2015**, *62* (5), 1148-55.
527. Dominguez-Perez, M.; Simoni-Nieves, A.; Rosales, P.; Nuno-Lambarri, N.; Rosas-Lemus, M.; Souza, V.; Miranda, R. U.; Bucio, L.; Uribe Carvajal, S.; Marquardt, J. U.; Seo, D.; Gomez-Quiroz, L. E.; Gutierrez-Ruiz, M. C., Cholesterol burden in the liver induces mitochondrial dynamic changes and resistance to apoptosis. *J Cell Physiol* **2019**, *234* (5), 7213-7223.
528. Yuan, Y.; Naito, H.; Nakajima, T., *The Role of Cholesterol in the Pathogenesis of Hypertension-Associated Nonalcoholic Steatohepatitis*. 2018; Vol. Chapter 7.

529. Fodor, J. G.; Frohlich, J. J.; Genest, J. J., Jr.; McPherson, P. R., Recommendations for the management and treatment of dyslipidemia. Report of the Working Group on Hypercholesterolemia and Other Dyslipidemias. *CMAJ* **2000**, *162* (10), 1441-7.
530. Wierzbicki, A. S.; Poston, R.; Ferro, A., The lipid and non-lipid effects of statins. *Pharmacol Ther* **2003**, *99* (1), 95-112.
531. Hawsawi, A. A.; University of Saskatchewan College of Graduate Studies and Research., Flaxseed Lignan Metabolites Modulate Hepatocellular Cholesterol Trafficking In HepaRG. **2018**. <http://hdl.handle.net/10388/10065>.
532. Sozen, E.; Ozer, N. K., Impact of high cholesterol and endoplasmic reticulum stress on metabolic diseases: An updated mini-review. *Redox Biol* **2017**, *12*, 456-461.
533. Corey, K. E.; Vuppalanchi, R.; Wilson, L. A.; Cummings, O. W.; Chalasani, N.; Nash, C. R. N., NASH resolution is associated with improvements in HDL and triglyceride levels but not improvement in LDL or non-HDL-C levels. *Aliment Pharmacol Ther* **2015**, *41* (3), 301-9.
534. Comeglio, P.; Cellai, I.; Mello, T.; Filippi, S.; Maneschi, E.; Corcetto, F.; Corno, C.; Sarchielli, E.; Morelli, A.; Rapizzi, E.; Bani, D.; Guasti, D.; Vannelli, G. B.; Galli, A.; Adorini, L.; Maggi, M.; Vignozzi, L., INT-767 prevents NASH and promotes visceral fat brown adipogenesis and mitochondrial function. *J Endocrinol* **2018**, *238* (2), 107-127.
535. Mason, J. K.; Thompson, L. U., Flaxseed and its lignan and oil components: can they play a role in reducing the risk of and improving the treatment of breast cancer? *Appl Physiol Nutr Metab* **2014**, *39* (6), 663-78.
536. Clavel, T.; Borrmann, D.; Braune, A.; Dore, J.; Blaut, M., Occurrence and activity of human intestinal bacteria involved in the conversion of dietary lignans. *Anaerobe* **2006**, *12* (3), 140-7.
537. Van De Wetering, K.; Feddema, W.; Helms, J. B.; Brouwers, J. F.; Borst, P., Targeted Metabolomics Identifies Glucuronides of Dietary Phytoestrogens as a Major Class of MRP3 Substrates In Vivo. *Gastroenterology* **2009**, *137* (5), 1725-1735.

APPENDIX A

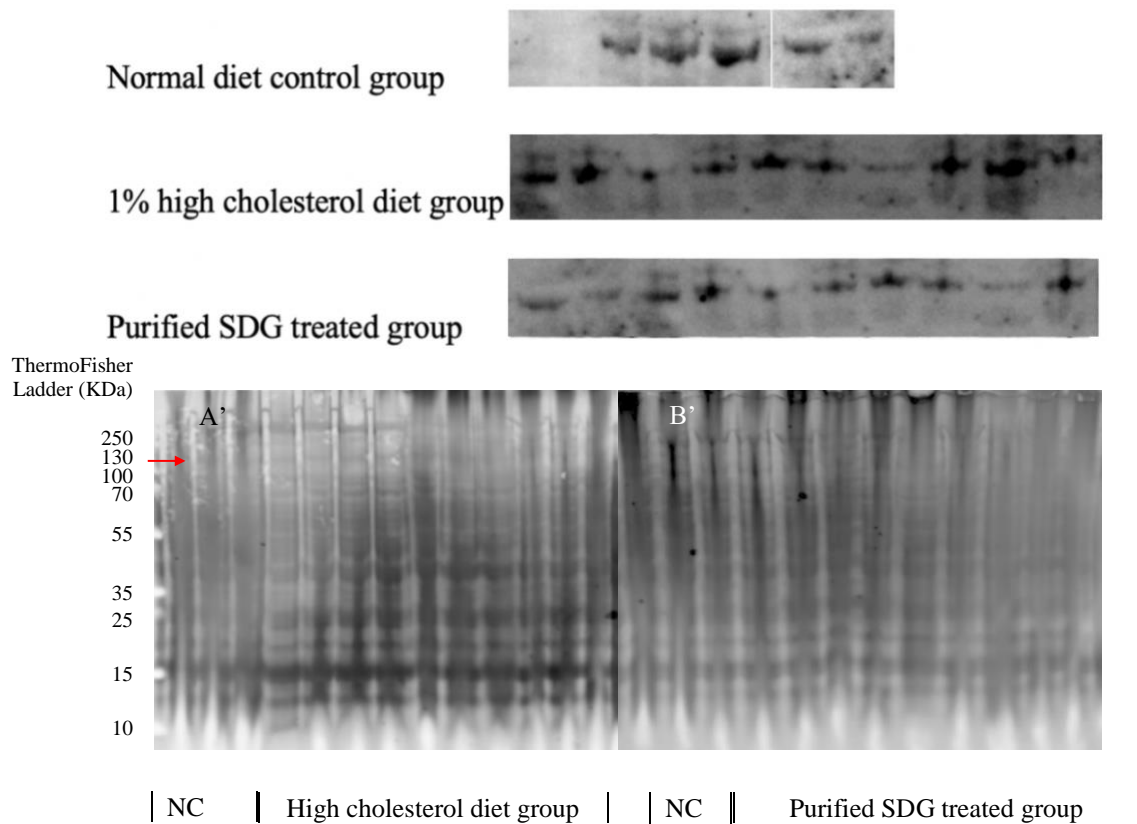


Figure A 1. The expression of collagen I in rat liver tissue after treatment with purified secoisolariciresinol diglucoside (SDG) in high cholesterol diet induced Wistar rats. The expression of collagen I in the individual rat liver samples were run separately, using total protein stained by SYPRO Ruby blot stain reagent (A' and B', protein ranges from 10 to 250 kDa according to ThermoFisher PageRuler™ Plus Prestained Protein Ladder) as normalizing reference. The expression of Collagen I protein was detected for each individual rat, located at the red arrow on the blot. N=5 for the normal control group and N=10 for high cholesterol diet and SDG groups.

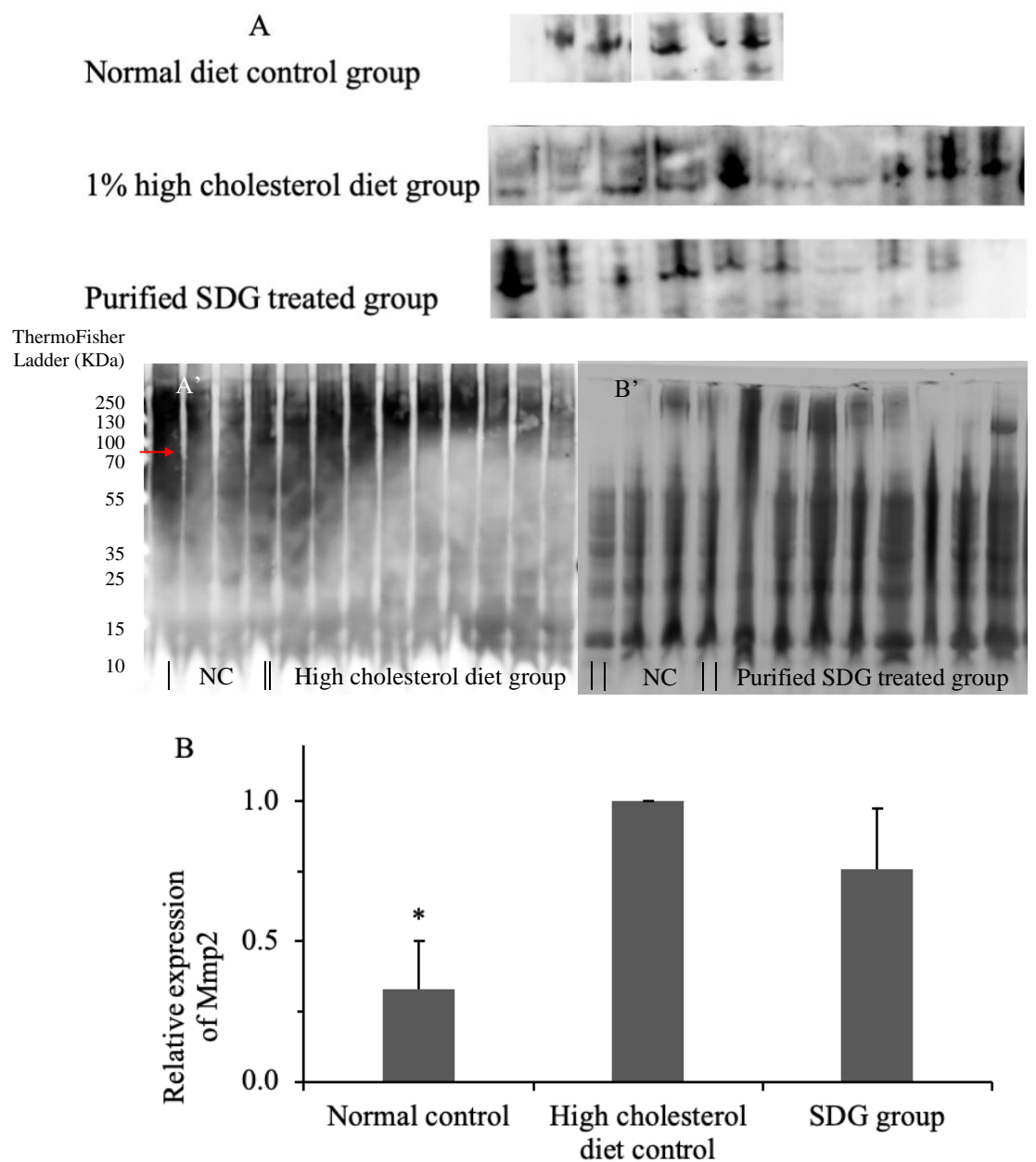


Figure A 2. The relative protein expression of Mmp2 in rat liver samples after treatment with purified secoisolariciresinol diglucoside (SDG) in high cholesterol diet induced Wistar rats. The relative expressions of Mmp2 in individual rat liver samples (A) and mean of relative expression for each group was normalized to the 1% high cholesterol diet group (B), using total protein stained by SYPRO Ruby blot stain reagent (A' and B', protein ranges from 10 to 250 kDa according to ThermoFisher PageRuler™ Plus Prestained Protein Ladder) as normalizing reference. Data were shown as mean \pm SD of the relative expression of Mmp2 protein in panel B, located at the red arrow on the blot (N=5 for the normal control group and N=8 for high cholesterol diet and SDG groups). * indicates significantly ($P < 0.05$) different from the High cholesterol diet control, by one-way ANOVA followed by Tukey test.

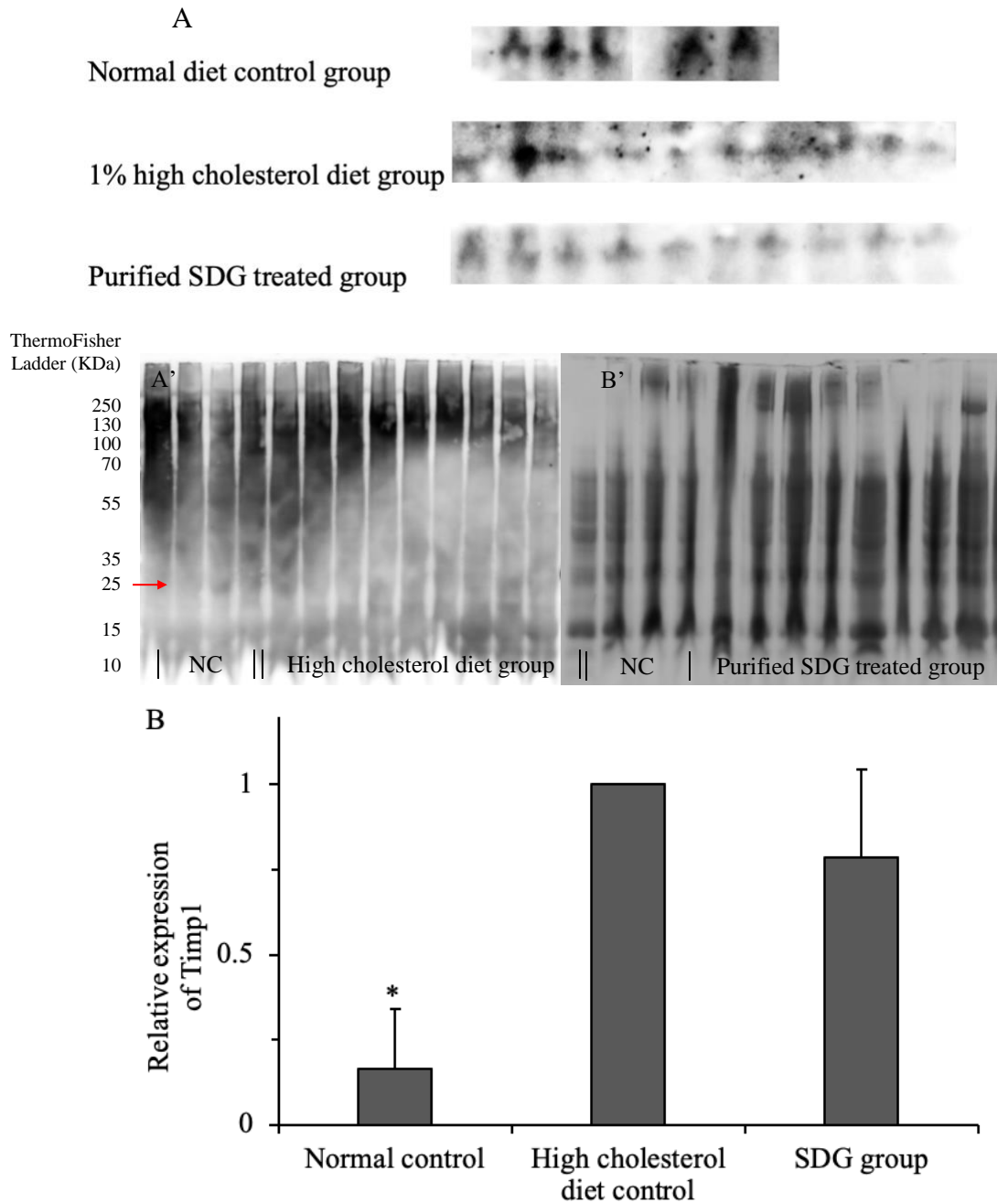


Figure A 3. The relative protein expression of Timp1 in rat liver samples after treated with purified secoisolariciresinol diglucoside (SDG) in high cholesterol diet supplied Wistar rats. The relative expressions of Timp1 in individual rat liver samples (A) and the mean relative expression for each group were normalized to the 1% high cholesterol diet group (B), using total protein stained by SYPRO Ruby blot stain reagent (A' and B', protein ranges from 10 to 250 kDa according to ThermoFisher PageRuler™ Plus Prestained Protein Ladder) as normalizing reference. Data were shown as mean \pm SD of the relative expression of Timp1 protein in panel B, located at the red arrow on the blot (N=5 for the normal control group and N=10 for high cholesterol diet and SDG groups). * indicates significantly ($P < 0.05$) different from the High cholesterol diet control, by one-way ANOVA with Tukey test.

APPENDIX B



Animal Research Ethics Board (AREB)

Certificate of Approval Protocol Modification

PRINCIPAL INVESTIGATOR Dr. Mary-Jane Alcorn	DEPARTMENT/ORGANIZATION Pharmacy & Nutrition	ANIMAL USE PROTOCOL # 20180044
--	---	-----------------------------------

TITLE
Comparative oral pharmacokinetics of purified SDG and SDG-enriched complex in female rats and efficacy of purified SDG and SDG-enriched complex in female hypercholesterolemic rats

APPROVAL DATE:
June 11, 2019

APPROVAL OF:
Change in Study Design or Procedures:
SDG complex was not soluble in saline or
Ensure. Changed dosing vehicles; 10%
ethanol, 30% PEG 400 and 60% saline; 4%
ethanol, 12% PEG 400, 24% saline and 60%
Ensure once daily.

EXPIRY DATE:
June 30, 2019

Full Board Meeting AREB Subcommittee AREB Chair and University Veterinarian AREB Chair

CERTIFICATION

The University of Saskatchewan Animal Research Ethics Board reviewed the above-named research project. The proposal was found to be acceptable on ethical grounds. The principal investigator has the responsibility for any other administrative or regulatory approvals that may pertain to this research project, and for ensuring that the authorized research is carried out according to the conditions outlined in the original protocol submitted for ethics review. This Certificate of Approval is valid for the above time period.

ONGOING REVIEW REQUIREMENTS

Research programs that extend beyond one year must receive annual review. For the annual renewal, an annual review form (and progress report) must be submitted to the AREB within one month of the current expiry date each year the study remains open, and upon study completion. Please refer to the [Research Services and Ethics Office website](#) for further instructions.

PROTOCOL MODIFICATIONS

Any further modifications to this protocol must be approved by the UACC AREB prior to implementation, using the [AUP Modification Form](#)

Sean Mulligan, Vice Chair
Animal Research Ethics Board
University of Saskatchewan

June 14, 2019
Date Issued

Please send all correspondence to:

Research Services and Ethics Office
University of Saskatchewan
Room 223 Thorvaldson, 110 Science Place
Saskatoon SK S7N 5C9
Telephone: (306) 966-4126 Fax: (306) 966-2069 Email: uacc.office@usask.ca